Progress of Theoretical Physics, Vol. 65, No. 5, May 1981

Dynamical Interplay of Pairing and Quadrupole Modes in Transitional Nuclei. III

Tōru SUZUKI, Masahiko FUYUKI*,†) and Kenichi MATSUYANAGI*

Institut für Kernphysik, Kernforschungsanlage Jülich
5170 Jülich
**Department of Physics, Kyoto University, Kyoto 606*

(Received January 12, 1981)

From the many-j shell model with pairing plus quadrupole force, we derive microscopic expressions for the pairing rotation-quasiparticle couplings as well as for the pairing vibration-quasiparticle couplings. In particular, we show it possible to construct a model space in a form analogous to the familiar particle-rotor model.

§ 1. Introduction

The purpose of the present paper is to derive a microscopic expression for the couplings between intrinsic quasiparticles and pairing collective excitations. A significant role of pairing vibration-quasiparticle couplings in transitional nuclei has been pointed out by Sakata et al.[1] On the other hand, the importance of explicitly treating the pairing rotation-quasiparticle couplings has been indicated in our previous papers.[2] The latter couplings are quite analogous to the more familiar particle-rotor couplings (in the ordinary coordinate space) associated with quadrupole deformations: As is well known, the intrinsic single-particle modes in the deformed Nilsson potential break the rotational symmetry. This broken-symmetry is restored, in the particle-rotor model, through the couplings of Nilsson particles to the rotational motions.[3] Analogously, Bogoliubov quasiparticles in the nuclear pairing problem may be regarded as intrinsic single-particle modes in a deformed pair potential. Due to the deformation of the pair field, the nucleon-number conservation law is necessarily broken in the intrinsic space. *We can, however, restore the broken-symmetry by taking into account the couplings of the quasiparticle motions to the pairing rotations.* This is just the mode-mode coupling point of view we intend to develop in this paper.

Let us denote the intrinsic quasiparticle operators by $(\boldsymbol{a}_\alpha^\dagger, \boldsymbol{a}_\alpha)$, the pairing vibrational modes by $(\Gamma_\nu^\dagger, \Gamma_\nu)$, and the angle operators for the pairing rotations by $\mathring{\Phi}$. Then, basis vectors of our model space may be written as direct products of intrinsic and pairing-collective states:

†) Present address: Department of Industrial Engineering, Kansai University, Suita, Osaka 564.

$$|\text{intrinsic}\rangle\otimes|\text{pairing collective}) = \boldsymbol{a}_\alpha^\dagger \boldsymbol{a}_\beta^\dagger \cdots \boldsymbol{a}_\delta^\dagger |0\rangle \otimes \exp(i\Pi\mathring{\Phi}) \prod_\nu \frac{1}{\sqrt{n_\nu!}} (\Gamma_\nu^\dagger)^{n_\nu} |\Psi_0^{\text{vib}}) \tag{1·1}$$

with

$$\boldsymbol{a}_\alpha|0\rangle = 0 \quad \text{and} \quad \Gamma_\nu|\Psi_0^{\text{vib}}) = 0\,. \tag{1·2}$$

Here $\exp(i\Pi\mathring{\Phi})$ represents the pairing rotation, Π being an eigenvalue of the nucleon-pair-number operator $\mathring{\Pi}$. Thus, our subject is to transform an original nuclear Hamiltonian H into an effective mode-mode coupling Hamiltonian $\mathcal{H}$ having the following form:

$$\mathcal{H} = \mathcal{H}_{\text{intri}}(\boldsymbol{a}^\dagger, \boldsymbol{a}) + \mathcal{H}_{\text{pair}}(\Gamma^\dagger, \Gamma, \mathring{\Pi}) + \mathcal{H}_{\text{coupl}}(\boldsymbol{a}^\dagger, \boldsymbol{a}, \Gamma^\dagger, \Gamma, \mathring{\Pi}). \tag{1·3}$$

Normal modes of pairing collective excitations are defined usually in terms of RPA. In this case, there is a serious problem in deriving a mode-mode coupling Hamiltonian (1·3); namely, the norm of the RPA vacuum diverges in association with the appearance of the zero-energy mode which corresponds to the pairing rotational degree of freedom.[4] Hence, the coupling matrix elements of interest inevitably diverge. In Ref. 5), this problem was formally *avoided* within the RPA by taking a special limiting procedure. In the present paper, we shall *overcome* this difficulty by introducing the exact number-angle variables (§ 2), and by performing a canonical transformation with auxiliary variables (§ 3). By this procedure, the pairing rotational mode manifests itself as a mode represented by the auxiliary number-angle variables (§ 4). We shall in this way obtain finite values for the coupling matrix elements between the intrinsic quasiparticle and pairing rotational modes (§§ 5 and 6).

Although a number of important papers[6)~12)] deal with the pairing vibrations and rotations, we feel that the study of their couplings to the intrinsic quasiparticle excitations is at a very early stage. In contrast, the presented microscopic method to derive the couplings of interest is applicable for any kind of effective interactions. For the sake of concreteness, however, we adopt in this paper the many-j shell model with pairing plus quadruple-quadruple (P+QQ) force.[13)]

§ 2. Number-angle representation of pairing Hamiltonian

2.1. *Pairing Hamiltonian*

With the nucleon creation and annihilation operators $(c_\alpha^\dagger, c_\alpha)$ in the shell-model state $\alpha \equiv (a, m_\alpha)$, the pairing Hamiltonian is written as

$$H = H_0 + H_P = \sum_\alpha \varepsilon_\alpha c_\alpha^\dagger c_\alpha - G\sum_{ab} \hat{S}_+(a)\hat{S}_-(b)\,, \tag{2·1}$$

$$\hat{S}_+(a)=\sum_{m_a>0} c_a^\dagger c_{\tilde{a}}^\dagger, \qquad \hat{S}_-(a)=\sum_{m_a>0} c_{\tilde{a}} c_a . \tag{2·2}$$

As in our previous papers,[2] we denote the intrinsic quasiparticle operators by $(\boldsymbol{a}_a^\dagger, \boldsymbol{a}_a)$, and the pairing boson operators by $(\boldsymbol{b}_a^\dagger, \boldsymbol{b}_a)$. Then, the nucleon operators $(c_a^\dagger, c_a)$ are expressed in the ideal boson-quasiparticle space[14] (constructed by these operators) as

$$c_a^\dagger = \boldsymbol{a}_a^\dagger \hat{u}_a + \hat{v}_a^\dagger \boldsymbol{a}_{\tilde{a}} , \tag{2·3}$$

$$\hat{u}_a=\sqrt{1-\frac{\hat{\boldsymbol{N}}_a}{\Omega_a-\hat{\boldsymbol{n}}_a}}, \qquad \hat{v}_a=\frac{\boldsymbol{b}_a}{\sqrt{\Omega_a-\hat{\boldsymbol{n}}_a}}, \tag{2·4}$$

$$\hat{\boldsymbol{n}}_a=\sum_{m_a}\boldsymbol{a}_a^\dagger \boldsymbol{a}_a, \quad \hat{\boldsymbol{N}}_a=\boldsymbol{b}_a^\dagger \boldsymbol{b}_a, \quad \Omega_a=j_a+\frac{1}{2}. \tag{2·5}$$

Inserting (2·3) into (2·1), we obtain the pairing Hamiltonian expressed in this space:

$$\begin{aligned}\boldsymbol{H}&=\boldsymbol{H}_0+\boldsymbol{H}_P\\ &=\sum_a \varepsilon_a(\hat{\boldsymbol{n}}_a+2\hat{\boldsymbol{N}}_a)-G\sum_{ab}\boldsymbol{b}_a^\dagger\sqrt{\Omega_a-\hat{\boldsymbol{n}}_a-\hat{\boldsymbol{N}}_a}\sqrt{\Omega_b-\hat{\boldsymbol{n}}_b-\hat{\boldsymbol{N}}_b}\,\boldsymbol{b}_b .\end{aligned} \tag{2·6}$$

2.2. *Number-angle operators*

Let us now introduce number-angle operators associated with individual shell-model orbits a

$$\hat{\Pi}_a=\frac{1}{2}\sum_{m_a} c_a^\dagger c_a=\boldsymbol{b}_a^\dagger \boldsymbol{b}_a+\frac{1}{2}\hat{\boldsymbol{n}}_a=\hat{\boldsymbol{N}}_a+\frac{1}{2}\hat{\boldsymbol{n}}_a , \tag{2·7}$$

$$\exp(i\hat{\Phi}_a)=\hat{S}_+(a)\frac{1}{\sqrt{\hat{S}_-(a)\hat{S}_+(a)}}=\boldsymbol{b}_a^\dagger\frac{1}{\sqrt{\boldsymbol{b}_a\boldsymbol{b}_a^\dagger}} , \tag{2·8}$$

which satisfy the commutation relations

$$[\hat{\Pi}_a, \exp(i\hat{\Phi}_a)]=[\hat{\boldsymbol{N}}_a, \exp(i\hat{\Phi}_a)]=\exp(i\hat{\Phi}_a) . \tag{2·9}$$

Note that the number operator of nucleon-pairs, $\hat{\Pi}_a$, is the sum of the number operator of pairing bosons $\hat{\boldsymbol{N}}_a$ and that of quasiparticle pairs $(1/2)\hat{\boldsymbol{n}}_a$, while $\exp(i\hat{\Phi}_a)$ depends only upon the pairing-boson degree of freedom.

In this number-angle representation, the pairing force in (2·6) is expressed as

$$\begin{aligned}\boldsymbol{H}_P=&-G\sum_{ab}\sqrt{\hat{\boldsymbol{N}}_a(\Omega_a+1-\hat{\boldsymbol{n}}_a-\hat{\boldsymbol{N}}_a)}\\ &\times\exp i(\hat{\Phi}_a-\hat{\Phi}_b)\cdot\sqrt{\boldsymbol{N}_b(\Omega_b+1-\hat{\boldsymbol{n}}_b-\boldsymbol{N}_b)} .\end{aligned} \tag{2·10}$$

Obviously, $\boldsymbol{H}_P$ depends only upon the relative angles $(\hat{\Phi}_a-\hat{\Phi}_b)$.

§ 3. $\Omega^{-1/2}$ expansion in a body-fixed frame

3.1. *Coherent-state representaion*

We assume that the pairing bosons form a condensate. Then, it is convenient to introduce a coherent state $|\mathrm{coh})$, and use new boson operators $\tilde{\boldsymbol{b}}_a$ defined by

$$\boldsymbol{b}_a = \sqrt{\Omega_a}\, v_a + \tilde{\boldsymbol{b}}_a \,. \tag{3·1}$$

Here the parameters v_a are defined by $\boldsymbol{b}_a|\mathrm{coh}) = \sqrt{\Omega_a}\, v_a|\mathrm{coh})$. Thus, we see that $\tilde{\boldsymbol{b}}_a|\mathrm{coh}) = 0$ for the bosons $\tilde{\boldsymbol{b}}_a$ which represent fluctuations of the deformed pair field. In this coherent-state representation,we have

$$\hat{\boldsymbol{N}}_a = \Omega_a v_a{}^2 + \tilde{\boldsymbol{N}}_a \,, \tag{3·2}$$

$$\tilde{\boldsymbol{N}}_a = \sqrt{\Omega_a}\, v_a(\tilde{\boldsymbol{b}}_a{}^\dagger + \tilde{\boldsymbol{b}}_a) + \tilde{\boldsymbol{b}}_a{}^\dagger \tilde{\boldsymbol{b}}_a \,. \tag{3·3}$$

Provided that the pairing-boson condensation generates a deformed pair potential, the angle operators $\hat{\Phi}_a$ can be well defined in terms of the following expansion:[11),2)]

$$\begin{aligned} i\hat{\Phi}_a &= \frac{1}{2}\left\{\ln\left(1+\frac{\tilde{\boldsymbol{b}}_a{}^\dagger}{\sqrt{\Omega_a}v_a}\right) - \ln\left(1+\frac{\tilde{\boldsymbol{b}}_a}{\sqrt{\Omega_a}v_a}\right)\right\} \\ &= \frac{1}{2\Omega_a^{1/2}v_a}(\tilde{\boldsymbol{b}}_a{}^\dagger - \tilde{\boldsymbol{b}}_a) - \frac{1}{4\Omega_a v_a{}^2}\{(\tilde{\boldsymbol{b}}_a{}^\dagger)^2 - (\tilde{\boldsymbol{b}}_a)^2\} \\ &\quad + \frac{1}{6\Omega_a^{3/2}v_a{}^3}\{(\tilde{\boldsymbol{b}}_a{}^\dagger)^3 - (\tilde{\boldsymbol{b}}_a)^3\} + \cdots . \end{aligned} \tag{3·4}$$

Note that this is an expansion in powers of the small parameter $\Omega_a{}^{-1/2}$, the leading order term being of $O(\Omega^{-1/2})$. In this expanded form, the angle operators $\hat{\Phi}_a$ satisfy the canonical commutaion relations

$$[\hat{\Phi}_a, \hat{\Pi}_b] = [\hat{\Phi}_a, \hat{\boldsymbol{N}}_b] = i\delta_{ab} \,. \tag{3·5}$$

3.2. *Use of the canonical transformation method with auxiliary variables*

The total number operators for the whole shell-model space are obviously given by

$$\hat{\Pi} = \sum_a \hat{\Pi}_a = \hat{\boldsymbol{N}} + \frac{1}{2}\hat{\boldsymbol{n}} \,, \tag{3·6}$$

$$\hat{\boldsymbol{N}} = \sum_a \hat{\boldsymbol{N}}_a, \qquad \hat{\boldsymbol{n}} = \sum_a \hat{\boldsymbol{n}}_a \,. \tag{3·7}$$

In the coherent-state representation,

$$\hat{\Pi} = \Pi_{\rm av} + \tilde{N} + \frac{1}{2}\hat{n}\ , \tag{3·8}$$

$$\Pi_{\rm av} = ({\rm coh}|\hat{\Pi}|{\rm coh}) = \sum_a \Omega_a v_a{}^2, \quad \tilde{N} = \sum_a \tilde{N}_a\ . \tag{3·9}$$

On the other hand, the total angle operator $\hat{\Phi}$ canonically conjugate to $\hat{\Pi}$ may be written as

$$\hat{\Phi} = \sum_a m_a \hat{\Phi}_a \quad \text{with} \quad \sum_a m_a = 1\ . \tag{3·10}$$

The above constraint on the (real) coefficients m_a comes from the kinematical condition $[\hat{\Phi}, \hat{\Pi}] = i$. Their values are explicitly determined through a dynamical consideration later in § 4.2.

Corresponding to $\hat{\Pi}$ and $\hat{\Phi}$ defined above let us introduce auxiliary variables $\mathring{\Pi}$ and $\mathring{\Phi}$ which satisfy $[\mathring{\Phi}, \mathring{\Pi}] = i$, and perform a canonical transformation[15]

$$U = U_1 U_2 U_1\ , \tag{3·11}$$

$$U_1 = \exp(i\mathring{\Phi}\hat{\Pi}), \qquad U_2 = \exp(-i\mathring{\Pi}\hat{\Phi}). \tag{3·12}$$

Then, we immediately see that

$$U\hat{\Pi}U^{-1} = \mathring{\Pi}, \qquad U\hat{\Phi}U^{-1} = \mathring{\Phi}, \tag{3·13}$$

$$U\hat{n}U^{-1} = \hat{n}, \qquad U\tilde{N}U^{-1} = \mathring{\Pi} - \frac{1}{2}\hat{n}\ . \tag{3·14}$$

Furthermore, we obtain

$$U\hat{N}_a U^{-1} = \hat{N}_a + m_a(\mathring{\Pi} - \hat{\Pi}), \tag{3·15}$$

$$U\hat{n}_a U^{-1} = \hat{n}_a\ , \tag{3·16}$$

$$U\hat{\Pi}_a U^{-1} = \hat{\Pi}_a + m_a(\mathring{\Pi} - \hat{\Pi}), \tag{3·17}$$

$$U\hat{\Phi}_a U^{-1} = \hat{\Phi}_a + (\mathring{\Phi} - \hat{\Phi}). \tag{3·18}$$

As was discussed in Ref. 15), the U-transformation implies an introduction of the body-fixed frame.

3.3. *Expansion in terms of* $\Omega^{-1/2}$

The realization of pairing deformation enables us to adopt an expansion in powers of $\Omega^{-1/2}$. For example, the angle oparator in (2·10) may be expanded as

$$\exp i(\hat{\Phi}_a - \hat{\Phi}_b) = 1 + i(\hat{\Phi}_a - \hat{\Phi}_b) - \frac{1}{2}(\hat{\Phi}_a - \hat{\Phi}_b)^2 + \cdots, \tag{3·19}$$

since $(\hat{\Phi}_a - \hat{\Phi}_b)$ are the quantities of $O(\Omega^{-1/2})$. In the same way, the square-root operators in (2·10) are expanded, after the U-transformation, as follows:

$$\sqrt{\{\hat{N}_a + m_a(\mathring{\Pi} - \tilde{\Pi})\}\{\Omega_a + 1 - \hat{n}_a - \hat{N}_a - m_a(\mathring{\Pi} - \tilde{\Pi})\}}$$

$$= \Omega_a u_a v_a + \frac{1}{2}(\mu_a \tilde{P}_a - \xi_a \tilde{n}_a + \eta_a)$$

$$- \frac{1}{8\Omega_a u_a v_a}(\xi_a \tilde{P}_a - \mu_a \tilde{n}_a - \eta_a)^2 + \cdots, \tag{3·20}$$

where

$$\tilde{P}_a \equiv 2(\tilde{\tilde{N}}_a + m_a \tilde{\Pi}) + \tilde{n}_a, \quad \tilde{\Pi} \equiv \mathring{\Pi} - \Pi_{\mathrm{av}}, \tag{3·21}$$

$$\tilde{\tilde{N}}_a \equiv \tilde{N}_a - m_a \tilde{N}, \quad \tilde{n}_a \equiv \hat{n}_a - m_a \hat{n}, \tag{3·22}$$

$$\xi_a = 1/2u_a v_a, \quad \mu_a = (u_a^2 - v_a^2)/2u_a v_a, \tag{3·23}$$

$$\eta_a = v_a/u_a, \quad u_a = \sqrt{1 - v_a^2}. \tag{3·24}$$

3.4. *Expanded Hamiltonian*

Let us apply the U-transformation to the pairing Hamiltonian with the chemical potential term $-2\lambda\hat{\Pi}$ added,

$$H' = H - 2\lambda\hat{\Pi}. \tag{3·25}$$

The term $-2\lambda\hat{\Pi}$ may be interpreted[7] as representing the pairing rotation-quasi-particle couplings *within the semi-classical approximation*. The semi-classical nature of such a "cranking model" treatment is removed by the U-transformation, because it introduces the body-fixed frame in a full quantum-mechanical way.[15]

Performing the $\Omega^{-1/2}$ expansion on $\mathcal{H}' = UH'U^{-1}$, obtained after the U-transformation, we have

$$\mathcal{H}' = W + \mathcal{H}_{\mathrm{danger}} + \mathcal{H}_{\mathrm{intri}} + \mathcal{H}_{\mathrm{pair}} + \mathcal{H}_{\mathrm{coupl.}} \tag{3·26}$$

The leading order terms of individual parts of r.h.s. are

$$W = 2\sum_a (\varepsilon_a - \lambda)\Omega_a v_a^2 - \Delta^2/G, \tag{3·27}$$

$$\mathcal{H}_{\mathrm{danger}} = \sum_a (\varepsilon_a - \lambda - \Delta \cdot \mu_a)(2\tilde{\tilde{N}}_a + 2m_a\tilde{\Pi} + \tilde{n}_a), \tag{3·28}$$

$$\mathcal{H}_{\mathrm{intri}} = \sum_a E_a \hat{n}_a, \tag{3·29}$$

$$\mathcal{H}_{\mathrm{pair}} = \frac{1}{2}G\sum_{ab}\Omega_a\Omega_b u_a v_a u_b v_b (\hat{\Phi}_a - \hat{\Phi}_b)^2$$

$$- G\{\sum_a \mu_a(\tilde{\tilde{N}}_a + m_a\tilde{\Pi})\}^2 + G\sum_a k_a(\tilde{\tilde{N}}_a + m_a\tilde{\Pi})^2, \tag{3·30}$$

$$\mathcal{H}_{\text{coupl}}=G\sum_a\mu_a(\tilde{\tilde{N}}_a+m_a\tilde{\Pi})\sum_b(\xi_b\tilde{n}_b-\mu_b\tilde{n}_b)$$
$$-G\sum_a k_a(\tilde{\tilde{N}}_a+m_a\tilde{\Pi})\{(u_a{}^2-v_a{}^2)\tilde{n}_a-\tilde{n}_a\}, \tag{3·31}$$

where

$$\Delta\equiv G\sum_a\Omega_a u_a v_a,\quad E_a\equiv\Delta/2u_a v_a, \tag{3·32}$$

$$k_a\equiv E_a/2G\Omega_a u_a{}^2 v_a{}^2\,. \tag{3·33}$$

If we define $G\Omega$ as order unity, the leading orders of individual parts are: $O(\Omega)$ for W, $O(\Omega^{1/2})$ for $\mathcal{H}_{\text{danger}}$, $O(1)$ for both $\mathcal{H}_{\text{intri}}$ and $\mathcal{H}_{\text{pair}}$, and $O(\Omega^{-1/2})$ for $\mathcal{H}_{\text{coupl}}$. Thus, we can determine the parameters v_a and the chemical potential λ as usual by putting $\mathcal{H}_{\text{danger}}=0$ and by requiring that the expectation value Π_{av} takes a specified value.

§ 4. Normal modes of pairing collective excitations

4.1. *Pairing vibrations*

The part $\mathcal{H}_{\text{pair}}$, (3·30), may be further decomposed into three parts:

$$\mathcal{H}_{\text{pair}}=\mathcal{H}_{\text{vib}}+\mathcal{H}_{\text{rot}}+\mathcal{H}_{\text{vib-rot}}\,, \tag{4·1}$$

$$\mathcal{H}_{\text{vib}}=\frac{1}{2}G\sum_{ab}\Omega_a\Omega_b u_a v_a u_b v_b(\tilde{\Phi}_a-\tilde{\Phi}_b)^2$$
$$-G(\sum_a\mu_a\tilde{\tilde{N}}_a)^2+G\sum_a k_a\tilde{\tilde{N}}_a{}^2\,, \tag{4·2}$$

$$\mathcal{H}_{\text{rot}}\doteq G(\sum_a m_a{}^2k_a-\mu^2)(\mathring{\Pi}-\Pi_{\text{av}})^2, \tag{4·3}$$

$$\mathcal{H}_{\text{vib-rot}}=2G(\mathring{\Pi}-\Pi_{\text{av}})\sum_a(m_a k_a-\mu\mu_a)\tilde{\tilde{N}}_a\,, \tag{4·4}$$

where $\mu\equiv\sum_a m_a\mu_a$. It is easy to find the normal modes $\Gamma_\nu{}^\dagger$ which diagonalize $\mathcal{H}_{\text{vib}}$. Let us write $\Gamma_\nu{}^\dagger$ as

$$\Gamma_\nu{}^\dagger=\sum_a(x_a{}^\nu\tilde{N}_a+iy_a{}^\nu\tilde{\Phi}_a). \tag{4·5}$$

Then, the requirements $[\Gamma_\nu,\Gamma_{\nu'}{}^\dagger]=\delta_{\nu\nu'}$ and $[\Gamma_\nu,\Gamma_{\nu'}]=0$ lead to the relations

$$\left.\begin{aligned}&\sum_a(x_a{}^\nu y_a{}^{\nu'}+y_a{}^\nu x_a{}^{\nu'})=\delta_{\nu\nu'}\,,\\&\sum_a(x_a{}^\nu y_a{}^{\nu'}-y_a{}^\nu x_a{}^{\nu'})=0\,.\end{aligned}\right\} \tag{4·6}$$

The equation of motion

$$[\mathcal{H}_{\text{vib}}, \Gamma_\nu^\dagger] = \omega_\nu \Gamma_\nu^\dagger \tag{4·7}$$

leads to the eigenvalue equation

$$\left.\begin{aligned} \omega_\nu X_a{}^\nu &= 2E_a Y_a{}^\nu - 4G\sum_b \sqrt{\Omega_a \Omega_b}\, u_a v_a u_b v_b \\ &\quad \times \{\tilde{\mu}_a \tilde{\mu}_b + m_a k_a + m_b k_b - \sum_c m_c{}^2 k_c\} Y_b{}^\nu , \\ \omega_\nu Y_a{}^\nu &= 2E_a X_a{}^\nu - G\sum_b \sqrt{\Omega_a \Omega_b}\, X_b{}^\nu . \end{aligned}\right\} \tag{4·8}$$

Here, $\tilde{\mu}_a \equiv \mu_a - \mu = \mu_a - \sum_b m_b \mu_b$ and

$$X_a{}^\nu \equiv 2\sqrt{\Omega_a}\, u_a v_a x_a{}^\nu , \qquad Y_a{}^\nu \equiv y_a{}^\nu / \sqrt{\Omega_a}\, u_a v_a . \tag{4·9}$$

The eigenvalue equation (4·8) differs from that of the conventional RPA[7] by the presence of terms depending on m's. This is because we are dealing with the Hamiltonian after the U-transformation.

We can easily solve (4·8) through the following dispersion equation:

$$\omega^2 \begin{vmatrix} \sum_a D_a(\omega) , & \sum_a \mu_a D_a(\omega) \\ \sum_a \mu_a D_a(\omega) , & \sum_a \mu_a{}^2 D_a(\omega) - (4\Delta)^{-1} \end{vmatrix} = 0 , \tag{4·10}$$

where

$$D_a(\omega) \equiv \frac{G\Omega_a u_a v_a}{(2E_a)^2 - \omega^2} . \tag{4·11}$$

We see that there always exists a zero-energy solution irrespective of the force-strength G (as long as $\Delta \neq 0$).

Let us investigate the properties of the $\omega = 0$ solution. Putting $\omega = 0$ in Eq. (4·8), we find that

$$x_a{}^{\nu=0} = \frac{1}{\sqrt{2}} \frac{1}{\Lambda} , \qquad y_a{}^{\nu=0} = \frac{1}{\sqrt{2}} \Lambda m_a \tag{4·12}$$

satisfy the relations (4·6). Here Λ is an arbitrary real number and the superscript $\nu = 0$ denotes the $\omega = 0$ solution. We thus obtain

$$\left.\begin{aligned} \Gamma_{\nu=0}^\dagger &= \frac{1}{\sqrt{2}} \left\{ \frac{1}{\Lambda} \tilde{N} + i\Lambda \tilde{\Phi} \right\}, \\ \Gamma_{\nu=0} &= \frac{1}{\sqrt{2}} \left\{ \frac{1}{\Lambda} \tilde{N} - i\Lambda \tilde{\Phi} \right\}, \end{aligned}\right\} \tag{4·13}$$

which clearly satisfy $[\Gamma_{\nu=0}, \Gamma_{\nu=0}^\dagger] = 1$. This fact is in clear contrast with the well-known result of the conventional RPA (in which the $\omega = 0$ mode cannot be normalized because their amplitudes diverge[4]). The reason why the finite values (4·12) are obtained in our case is that we have the additional m_a-dependent terms

in (4·8). Since these terms do not appear in the dispersion equation (4·10), they cannot affect the properties of the $\omega \neq 0$ modes. However, they do play a role of giving the finite amplitudes (4·12) for the $\omega = 0$ mode.

In terms of the normal modes satisfying Eq. (4·7), an arbitrary one-body operator O may be expanded as

$$O = \sum_{\nu} \{ [\Gamma_\nu, O] \Gamma_\nu^\dagger - [\Gamma_\nu^\dagger, O] \Gamma_\nu \} , \tag{4·14}$$

where the sum includes $\nu = 0$. For example, we have

$$\tilde{N}_a = \sum_{\nu \neq 0} y_a^\nu (\Gamma_\nu^\dagger + \Gamma_\nu) + m_a \tilde{N} , \tag{4·15}$$

$$i\tilde{\Phi}_a = \sum_{\nu \neq 0} x_a^\nu (\Gamma_\nu^\dagger - \Gamma_\nu) + i\tilde{\Phi} . \tag{4·16}$$

The above equations show that $\tilde{\tilde{N}}_a (\equiv \tilde{N}_a - m_a \tilde{N})$ and $i(\tilde{\Phi}_a - \tilde{\Phi}_b)$ are the quantities independent of the $\omega = 0$ mode, $\Gamma_{\nu=0}^\dagger$ and $\Gamma_{\nu=0}$.

4.2. *Separation of pairing rotation*

Now let us determine the coefficients m_a in the total angle operator $\tilde{\Phi}$ defined by (3·10). These values are determined by the dynamical consideration that the rotation-vibration couplings vanish to the order unity. Since $\sum_a \tilde{\tilde{N}}_a = 0$ by definition, the requirement, $\mathcal{H}_{\text{rot-vib}} = 0$, is equivalent to setting $m_a k_a - \mu \mu_a = \text{const} \equiv \varkappa$. Combining this relation with the constraint $\sum_a m_a = 1$, we can determine the constants $\varkappa$ and μ. The explicit expression of m_a obtained in this way is

$$m_a = (\varkappa + \mu \mu_a)/k_a \tag{4·17}$$

with

$$\varkappa = \frac{\sum_a k_a^{-1}}{(\sum_a k_a^{-1})^2 + (\sum_a \mu_a / k_a)^2} , \quad \mu = \frac{\sum_a \mu_a / k_a}{(\sum_a k_a^{-1})^2 + (\sum_a \mu_a / k_a)^2} . \tag{4·18}$$

If we expand the $\tilde{\Phi}$ thus determined in powers of $\Omega^{-1/2}$, we see that the leading order term coincides with the angle operator of the conventional RPA.[7),8)] Inserting (4·17) into $\mathcal{H}_{\text{rot}}$ in (4·1), we arrive at the expression

$$\mathcal{H}_{\text{pair}} = \sum_{\nu \neq 0} \omega_\nu (\Gamma_\nu^\dagger \Gamma_\nu + \frac{1}{2}) + \frac{1}{2\mathcal{J}} (\mathring{\Pi} - \Pi_{\text{av}})^2 , \tag{4·19}$$

$$2\mathcal{J} = (G\varkappa)^{-1} . \tag{4·20}$$

Note that the zero-energy mode $\Gamma_{\nu=0}^\dagger$ does not appear in this final expression. This is because it has already been replaced by the auxiliary variable $\mathring{\Pi} - \Pi_{\text{av}}$.

4.3. *Structure of the correlated ground state*

We first show it possible to construct the correlated ground state $|\Psi_0)$ satisfying the conditions

$$\Gamma_{\nu\neq 0}|\,\Psi_0)=0 \quad \text{and} \quad \tilde{N}|\,\Psi_0)=(\Pi-\Pi_{\rm av})|\,\Psi_0). \tag{4·21}$$

Here Π denotes a nucleon-pair number which may generally take a value different from $\Pi_{\rm av}(\equiv\sum_a \Omega_a v_a{}^2)$. If we write $|\,\Psi_0)$ as[4]

$$|\,\Psi_0)=\mathcal{N}\exp\Big(-\frac{1}{2}\sum_{\nu\neq 0}Q_\nu{}^2\Big)|P=0), \tag{4·22}$$

where

$$P_\nu=\frac{1}{\sqrt{2}}(\Gamma_\nu{}^+ + \Gamma_\nu), \quad iQ_\nu=\frac{1}{\sqrt{2}}(\Gamma_\nu{}^+ - \Gamma_\nu), \tag{4·23}$$

and $\mathcal{N}$ is a normalization constant, (4·21) reduces to the following conditions on the state $|P=0)$:

$$P_{\nu\neq 0}|P=0)=0 \quad \text{and} \quad \tilde{N}|P=0)=(\Pi-\Pi_{\rm av})|P=0). \tag{4·24}$$

By writing $|P=0)$ as

$$|P=0)=\exp(i\textstyle\sum_a \pi_a \hat{\Phi}_a)|0) \quad \text{with} \quad \boldsymbol{b}_a|0)=0\,, \tag{4·25}$$

we obtain from (4·24) the linear inhomogeneous equation

$$\sum_a x_a^{\nu\neq 0}\pi_a=\sum_a x_a^{\nu\neq 0}\Omega_a v_a{}^2 \quad \text{and} \quad \sum_a \pi_a=\Pi\,, \tag{4·26}$$

which uniquely determines the coefficients π_a.

We next perform the U-transformation on $|\,\Psi_0)$ thus obtained. Since this transformation does not affect the pairing vibrations with $\omega_\nu\neq 0$, i.e., $UQ_{\nu\neq 0}U^{-1}=Q_{\nu\neq 0}$, the exponential factor in (4·22) remains unchanged. On the other hand, $|P=0)$ given by (4·25) is transformed to

$$U|P=0)=\exp(i\Pi\mathring{\Phi})\exp\Big(i\sum_{\nu\neq 0}q_\nu Q_\nu\Big)|\mathring{0}) \tag{4·27}$$

with $q_\nu\equiv\sqrt{2}\sum_a \pi_a x_a{}^\nu$ and $|\mathring{0})\equiv U|0)$. In obtaining (4·27) we have used (4·16), (4·23) and (3·13). *Note that the rotational "wave function"* $\exp(i\Pi\mathring{\Phi})$ *has appeared after the U-transformation.* Thus, after the U-transformation, explicit structure of the correlated ground state becomes

$$|\,\mathring{\Psi}_0)\equiv U|\,\Psi_0)=\exp(i\Pi\mathring{\Phi})|\,\Psi_0^{\rm vib}),$$

$$|\,\Psi_0^{\rm vib})=\mathcal{N}\exp\Big(-\frac{1}{2}\sum_{\nu\neq 0}q_\nu{}^2\Big)\exp-\frac{1}{2}\sum_{\nu\neq 0}(Q_\nu-iq_\nu)^2\cdot|\mathring{0}). \tag{4·28}$$

In place of (4·21), $|\,\mathring{\Psi}_0)$ satisfies the conditions

$$\Gamma_{\nu\neq 0}|\,\mathring{\Psi}_0)=0 \quad \text{and} \quad \mathring{\Pi}|\,\mathring{\Psi}_0)=\Pi\,|\,\mathring{\Psi}_0). \tag{4·29}$$

Evidently, it also satisfies the supplementary condition $\mathring{\Phi}|\,\mathring{\Psi}_0)=0$. As was discussed in Ref. 2), all state vectors $|\,\mathring{\Psi})$ after the U-transformation generally satisfy the supplementary condition

$$\mathring{\Phi}|\,\mathring{\Psi})=0 \tag{4·30}$$

and thus compensate for the overcompleteness in the degree of freedom due to our introduction of the auxiliary variables, $\mathring{\Pi}$ and $\mathring{\Phi}$.

§ 5. Quasiparticle-collective couplings originating from pairing force

In terms of the pairing vibrational and rotational modes obtained in §4, the coupling Hamiltonian $\mathcal{H}_{\text{coupl}}$, (3·31), may be rewritten as

$$\mathcal{H}_{\text{coupl}}=\mathcal{H}_{\text{part-vib}}+\mathcal{H}_{\text{part-rot}}\,, \tag{5·1}$$

$$\begin{aligned}\mathcal{H}_{\text{part-vib}}=&2G\sum_{\nu\neq 0}\sum_{a}(k_a v_a{}^2 y_a{}^{\nu})(\Gamma_{\nu}{}^{\dagger}+\Gamma_{\nu})\hat{\boldsymbol{n}}_a\\&+G\sum_{\nu\neq 0}\sum_{a}\eta_a\Big(\sum_{b}\mu_b y_b{}^{\nu}\Big)(\Gamma_{\nu}{}^{\dagger}+\Gamma_{\nu})\hat{\boldsymbol{n}}_a\,,\end{aligned} \tag{5·2}$$

$$\begin{aligned}\mathcal{H}_{\text{part-rot}}=&-\frac{1}{\mathcal{J}}(\mathring{\Pi}-\Pi_{\text{av}})\Big(\frac{\hat{\boldsymbol{n}}}{2}\Big)+\frac{1}{\mathcal{J}}(\mathring{\Pi}-\Pi_{\text{av}})\sum_{a}\Big(v_a{}^2+\frac{\mu}{\chi}u_a v_a\Big)\hat{\boldsymbol{n}}_a\\=&-\frac{1}{\mathcal{J}}(\mathring{\Pi}-\Pi_{\text{av}})\sum_{a}(u_a{}^2-v_a{}^2)\Big(\frac{\hat{\boldsymbol{n}}_a}{2}\Big)\\&+\frac{1}{\mathcal{J}}(\mathring{\Pi}-\Pi_{\text{av}})\frac{\mu}{\chi}\sum_{a}(2u_a v_a)\Big(\frac{\hat{\boldsymbol{n}}_a}{2}\Big).\end{aligned} \tag{5·3}$$

The term $\mathcal{H}_{\text{part-vib}}$ represents the pairing vibration-quasiparticle couplings, while $\mathcal{H}_{\text{part-rot}}$ represents the pairing rotation-quasiparticle couplings. The latter coupling exhibits a very interesting property: The second term in (5·3) has a structure which exactly cancels out the first term for the special case of single j-shell, and causes $\mathcal{H}_{\text{part-rot}}$ to vanish.

With the concept of pairing rotation-quasiparticle couplings, we can describe a nucleus whose nucleon-pair number Π (an eigenvalue of $\mathring{\Pi}$) is different from Π_{av}: Namely, by keeping the values of parameters v_a and λ (characterizing the intrinsic quasiparticle modes) *fixed* at the specified value Π_{av}, one may evaluate $\mathcal{H}=\mathcal{H}'+2\lambda\Pi$ to get the true energy of the nucleus whose nucleon-pair number is Π ($\neq\Pi_{\text{av}}$). Of course, $\mathcal{H}_{\text{part-rot}}$ vanishes if we choose Π_{av} so as to just coincide with Π. Even in this case, however, the effects of pairing rotational modes on the quasi-

particle excitation still remain: If we explicitly write down the intrinsic Hamiltonian $\mathcal{H}_{\text{intri}}$, (3·29), including the next order, $O(\Omega^{-1})$, we have

$$\mathcal{H}_{\text{intri}}=\sum_a E_a\hat{\boldsymbol{n}}_a+\frac{1}{2\mathcal{I}}\left(\frac{\hat{\boldsymbol{n}}}{2}\right)^2-\frac{1}{\mathcal{I}}\left(\frac{\hat{\boldsymbol{n}}}{2}\right)\sum_a\left(v_a{}^2+\frac{\mu}{\chi}u_av_a\right)\hat{\boldsymbol{n}}_a$$

$$+G\sum_a k_av_a{}^4\hat{\boldsymbol{n}}_a{}^2-\frac{1}{4}G(\sum_a\eta_a\hat{\boldsymbol{n}}_a)^2$$

$$+\frac{1}{2}G(\sum_b\xi_b)\sum_a\xi_a\hat{\boldsymbol{n}}_a-\frac{1}{2}G\sum_a k_a(u_a{}^2-v_a{}^2)^2\hat{\boldsymbol{n}}_a\ . \tag{5·4}$$

In this expression, the terms depending on $\hat{\boldsymbol{n}}_a{}^2$ or $\hat{\boldsymbol{n}}_a\cdot\hat{\boldsymbol{n}}_b$ may be interpreted as a kind of recoil effect (due to the pairing rotation), although an analogy to the well-known recoil term of the particle-rotor model does not hold perfectly. The importance of these terms may be seen most clearly by considering (5·4) in the single j-shell case: With the above $\mathcal{H}_{\text{intri}}$ and with inclusion of the Hartree contribution of the pairing force, the eigenvalue of the pairing Hamiltonian becomes

$$E=E'+2\lambda\Pi$$

$$=2\left(\varepsilon-\lambda-\frac{1}{2}G\right)\Omega v^2-\Delta^2/G$$

$$+G(\Omega+1)\left(\frac{\boldsymbol{n}}{2}\right)-G\left(\frac{\boldsymbol{n}}{2}\right)^2+G(\Pi-\Pi_{\text{av}})^2+2\lambda\Pi\ . \tag{5·5}$$

Comparing this expression (after eliminating λ which is determined by the conditions $\mathcal{H}_{\text{danger}}=0$ and $\Pi_{\text{av}}=\Omega v^2$) with the exact solution,

$$E_{\text{exact}}=2\varepsilon\Pi-G\Pi(\Omega-\Pi+1)+G\left(\frac{\boldsymbol{n}}{2}\right)\left\{\Omega-\left(\frac{\boldsymbol{n}}{2}\right)+1\right\}, \tag{5·6}$$

we see that the two are in perfect agreement irrespective of the value of Π_{av} chosen.*) Obviously, the $\hat{\boldsymbol{n}}^2$ term plays an indispensable role in bringing about this agreement, which indicates that the nucleon-number conservation law is recovered.

§ 6. Quadrupole force

Let us proceed to investigate the mode-mode couplings originating from the quadrupole force

$$H_{\text{QQ}}=-\frac{1}{2}\chi\sum_M Q_M{}^\dagger Q_M\ , \tag{6·1}$$

*) A special choice, $\Pi_{\text{av}}=\Pi$, was adopted in Ref. 2).

$$Q_M=\sum_{\alpha\beta}\langle\alpha|r^2\,Y_{2M}|\beta\rangle c_\alpha^\dagger c_\beta\,. \tag{6·2}$$

The mass-quadrupole operator Q_M may be expressed in the ideal boson-quasiparticle space as

$$Q_M=\frac{1}{\sqrt{2}}\sum_{ab}\{\boldsymbol{A}_{2M}^\dagger(ab)\hat{Q}(ab)+\text{h. conj.}\}+\sum_{ab}\boldsymbol{B}_{2M}^\dagger(ab)\hat{R}(ab), \tag{6·3}$$

where

$$\boldsymbol{A}_{2M}^\dagger(ab)\equiv\frac{1}{\sqrt{2}}\sum_{m_\alpha m_\beta}\langle j_\alpha m_\alpha j_b m_\beta|2M\rangle\boldsymbol{a}_\alpha^\dagger\boldsymbol{a}_\beta^\dagger\,, \tag{6·4}$$

$$\boldsymbol{B}_{2M}^\dagger(ab)\equiv-\sum_{m_\alpha m_\beta}\langle j_\alpha m_\alpha j_b m_\beta|2M\rangle\boldsymbol{a}_\alpha^\dagger\boldsymbol{a}_{\bar\beta}\,, \tag{6·5}$$

$$\hat{Q}(ab)\equiv q(ab)(\hat{u}_\alpha\hat{v}_b+\hat{u}_b\hat{v}_\alpha), \tag{6·6}$$

$$\hat{R}(ab)\equiv q(ab)(\hat{u}_b^\dagger\hat{u}_\alpha-\hat{v}_b^\dagger v_\alpha) \tag{6·7}$$

and $q(ab)\equiv\langle a\|r^2\,Y_2\|b\rangle/\sqrt{5}$. To remove unnecessary complication, we have dropped in (6·3) the contraction terms resulting from the non-commutability between $(\boldsymbol{a}_\alpha^\dagger,\boldsymbol{a}_\alpha)$ and $(\hat{u}_\alpha,\hat{v}_\alpha)$.

We follow the same procedure as in the previous sections, i.e., 1) use the coherent-state representation, 2) perform the U-transformation, 3) expand in powers of the small parameter $\Omega^{-1/2}$, and 4) express the pairing degrees of freedom in terms of the normal modes defined in § 4. By this procedure, the quadrupole operator is transformed into the following form:

$$\mathcal{Q}_M\equiv U\boldsymbol{Q}_M U^{-1}=\mathcal{Q}_M^{(\text{intri})}+\mathcal{Q}_M^{(\text{coupl})}, \tag{6·8}$$

$$\begin{aligned}\mathcal{Q}_M^{(\text{intri})}=&\sum_{ab}\{Q(ab)\boldsymbol{A}_{2M}^{(+)}(ab)+R(ab)\boldsymbol{B}_{2M}^\dagger(ab)\}\\&+\frac{1}{2}\sum_{ab}\{\hat{\boldsymbol{n}}(ab)-M(ab)\hat{\boldsymbol{n}}\}\{R(ab)\boldsymbol{A}_{2M}^{(+)}(ab)-Q(ab)\boldsymbol{B}_{2M}^\dagger(ab)\},\end{aligned} \tag{6·9}$$

$$\mathcal{Q}_M^{(\text{coupl})}=\mathcal{Q}_M^{(\text{part-vib})}+\mathcal{Q}_M^{(\text{part-rot})}\,, \tag{6·10}$$

$$\begin{aligned}\mathcal{Q}_M^{(\text{part-vib})}=&\sum_{\nu\neq0}\sum_{ab}Y_\nu(ab)(\Gamma_\nu^\dagger+\Gamma_\nu)\{R(ab)\boldsymbol{A}_{2M}^{(+)}(ab)-Q(ab)\boldsymbol{B}_{2M}^\dagger(ab)\}\\&-\sum_{\nu\neq0}\sum_{ab}q(ab)(u_a v_b x_b^\nu+u_b v_a x_a^\nu)(\Gamma_\nu^\dagger-\Gamma_\nu)\boldsymbol{A}_{2M}^{(-)}(ab)\\&+\sum_{\nu\neq0}\sum_{ab}q(ab)v_a v_b(x_a^\nu-x_b^\nu)(\Gamma_\nu^\dagger-\Gamma_\nu)\boldsymbol{B}_{2M}^\dagger(ab),\end{aligned} \tag{6·11}$$

$$\mathcal{Q}_M^{(\text{part-rot})}=(\mathring{\Pi}-\Pi_{\text{av}})\sum_{ab}M(ab)\{R(ab)\boldsymbol{A}_{2M}^{(+)}(ab)-Q(ab)\boldsymbol{B}_{2M}^\dagger(ab)\}, \tag{6·12}$$

where terms higher than the order $1/\Omega$ are neglected. Here, $Q(ab)$ and $R(ab)$

are the quantities obtained by replacing the operators $\hat{u}_a$ and $\hat{v}_a$ in $\hat{Q}(ab)$ and $\hat{R}(ab)$ with the corresponding c-numbers u_a and v_a. Also, the following notations are used:

$$A^{(\pm)}_{2M}(ab)\equiv\frac{1}{\sqrt{2}}\{\exp(-i\hat{\Phi})A^{\dagger}_{2M}(ab)\pm A_{2\widetilde{M}}(ab)\exp(i\hat{\Phi})\}, \tag{6·13}$$

$$\hat{\boldsymbol{n}}(ab)\equiv\eta_a\hat{\boldsymbol{n}}_a/\Omega_a+\eta_b\hat{\boldsymbol{n}}_b/\Omega_b\ , \tag{6·14}$$

$$M(ab)\equiv\xi_a m_a/\Omega+\xi_b m_b/\Omega_b\ , \tag{6·15}$$

$$Y_\nu(ab)\equiv\xi_a y_a{}^\nu/\Omega_a+\xi_b y_b{}^\nu/\Omega_b\ . \tag{6·16}$$

In practice, the angle operator $\exp(i\hat{\Phi})$ in (6·13) can be dropped, because of the supplementary condition (4·30). The obtained expression (6·8) may be directly used for calculating $E2$-transitions and $E2$-moments. Furthermore, it immediately leads us to an expression of the quadrupole force in a mode-mode coupling form. The result is given in the Appendix.

§ 7. Concluding remarks

Starting with the many-j shell model with P+QQ force, we have derived microscopic expressions for the pairing rotation-quasiparticle couplings as well as for the pairing vibration-quasiparticle couplings. The expressions obtained in this paper are useful irrespective of models which may be later introduced to treat the intrinsic quasiparticle excitations. In practice, we plan to combine the present result with the many-phonon approaches developed in Refs. 16)~20) in order to describe quadrupole collective motions. If we introduce the phonon operator $X^{\dagger}_{2M}$,

$$X^{\dagger}_{2M}=\sum_{ab}\psi(ab)A^{\dagger}_{2M}(ab), \tag{7·1}$$

as a building block of the quadrupole collective subspace *in the intrinsic space*,[20] the intrinsic space may be truncated as

$$\{\boldsymbol{a}_\alpha{}^\dagger\boldsymbol{a}_\beta{}^\dagger\cdots\boldsymbol{a}_\delta{}^\dagger|0\rangle\}\longrightarrow\left\{\frac{1}{n!}(X^\dagger)^n_{\lambda M}|0\rangle\right\}. \tag{7·2}$$

Any matrix element of the quasiparticle operators within this quadrupole collective subspace may be easily calculated by using the method of Refs. 18) and 19). After this is done, we finally obtain a mode-mode coupling Hamiltonian of the following form:

$$\mathcal{H}=\mathcal{H}_{\rm quad}(X^\dagger, X)+\mathcal{H}_{\rm pair}(\Gamma^\dagger, \Gamma, \overset{\circ}{H})+\mathcal{H}_{\rm coupl}(X^\dagger, X, \Gamma^\dagger, \Gamma, \overset{\circ}{H}). \tag{7·3}$$

The basis vectors of the corresponding model space are

$$|\text{quadrupole}\rangle\otimes|\text{pairing}\rangle$$

$$=\frac{1}{\sqrt{n!}}(X^{\dagger})^{n}_{\alpha JM}|0\rangle\otimes\exp(i\Pi\mathring{\Phi})\prod_{\nu\neq 0}\frac{1}{\sqrt{n_{\nu}!}}(\Gamma_{\nu}^{\dagger})^{n_{\nu}}|\Psi_{0}^{\text{vib}}). \tag{7·4}$$

With the aid of this collective model space, it becomes feasible to analyse the dynamical interplay of pairing and quadrupole modes in a visual and systematic way.

Evidently, there is no difficulty to extend the quadrupole collective subspace in (7·2) into a form suitable for odd-A nuclei. It is also quite possible to include the quasiparticle pairs coupled to angular momenta $J\geq 4$ in the quadrupole collective subspace.[21]

After the completion of this work, we learned that expressions similar to ours for the pairing collective-quasiparticle couplings were derived[22] by Kishimoto. It is interesting to compare our result with his result in the future.

Acknowledgements

We are grateful to Professor M. Yamamura and Professor T. Kishimoto for valuable disscussions. One of us (T. S.)would like to thank Professor Speth for his warm hospitality at the Institut für Kernphysik, Kernforschungsanlage Jülich. Our thanks are also due to Mr. S. Karpa for his advice on English expression of the original manuscript.

Appendix

The quadrupole force (6·1) is represented in the following form explicitly showing the mode-mode coupling of interest:

$$\mathcal{H}_{QQ}\equiv U\boldsymbol{H}_{QQ}U^{-1}=\mathcal{H}^{QQ}_{\text{intri}}+\mathcal{H}^{QQ}_{\text{coupl}}, \tag{A·1}$$

$$\begin{aligned}\mathcal{H}^{QQ}_{\text{intri}}=&-\frac{1}{4}\chi\sum\{Q(ab)Q(cd)+R(ab)Q(cd)(\hat{\boldsymbol{n}}(ab)-M(ab)\hat{\boldsymbol{n}})\}\\&\times\boldsymbol{A}^{(+)}_{2M}(ab)\boldsymbol{A}^{(+)}_{2\widehat{M}}(cd)\\&-\frac{1}{2}\chi\sum\Big\{Q(ab)R(cd)-\frac{1}{2}Q(ab)Q(cd)(\hat{\boldsymbol{n}}(cd)-M(cd)\hat{\boldsymbol{n}})\\&+\frac{1}{2}R(ab)R(cd)(\hat{\boldsymbol{n}}(ab)-M(ab)\hat{\boldsymbol{n}})\Big\}\boldsymbol{A}^{(+)}_{2M}(ab)\boldsymbol{B}_{2M}(cd)\\&+\text{h. conj. of the above terms,}\end{aligned} \tag{A·2}$$

$$\mathcal{H}^{QQ}_{\text{coupl}}=\mathcal{H}^{QQ}_{\text{part-vib}}+\mathcal{H}^{QQ}_{\text{part-rot}}, \tag{A·3}$$

$$\mathcal{H}^{QQ}_{\text{part-vib}} = -\frac{1}{2}\chi\sum Q(ab)R(cd)\,Y_\nu(cd)(\Gamma_\nu^\dagger+\Gamma_\nu)\boldsymbol{A}^{(+)}_{2M}(ab)\boldsymbol{A}^{(+)}_{2M}(cd)$$

$$+\frac{1}{2}\chi\sum\{Q(ab)Q(cd)\,Y_\nu(cd)-R(ab)R(cd)\,Y_\nu(ab)\}$$

$$\times(\Gamma_\nu^\dagger+\Gamma_\nu)\boldsymbol{A}^{(+)}_{2M}(ab)\boldsymbol{B}_{2M}(cd)$$

$$+\frac{1}{2}\chi\sum Q(ab)q(cd)(u_cv_dx_d{}^\nu+u_dv_cx_c{}^\nu)(\Gamma_\nu^\dagger-\Gamma_\nu)\boldsymbol{A}^{(+)}_{2M}(ab)\boldsymbol{A}^{(-)}_{2M}(cd)$$

$$+\frac{1}{2}\chi\sum Q(ab)q(cd)v_cv_d(x_c{}^\nu-x_d{}^\nu)(\Gamma_\nu^\dagger-\Gamma_\nu)\boldsymbol{A}^{(+)}_{2M}(ab)\boldsymbol{B}_{2M}(cd)$$

$$+\frac{1}{2}\chi\sum q(ab)(u_av_bx_b{}^\nu+u_bv_ax_a{}^\nu)R(cd)(\Gamma_\nu^\dagger-\Gamma_\nu)\boldsymbol{A}^{(-)}_{2M}(ab)\boldsymbol{B}_{2M}(cd)$$

$$+\text{h. conj. of the above terms,} \qquad (A\cdot4)$$

$$\mathcal{H}^{QQ}_{\text{part-rot}} = -\frac{1}{2}\chi(\overset{\circ}{\Pi}-\Pi_{\text{av}})\sum Q(ab)R(cd)M(cd)\boldsymbol{A}^{(+)}_{2M}(ab)\boldsymbol{A}^{(+)}_{2M}(cd)$$

$$+\frac{1}{2}\chi(\overset{\circ}{\Pi}-\Pi_{\text{av}})\sum\{Q(ab)Q(cd)M(cd)-R(ab)R(cd)M(ab)\}$$

$$\times\boldsymbol{A}^{(+)}_{2M}(ab)\boldsymbol{B}_{2M}(cd)+\text{h. conj. of the above terms.} \qquad (A\cdot5)$$

In the above expressions, we have neglected, 1) the terms higher than $O(1/\Omega)$, and 2) the recoupling terms containing the operators $\boldsymbol{B}^\dagger_{2M}(ab)\boldsymbol{B}_{2M}(cd)$.

References

1) F. Sakata, S. Iwasaki, T. Marumori and K. Takada, Z. Phys. **A286** (1978), 195; Prog. Theor. Phys. **56** (1976), 1140; *Proc. Int. Conf. Nuclear Structure, Tokyo, 1977* [J. Phys. Soc. Japan **44** (1978), Suppl.], p. 520.
2) T. Suzuki, M. Fuyuki and K. Matsuyanagi, Prog. Theor. Phys. **61** (1979), 1682; **62** (1979), 690.
3) A. Bohr and B. R. Mottelson, *Nuclear Structure*, vol. II (Benjamin, 1975).
4) E. R. Marshalek and J. Weneser, Ann. of Phys. **53** (1969), 569.
5) A. Kuriyama, T. Marumori, K. Matsuyanagi, F. Sakata and T. Suzuki, Prog. Theor. Phys. Suppl. No. 58 (1975), 9.
6) A. Bohr, *Nuclear Structure*: *Dubna Symposium 1968* (International Atomic Energy Agency, Vienna, 1969), p. 179.
7) D. R. Bès and R. A. Broglia, *Proceedings of the International School of Physics, "Enrico Fermi"*, course LXIX (1977), p. 55.
8) R. Beck, M. Kleber and H. Schmidt, Z. Phys. **250** (1972), 155.
9) S. T. Belyaev and V. G. Zelevinsky, Yadern Fiz. **16** (1972), 1195; Soviet J. Nucl. Phys. **16** (1973), 657.
10) R. V. Jolos, V. G. Kartavenko and V. Rybarska, Teor. Mat. Fiz. **20** (1974), 353; Theor. Math. Phys. **20** (1975), 873.
11) V. Alessandrini, D. R. Bès and B. Machet, Nucl. Phys. **B142** (1978), 489.
12) Y. Miyanishi and G. Watanuki, Prog. Theor. Phys. **63** (1980), 329.
13) D. R. Bès and R. A. Sorensen, *The Pairing-Plus-Quadrupole Model, Advances in Nuclear Physics* (Plenum Press), vol. 2 (1969), p. 129.

14) T. Suzuki and K. Matsuyanagi, Prog. Theor. Phys. **56** (1976), 1156.
15) S. Hayakawa and T. Marumori, Prog. Theor. Phys. **18** (1957), 396, and references therein.
16) S. Iwasaki, T. Marumori, F. Sakata and K. Takada, Prog. Theor. Phys. **56** (1976), 846.
17) S. G. Lie and G. Holzwarth, Phys. Rev. **C12** (1975), 1035.
18) G. Holzwarth, D. Janssen and R. V. Jolos, Nucl. Phys. **A261** (1976), 1.
19) S. Iwasaki, F. Sakata and K. Takada, Prog. Theor. Phys. **57** (1977), 1289.
20) T. Suzuki, M.Fuyuki and K. Matsuyanagi, Prog. Theor. Phys. **61** (1979), 1082.
21) M. Fuyuki, Prog. Theor. Phys. **64** (1980), 1470.
22) T. Kishimoto, private communication.

Progress of Theoretical Physics, Vol. 67, No. 5, May 1982

Attenuation Factors for $B(E2)$ in the Microscopic Description of Multiphonon States

— *A Simple Model Analysis* —

Kenichi MATSUYANAGI

Department of Physics, Kyoto University, Kyoto 606

(Received July 13, 1981)

With an exactly solvable $O(4)$ model of Piepenbring, Silvestre-Brac and Szymanski, we demonstrate that the attenuation factor for the $B(E2)$ values, derived by the lowest-order approximation of the multiphonon method, takes excellent care of the kinematical anharmonicity effects, if multiphonon states are defined in the intrinsic subspace orthogonal to the pairing rotation. It is also shown that the other attenuation effect characterizing the interacting boson model is not a dominant effect in the model analysed here.

§ 1. Introduction

An important characteristic of the $SU(6)$ phonon model of Janssen, Jolos and Dönau[1] is that it introduces an attenuation factor of the form $\sqrt{1-Cn_d}$. Here n_d is the number of the quadrupole phonons and C is a constant. This attenuation factor results from the Pauli principle between the constituent quasiparticles of the quadrupole phonon modes, and has been expected to represent the major part of the kinematical anharmonicity effects associated with multiphonon excitations in even-even nuclei.

Holzwarth et al.[2] and Iwasaki et al.[3] have shown that this factor is obtainable as the lowest-order approximation of a new microscopic method for describing the multiphonon states, referred to as the multiphonon method (MPM).[2)~4)] These works have made it possible to relate the phenomenological constant C to the microscopic quantities characterizing the Pauli principle effects on the two-phonon states.

There is another attenuation factor $\sqrt{1-n_d/n_B}$ characterizing the interacting boson model (IBM) of Arima and Iachello.[5] This factor stems from the explicit treatment of s-bosons and arises through the equality $\sqrt{n_s}=\sqrt{n_B-n_d}$. Here n_s denotes the number of the $J=0$-coupled nucleon pairs, and n_B is regarded as the total number of nucleon pairs in the spherical valence shell. Although this factor plays a similar role to that of Janssen et al.[1] and hence indistinguishable in the phenomenological level, their microscopic origins are to be interpreted[6),7)] in distinctively different ways to each other.

The main purpose of this paper is to make a critical analysis of the assumptions on the basis of which the above-mentioned attenuation factors are extracted

from among the complicated anharmonicity effects. For this aim, we study an exactly solvable model with $O(4)$ symmetry, which Piepenbring, Silvestre-Brac and Szymanski[8] developed to describe the $K^\pi=0^+$ excitations in deformed nuclei. As they pointed out, this model well simulates the pairing plus quadrupole-quadrupole ($P+QQ$) force model and thus one can expect that the essential points of the analysis based on the $O(4)$ model are kept valid even for more realistic cases. They have extensively studied this model in order to test the accuracy of the MPM. In their work, however, the spurious states due to the nucleon-number fluctuations in the quasiparticle representation are not removed from their collective model space. It will become evident in this paper that the deviations of their numerical results[8] from the exact solutions are entirely due to this shortcoming.

In § 2, the $O(4)$ model is described. In § 3, we first perform a mapping of the nucleon state space into the "ideal boson-quasiparticle space." We then apply the multiphonon method to the intrinsic subspace*) in the ideal space, which is orthogonal to the monopole pair degree of freedom.[12),13)] This two-step approach has been developed[14)~16)] in order to systematically study the competition between the pairing and quadrupole modes of excitations in transitional nuclei. In § 4, we present numerical examples, which will clearly exhibit the quality of approximations currently used to treat the kinematical anharmonicity effects.

We should remark that the analysis in terms of a solvable model (i.e., a model completely characterized by a closed algebra) leaves the dynamical questions (which inevitably arise in realistic cases)[9),10)] untouched; e.g., whether the essential effect of nuclear deformation is describable after the truncation to some specific nucleon pairs (such as $J=0$ and 2 pairs or $A^\dagger$ and $B^\dagger$ pairs in the $O(4)$ model discussed hereon). An answer to this question has been recently discussed by Bohr and Mottelson.[11)]

§ 2. The $O(4)$ model

Let us consider the j^N configuration and define the nucleon operators in the following way:

$$A^\dagger=\sum_{m>0} c_m^\dagger c_{\tilde{m}}^\dagger \ , \qquad B^\dagger=\sum_{m>0} \sigma_m c_m^\dagger c_{\tilde{m}}^\dagger \ , \tag{2·1a}$$

$$N=\sum_m c_m^\dagger c_m \ , \qquad Q=\sum_m \sigma_m c_m^\dagger c_m \ , \tag{2·1b}$$

$$\sigma_m=\begin{cases}+1 & \text{for } |m|<\Omega/2 \ , \\ -1 & \text{for } |m|>\Omega/2 \ , \end{cases} \qquad \Omega=j+1/2 \ , \tag{2·1c}$$

where $c_{\tilde{m}}$ denotes the time-reverse of c_m, i.e., $(-)^{j-m}c_{-m}$. We consider the case

*) The term "intrinsic" is used because it is orthogonal to the pairing rotation.[15)]

that Ω=even. These pair operators constitute the Lie algebra for $O(4)$:

$$[A, A^\dagger]=\Omega-N\,, \qquad [B, B^\dagger]=\Omega-N\,, \tag{2·2a}$$

$$[N, A^\dagger]=2A^\dagger\,, \qquad [N, B^\dagger]=2B^\dagger\,, \tag{2·2b}$$

$$[Q, A^\dagger]=2B^\dagger\,, \qquad [Q, B^\dagger]=2A^\dagger\,, \tag{2·2c}$$

$$[A, B^\dagger]=-Q\,, \qquad [N, Q]=0\,. \tag{2·2d}$$

As is well known in the group theory for the hydrogen atom,[17] $O(4)$ is isomorphic to $SU(2)\otimes SU(2)$: The operators $\boldsymbol{K}$ and $\boldsymbol{L}$ defined by[8]

$$K_+=\frac{1}{2}(A^\dagger+B^\dagger), \qquad L_+=\frac{1}{2}(A^\dagger-B^\dagger), \tag{2·3a}$$

$$K_-=\frac{1}{2}(A+B), \qquad L_-=\frac{1}{2}(A-B), \tag{2·3b}$$

$$K_0=\frac{1}{4}(N+Q-\Omega), \qquad L_0=\frac{1}{4}(N-Q-\Omega) \tag{2·3c}$$

separately satisfy the commutation relations of $SU(2)$

$$[K_+, K_-]=2K_0\,, \qquad [L_+, L_-]=2L_0\,, \tag{2·4a}$$

$$[K_0, K_\pm]=\pm K_\pm\,, \qquad [L_0, L_\pm]=\pm L_\pm\,, \tag{2·4b}$$

$$[K_-, L_+]=0\,. \tag{2·4c}$$

Let us introduce the Hamiltonian

$$H=-GA^\dagger A-\frac{1}{2}\chi Q^\dagger Q\,, \tag{2·5}$$

which consists of the monopole pairing force and the quadrupole-like force. Though the Q is not a usual quadrupole operator (in fact, a mixed-multipole one), we will call it "quadrupole" operator from now on because the quantity σ_m simulates the properties of $\langle jm|Y_{20}|jm\rangle$. Likewise, we use the term "$E2$"-transitions for those caused by the present Q operator of Eq. (2·1b).

If the pairing is a dominant correlation, one can start the discussion with the BCS state

$$|\phi(\alpha)\rangle=e^{\alpha(A^\dagger-A)}|0\rangle\,. \tag{2·6}$$

With increasing "quadrupole" correlation, the structure of the Hartree-Bogoliubov vacuum may change into

$$\begin{aligned}|\phi(\alpha,\beta)\rangle&=e^{\beta(B^\dagger-B)}|\phi(\alpha)\rangle\\&=e^{(\alpha A^\dagger+\beta B^\dagger)-\text{h.c.}}|0\rangle\,.\end{aligned} \tag{2·7}$$

The parameters α and β characterize the pairing and "quadrupole" deformations of the system, respectively. The potential energy function is obtained as

$$\begin{aligned} V(\alpha,\beta) &= \langle\phi(\alpha,\beta)|H-\lambda N|\phi(\alpha,\beta)\rangle \\ &= -G\Omega^2u^2v^2+(G-2\chi)\Omega^2u^2v^2(\sin 2\beta)^2-\lambda\{2\Omega v^2+2\Omega(u^2-v^2)\sin^2\beta\} \end{aligned} \tag{2·8}$$

in the leading-order approximation with respect to Ω^{-1}. Here $u=\cos\alpha$ and $v=\sin\alpha$. If we neglect the variation of the chemical potential λ due to the "quadrupole" deformation, which is the same approximation as in the conventional quasiparticle RPA, we find that the structural change of the vacuum into the form (2·7) occurs when the interaction strengths G and χ satisfy the relation $8\chi u^2v^2>G$. The equilibrium deformation β is given by

$$\sin^2\beta=\frac{8u^2v^2\chi-G}{8u^2v^2(2\chi-G)}, \tag{2·9}$$

which implies that $\beta=\pm\pi/4$ for $N=\Omega$ where $u^2=v^2=1/2$. Namely, the condensate of monopole pairs $A^\dagger$ changes its structure toward that of K_+ or L_+ with increasing strength of the "quadrupole" force. The structure of $|\phi(\alpha,\beta)\rangle$ simulates the well-known deformed BCS state: For positive (negative) β, we have a condensate of $K_+(L_+)$ which corresponds to the prolate (oblate) deformation. Thus, the $SU(2)\otimes SU(2)$ picture[8] is appropriate for the "quadrupole" dominant phase, while the $O(4)$ picture is suitable for the pairing dominant phase.

§ 3. Boson representation of the $O(4)$ model

3.1. *Mapping into the "ideal boson-quasiparticle space"*

The nucleon state space spanned by the non-orthogonal vectors $(A^\dagger)^{n_1}(B^\dagger)^{n_2}|0\rangle$ can be mapped into the "ideal boson-quasiparticle space"[18] which is a direct product space of the pairing boson space $\{(b^\dagger)^{n_1}|0)\}$ and the intrinsic quasiparticle space $\{(\boldsymbol{B}^\dagger)^{n_2}|0\rangle\}$:

$$\{(A^\dagger)^{n_1}(B^\dagger)^{n_2}|0\rangle\}\longrightarrow\{(b^\dagger)^{n_1}|0)\otimes(\boldsymbol{B}^\dagger)^{n_2}|0\rangle\}. \tag{3·1}$$

The nucleon-pair operators are transcribed into the ideal space as[18]

$$A^\dagger\longrightarrow b^\dagger\sqrt{\Omega-\hat{\boldsymbol{n}}-b^\dagger b}\,, \tag{3·2a}$$

$$B^\dagger=\boldsymbol{B}^\dagger\hat{u}\hat{u}'-\hat{v}^\dagger\hat{v}'^\dagger\boldsymbol{B}+\hat{v}^\dagger\hat{u}\boldsymbol{Q}\,, \tag{3·2b}$$

$$N\longrightarrow\hat{\boldsymbol{n}}+2b^\dagger b\,, \tag{3·2c}$$

$$Q\longrightarrow 2\boldsymbol{B}^\dagger\hat{u}'\hat{v}+2\hat{v}^\dagger\hat{u}'\boldsymbol{B}+(\hat{u}\hat{u}-\hat{v}^\dagger\hat{v})\boldsymbol{Q}\,, \tag{3·2d}$$

where $\boldsymbol{B}^\dagger$, $\hat{\boldsymbol{n}}$, $\boldsymbol{Q}$ are operators in terms of the intrinsic quasiparticles

$$\boldsymbol{B}^\dagger=\sum_{m>0}\sigma_m a_m^\dagger a_{\tilde{m}}^\dagger\ , \qquad \hat{\boldsymbol{n}}=\sum_m a_m^\dagger a_m\ , \tag{3·3a}$$

$$\boldsymbol{Q}=\sum_m \sigma_m a_m^\dagger a_m\ , \tag{3·3b}$$

and

$$\hat{u}=\sqrt{1-\frac{b^\dagger b}{2\hat{S}}}\ , \qquad \hat{v}=\frac{b}{\sqrt{2\hat{S}}}\ , \tag{3·4a}$$

$$\hat{u}'=\sqrt{1-\frac{b^\dagger b}{2\hat{S}-1}}\ , \quad \hat{v}'=\frac{b}{\sqrt{2\hat{S}-1}}\ , \tag{3·4b}$$

$$2\hat{S}=\Omega-\hat{\boldsymbol{n}}\ . \tag{3·5}$$

The intrinsic quasiparticle operators ($a^\dagger$, a) exactly transfer the seniority quantum number by one unit, and satisfy

$$\{a_m,\ a_{\tilde{m}'}^\dagger\}_+=\delta_{mm'}-a_{\tilde{m}}^\dagger\frac{1}{2\hat{S}}a_{\tilde{m}'}\ . \tag{3·6}$$

This anticommutation relation guarantees that the quasiparticle operators ($a^\dagger$, a) are independent of the pairing-boson operators ($b^\dagger$, b). From (3·6) we obtain the following commutation relations:

$$[\boldsymbol{B},\boldsymbol{B}^\dagger]=2\hat{S}-\frac{2}{(2\hat{S}+1)(2\hat{S}+2)}\boldsymbol{B}^\dagger\boldsymbol{B}-\frac{1}{2\hat{S}}\boldsymbol{Q}^2\ , \tag{3·7a}$$

$$[\boldsymbol{Q},\boldsymbol{B}^\dagger]=\frac{2\hat{S}}{2\hat{S}+2}\boldsymbol{B}^\dagger\boldsymbol{Q}\ , \tag{3·7b}$$

$$[\hat{\boldsymbol{n}},\boldsymbol{B}^\dagger]=2\boldsymbol{B}^\dagger\ , \qquad [\boldsymbol{Q},\hat{\boldsymbol{n}}]=0\ . \tag{3·7c}$$

We note that the operator $\boldsymbol{Q}$ plays no role in the subspace $\{(\boldsymbol{B}^\dagger)^{n_2}|0\rangle\}$, because of the relation (3·7b). Eliminating $\boldsymbol{Q}$, we obtain higher commutators as follows:

$$[[\boldsymbol{B},\boldsymbol{B}^\dagger],\boldsymbol{B}^\dagger]=-2\boldsymbol{B}^\dagger-\boldsymbol{B}^\dagger\frac{2^2\cdot 2!}{4(2\hat{S}-1)}\left\{1+\frac{4}{(2\hat{S}+1)(2\hat{S}+2)}\boldsymbol{B}^\dagger\boldsymbol{B}\right\}, \tag{3·8}$$

$$[\cdots[\boldsymbol{B},\underbrace{\boldsymbol{B}^\dagger],\cdots,\boldsymbol{B}^\dagger}_{k}]=-(\boldsymbol{B}^\dagger)^{k-1}\frac{2^k\cdot k!(2\hat{S}-2k+1)!!}{4(2\hat{S}-1)!!}$$
$$\times\left\{1+\frac{4}{(2\hat{S}+1)(2\hat{S}+2)}\boldsymbol{B}^\dagger\boldsymbol{B}\right\}. \quad (k\geq 3) \tag{3·9}$$

3.2. *Application of the multiphonon method to the intrinsic subspace*

In the $O(4)$ model, the quasiparticle-pair operator $(\boldsymbol{B}^\dagger, \boldsymbol{B})$ defined by (3·3a) just corresponds to the phonon operator in the MPM. Let us derive a boson representation of $(\boldsymbol{B}^\dagger, \boldsymbol{B})$ such that a one-to-one correspondence between the multiphonon states $(\boldsymbol{B}^\dagger)^{n_d}|0\rangle$ and the d-boson states $(d^\dagger)^{n_d}|0)$ holds:

$$|n_d\rangle = \frac{1}{\sqrt{n_d!}}(\bar{\boldsymbol{B}}^\dagger)^{n_d}|0\rangle \longleftrightarrow |n_d) = \frac{1}{\sqrt{n_d!}}(d^\dagger)^{n_d}|0). \tag{3·10}$$

Here we have defined $\bar{\boldsymbol{B}} = \boldsymbol{B}/\sqrt{\Omega}$ for convenience. The multiphonon states $|n_d\rangle$ above have to be normalized:

$$|\bar{n}_d\rangle = \frac{1}{\sqrt{\langle n_d|n_d\rangle}} \cdot |n_d\rangle . \tag{3·11}$$

With $|\bar{n}_d\rangle$, we can introduce a transformation U:

$$U = \sum_{n_d=0}^{\Omega/2} |n_d)\langle \bar{n}_d| . \tag{3·12}$$

The upper limit of the sum with respect to n_d is $\Omega/2$. This is because the maximum seniority in the j^N configuration is $\Omega = j + 1/2$. (The phonon operator $\boldsymbol{B}^\dagger$ composed of two quasiparticles exactly transfers the seniority quantum number by two units.) By the U-transformation, $\bar{\boldsymbol{B}}$ is mapped into the d-boson space as

$$\bar{\boldsymbol{B}} \to \mathring{\boldsymbol{B}} \equiv U\bar{\boldsymbol{B}}U^{-1} = \sum_{n_d=1}^{\Omega/2} \langle \sqrt{n_d - 1}|\bar{\boldsymbol{B}}|\bar{n}_d\rangle \cdot |n_d - 1)(n_d| . \tag{3·13}$$

Inserting the boson-vacuum projector $|0)(0| = 1 - d^\dagger d + \frac{1}{2} d^\dagger d^\dagger dd - + \cdots$ in the r.h.s. of this equation, we obtain

$$\begin{aligned} \mathring{\boldsymbol{B}} &= \langle 0|\bar{\boldsymbol{B}}|1\rangle d + \left\{ \frac{1}{\sqrt{2}} \langle 1|\bar{\boldsymbol{B}}|\bar{2}\rangle - \langle 0|\bar{\boldsymbol{B}}|1\rangle \right\} d^\dagger dd + \cdots \\ &= d + \left(\sqrt{1 - \frac{1}{\Omega - 1}} - 1 \right) d^\dagger dd + \cdots . \end{aligned} \tag{3·14}$$

This is just the modified Marumori boson expansion.[19)~21)] On the other hand, it is possible to obtain an exact and closed representation if the multiphonon norm $\langle n_d|n_d\rangle$ is exactly calculable. We can clearly see this fact by rewriting (3·13) as follows:

$$\begin{aligned} \mathring{\boldsymbol{B}} &= \sum_{n_d=1}^{\Omega/2} \sqrt{n_d}\, |n_d - 1)(n_d|g(n_d) \\ &= d \sum_{n_d=1}^{\Omega/2} |n_d)(n_d|g(\hat{n}_d) = d \cdot g(\hat{n}_d)\mathbf{1} . \end{aligned} \tag{3·15}$$

Here $g(\hat{n}_d)$ is the operator obtained by the replacement $n_d \to \hat{n}_d = d^\dagger d$ in the

function

$$g(n_d)=\sqrt{\frac{\langle n_d|n_d\rangle}{\langle n_d-1|n_d-1\rangle}}\,, \tag{3·16}$$

and **1** is the projector onto the physical subspace of the d-boson space:

$$\mathbf{1}=\sum_{n_d=0}^{\Omega/2}|n_d)(n_d|. \tag{3·17}$$

Now, Eq. (3·15) indicates that, if a good lowest-order approximation for $g(n_d)$ is found, we can perform an approximate summing up of all orders of the modified Marumori expansion. This is the basic idea of the MPM.

The multiphonon norm $\langle n_d|n_d\rangle$ may be expanded with respect to the order of commutators as follows:

$$\begin{aligned}\langle n_d|n_d\rangle&=\frac{1}{n_d!}\langle 0|(\bar{\boldsymbol{B}})^{n_d-1}[\bar{\boldsymbol{B}},(\bar{\boldsymbol{B}}^\dagger)^{n_d}]|0\rangle\\&=\frac{1}{n_d!}\sum_{k=1}^{n_d}\binom{n_d}{k}\langle 0|(\bar{\boldsymbol{B}})^{n_d-1}(\bar{\boldsymbol{B}}^\dagger)^{n_d-k}[\cdots[\bar{\boldsymbol{B}},\underbrace{\bar{\boldsymbol{B}}^\dagger],\cdots,\bar{\boldsymbol{B}}^\dagger}_{k}]|0\rangle\,.\end{aligned} \tag{3·18}$$

For the $O(4)$ model, it is exactly calculable by the use of (3·9); the result is

$$\frac{\langle n_d|n_d\rangle}{\langle n_d-1|n_d-1\rangle}=1-C\cdot(n_d-1)-\frac{(n_d-1)!}{4\Omega\cdot(\Omega-1)!!}\sum_{k=3}^{n_d}\frac{2^k\cdot(\Omega-2k+1)!!}{(n_d-k)!} \tag{3·19}$$

with

$$C\equiv 1-\langle n_d=2|n_d=2\rangle=\frac{1}{\Omega-1}\,. \tag{3·20}$$

The lowest-order approximation of MPM consists in neglecting the third term in the r.h.s. of (3·19) which results from the commutator higher than double. The neglected terms are of $O(\Omega^{-k})$, $k=3, 4, \cdots, n_d$. Thus, we obtain in the lowest-order approximation

$$\overset{\circ}{\boldsymbol{B}}=d\sqrt{1-C(\hat{n}_d-1)}\cdot\mathbf{1}=\sqrt{1-C\hat{n}_d}\cdot d\cdot\mathbf{1}\,, \tag{3·21a}$$

$$\overset{\circ}{\boldsymbol{B}}^\dagger=\mathbf{1}\cdot d^\dagger\sqrt{1-C\hat{n}_d}\,. \tag{3·21b}$$

A seeming shortcoming of the above representation is that, unlike the well-known Holstein-Primakoff representation, the square-root operator does not vanish even when it operates on the maximum d-boson state with $n_d=\Omega/2$.

Thus, we adopted in Ref. 14) an additional approximation $C\simeq 2/\Omega$,*) and replaced (3·21) with

$$\overset{\circ}{\boldsymbol{B}}{}^{\dagger}=\mathbf{1}\cdot d^{\dagger}\sqrt{1-\frac{2}{\Omega}\hat{n}_d}\ . \tag{3·22}$$

However, the square-root operator need not satisfy the boundary condition stated above, since the projector $\mathbf{1}$ automatically cuts off the unphysical states with $n_d > (n_d)_{\max}$. In § 4, we extensively study the difference between the approximation (3·21) with the relation (3·20) [$C=1/(\Omega-1)$] and the other approximation (3·22) [$C=2/\Omega$]. It should be pointed out that the latter approximation is equivalent to the leading-order approximation adopted by Otsuka et al.[6),7)] in their works to give a microscopic interpretation of the phenomenological IBM (proof is given in the Appendix).

3.3. *s-d boson representation*

By the two-step mapping described above, the original nucleon state space has been mapped onto the s-d boson space as

$$\{(A^{\dagger})^{n_s}(B^{\dagger})^{n_d}|0\rangle\}\longrightarrow\{(s^{\dagger})^{n_s}(d^{\dagger})^{n_d}|0\rangle\}.\quad (n_s+n_d=N/2) \tag{3·23}$$

Here our previous notation for the pairing boson ($b^{\dagger}$, b) is changed into ($s^{\dagger}$, s). Corresponding to the mapping (3·23), the nucleon-pair operators have been transcribed as**)

$$A^{\dagger}\to s^{\dagger}\sqrt{\Omega-\hat{n}_B-\hat{n}_d}\ , \tag{3·24a}$$

$$Q\to\sqrt{\Omega}\{f(\hat{n}_d)\overset{\circ}{\boldsymbol{B}}{}^{\dagger}s+s^{\dagger}\overset{\circ}{\boldsymbol{B}}f(\hat{n}_d)\}, \tag{3·24b}$$

$$N\to 2\hat{n}_B=2(\hat{n}_s+\hat{n}_d),\qquad \hat{n}_s\equiv s^{\dagger}s\ , \tag{3·24c}$$

where

$$f(\hat{n}_d)=2\sqrt{\frac{\Omega-\hat{n}_B-\hat{n}_d+1}{(\Omega-2\hat{n}_d+1)(\Omega-2\hat{n}_d+2)}}\ . \tag{3·25}$$

The operator $f(\hat{n}_d)$ combined with the s-boson, $f(\hat{n}_s)s$, is equivalent to the operator $2\hat{u}'\hat{v}$ in the previous expression (3·2d): This is easy to see if we notice that the quasiparticle-number operator $\hat{\boldsymbol{n}}$ is transcribed into $2\hat{n}_d$ in the second-step mapping. Let us recall that these ($\hat{u}$, $\hat{v}$) operators may be regarded[18)] as

*) In the realistic case, there appear three quantities C_0, C_2 and C_4 in place of the present C. Their values are given, to the order Ω^{-2}, by

$$C_0=\frac{5}{\Omega-1}\ ,\qquad C_2=C_4=\frac{10}{7}\cdot\frac{1}{\Omega-2}\ .$$

These were replaced in Ref. 14) with the "average" value $\bar{C}=2/\Omega$.

**) The notation Π was used in Ref. 14) for the quantity $n_B\equiv N/2$.

"quantized" coefficients of the Bogoliubov transformation.

The *s-d* boson representation above is exact, if we use the representation (3·15) for $\overset{\circ}{\boldsymbol{B}}$ in combination with the operator $g(\hat{n}_d)$ obtained from the exact expression (3·19) for the multiphonon norm.

§ 4. Numerical examples and discussion

Figure 1 compares the exact and approximate values of the multiphonon norms. We see that the lowest-order MPM reproduces the exact norms with high degree of precision: The deviations from the exact values are negligible except when n_d approaches its maximum $(n_d)_{\max}=\Omega/2$. On the other hand, the replacement $C\to 2/\Omega$ discussed in § 3.2 brings about a large error in the whole range of n_d.

Figure 2 shows the n_d-dependence of the intrinsic matrix elements

$$(n_d-1|\overset{\circ}{\boldsymbol{B}}|n_d)^2=n_d\frac{\langle n_d|n_d\rangle}{\langle n_d-1|n_d-1\rangle}, \tag{4·1}$$

which contributes to the $B(E2)$'s between the multiphonon states. As expected from Fig. 1, the lowest-order MPM reproduces the exact values very well, except for the vicinity of $(n_d)_{\max}$. It is also seen that the third-order approximation of the modified Marumori expansion, i.e., the first two terms of (3·14), already gives a very good result.

The above characteristics remain essentially the same for the total $B(E2)$ values

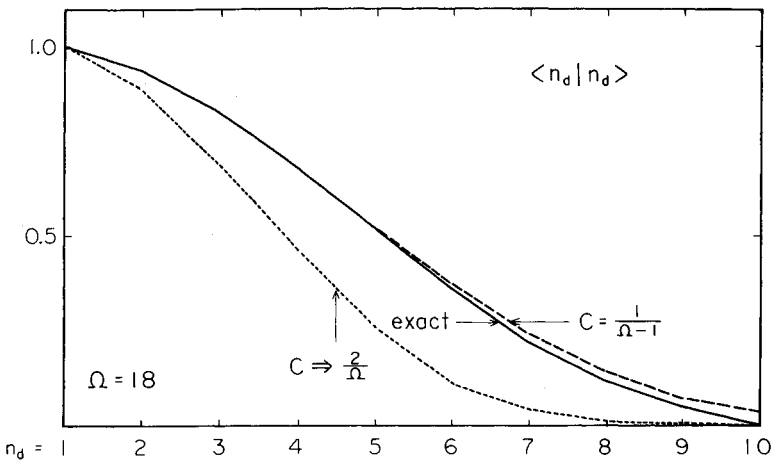

Fig. 1. Norms of the multiphonon states. The solid lines show the exact values; the dashed lines the lowest-order result of the MPM; the dotted lines the result with the replacement $C\to 2/\Omega$. Note that $(n_d)_{\max}=9$ for $\Omega=18$.

$$(n_s+1,\ n_d-1|Q|n_s,\ n_d)^2$$

$$=\Omega f(n_d)^2\cdot(n_s+1)\cdot(n_d-1|\mathring{B}|n_d)^2$$

$$=\frac{4\Omega(\Omega-n_B-n_d+1)}{(\Omega-2n_d+1)(\Omega-2n_d+2)}\cdot(n_B-n_d+1)n_d\{1-C(n_d-1)\},\qquad(4\cdot2)$$

which are shown in Fig. 3.

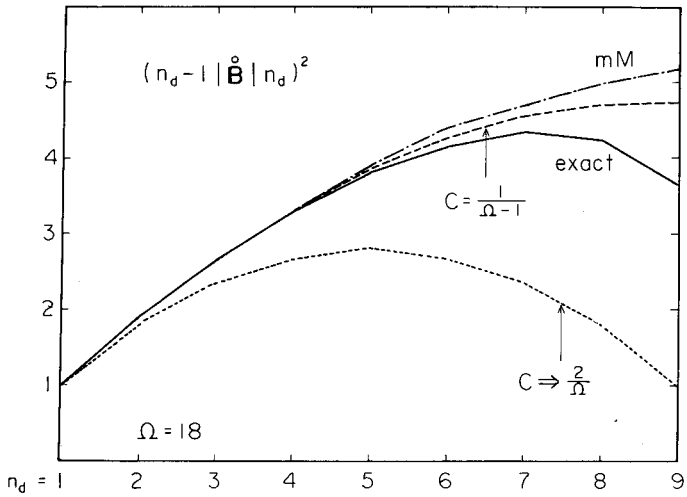

Fig. 2. Intrinsic contributions to the $B(E2)$ between the multiphonon states. The solid lines show the exact values; the dashed lines the lowest-order result of the MPM; The dash-dotted lines the 3rd order result of the modified Marumori (mM) method; the dotted lines the result with the replacement $C\to 2/\Omega$.

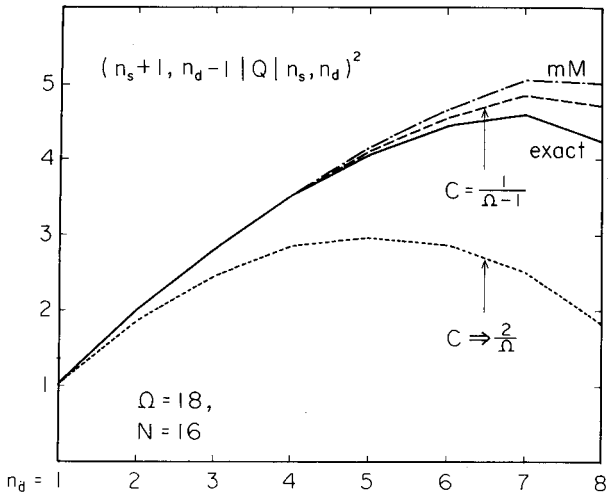

Fig. 3. $B(E2)$ for transitions between the multiphonon states. Notations are the same as in Fig. 2.

The reason why Figs. 2 and 3 are similar may be clear from Fig. 4. This figure shows the n_d-dependence of the matrix elements $f(n_d)\sqrt{n_s+1}$ of the pairing operator $f(\hat{n}_d)s^\dagger$. We see that the decrease due to $\sqrt{n_s+1}=\sqrt{n_B-n_d+1}$ is largely counterbalanced by the increase of $f(n_d)$. Namely, there is a tendency to keep the product $f(n_d)\cdot\sqrt{n_s+1}$ almost constant. This property is not surprising in view of the fact that the s-boson is merely a piece of the total pairing operator $2\hat{u}\hat{v}$. Thus, if the function $f(n_d)$ is replaced with its value at $n_d=1$, a large error comes about. The counteraction of $f(n_d)$ stated above becomes weak only when N becomes appreciably smaller than Ω.

If we replace the constant C in (4·2) with the value $2/\Omega$, then the attenuation factor associated with $(n_d-1|\mathring{\boldsymbol{B}}|n_d)$ cancels the same factor contained in the denominator of $f(n_d)$, diminishing the counteraction discussed above. Implicitly based on this approximation, Arima and Iachello[5] emphasized the importance of the attenuation effect due to the factor $\sqrt{n_s+1}$ exclusively. However, the replacement $(C\to 2/\Omega)$ is not a good approximation in the present model as is seen in Fig. 3, and the factor $\sqrt{n_s+1}$ does not (exclusively) represent the anharmonic effects dominant in the solvable model under consideration.

Figure 5(a) shows the excitation spectrum as a function of the force-strengths G and χ. It is seen that the lowest-order MPM reproduces the exact spectrum almost perfectly. On the other hand, the replacement $C\to 2/\Omega$ again brings about a discrepancy (see Fig. 5(b)). We have also made calculations with the fourth-order approximation of the modified Marumori method. It gives the result which almost overlaps upon the dotted lines in Fig. 5(a). The reason why it gives a

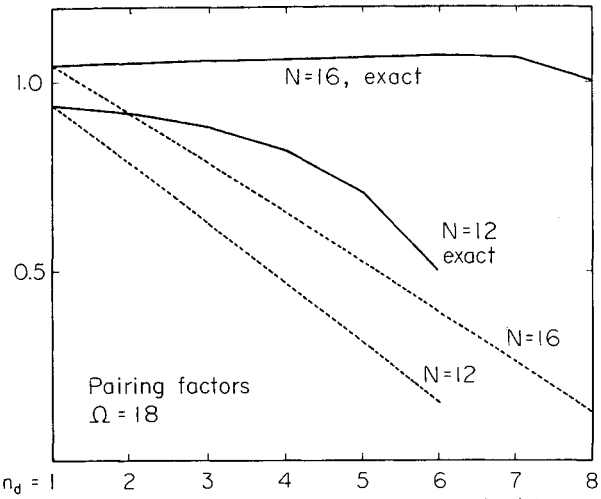

Fig. 4. Pairing factors squared which contribute to the $B(E2)$ between the multi-phonon states. The solid lines show the exact values, while the dotted lines the approximate values where the values of $f(n_d)$ are replaced by the constant $f(n_d=1)$.

better accuracy for the excitation spectrum than for $B(E2)$ is that the intrinsic Hamiltonian (as a function of the products $\boldsymbol{B}^{\dagger}\boldsymbol{B}^{\dagger}$, $\boldsymbol{B}^{\dagger}\boldsymbol{B}$ and $\boldsymbol{BB}$) is directly mapped onto the d-boson space. Namely, the fifth-order term in the expansion (3·14) is partially taken into account in the course of the normal ordering with respect to $d^{\dagger}$ and d.

With decreasing N, agreement with the exact spectrum becomes better than that of Fig. 5(a). This is because actual values of n_d are cut off at $N/2<(n_d)_{\max}$ for systems with $N<\Omega$. On the other hand, an exceptional case occurs for $N=\Omega$.

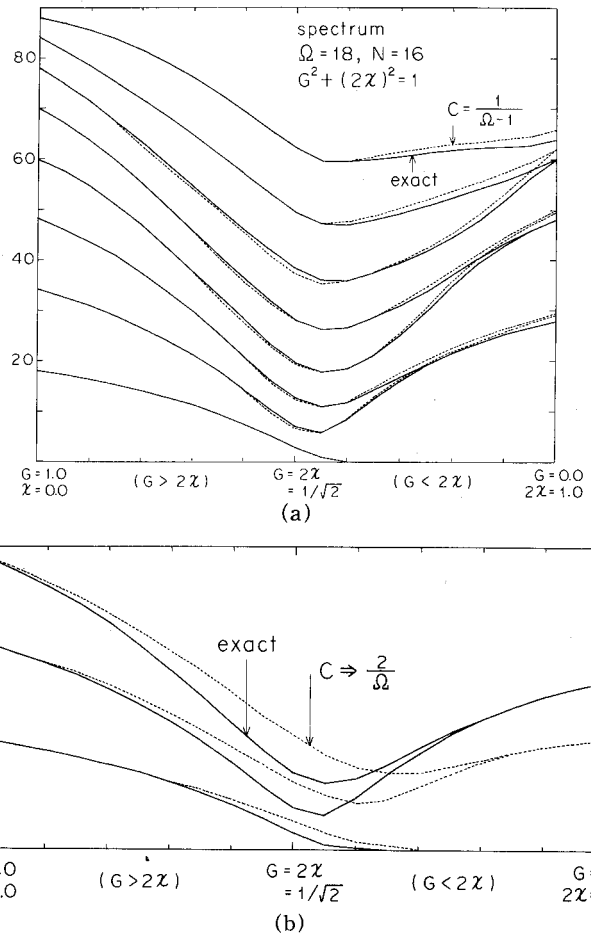

Fig. 5. Excitation spectrum of the $O(4)$ model, for the case $\Omega=18$ and $N=16$. The interaction-strengths G and χ are parametrized such that $(G)^2+(2\chi)^2=1$. Note that the Hartree-Bogoliubov vacuum acquires in the region $G<2\chi$ an equilibrium deformation β given by (2·9) in the text. (a) The solid lines show the exact values, while the dotted lines the lowest-order result of the MPM. (b) Same as above except that the dotted lines here show the result with the replacement $C\to 2/\Omega$.

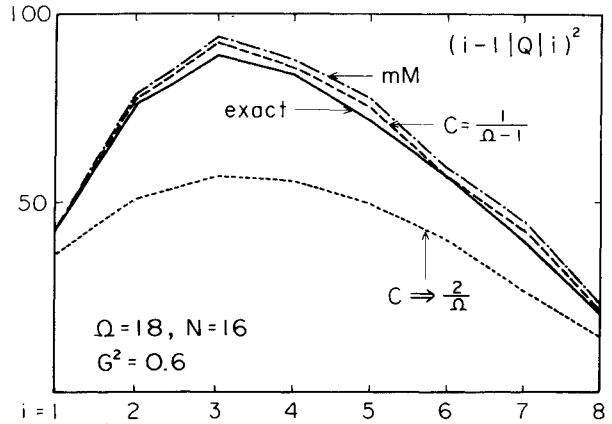

Fig. 6. $B(E2)$ values after the diagonalization of the Hamiltonian with $G^2=0.6$ and $(2\chi)^2=0.4$. Notations are the same as in Fig. 2.

In this specific case, deviation from the exact solution becomes nonnegligible in the "quadrupole" limit, because the maximum d-boson state (for which the accuracy of the approximation is worst) plays an important role there.

Figure 6 summarizes the exact and approximate results for the attenuation effects on the $B(E2)$ values between the eigenstates of the Hamiltonian for a situation just before the occurrence of the instability toward the static "quadrupole" deformation.

We have used the $O(4)$ model for a rather restricted aim of testing the accuracy of the MPM. Thus, many interesting properties of this model have not been discussed in this paper; for instance, properties in the "quadrupole" limit resulting from the degeneracy between the prolate and oblate deformations. It is expected[22] that this model is useful to elucidate some of the features of nuclear transition phenomena.

Acknowledgements

Part of this work has been done during the author's stay at NORDITA in the summer of 1979, and he would like to express his thanks to Professor B. R. Mottelson for suggesting the $O(4)$ model. The author also wishes to acknowledge stimulating discussions with Professor Z. Szymanski, Professor R. Broglia, Professor M. Yamamura and Dr. T. Suzuki.

Appendix

Since the number of intrinsic quasiparticles exactly corresponds to the seniority quantum number ν,[18] we have in the present model the following one-

to-one correspondence:

$$\frac{1}{\sqrt{\langle n_d|n_d\rangle}}|n_d\rangle|0\rangle \hat{=} |j^\nu, \nu\rangle ,$$

where $|j^N, \nu\rangle$ denotes the normalized N-nucleon state with seniority $\nu=2n_d$. From (3·24a), we also see that

$$\frac{1}{\sqrt{\langle n_d-1|n_d-1\rangle}}A^\dagger|n_d-1\rangle|0\rangle \hat{=} \sqrt{\Omega-2(n_d-1)}|j^\nu, \nu-2\rangle .$$

Therefore, we can rewrite the seniority-changing matrix elements of the "quadrupole" operator (between the states with the same nucleon number ν) as

$$\begin{aligned}
&\langle j^\nu, \nu|Q|j^\nu, \nu-2\rangle \\
&\hat{=} \frac{1}{\sqrt{\Omega-2(n_d-1)}}\cdot\frac{1}{\sqrt{\langle n_d|n_d\rangle}}\cdot\frac{1}{\sqrt{\langle n_d-1|n_d-1\rangle}}\cdot(0|\langle n_d|[Q, A^\dagger]|n_d-1\rangle|0) \\
&= \frac{1}{\sqrt{\Omega-2(n_d-1)}}\cdot\frac{1}{\sqrt{\langle n_d|n_d\rangle}}\cdot\frac{1}{\sqrt{\langle n_d-1|n_d-1\rangle}}\cdot 2\langle n_d|\boldsymbol{B}^\dagger|n_d-1\rangle \\
&= \frac{1}{\sqrt{1-\frac{2}{\Omega}(n_d-1)}}\cdot\sqrt{\frac{\langle n_d|n_d\rangle}{\langle n_d-1|n_d-1\rangle}}\sqrt{n_d}\langle j^2, \nu=2|Q|j^2, \nu=0\rangle .
\end{aligned}$$

Thus, the replacement of $\langle j^\nu, \nu|Q|j^\nu, \nu-2\rangle$ with $\sqrt{n_d}\langle j^2, \nu=2|Q|j^2, \nu=0\rangle$ is equivalent to the approximation

$$\frac{\langle n_d|n_d\rangle}{\langle n_d-1|n_d-1\rangle}\simeq 1-\frac{2}{\Omega}(n_d-1).$$

Essentially the same replacement was adopted in the work of Otsuka et al.[6] in order to derive Eq. (7) of their paper.

References

1) D. Janssen, R. V. Jolos and F. Dönau, Yadern Fiz. **22** (1975), 965; Soviet J. Nucl. Phys. **22** (1976), 503; Nucl. Phys. **A224** (1974), 93.
R. V. Jolos and D. Janssen, Fiz. Elm. Chastits At. Yadra 8 (1977), 330; Soviet J. Part. Nucl. 8 (1977), 138.
2) G. Holzwarth, D. Janssen and R. V. Jolos, Nucl. Phys. **A261** (1976), 1.
3) S. Iwasaki, F. Sakata and K. Takada, Prog. Theor. Phys. **57** (1977), 1289.
4) B. Silvestre-Brac and R. Piepenbring, Phys. Rev. **C16** (1977), 1638; **C17** (1978), 364; **C20** (1979), 1161.
5) A. Arima and F. Iachello, Phys. Rev. Letters **35** (1975), 1069; Ann. of Phys. **99** (1976), 253; **111** (1978), 201; **123** (1979), 468.
6) T. Otsuka, A. Arima, F. Iachello and I. Talmi, Phys. Letters **76B** (1978), 139.
7) T. Otsuka, A. Arima and F. Iachello, Nucl. Phys. **A309** (1978), 1.
8) R. Piepenbring, B. Silvestre-Brac and Z. Szymanski, Nucl. Phys. **A348** (1980), 77.
9) T. Marumori, M. Yamamura, Y. Miyanishi and S. Nishiyama, Prog. Theor. Phys. Suppl.

Extra Number (1968), 179; Yadern. Fiz. **9** (1969), 501; Soviet J. Nucl. Phys. **9** (1969), 287.
10) S. T. Belyaev and V. G. Zelevinsky, Yadern. Fiz. **11** (1970), 741; Soviet J. Nucl. Phys. **11** (1970), 416.
11) A. Bohr and B. R. Mottelson, Phys. Scripta **22** (1980), 468.
12) A. Kuriyama, T. Marumori, K. Matsuyanagi, F. Sakata and T. Suzuki, Prog. Theor. Phys. Suppl. No. 58 (1975), 9.
13) S. Iwasaki, T. Marumori, F. Sakata and K. Takada, Prog. Theor. Phys. **56** (1976), 846.
14) T. Suzuki, M. Fuyuki and K. Matsuyanagi, Prog. Theor. Phys. **61** (1979), 1682.
15) T. Suzuki, M. Fuyuki and K. Matsuyanagi, Prog. Theor. Phys. **61** (1979), 1082; **62** (1979), 690; **65** (1981), 1667.
16) M. Fuyuki, Prog. Theor. Phys. **64** (1980), 1470.
17) M. Bander and C. Itzykson, Rev. Mod. Phys. **38** (1966), 330.
18) T. Suzuki and K. Matsuyanagi, Prog. Theor. Phys. **56** (1976), 1156.
19) S. G. Lie and G. Holzwarth, Phys. Rev. **C12** (1975), 1035.
20) M. Kleber, Phys. Letters **30B** (1969), 588.
21) S. Y. Li, R. M. Dreizler and A. Klein, Phys. Rev. **C4** (1971), 1571.
22) Y. Mizobuchi, Prog. Theor. Phys. **65** (1981), 1450.

Prog. Theor. Phys. Vol. 67, No. 5, May 1982, Progress Letters

Rotational Frequency Dependence of Gamma Vibration and Pairing Potential in ^{164}Er

Yoshifumi R. SHIMIZU and Kenichi MATSUYANAGI
Department of Physics, Kyoto University, Kyoto 606
(Received January 20, 1982)

By performing the "shell-model plus RPA" calculation in a rotating frame, we suggest that the observed properties of the γ-vibrational energies are connected with the weak dependence of the pairing potential of the ground band upon the rotational frequency in the region $\hbar\omega_{\rm rot}<0.32$ MeV.

Recent studies of nuclear high-spin states have demonstrated the validity of superposing the independent quasiparticle excitations defined in a frame uniformly rotating about the axis with maximum moment of inertia. The success of such a "shell model in a rotating frame"[1)~4)] opens the possibility for analyzing the effects of rapid rotation on the collective vibrational excitations in the neighborhood of the yrast line by means of an application of the RPA to the rotating frame.

As the first theme of the "shell-model plus RPA in the rotating frame", we have performed an analysis of the microscopic structure of the γ-band in ^{164}Er. The calculation has been performed up to $\hbar\omega_{\rm rot}=0.32$ MeV which is higher than the critical rotational frequency $\hbar\omega^{(1)}_{\rm crit}=0.28$ MeV for the occurrence of the band crossing between the ground band (g-band) and the Stockholm band (s-band). To describe the γ-band for $\omega_{\rm rot}>\omega^{(1)}_{\rm crit}$, we have therefore constructed the RPA excitation modes by regarding the configuration with two quasiparticles in the two lowest positive-energy states as the RPA vacuum.

Although the RPA formalism based on the Hartree-Bogoliubov-cranking model is known,[5) 7)] we want to emphasize the following two important points which distinguish our work from Refs. 5)~7):

1) We interpret the RPA excitation energies as the relative energies between two states *with the same rotational frequency*. Thus, we avoid the difficulty of estimating the amount of the angular momentum transferred by the RPA excitation modes.

2) We have eliminated the band-band interactions originating from the neutron $i_{13/2}$ orbit when diagonalizing the cranking Hamiltonian. For this purpose, the method of Tanaka and Suekane[8)] was used. The quasiparticle energy diagram obtained in this way and used in the RPA calculation is shown in Fig. 1. The elimination of the band-band interactions is crucial to get a clear lowest-order picture presented below.

We have constructed the Hamiltonian to be used in the RPA in the body-fixed frame, $H_{\rm body}$, by starting with the experimental fact that there exists a rotating and superconducting Nilsson potential. With the conventional notations,[6)] the $H_{\rm body}$ is assumed to be written as

$$H_{\rm body}=H_{\rm sp}+H_{\rm int}-H_{\rm rot}$$
$$=H'_{\rm sp}+H'_{\rm int}\,, \tag{1}$$
$$H'_{\rm sp}=H_{\rm Nilsson}-\Delta(P^{\dagger}+P)-\omega_{\rm rot}J_x\,, \tag{2}$$
$$H'_{\rm int}=-\sum_{\tau=n,p}G_\tau:P_\tau^{\dagger}P_\tau:$$
$$-\frac{1}{2}\sum_{K=0,1,2}\chi_K:Q_K^{\dagger}Q_K:-\sum_{i=x,y,z}\mu_i\tilde{J}_i^{\,2}\,, \tag{3}$$

where $\tilde{J}_x=J_x-\langle J_x\rangle$, $\tilde{J}_y=J_y$ and $\tilde{J}_z=J_z$. The force-strengths, $G_{\tau=n,p}$ and $\chi_{K=0,2}$, were determined so as to reproduce the magnitudes

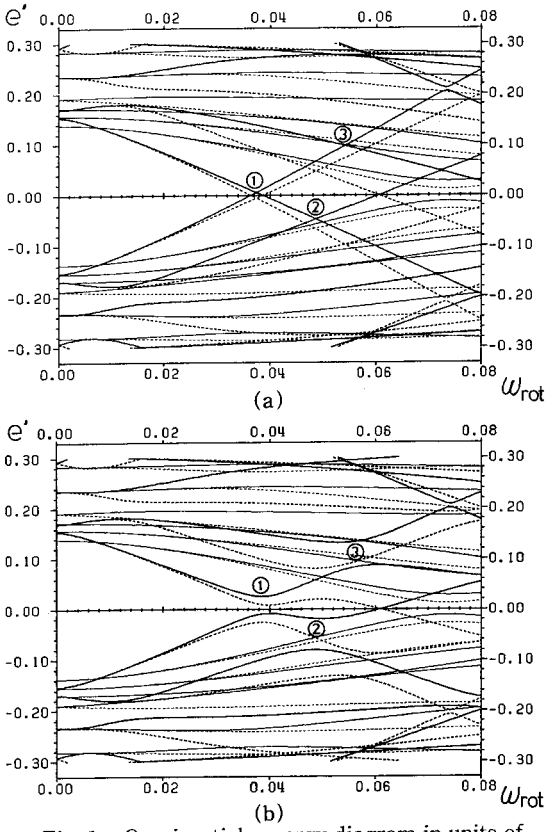

Fig. 1. Quasiparticle energy diagram in units of $\hbar\bar{\omega}=7.56$ MeV, used in the RPA calculation for the γ-band. The dotted (solid) lines show the quasiparticle states with signature $r=+i$ $(-i)$. The critical rotational frequencies for the occurrence of the band crossings are indicated by the simplified notations like ①$\equiv\omega^{(1)}_{crit}$ and ②$\equiv\omega^{(2)}_{crit}$. The deformation parameters are: $\delta_{osc}=0.269$ and $\Delta_g(\omega_{rot}=0)=1.04$ MeV. The shell-model spaces used are: $N_{osc}=4$, 5 and 6 for neutrons, and $N_{osc}=3$, 4 and 5 for protons (the proton part is not presented).
(a) The band-band interactions originating from the neutron $i_{13/2}$ orbit are eliminated.
(b) The band-band interactions are included. Compare with the case (a).

of the pairing potentials Δ (for both protons and neutrons) and the excitation energies of the β- and γ-vibration at $\omega_{rot}=0$, while $\chi_{K=1}$ was determined such that the Nambu-Goldstone modes ($\tilde{J}_x$ and $\tilde{J}_y\pm i\tilde{J}_z$) are analytically decoupled in the RPA order. As shown in Ref. 6), the coefficients μ_i in the last term of H'_{int}, which is the RPA-order term of the rotational energy H_{rot}, can be uniquely determined as functions of G and χ. Thus, there is no adjustable parameter in the present calculation. It turned out that the K-dependence of the quadrupole-force strengths $\chi_{K=1,2}$ obtained in this way agrees within 3% with the one expected from the scaling argument of Refs. 9) and 10). [Only the value of $\chi_{K=0}$ deviates about 10%.] Details of the method for constructing the H_{body} which guarantees the decoupling of the Nambu-Goldstone modes will be presented in a forthcoming paper.[11]

The pairing potential Δ was calculated (for both protons and neutrons) self-consistently at each value of ω_{rot}, while the quadrupole deformation of the Nilsson potential was fixed at its value for $\omega_{rot}=0$.

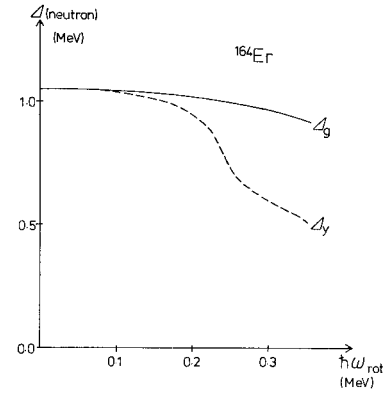

Fig. 2. The neutron pairing potential Δ_g of the g-band (solid line) calculated self-consistently at each value of ω_{rot}. Note that, for $\omega_{rot}>\omega^{(1)}_{crit}$, the g-band corresponds to the lowest-energy two quasiparticle states in the quasiparticle energy diagram shown in Fig. 1(a). For comparison, the pairing potential Δ_y of the yrast states calculated without eliminating the band-band interactions is shown by the dashed line.

Figure 2 shows the theoretical values for the magnitude of the neutron pairing potential Δ_g of the g-band. We see that the Δ_g is quite stable against an increase of $\omega_{\rm rot}$. This result is consistent with the assumption of constant Δ adopted by Bengtsson and Frauendorf in their rotating-shell-model calculations.[2] Of course, it does not imply that Δ is almost constant for *different* bands in the vicinity of the yrast line. In fact, the value of Δ_y for the yrast states calculated in the conventional manner (without eliminating the band-band interactions) considerably decreases in the region $\hbar\omega_{\rm rot} > 0.2$ MeV with increasing $\omega_{\rm rot}$. The drastic decrease of Δ_y in the vicinity of the band-crossing frequency $\omega_{\rm crit}$ is mainly caused by the strong mixing between the g-band and s-band whose pairing potential Δ_s is considerably smaller than Δ_g. Such a strong band-mixing in the vicinity of the band-crossing frequency is unavoidable in the conventional cranking-model calculation. As pointed out by Hamamoto,[12] however, proper description of the band-band interactions would require a full quantum-mechanical treatment beyond the semi-classical approximation inherent in the cranking model. On the other hand, the elimination of the band-band interactions provides us with a clear lowest-order picture that the magnitude

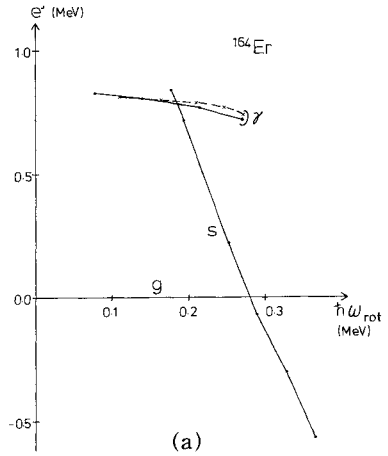

(a)

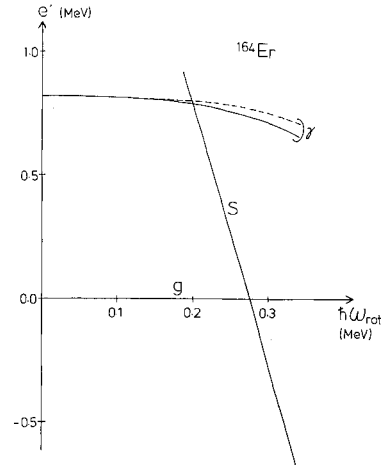

(b)

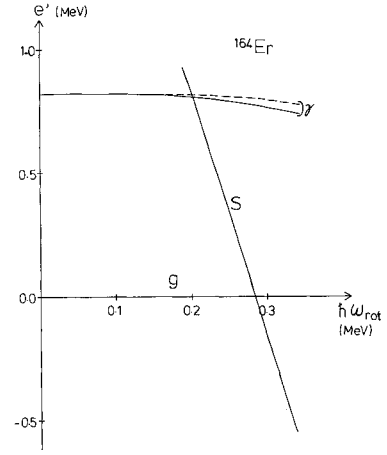

(c)

Fig. 3. Excitation energies of the γ-vibration in ^{164}Er, defined in a rotating frame associated with the ground band. The solid (dashed) lines show the states with positive (negative) signature.
(a) Experimental data from Ref. 14).
(b) Theoretical values with Δ_g shown in Fig. 2.
(c) Theoretical values with Δ_g fixed at its values for $\omega_{\rm rot}=0$.
For reference, the excitation energies of the s-band relative to the g-band are also shown.

of the pairing potential discontinuously decreases at the band-crossing point along the yrast line. It seems to us that this picture is more appropriate than the one associated with Δ_γ, in such a situation where the band-band interaction between the g-band and the s-band is experimentally known to be weak as in the case of ^{164}Er under discussion.

Figure 3 shows the excitation energies of the γ-band (relative to the g-band) as a function of $\omega_{\rm rot}$. We see that the weak $\omega_{\rm rot}$-dependence of the experimental γ-vibrational energies is well reproduced in the theoretical calculation. The theoretical dependence on $\omega_{\rm rot}$ of the RPA excitation energies $\omega_{\rm RPA}^{(\gamma)}$ is mainly determined by the corresponding dependence of the pairing potential Δ_g of the g-band. This may be confirmed by comparing Fig. 3(b) with Fig. 3(c) where Δ_g is fixed at its value for $\omega_{\rm rot}=0$. We want to emphasize that it would be difficult to understand the weak $\omega_{\rm rot}$-dependence of the experimental γ-vibrational energies, if Δ_g depends on $\omega_{\rm rot}$ much stronger than shown in Fig. 2. The presented result of the "shell-model plus RPA in the rotating frame" thus indicates that the observed property of the γ-vibrational energies is connected with the weak $\omega_{\rm rot}$-dependence of the pairing potential of the g-band. On the other hand, the γ-band in ^{164}Er is known[13),14)] to exhibit a band-crossing phenomenon with another unknown band at $\hbar\omega_{\rm rot}\approx 0.25$ MeV. The result of the analysis of this phenomenon will be reported in a separate letter.[15)]

This work was initiated as a part of the 1980 annual research projects on "Theoretical Study of the High-Spin States of the Nucleus" organized by the Research Institute for Fundamental Physics, Kyoto University, and the computer calculation for this work has been financially supported in 1981 by Institute for Nuclear Study, University of Tokyo.

1) A. Bohr and B. R. Mottelson, *Proc. Int. Conf. Nuclear Structure, Tokyo, 1977* [J. Phys. Soc. Japan **44** (1978) Suppl.], p. 157.
2) R. Bengtsson and S. Frauendorf, Nucl. Phys. **A327** (1979), 139.
3) S. Frauendorf, *Proc. Int. Conf. Extreme States in Nuclear Systems, Dresden, 1980,* p. 204.
4) L. L. Riedinger, Nucl. Phys. **A347** (1980), 141.
5) E. R. Marshalek, Nucl. Phys. **A275** (1977), 416.
6) D. Janssen and I. N. Mikhailov, Nucl. Phys. **A318** (1979), 390.
7) J. L. Egido, H. J. Mang and P. Ring, Nucl. Phys. **A339** (1980), 390.
8) Y. Tanaka and S. Suekane, Prog. Theor. Phys. **66** (1981), 1639.
9) T. Kishimoto et al., Phys. Rev. Letters **35** (1975), 552.
10) T. Suzuki and D. J. Rowe, Nucl. Phys. **A289** (1977), 461.
11) Y. R. Shimizu and K. Matsuyanagi, in preparation.
12) I. Hamamoto, Nucl. Phys. **A271** (1976), 15.
13) N. R. Johnson, D. Cline, S. W. Yates, F. S. Stephens, L. L. Riedinger and R. M. Ronningen, Phys. Rev. Letters **40** (1978), 151.
14) O. C. Kistner, A. W. Sunyar and E. der Mateosian, Phys. Rev. **C17** (1978), 1417.
15) Y. R. Shimizu and K. Matsuyanagi, Prog. Theor. Phys. **67** (1982), 1641.

Prog. Theor. Phys. Vol. 67, No. 5, May 1982, Progress Letters

High-Spin Anomaly of Gamma Band and Rotation-Alignment Effects in ^{164}Er

Yoshifumi R. SHIMIZU and Kenichi MATSUYANAGI
Department of Physics, Kyoto University, Kyoto 606
(Received January 20, 1982)

The "shell-model plus RPA" calculation in a rotating frame indicates that the nature of the γ-vibrational mode in ^{164}Er is drastically changed by the excitation of the rotation-aligned two-quasiparticles.

The γ-band in ^{164}Er is known[1),2)] to exhibit a band-crossing phenomenon with another unidentified band at about the same rotational frequency for the occurrence of the band-crossing between the ground band (g-band) and the Stockholm band (s-band). It has been conjectured[1),3),4)] that there are two candidates for the intersecting band. One candidate is the second-lowest aligned band (s'-band) generated, in a way similar to the s-band, by the rotation-alignment of the two quasiparticles in the neutron $i_{13/2}$ orbit. The other candidate is the γ-vibrational mode built on the s-band. To identify the nature of the intersecting band, it is desirable to determine whether or not the γ-vibrational mode can be excited from the s-band in the same way, as it is excited from the g-band. Thus, we have investigated how the properties of the γ-vibrational mode are modified by the presence of the rotation-aligned two-quasiparticles (with the lowest energy). The theoretical calculation has been done in the framework of the "shell-model plus RPA in the rotating frame"[5)~7)] with the parametrizations presented in Ref. 8). The result clearly indicates that the aligned two-quasiparticles cause drastic changes of the nature of the γ-vibration.

Figure 1 shows the neutron pairing potentials for the g-band (Δ_g) and the s-band (Δ_s), separately calculated in a self-consistent way by eliminating as in Ref. 9) the band-band interaction between the two bands. By virtue of the elimination, both the values Δ_g and Δ_s vary quite smoothly across the band-crossing region. The critical rotational frequencies for the occurrence of the band crossing are indicated in the figure by the symbols $\times$. [Because $\Delta_s \neq \Delta_g$, they take different values according to the bands in which they are defined.] We see that the dependence of Δ on the rotational frequency $\omega_{\rm rot}$ is weak, and that $\Delta_s \approx 0.6\Delta_g$. The reduction of Δ of the s-band is caused by the blocking effect of the rotation-aligned two quasiparticles on the

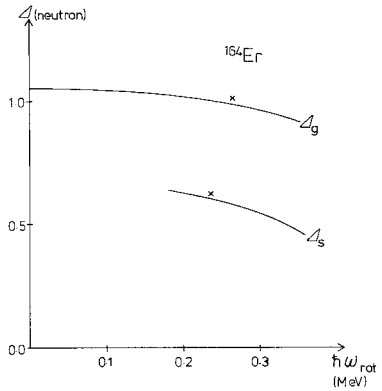

Fig. 1. Theoretical values of the neutron pairing potential of the ground band (Δ_g) and of the Stockholm band (Δ_s) in ^{164}Er are shown as the functions of the rotational frequency $\omega_{\rm rot}$. The symbols $\times$ denote the critical rotational frequencies at which the two bands intersect with each other. The band-band interaction is eliminated in this calculation.

pairing correlation.

Figure 2 shows the excitation energies (relative to the g-band) of the γ-vibrational modes as functions of $\omega_{\rm rot}$, which were obtained by the RPA in a rotating frame. The symbol $g\gamma$ denotes the γ-band built on the g-band, while the symbol $s\gamma$ is used for that on the s-band. For reference, the second-lowest aligned band (s'-band) is also shown in the same figure. To describe the $s\gamma$-band for $\omega_{\rm rot} < \omega_{\rm crit}^{(1)}$, we have constructed the excitation mode generating the $s\gamma$-band by regarding the lowest-energy two-quasiparticle state (corresponding to the s-band) as an RPA vacuum. In a similar manner, we have described the $g\gamma$-band in the region $\omega_{\rm rot} > \omega_{\rm crit}^{(1)}$ by regarding the lowest-energy two-quasiparticle state (which corresponds to the g-band) as an RPA vacuum. All calculations shown in this figure have been performed by using the pairing potential Δ_g of the g-band (including the $\omega_{\rm rot}$-dependence). We see that the excitation energy of the $s\gamma$-band relative to the s-band is much smaller than that of the $g\gamma$-band, i.e., $\omega_{\rm RPA}^{(s\gamma)} < \omega_{\rm RPA}^{(g\gamma)}$. In particular, a drastic decrease of the excitation energies occurs for the negative-signature states ($r=-1$). Thus, the property of signature splitting changes between the $g\gamma$-band and the $s\gamma$-band. Namely, $\omega_{\rm RPA}^{(s\gamma)}(r=-1) < \omega_{\rm RPA}^{(s\gamma)}(r=+1)$ whereas $\omega_{\rm RPA}^{(g\gamma)}(r=+1) < \omega_{\rm RPA}^{(g\gamma)}(r=-1)$. The reason for the drastic decrease of $\omega_{\rm RPA}^{(s\gamma)}(r=-1)$ may be directly seen in Fig. 3 which displays the distribution of two-quasiparticle transition strength for the operator $Q_2^{(-)} = (1/\sqrt{2})(Q_{22} - Q_{2-2})$. Comparing the upper part (for the excitations from the g-band) with the lower part (for that from the s-band), we see that the low-energy two-quasiparticle states acquire an appreciable amount of the transition strength in the latter case. In this way, the presence of the rotation-aligned two quasiparticles plays the role of softening the γ-vibrational mode. Similar tendency exists also in the positive-signature mode ($r=+1$), though the degree of the softening is less than that of $r=-1$.

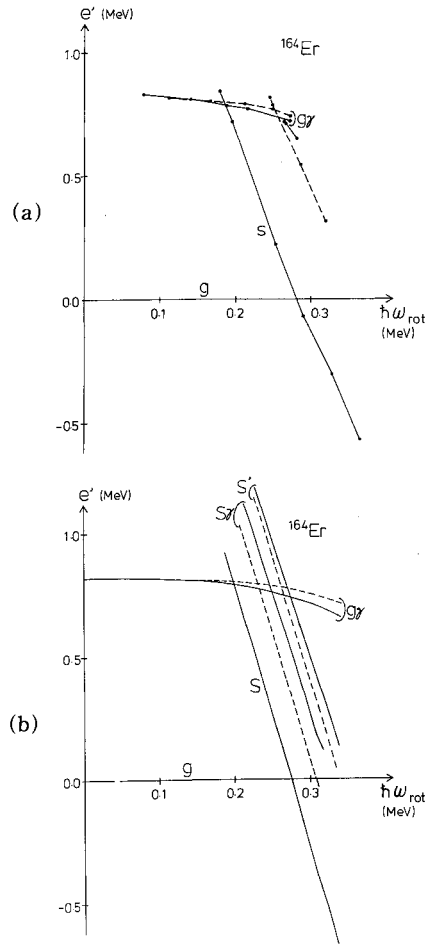

Fig. 2. Yrast spectrum with positive parity in ^{164}Er plotted as a function of $\omega_{\rm rot}$. The solid (dashed) lines show the states with positive (negative) signature.
(a) Experimental data from Ref. 1).
(b) Theoretical spectra. The notation $g\gamma$($s\gamma$) means the γ-band built on the g-band (s-band). A common pairing potential Δ_g is used in calculating the $g\gamma$- and $s\gamma$-bands.

Figure 4 shows the dependence of the γ-vibrational energies, $\omega_{\rm RPA}$, upon the magnitude Δ of the neutron pairing potential. As expected, the $\omega_{\rm RPA}$ decreases with decreasing Δ, since the pairing correlation favors the

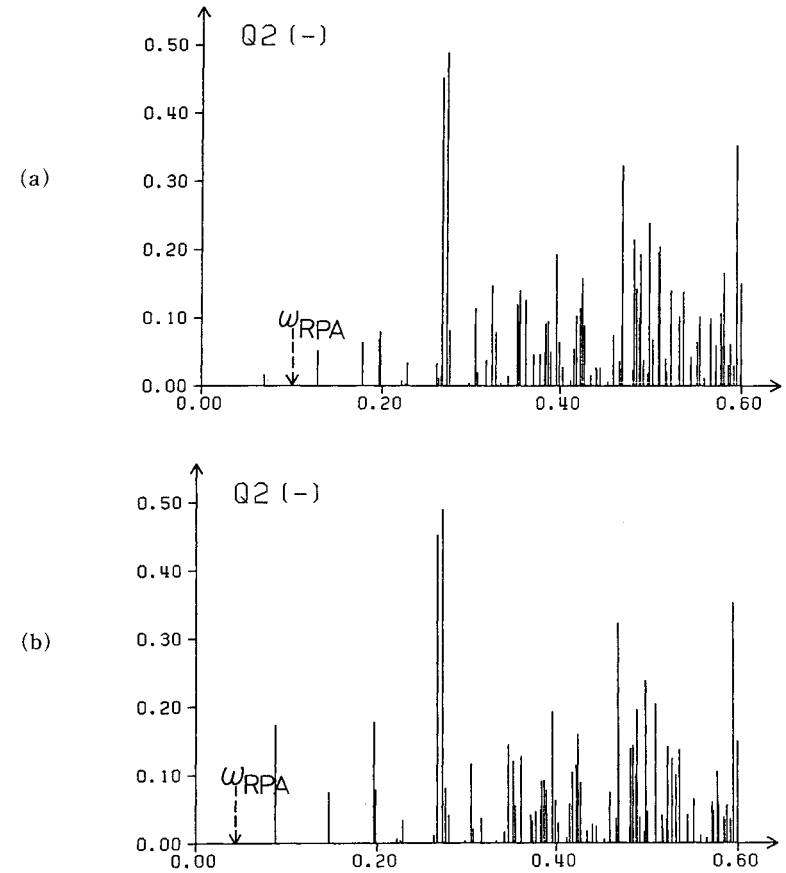

Fig. 3. Distribution of two-quasiparticle transition strengths for the operator $Q_2^{(-)} = (1/\sqrt{2})(Q_{22} - Q_{2-2})$, which contribute to the negative-signature γ-vibrational excitations from the g-band (upper part) and from the s-band (lower part) at $\hbar\omega_{rot} = 0.29$ MeV. The abscissa means the two-quasiparticle excitation energies in units of $\hbar\bar{\omega} = 7.56$ MeV. The ordinate is in units of $\bar{b}^2 = 5.48$ fm^2. The resulting γ-vibrational energies in the RPA are denoted by the notation ω_{RPA}. Only the neutron part is presented here.

axial symmetry and acts against the γ-deformation. The self-consistent value of Δ for the s-band is 0.62 MeV at $\hbar\omega_{rot} = 0.21$ MeV, as seen in Fig. 1. Hence, an instability would occur in the γ-vibrational mode built on the s-band, if this value of Δ_s is used in the RPA calculation to describe the $s\gamma$-band.

The principal effects of the rotation-aligned two quasiparticles on the properties of the γ-vibration may be summarized as follows: The first is the blocking effect leading to a decrease of the neutron pairing potential. The second is the softening of the γ-vibrational mode through the redistribution of the transition strength of the Y_{22} type. A consequence of the combined action of the above two effects is an occurrence of the instability toward a static γ-deformation. It should be stressed that the second effect alone is insufficient to realize the γ-instability. In the light of the major modification of the nature of the γ-vibration mentioned above, it

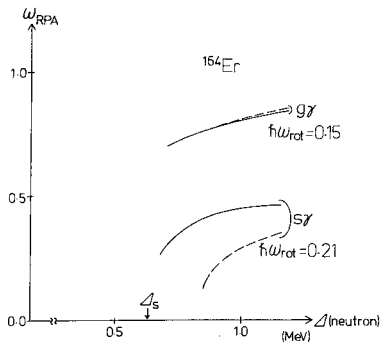

Fig. 4. Dependence of the theoretical γ-vibrational energies upon the magnitude of the neutron pairing potential. The solid (dashed) lines show the excitations with positive (negative) signature. This is the example calculated at $\hbar\omega_{rot}=0.15$ MeV (0.21 MeV) for the γ-vibration built on the g-band (s-band). The self-consistent value of the pairing potential of the s-band (Δ_s) is denoted by an arrow.

appears difficult to interpret the intersecting band as the $s\gamma$-band.

The above interpretation is somewhat different from that of Egido, Mang and Ring.[7] We here note that the magnitude of the static γ-deformation has been assumed to be negligibly small in our calculation while their single-particle potential (resulting from the Hartree-Bogoliubov calculation) is always non-axial symmetric. The question whether or not the existence of the finite γ-deformation in the s-band is the main reason for the above difference will be discussed in a forthcoming paper.[10]

The computer calculation for this work has been financially supported by Research Center for Nuclear Physics, Osaka University.

1) N. R. Johnson, D. Cline, S. W. Yates, F. S. Stephens, L. L. Riedinger and R. M. Ronningen, Phys. Rev. Letters **40** (1978), 151.
2) O. C. Kistner, A. W. Sunyar and E. der Mateosian, Phys. Rev. **C17** (1978), 1417.
3) A. Bohr and B. R. Mottelson, *Proc. Int. Conf. Nuclear Structure, Tokyo, 1977* [J. Phys. Soc. Japan **44** (1978) Suppl.], p. 157.
4) R. Bengtsson and S. Frauendorf, Nucl. Phys. **A327** (1979), 139.
5) E. R. Marshalek, Nucl. Phys. **A275** (1977), 416.
6) D. Janssen and I. N. Mikhailov, Nucl. Phys. **A318** (1979), 390.
7) J. L. Egido, H. J. Mang and P. Ring, Nucl. Phys. **A339** (1980), 390.
8) Y. R. Shimizu and K. Matsuyanagi, Prog. Theor. Phys. **67** (1982), 1637.
9) Y. Tanaka and S. Suekane, Prog. Theor. Phys. **66** (1981), 1639.
10) Y. R. Shimizu and K. Matsuyanagi, in preparation.

Progress of Theoretical Physics, Vol. 70, No. 1, July 1983

An Extension of the Rotating Shell Model and Its Application to ^{164}Er

Yoshifumi R. SHIMIZU and Kenichi MATSUYANAGI

Department of Physics, Kyoto University, Kyoto 606

(Received October 20, 1982)

We develop an RPA approach based on rotating potentials as an extension of the rotating shell model of nuclear high-spin states. The RPA formalism is applied to the positive-parity yrast spectrum of ^{164}Er. Properties at high spin of the pairing potentials and of the γ-vibrational bands are analyzed as functions of the rotational frequency. The result of calculation indicates an onset in the s-band of instability toward triaxial deformation.

§ 1. Introduction

Recent study on nuclear band structure in the high-spin yrast region has clarified the usefulness and validity of the concept of quasiparticle motion in rotating potentials:[1)~3)] The quasiparticle motion is defined as a function of rotational frequency $\omega_{\rm rot}$ which is a collective parameter characterizing a uniform rotation of a superconducting deformed potential. The approach developed by Bengtsson and Frauendorf[2)] has been called "cranked shell model" or "rotating shell model (RSM)" in order to distinguish it from the more familiar Constrained Hartree-Bogoliubov (CHB) method,[4),5)] because it aims at studying variety of excitation spectra with respect to a reference band which may be taken, for instance, as the ground-state rotational band (g-band). Namely, the interest of the RSM lies in the *relative* energies between the states with the same values of $\omega_{\rm rot}$, rather than the absolute energies of the yrast states themselves.

The quasiparticle states in a *fixed* single-particle potential of the RSM span an orthogonal basis *for each given value of* $\omega_{\rm rot}$ *of the reference band.* This is an important merit of the RSM; for instance, possible quasiparticle correlations may be easily treated in terms of the residual interactions among the quasiparticles that move in the RSM potential. In this way, the RSM treats intrinsic excitations quantum-mechanically while the rotational energies within the semi-classical approximation. On the other hand, the CHB method adopts an alternative approach; namely different potentials would be associated with individual nuclear states, since selfconsistent potential would change from one quasiparticle configuration to another. Obviously, part of the residual interactions in the RSM should correspond to the variation of the selfconsistent potential (in the CHB method) due to the quasiparticle excitations, Thus, the RSM and CHB viewpoints are to be regarded as complements each of the other.

We intend to extend the scope of the RSM by taking into account the quasiparticle correlations. In this paper, we particularly aim at describing the collective vibrational bands in the high-spin yrast region by means of the random-phase approximation (RPA) formulated in a rotating frame. This extension of the RSM would enable us to study the influence of the rapid rotation on microscopic structure of collective vibrations.

The RPA formalism in a rotating frame is briefly outlined in § 2. Several authors have already explored the RPA formalism based on the CHB method, so that formal

aspect of § 2 is rather well known.[6)~11)] However, our approach has a number of new features different from Refs. 6)~11); especially important differences are the followings.
1) Following the RSM point of view, we identify the RPA excitation energies with the relative energies between the two states that are transformed into the rotating frame specified by a definite value of $\omega_{\rm rot}$. This approach avoids the difficult problem of evaluating the amount of the angular momenta transferred by the RPA excitation modes in the laboratory frame.
2) We eliminate the band-band interaction originating from the neutron $i_{13/2}$ orbit when diagonalizing the Coriolis term. This makes it possible to define individual rotational bands as series of states with smoothly changing internal structures.
3) We use, as a residual interaction, the modified quadrupole-quadrupole interaction which is appropriate to rotating deformed potentials. This modification is inevitable in order to adequately describe the β-and γ-vibrations in deformed nuclei. Details of the RSM-plus-RPA approach are described in §§ 3 and 4.

In §§ 5 and 6 we present the result of the analysis of the positive-parity yrast spectrum of ^{164}Er. We first evaluate in § 5 the change of the pairing deformation Δ as a function of $\omega_{\rm rot}$, as well as the difference of Δ according to the choice of the reference band. We then discuss in § 6 the nature of the high-spin portion of the γ-vibrational band by separately calculating the γ-vibrations built on the g-band and those built on the rotation-aligned two-quasiparticle band (s-band). An implication of our result of calculation is pointed out in § 7.

A preliminary version of this work was previously reported in this journal.[12)]

§ 2. The RPA in a rotating frame

2.1. *Construction of the Hamiltonian*

We start with the quasiparticle Hamiltonian in a rotating frame:

$$h'=h_{\rm def}-\Delta(\hat{P}^{\dagger}+\hat{P})-\lambda\hat{N}-\omega_{\rm rot}\hat{J}_x\,, \tag{2·1}$$

where $h_{\rm def}$ describes single-particle motions in a deformed potential and $\hat{P}$ is the nucleon-pair operator defined by $\hat{P}=\sum' c_{\bar{i}}c_i$ with i labeling the single-particle states in an axially symmetric potential and $\bar{i}$ the time-reversed of i. The notation $\sum'$ means the sum over the single-particle states with $m_i-\frac{1}{2}=$even, m_i being the projections of angular momenta on the symmetry axis. The h' can be easily diagonalized by means of the generalized Bogoliubov transformation[5)]

$$\begin{aligned} a_\mu&=\sum_i'(U_{\mu i}d_i+V_{\mu i}d_{\bar{i}}^{\dagger}),\\ a_{\bar{\mu}}&=\sum_i'(\bar{U}_{\mu i}d_{\bar{i}}+\bar{V}_{\mu i}d_i^{\dagger}) \end{aligned} \tag{2·2}$$

with real coefficients U, V, $\bar{U}$ and $\bar{V}$, so that, aside from a constant,

$$h'=\sum_\mu E_\mu a_\mu^{\dagger}a_\mu+\sum_{\bar{\mu}}E_{\bar{\mu}}a_{\bar{\mu}}^{\dagger}a_{\bar{\mu}}\,. \tag{2·3}$$

The operators $(d_i,d_{\bar{i}})$ connected with the nucleon operators $(c_i,c_{\bar{i}})$ by

$$d_i=(c_{\bar{i}}+c_i)/\sqrt{2}\,,$$

$$d_{\bar{i}}=(c_{\bar{i}}-c_i)/\sqrt{2}\,, \tag{2·4}$$

are used in (2·2) so that the quasiparticle operators $(a_\mu, a_{\bar{\mu}})$ satisfy the property

$$e^{-i\pi\hat{J}_x}\begin{pmatrix}a_\mu\\ a_{\bar{\mu}}\end{pmatrix}e^{i\pi\hat{J}_x}=\pm i\begin{pmatrix}a_\mu\\ a_i\end{pmatrix}. \tag{2·5}$$

The quasiparticle states $\mu(\bar{\mu})$ are called the states with signature quantum number[13] $r=-i(r=+i)$.

Let us now introduce the residual interactions between quasiparticles that are consistent with the single-particle Hamiltonian (2·1). The residual pairing interaction associated with the pairing potential $\Delta(\hat{P}^\dagger+\hat{P})$ is readily found to be

$$H_P^{\rm int}=-G\tilde{P}^\dagger\tilde{P}, \qquad \tilde{P}=\hat{P}-\langle\hat{P}\rangle, \tag{2·6}$$

where $\langle\hat{P}\rangle$ denotes an expectation value with respect to a quasiparticle configuration chosen as a reference configuration, and is related to the pairing deformation Δ through the selfconsistency condition $\Delta=G\langle\hat{P}\rangle$.

In a similar manner, assuming a quadrupole deformation for $h_{\rm def}$, we can derive the following residual interaction of the quadrupole-quadrupole type:

$$H_{QQ}^{\rm int}=-\frac{1}{2}\sum_{K=0,1,2}\chi_K^{(+)}\tilde{Q}_K^{(+)\dagger}\tilde{Q}_K^{(+)}-\frac{1}{2}\sum_{K=1,2}\chi_K^{(-)}\tilde{Q}_K^{(-)\dagger}\tilde{Q}_K^{(-)}, \tag{2·7}$$

where $\tilde{Q}_K^{(\pm)}$ are the modified quadrupole operators obtained from the ordinary quadrupole operators

$$\hat{Q}_K^{(\pm)}=\frac{1}{\sqrt{2(1+\delta_{K0})}}\sum_{ij}\langle i|(r^2Y_{2K}\pm r^2Y_{2-K})|j\rangle c_i^\dagger c_j\,, \tag{2·8}$$

through the replacement $x_k\to x_k''$. Here x_k'' are the doubly stretched coordinates defined in Appendix A. The $\tilde{Q}_K^{(\pm)}$ satisfy the same symmetry properties as those of $\hat{Q}_K^{(\pm)}$,

$$e^{-i\pi\hat{J}_x}\tilde{Q}_K^{(\pm)}e^{i\pi\hat{J}_x}=\pm\tilde{Q}_K^{(\pm)}, \quad \tilde{Q}_K^{(\pm)\dagger}=\pm(-1)^K\tilde{Q}_K^{(\pm)} \tag{2·9}$$

so that $\tilde{Q}_K^{(+)}$ $(\tilde{Q}_K^{(-)})$ is the operator with positive (negative) signature. The interaction (2·7) is derived from the consideration of rotating harmonic-oscillator potentials, along the line of Kishimoto et al.[14] (see Appendix A). It should be stressed here that, in contrast to the case of the residual pairing interaction, the operators $\tilde{Q}_K^{(\pm)}$ appearing in $H_{QQ}^{\rm int}$ are different from the quantities $\hat{Q}_K^{(\pm)}-\langle\hat{Q}_K^{(\pm)}\rangle$: The ordinary quadrupole interaction (in terms of $\hat{Q}_K^{(\pm)}$) does not satisfy the selfconsistency condition that the shape of the potential should be proportional to that of density distribution, and thus it cannot reproduce the excitation energies of the β-and γ-vibrations in deformed nuclei.[14)~16] We furthermore note that the force-strength χ for rotating deformed potential might in general depend not only on the K-quantum number but also on the signature $r=\pm1$.

In this way, we obtain the total Hamiltonian that is consistent with (2·1):

$$H=h'+H_P^{\rm int}+H_{QQ}^{\rm int}\,. \tag{2·10}$$

If the quadrupole-pairing deformation is added to the single-particle Hamiltonian h', we

Table I. Quasiparticle representation of the basic operators. All coefficients below are real and satisfy the properties listed in the lower part of this table. The double primes attached to Σ indicate that when the component $(\mu\nu)$ is summed its signature partner $(\bar{\mu}\bar{\nu})$ should also be summed, and the inequality $\mu<\nu$ means that the component $(\nu\mu)$ should *not* be counted independently of $(\mu\nu)$. The quadrupole operators in terms of the doubly stretched coordinates, $\hat{Q}_K^{(\pm)}$, satisfy the same properties as those of $\hat{Q}_K^{(\pm)}$.

$$\hat{N}=\langle\hat{N}\rangle+\Sigma N(\mu\bar{\nu})(A^\dagger_{\mu\bar{\nu}}+A_{\mu\bar{\nu}})\qquad+\Sigma'' N(\mu\nu)B^\dagger_{\mu\nu}$$

$$\hat{P}_\pm=\langle\hat{P}_\pm\rangle+\Sigma P_\pm(\mu\bar{\nu})(A^\dagger_{\mu\bar{\nu}}\pm A_{\mu\bar{\nu}})\qquad+\Sigma'' P_\pm(\mu\nu)B^\dagger_{\mu\nu}$$

$$\hat{J}_x=\langle\hat{J}_x\rangle+\Sigma J_x(\mu\bar{\nu})(A^\dagger_{\mu\bar{\nu}}+A_{\mu\bar{\nu}})\qquad+\Sigma'' J_x(\mu\nu)B^\dagger_{\mu\nu}$$

$$i\hat{J}_y=\sum_{\mu<\nu}{}'' J_y(\mu\nu)(A^\dagger_{\mu\nu}-A_{\mu\nu})\qquad+\Sigma J_y(\mu\bar{\nu})(B^\dagger_{\mu\bar{\nu}}-B_{\mu\bar{\nu}})$$

$$\hat{J}_z=\sum_{\mu<\nu}{}'' J_z(\mu\nu)(A^\dagger_{\mu\nu}+A_{\mu\nu})\qquad+\Sigma J_z(\mu\bar{\nu})(B^\dagger_{\mu\bar{\nu}}+B_{\mu\bar{\nu}})$$

$$\hat{Q}_K^{(+)}=\langle\hat{Q}_K^{(+)}\rangle+\Sigma Q_K^{(+)}(\mu\bar{\nu})(A^\dagger_{\mu\bar{\nu}}+(-1)^K A_{\mu\bar{\nu}})\qquad+\Sigma'' Q_K^{(+)}(\mu\nu)B^\dagger_{\mu\nu}$$

$$\hat{Q}_K^{(-)}=\sum_{\mu<\nu}{}'' Q_K^{(-)}(\mu\nu)(A^{\dagger *}_{\mu\nu}-(-1)^K A_{\mu\nu})\qquad+\Sigma Q_K^{(-)}(\mu\bar{\nu})(B^\dagger_{\mu\bar{\nu}}-(-1)^K B_{\mu\bar{\nu}})$$

$$N(\nu\mu)=N(\mu\nu),\qquad P_\pm(\nu\mu)=\pm P_\pm(\mu\nu),$$

$$J_x(\nu\mu)=J_x(\mu\nu),\quad J_y(\nu\mu)=-J_y(\mu\nu),\quad J_z(\nu\mu)=-J_z(\mu\nu),$$

$$Q_K^{(+)}(\nu\mu)=(-1)^K Q_K^{(+)}(\mu\nu),\quad Q_K^{(-)}(\nu\mu)=-Q_K^{(-)}(\mu\nu)$$

should also add the corresponding residual interaction. However, we restrict in this paper to the simple case of (2·10), leaving this subject for a future work.

2.2. *Coupled dispersion equation*

The basic operators (nucleon number $\hat{N}$, nucleon-pair $\hat{P}$, angular momentum $\hat{\boldsymbol{J}}$, quadrupole moment $\hat{Q}$) can be expressed in terms of the bilinear quasiparticle operators

$$A^\dagger_{\mu\nu}=a^\dagger_\mu a^\dagger_\nu,\qquad A^\dagger_{\mu\bar{\nu}}=a^\dagger_\mu a^\dagger_{\bar{\nu}},$$

$$B^\dagger_{\mu\nu}=a^\dagger_\mu a_\nu,\qquad B^\dagger_{\mu\bar{\nu}}=a^\dagger_\mu a_{\bar{\nu}},\tag{2·11}$$

and their conjugates, as listed in Table I. As is well known, the parts containing the scattering operators $B^\dagger$ or B in the residual interactions do not contribute in the RPA order, and therefore the Hamiltonian (2·10) reduces in this order to the following form:

$$H=\sum_\mu E_\mu a^\dagger_\mu a_\mu+\sum_{\bar{\mu}}E_{\bar{\mu}}a^\dagger_{\bar{\mu}}a_{\bar{\mu}}+H^{(+)}_{\rm int}+H^{(-)}_{\rm int},\tag{2·12}$$

$$H^{(\pm)}_{\rm int}=-\frac{1}{2}\sum_\rho\{\hat{R}^{(\pm)}_\rho\}^2,\tag{2·13}$$

$$\hat{R}^{(+)}_\rho=\sum_{\mu\bar{\nu}}\{R^{(+)}_\rho(\mu\bar{\nu})A^\dagger_{\mu\bar{\nu}}+R^{(+)*}_\rho(\mu\bar{\nu})A_{\mu\bar{\nu}}\},\tag{2·14}$$

$$\hat{R}^{(-)}_\rho=\sum_{\mu<\nu}{}''\{R^{(-)}_\rho(\mu\nu)A^\dagger_{\mu\nu}+R^{(-)*}_\rho(\mu\nu)A_{\mu\nu}\}.\tag{2·15}$$

Here, the positive-signature operators $\hat{R}^{(+)}_\rho$ are defined by

$$\hat{R}^{(+)}_\rho=\sqrt{\frac{G}{2}}\hat{P}_+,\quad i\sqrt{\frac{G}{2}}\hat{P}_-,\quad\sqrt{\chi^{(+)}_0}\,\tilde{Q}^{(+)}_0,\quad i\sqrt{\chi^{(+)}_1}\,\tilde{Q}^{(+)}_1,\quad\sqrt{\chi^{(+)}_2}\,\tilde{Q}^{(+)}_2,\tag{2·16}$$

for $\rho=+$, $-$, 0, 1 and 2, respectively, where $\hat{P}_\pm=\hat{P}^\dagger\pm\hat{P}$. The negative-signature operators $\hat{R}^{(-)}_\rho$ are given by

$$\hat{R}_\rho^{(-)}=\sqrt{\chi_1^{(-)}}\,\tilde{Q}_1^{(-)},\qquad i\sqrt{\chi_2^{(-)}}\,\tilde{Q}_2^{(-)}, \tag{2·17}$$

for $\rho=1$ and 2, respectively. They are all Hermitian. In (2·15), the double primes attached to $\sum$ indicate that, when the component $(\mu\nu)$ is summed, its signature partner $(\bar{\mu}\bar{\nu})$ should also be summed.

The RPA equation of motion

$$[H,\ X_n^{(\pm)\dagger}]_{\mathrm{RPA}}=\hbar\omega_n^{(\pm)}X_n^{(\pm)\dagger} \tag{2·18}$$

for the excitation operators

$$X_n^{(+)\dagger}=\sum_{\mu\bar{\nu}}\{\psi_n^{(+)}(\mu\bar{\nu})A_{\mu\bar{\nu}}^\dagger+\varphi_n^{(+)}(\mu\bar{\nu})A_{\mu\bar{\nu}}\}, \tag{2·19}$$

$$X_n^{(-)\dagger}=\sum_{\mu<\nu}{}''\{\psi_n^{(-)}(\mu\nu)A_{\mu\nu}^\dagger+\varphi_n^{(-)}(\mu\nu)A_{\mu\nu}\}, \tag{2·20}$$

yields the linear homogeneous equation

$$t_\rho^{(\pm)}(\omega)=\sum_{\rho'}S_{\rho\rho'}^{(\pm)}(\omega)t_{\rho'}^{(\pm)}(\omega) \tag{2·21}$$

for the quantities

$$t_\rho^{(\pm)}(\omega)=[\hat{R}_\rho^{(\pm)},\ X_n^{(\pm)\dagger}]_{\mathrm{RPA}}, \tag{2·22}$$

separately for the positive- and negative-signature modes, $X_n^{(+)}$ and $X_n^{(-)}$.*) Here the quantities

$$S_{\rho\rho'}^{(+)}(\omega)=\sum_{\mu\bar{\nu}}\left\{\frac{R_\rho^{(+)*}(\mu\bar{\nu})R_{\rho'}^{(+)}(\mu\bar{\nu})}{E_{\mu\bar{\nu}}-\hbar\omega}+\frac{R_\rho^{(+)}(\mu\bar{\nu})R_{\rho'}^{(+)*}(\mu\bar{\nu})}{E_{\mu\bar{\nu}}+\hbar\omega}\right\}, \tag{2·23}$$

$$S_{\rho\rho'}^{(-)}(\omega)=\sum_{\mu<\nu}{}''\left\{\frac{R_\rho^{(-)*}(\mu\nu)R_{\rho'}^{(-)}(\mu\nu)}{E_{\mu\nu}-\hbar\omega}+\frac{R_\rho^{(-)}(\mu\nu)R_{\rho'}^{(-)*}(\mu\nu)}{E_{\mu\nu}+\hbar\omega}\right\} \tag{2·24}$$

with $E_{\mu\bar{\nu}}=E_\mu+E_{\bar{\nu}}$ and $E_{\mu\nu}=E_\mu+E_\nu$ satisfy the property $S_{\rho\rho'}^{(\pm)}(\omega)=S_{\rho\rho'}^{(\pm)}(-\omega)$. From (2·21) we obtain a coupled dispersion equation which determines the eigenfrequencies ω of the excitations:

$$\det(S_{\rho\rho'}^{(\pm)}(\omega)-\delta_{\rho\rho'})=0\,. \tag{2·25}$$

The quantities $t_\rho^{(\pm)}$, which are connected with the transition matrix elements for the operators $\hat{Q}_K^{(\pm)}$, etc., as well as the RPA amplitudes ψ and φ can be calculated with the normalization condition $[X_n^{(\pm)},\ X_{n'}^{(\pm)\dagger}]_{\mathrm{RPA}}=\delta_{nn'}$ for the positive-frequency modes, n and n'.

2.3. *Explicit separation of the Nambu-Goldstone modes*

The symmetries broken in h' are restored in the RPA order by the residual interactions (2·13) so that Eq. (2·25) contains the solutions corresponding to the relations

$$[H,\ \hat{N}]_{\mathrm{RPA}}=0,\qquad [H,\ \hat{J}_x]_{\mathrm{RPA}}=0\,, \tag{2·26}$$

$$[H,\ \hat{J}_y\mp i\hat{J}_z]_{\mathrm{RPA}}=\pm\hbar\omega_{\mathrm{rot}}(\hat{J}_y\mp i\hat{J}_z). \tag{2·27}$$

The finite energy $\hbar\omega=\hbar\omega_{\mathrm{rot}}$ in (2·27), which is due to the Coriolis term $-\omega_{\mathrm{rot}}\hat{J}_x$ in h', can

*) The subscript RPA attached to the commutator means that it is evaluated within the RPA. Note also that the exchange terms (i.e., the $B^\dagger B$ terms) in the separable interaction $H_{\mathrm{int}}^{(\pm)}$ are neglected in this approximation.

be easily shifted down to zero (see Appendix B), so that the operators $\hat{N}$, $\hat{J}_x$ and $\hat{J}_y \mp i\hat{J}_z$ in the RPA may be called the Nambu-Goldstone (NG) modes.

By making use of Eqs. (A·21)~(A·25),*) and the identities listed in Table III, we can explicitly separate the NG modes out of Eq. (2·25).

For the positive-signature sector, we obtain

$$\omega^4 \det(\bar{S}^{(+)}_{\rho\rho'}(\omega) - x_\rho \delta_{\rho\rho'}) = 0 , \tag{2·28}$$

where

$$\bar{S}^{(+)}_{\rho\rho'}(\omega) = \sum_{\mu\bar{\nu}} \frac{2E_{\mu\bar{\nu}} \bar{R}^{(+)}_\rho(\mu\bar{\nu}) \bar{R}^{(+)}_{\rho'}(\mu\bar{\nu})}{E^2_{\mu\bar{\nu}} - (\hbar\omega)^2} \tag{2·29}$$

Table II. Some kinematical identities resulting from the commutation relations between the basic operators ($\hat{N}$, $\hat{P}_\pm$, $\hat{J}_{x,y,z}$, $\hat{Q}^{(\pm)}_K$). The numbers in the second and third columns indicate the degree of fulfilling the identities within the truncated space of the Nilsson model space. The upper (lower) numbers are those evaluated at $\hbar\omega_{\rm rot} = 0.3$ MeV for neutrons (protons).

	3 major shells	5 major shells
$\sum_{\mu\bar{\nu}} N(\mu\bar{\nu}) P_-(\mu\bar{\nu}) = \langle \hat{P}_+ \rangle$	100% / 100	100% / 100
$2\sum_{\mu\bar{\nu}} J_x(\mu\bar{\nu}) Q^{(+)}_1(\mu\bar{\nu}) = \sqrt{3}\langle \hat{Q}^{(+)}_0 \rangle + \langle \hat{Q}^{(+)}_2 \rangle$	78 / 66	97 / 89
$2\sum''_{\mu<\nu} J_y(\mu\nu) Q^{(-)}_1(\mu\nu) = \sqrt{3}\langle \hat{Q}^{(+)}_0 \rangle - \langle \hat{Q}^{(+)}_2 \rangle$	78 / 66	97 / 89
$2\sum''_{\mu<\nu} J_z(\mu\nu) Q^{(-)}_2(\mu\nu) = 2\langle \hat{Q}^{(+)}_2 \rangle$	100 / 100	100 / 100
$2\sum''_{\mu<\nu} J_y(\mu\nu) J_z(\mu\nu) = \langle \hat{J}_x \rangle$	100 / 100	100 / 100

Table III. Identities derived from the commutators and double-commutators between h' defined by (2·1) and ($\hat{N}$, $\hat{J}_x$, $i\hat{J}_y$, $\hat{J}_z$). Here $h_{\rm def}$ in h' is assumed to be written as $h_{\rm def} = h_{\rm sph} - \alpha_0 \hat{Q}^{(+)}_0 - \alpha_2 \hat{Q}^{(+)}_2$ with $h_{\rm sph}$ being the spherical symmetric part of $h_{\rm def}$. The numbers in the second and third columns indicate the degree of fulfilling the identities within the truncated space of the Nilsson model space. The upper (lower) numbers are those evaluated at $\hbar\omega_{\rm rot} = 0.3$ MeV for neutrons (protons).

$$E_{\mu\bar{\nu}} N(\mu\bar{\nu}) = 2\Delta P_-(\mu\bar{\nu})$$
$$E_{\mu\bar{\nu}} J_x(\mu\bar{\nu}) = (\sqrt{3}\alpha_0 + \alpha_2) Q^{(+)}_1(\mu\bar{\nu})$$
$$E_{\mu\nu} J_y(\mu\nu) = (\sqrt{3}\alpha_0 - \alpha_2) Q^{(-)}_1(\mu\nu) + \omega_{\rm rot} J_z(\mu\nu)$$
$$E_{\mu\nu} J_z(\mu\nu) = 2\alpha_2 Q^{(-)}_2(\mu\nu) + \omega_{\rm rot} J_y(\mu\nu)$$

	3 major shells	5 major shells
$\sum E_{\mu\bar{\nu}} \lvert N(\mu\bar{\nu}) \rvert^2 = 2\Delta \langle \hat{P}_+ \rangle$	100% / 100	100% / 100
$2\sum E_{\mu\bar{\nu}} \lvert J_x(\mu\bar{\nu}) \rvert^2 = (\sqrt{3}\alpha_0 + \alpha_2)(\sqrt{3}\langle \hat{Q}^{(+)}_0 \rangle + \langle \hat{Q}^{(+)}_2 \rangle)$	78 / 67	96 / 87
$2\sum''_{\mu<\nu} E_{\mu\nu} \lvert J_y(\mu\nu) \rvert^2 = (\sqrt{3}\alpha_0 - \alpha_2)(\sqrt{3}\langle \hat{Q}^{(+)}_0 \rangle - \langle \hat{Q}^{(+)}_2 \rangle) + \omega_{\rm rot} \langle \hat{J}_x \rangle$	78 / 67	96 / 87
$2\sum''_{\mu<\nu} E_{\mu\nu} \lvert J_z(\mu\nu) \rvert^2 = 2\alpha_2 \cdot 2\langle \hat{Q}^{(+)}_2 \rangle + \omega_{\rm rot} \langle \hat{J}_x \rangle$	100 / 100	100 / 100

*) The expectation values appearing in the r.h.s. of (A·23)~(A·25) are here to be taken with respect to the actual quasiparticle configuration of the reference band, instead of the pure harmonic oscillator ones considered in Appendix A.

with

$$\bar{R}_\rho^{(+)}(\mu\bar{\nu})=P_+(\mu\bar{\nu}),\quad N(\mu\bar{\nu}),\quad \tilde{Q}_0^{(+)}(\mu\bar{\nu}),\quad J_x(\mu\bar{\nu}),\quad \tilde{Q}_2^{(+)}(\mu\bar{\nu}), \tag{2·30}$$

$$x_\rho=2/G,\qquad 0,\qquad 1/\varkappa_0^{(+)},\qquad 0,\qquad 1/\varkappa_2^{(+)}, \tag{2·31}$$

for $\rho=+$, $-$, 0, 1 and 2, respectively.

For the negative-signature sector, we obtain, on the assumption that $\langle\hat{Q}_2^{(+)}\rangle\neq 0$,

$$(\omega^2-\omega_{\rm rot}^2)\begin{vmatrix}\omega\mathcal{I}_y-\omega_{\rm rot}\mathcal{I}_{yz}, & \omega_{\rm rot}(\mathcal{I}_z-\mathcal{I}_x)-\omega\mathcal{I}_{yz}\\ \omega_{\rm rot}(\mathcal{I}_y-\mathcal{I}_x)-\omega\mathcal{I}_{yz}, & \omega\mathcal{I}_z-\omega_{\rm rot}\mathcal{I}_{yz}\end{vmatrix}=0, \tag{2·32}$$

where

$$\mathcal{I}_y(\omega)=\sum_{\mu<\nu}{}''\frac{2E_{\mu\nu}|J_y(\mu\nu)|^2}{E_{\mu\nu}^2-(\hbar\omega)^2},\quad \mathcal{I}_z(\omega)=\sum_{\mu<\nu}{}''\frac{2E_{\mu\nu}|J_z(\mu\nu)|^2}{E_{\mu\nu}^2-(\hbar\omega)^2}, \tag{2·33}$$

$$\mathcal{I}_{yz}(\omega)=\sum_{\mu<\nu}{}''\frac{2\hbar\omega J_y(\mu\nu)J_z(\mu\nu)}{E_{\mu\nu}^2-(\hbar\omega)^2}, \tag{2·34}$$

and $\mathcal{I}_x=\langle\hat{J}_x\rangle/\omega_{\rm rot}$. As shown by Janssen and Mikhailov[7] and by Marshalek,[8] Eq.(2·32) can be cast into a form suitable for extracting the wobbling modes that are expected in situations characterized by large values of $\langle\hat{Q}_2^{(+)}\rangle$. Furthermore, we can show that Eq. (2·32) coincides with the dispersion equation for the precession modes built on the oblate high-K isomers, investigated by Andersson et al.,[17),18)] in the oblate limit of the deformed potential. On the other hand, in the prolate limit we obtain, by putting $\langle\hat{Q}_2^{(+)}\rangle=0$, the following expression instead of (2·32):

$$(\omega^2-\omega_{\rm rot}^2)\begin{vmatrix}\sum_{\mu<\nu}{}''\frac{2E_{\mu\nu}\{|J_y(\mu\nu)|^2-|J_z(\mu\nu)|^2\}}{E_{\mu\nu}^2-(\hbar\omega)^2}, & \sum_{\mu<\nu}{}''\frac{2\{E_{\mu\nu}J_y(\mu\nu)+\hbar\omega J_z(\mu\nu)\}\tilde{Q}_2^{(-)}(\mu\nu)}{E_{\mu\nu}^2-(\hbar\omega)^2}\\ \sum_{\mu<\nu}{}''\frac{2\{E_{\mu\nu}J_y(\mu\nu)-\hbar\omega J_z(\mu\nu)\}\tilde{Q}_2^{(-)}(\mu\nu)}{E_{\mu\nu}^2-(\hbar\omega)^2}, & \sum_{\mu<\nu}{}''\frac{2E_{\mu\nu}|\tilde{Q}_2^{(-)}(\mu\nu)|^2}{E_{\mu\nu}^2-(\hbar\omega)^2}-\frac{1}{\varkappa_2^{(-)}}\end{vmatrix}=0. \tag{2·35}$$

Needless to say, in actual calculations, the sum with respect to the quasiparticle pairs $(\mu\nu)$, etc., in the $\hat{J}$ and $\hat{Q}$ operators should be taken over protons and neutrons, while the residual pairing interaction should be separately considered for protons and neutrons so that Eq. (2·28) is in fact the 7×7 matrix (instead of 5×5).

§ 3. Specificity of the band

3.1. *Elimination of the interaction between the g- and s-bands*

The band-band interactions between different rotational bands are described in the RSM as the interactions between different quasiparticle configurations in rotating potentials. This description is semi-classical since the bands are treated as wave packets characterized by $\omega_{\rm rot}$ and, therefore, the band-band interaction in the RSM should be distinguished from the interactions between individual rotational *states* with definite angular momenta.[19)]

There are many nuclei for which we know that the elimination of the RSM interaction between the g- and s-bands provides us with a clear lowest-order picture for the microscopic structure of the individual bands.[2),3)] Keeping in mind an application to such situa-

tions, we use the method proposed by Tanaka and Suekane[20] to eliminate the g-s interaction.

Let us first introduce the BCS quasiparticle operators $(b_i^\dagger, b_i)$ by means of the

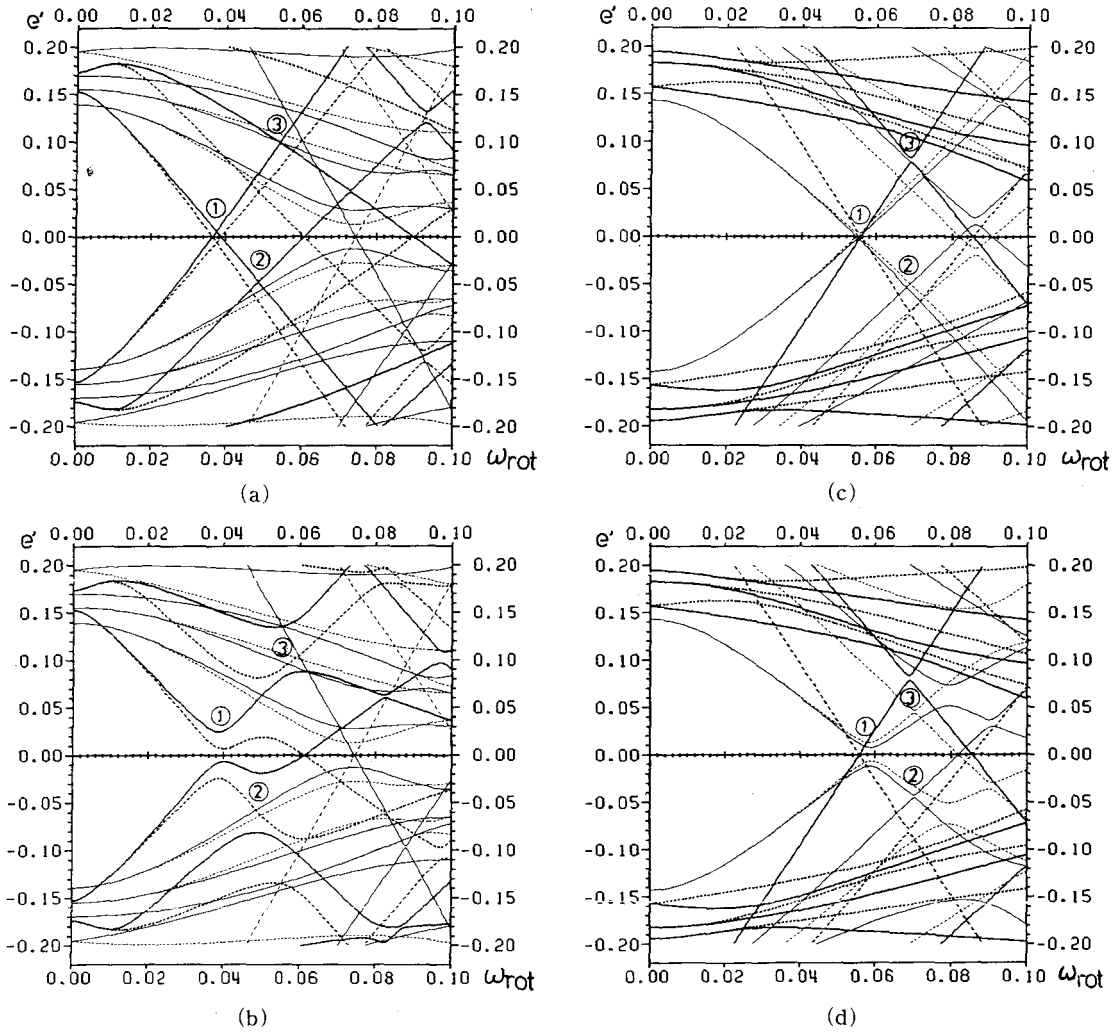

Fig. 1. Quasiparticle energy diagram in units of $\hbar\omega_0 = 7.49$ MeV. The quasiparticle states with signature $r = +i$ $(-i)$ are shown by the solid (dotted) lines. The positive (negative)-parity states are drawn by the thick (thin) lines. The critical rotational frequencies for the occurrence of the band crossings are indicated by the simplified notations like ① $= \omega_{\rm crit}^{(1)}$, ② $= \omega_{\rm crit}^{(2)}$. The deformation parameters used are: $\delta_{\rm osc} = 0.269$, $\Delta = 1.04$ MeV for neutrons, $\Delta = 1.06$ MeV for protons. These values, together with the chemical potentials λ, are fixed at $\omega_{\rm rot} = 0$. The shell-model space used is: $N_{\rm osc} = 3$, 4, 5, 6 and 7 for neutrons, $N_{\rm osc} = 2$, 3, 4, 5 and 6 for protons. Notice that the states with the largest alignment result from the $j_{15/2}$ ($N_{\rm osc} = 7$) and $i_{13/2}$ ($N_{\rm osc} = 6$) orbits for neutrons and protons, respectively.

(a) The neutron part. The band-band interactions originating from the neutron $i_{13/2}$ orbit are eliminated.

(b) The neutron part. The band-band ineractions are included.

(c) The proton part. The band-band interactions originating from the proton $h_{11/2}$ orbit are eliminated.

(d) The proton part. The band-band interactions are included.

ordinary Bogoliubov transformation, $d_i^\dagger = u_i b_i^\dagger + v_i b_{\bar{i}}$, which diagonalizes the Nilsson-plus-BCS Hamiltonian $h_{\rm Nils}$,

$$h_{\rm Nils} = h_{\rm sph} - \alpha_0 \hat{Q}_0^{(+)} - \Delta(\hat{P}^\dagger + \hat{P}) - \lambda \hat{N} \,, \tag{3·1}$$

where $h_{\rm sph}$ denotes the spherically symmetric part. Then, the angular momentum operator is expressed in this basis as

$$\hat{J}_x = \sum_{ij}{}' \langle i|\hat{J}_x|\bar{j}\rangle (u_i u_j + v_i v_j)(b_i^\dagger b_j - b_{\bar{i}}^\dagger b_{\bar{j}}) + \sum_{ij}{}' \langle i|\hat{J}_x|\bar{j}\rangle (u_i v_j - v_i u_j)(b_i^\dagger b_{\bar{j}}^\dagger + b_{\bar{j}} b_i). \tag{3·2}$$

The g-s interaction stems mainly from the specific (ij) components in the second term of (3·2), where both i and j belong to the Nilsson states made mainly out of the neutron $i_{13/2}$ orbit, i.e., roughly speaking, $(ij) \approx (\nu i_{13/2})^2$. Hence, by excluding such specific (ij) components when we diagonalize the h' represented in the $(b^\dagger, b)$ basis, the g-s interaction is removed almost perfectly.*)

The quasiparticle level diagram calculated by the above method is displayed in Fig. 1(a) and compared with the ordinary one, Fig. 1(b), that includes the g-s interaction.

3.2. *Collective vibrations built on a specified rotational band*

Since we have separated out the s-band from the g-band by eliminating their interactions, we are now able to smoothly join the RPA excitations buit on each band across the band-crossing region: To describe the collective vibrations built on the g-band (s-band) after (before) the band-crossing frequency $\omega_{\rm cri}^{(1)}$, we apply the RPA formalism given in § 2 by regarding the lowest-energy two-quasiparticle configuration as the RPA-vacuum. In this way, we can avoid the mixing of different vibrations (built on the g- and s-bands). This mixing would inevitably occur in the case of conventional treatments of the RPA where the *yrast states* are always regarded as the RPA-vacuum, since the yrast states continuously change their characters over the band-crossing region.

§ 4. Calculational procedure

As stated in Introduction, the RSM provides a fixed orthogonal basis for a given $\omega_{\rm rot}$, and does not attempt to calculate the selfconsistent potentials for *individual* excited states. However, the selfconsistent potential for the *reference band* itself is in principle allowed to change as a function of $\omega_{\rm rot}$.

In this paper, we selfconsistently calculate the pairing deformation Δ of the reference band with the use of the pairing-force strength G determined at $\omega_{\rm rot}=0$ by the empirical data for the Δ value of the g-band. On the other hand, we fix the magnitudes of the quadrupole deformations to their empirical values for $\omega_{\rm rot}=0$, i. e., we restrict ourselves to the prolate deformation and neglect their variations with $\omega_{\rm rot}$. This is because there are no definite experimental evidence of a significant change of the quadrupole deformation of the g-band in the range $0 \leq \hbar\omega_{\rm rot} \leq 0.4$ MeV in ^{164}Er which we discuss in this paper.

*) The excluded components are only a small portion of the second term of (3·2), i.e., 7 out of 64 components (in the case of neutrons within the 3 major shells). However, their effect need to be investigated in the future. A possible method that may be used for such a purpose is proposed in Appendix C.

The deformed potential $h_{\rm def}$ used is the one given by Bohr and Mottelson's textbook.[21] As is usually done, the $\Delta N_{\rm osc}=2$ coupling terms arising from the $\boldsymbol{l}\cdot\boldsymbol{s}$ and $\boldsymbol{l}^2$ terms in $h_{\rm def}$ are neglected when diagonalizing h'.*)

The determination of the quadrupole-force strengths $\chi_K^{(\pm)}$ is rather intricate: Firstly, the actual deformed potential in h' is different (because of the $\boldsymbol{l}\cdot\boldsymbol{s}$, $\boldsymbol{l}^2$ and pairing terms) from the harmonic-oscillator potential for which we obtain in Appendix A the analytical expressions of $\chi_K^{(\pm)}$. Secondly, we have in practice to truncate the Nilsson-model space in numerical calculations, although the formulation given in § 2 does not presuppose any space-truncation. Thus, we adopt in this paper the following prescription:

$$\chi_K^{(\pm)}(\omega_{\rm rot})=\chi_K^{(\pm)}(\omega_{\rm rot})\Big|_{\rm theory}\times\frac{\chi_K^{(\pm)}(\omega_{\rm rot}=0)|_{\rm empirical}}{\chi_K^{(\pm)}(\omega_{\rm rot}=0)|_{\rm theory}}\equiv\chi_K^{(\pm)}(\omega_{\rm rot})\Big|_{\rm theory}\times f_K^{(\pm)}. \tag{4·1}$$

Here the index "theory" denotes the theoretical values obtained by replacing the harmonic-oscillator expectation values in the expressions (A·8) and (A·17) for $\chi_K^{(\pm)}$ given in Appendix A, with the ones taken with respect to the actual RPA vacuum, while the index "empirical" those determined at $\omega_{\rm rot}=0$ such that they reproduce 1) the observed β-and γ-vibrational states and 2) the NG modes at zero energy. Actually, as pointed out in Appendix A, the value $\chi_2^{(-)}$ is undefined in the prolate limit so that we adopt an additional assumption $\chi_2^{(-)}=\chi_2^{(+)}$.

It should be stressed that, since all parameters of the calculations are determined at $\omega_{\rm rot}=0$, there are no adjustable parameters for the calculations at finite $\omega_{\rm rot}$.

To see the effect of truncation of the Nilsson-model space, we perform both calculations with five-major shells and with three-major shells, and compare their results. It is always very important to keep in mind that the kinematical identities resulting from the commutation relations, listed in Tables II and III, are not exactly satisfied, once the space is truncated.

§ 5. Configuration- and $\omega_{\rm rot}$-dependence of the pairing potential

The RSM approach is flexible about the choice of the reference band. Thus, we may choose either the g-band or the s-band as the reference band, and calculate the pairing deformation Δ for each band by solving

$$G\langle\phi|\hat{P}|\phi\rangle=\Delta,\qquad \langle\phi|\hat{N}|\phi\rangle=N\,. \tag{5·1}$$

For the g-band, we should use in the above equations

$$|\phi\rangle=\begin{cases}|\phi_0\rangle & \text{for } \omega_{\rm rot}<\omega_{\rm cri}^{(1)},\\ a_\mu^\dagger a_{\bar\nu}^\dagger|\phi_0\rangle & \text{for } \omega_{\rm cri}^{(1)}<\omega_{\rm rot}<\omega_{\rm cri}^{(2)},\\ a_\mu^\dagger a_{\bar\nu}^\dagger|\phi_0 & \text{for } \omega_{\rm cri}^{(2)}<\omega_{\rm rot}<\omega_{\rm cri}^{(3)},\end{cases} \tag{5·2}$$

where $|\phi_0\rangle$ is the quasiparticle vacuum, $(\mu\bar\nu)$ the lowest-energy quasiparticle pair, $(\mu'\bar\nu')$ the second lowest-energy quasiparticle pair formed mainly out of the neutron $i_{13/2}$ orbit, $\omega_{\rm cri}^{(i)}$ the critical rotational frequencies for the band crossings indicated in Fig. 1. On the other hand, we use for the s-band

*) Note that the major part of the $\Delta N=2$ coupling terms in the spherical basis is already taken into account through the use of the deformed harmonic-oscillator basis $\{a_i^\dagger\}$ (see Appendix A).

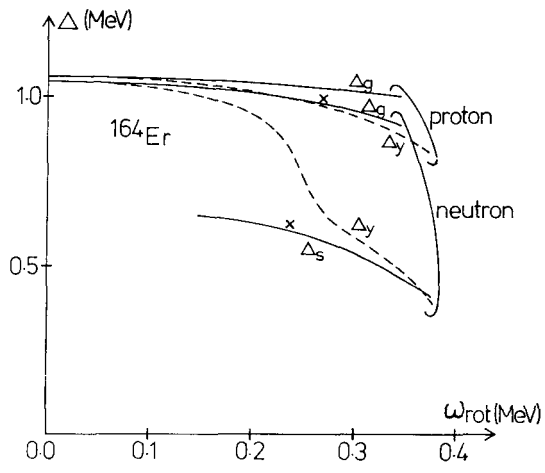

Fig. 2. Pairing deformations of the ground band (Δ_g) and of the Stockholm band (Δ_s) in ^{164}Er calculated as functions of the rotational frequency $\omega_{\rm rot}$. The symbols × denote the critical points at which the two bands intersect each other. The band-band interactions originating from the neutron $i_{13/2}$ (proton $h_{11/2}$) orbit are eliminated in the calculation for neutrons (protons). For comparison, the pairing deformations Δ_y of the yrast states calculated without eliminating the band-band interactions are also shown by the dashed lines, for both neutrons and protons. Note that the proton pairing deformation is common to both g- and s-bands (in the range of $\omega_{\rm rot}$ before the proton alignment occurs).

$$|\phi\rangle=\begin{cases} a_\mu^\dagger a_\nu^\dagger|\phi_0\rangle & \text{for } \omega_{\rm rot}<\omega_{\rm cri}^{(1)}, \\ |\phi_0\rangle & \text{for } \omega_{\rm cri}^{(1)}<\omega_{\rm rot}\,. \end{cases} \tag{5·3}$$

We present in Fig. 2 a theoretical picture on the behaviour of the pairing deformations Δ at high spin in ^{164}Er. The following characteristics are immediately seen:

1) The value Δ decreases only little with increasing $\omega_{\rm rot}$ in each band.*)

2) The Δ_s of the s-band is much smaller than the Δ_g of the g-band, i.e., $\Delta_s \approx 0.6\Delta_g$. Obviously, the reduction of Δ of the s-band is caused by the blocking effect of the rotation-aligned two quasiparticles on the pairing correlation. Thus, if we follow the yrast line, we see that the pairing deformation decreases *stepwise* at the band crossing point.

For comparison, we present in the same figure what we would obtain for the quasiparticle vacuum $|\phi_0\rangle$ if the band-band interaction is not removed. In this case, the pairing deformation Δ_y of the yrast states decreases smoothly over a rather wide region of $\omega_{\rm rot}$. Evidently, this behaviour is caused by the mixing between the g-band and the s-band. As discussed in § 3, however, this mixing evaluated with the semi-classical approximation might be quite different from the mixing effect in the quantum mechanical sense. Thus, the former picture (obtained by removing the g-s interaction) seems to be more realistic at least in a situation in ^{164}Er where experimental data[23),24)] indicate that the band-band interaction is very weak.

In concluding this section, we should emphasize the difference in the physical meaning of Δ between the approach under consideration and the variation after number-projection method.[4),5)] In the latter method, the Δ is treated as a variational parameter and will never vanish as long as there are pairing correlations. In contrast, the Δ determined by (5·1) is meant to be an equilibrium value of the pairing deformation of the *pairing potential,* and therefore it will eventually vanish with increasing number of rotation-aligned nucleons (indicating the occurrence of the phase transition to the normal phase). This is the reason why we prefer to call Δ the *pairing deformation.*

§ 6. Gamma bands in ^{164}Er at high spin

Figure 3(a) shows the experimental data[23)~25)] on the yrast spectrum with positive parity in ^{164}Er, which are transformed into the rotating frame according to the prescrip-

*) A similar result has been reported by Bengtsson and Zhang.[22)]

tion of Ref. 2). Here the reference band is taken to be the g-band. We see that 1) the s-band intersects with the γ-vibrational band at $\hbar\omega_{\rm rot}\approx 0.19$ MeV, but the interaction between the s- and γ-bands is weak (so that it is not visible in this figure). 2) The γ-band comes across another new band at $\hbar\omega_{\rm rot}\approx 0.25$ MeV. This crossing frequency is slightly

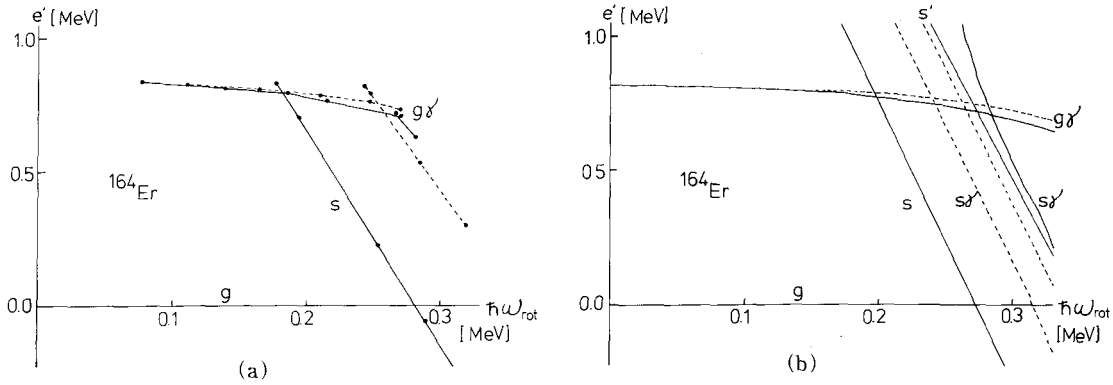

Fig. 3. Yrast spectrum with positive parity in ^{164}Er plotted as a function of $\omega_{\rm rot}$. The solid (dashed) lines show the states with positive (negative) signature.
(a) Experimental data from Ref. 23).
(b) Solutions of the RPA equation (2·25) with the use of five major shells; $N_{\rm osc}=3$, 4, 5, 6 and 7 for neutrons, and $N_{\rm osc}=2$, 3, 4, 5 and 6 for protons. The notation $g\gamma$ ($s\gamma$) means the γ-band built on the g-band (s-band). A common pairing deformation Δ_g is used in calculating the $g\gamma$-and $s\gamma$-bands. For reference, the excitation energies of the s-band and of the s'-band (the second-lowest two-quasipartice aligned states) relative to the g-band are also shown. Notice that this figure is different from the one previously published in Ref. 12).

Table IV. Quadrupole-force strengths $\chi_K^{(\pm)}$ in units of $b_0^{-4}A^{-5/3}$ MeV fm^{-4}, where $b_0^2=\hbar/M\omega_0$ with $\hbar\omega_0=41.0\ A^{-1/3}$ MeV$=7.49$ MeV. Compare with the well-known standard value, 120 $b_0^{-4}\ A^{-5/3}$ MeV fm^{-4}. (a) The values determined at $\omega_{\rm rot}=0$. In the parenthesis are shown the values of $\chi_K^{(\pm)}$ defined in Appendix A. (b) The renormalization factors $f_K^{(\pm)}$ defined by (4·1). (c) The values at $\hbar\omega_{\rm rot}=0.3$ MeV. The upper (lower) numbers in each line are those for the g-band (s-band).

(a)

	$\chi_0^{(+)}$	$\chi_1^{(\pm)}$	$\chi_2^{(\pm)}$
5 major shells	163.7	133.4	126.6
	(120.9)	(110.4)	(184.8)
3 major shells	272.2	195.7	182.5
	(201.1)	(162.0)	(266.4)

(b)

	$f_0^{(+)}$	$f_1^{(\pm)}$	$f_2^{(\pm)}$
5 major shells	1.271	1.032	0.984
3 major shells	1.719	1.370	1.153

(c)

	$\chi_0^{(+)}$	$\chi_1^{(+)}$	$\chi_1^{(-)}$	$\chi_2^{(\pm)}$
5 major shells	163.8	132.8	133.2	126.7
	164.7	135.2	136.2	127.4
3 major shells	272.2	194.4	195.1	182.6
	274.0	198.4	199.9	183.8

smaller than $\hbar\omega_{cri}^{(1)} \approx 0.28$ MeV for the g-s crossing. 3) The negative-signature part of the new band appears in energy significantly below the positive-signature part if they are regarded as signature-doublets.

We present in Fig. 3(b) the result of the RPA calculation that takes into account five major shells of the Nilsson model space. We have always used for this calculation the self-consistent pairing deformations Δ_g for the g-band. The quadrupole-force strengths used are listed in Table IV, in which the values for $f_K^{(\pm)}$ defined by (4·1) are also included.*) As expected from the expressions (A·8) and (A·17), the ω_{rot}- and quasiparticle configuration-dependences of $\varkappa_K^{(\pm)}$ are very weak.

The following points are to be mentioned concerning Fig. 3(b):

1) The s-γ interaction was found to be very weak so that we have drawn this figure as if the s-γ crossing is an interaction-free crossing. The same applies also to other band-crossings shown in this figure, except for the positive-signature γ-vibration built on the s-band mentioned below.

2) Since non-collective two-quasiparticle states intervene in the same energy region, a careful numerical calculation was necessary to find the RPA solution corresponding to the γ-vibration. This especially applies to the positive-signature γ-vibration built on the s-band, where the interactions with the higher-lying non-collective two-neutron-quasiparticle states as well as with the aligned two-proton-quasiparticle states are not always weak.

3) In order to ascertain the reliability of the numerical calculations, we have performed two independent calculations by using either expression (2·25) in § 2.2 or (2·28) and (2·35) given in § 2.3 for the RPA dispersion equation. We found that the resulting eigenfrequencies for the γ-vibrations agree within 50 keV/$\hbar$ in spite of the fact that the two kinds of expressions are, strictly speaking, not equivalent under the truncation of the Nilsson-model space.

4) We have also made calculations using only three major shells and compared with Fig. 3(b). As far as the excitation spectrum is concerned, the difference was found to be negligible (the largest deviation being -20 keV at $\hbar\omega_{rot}=0.3$ MeV for the γ-vibrational energies built on the g-band). Therefore, the effect of space truncation may be said to be renormalizable into the force-strengths (see Table IV). We note, however, that the identities listed in Tables II and III are not well fulfilled in the case of the three major-shell calculation (see the numbers in the right-hand columns of these Tables).

5) The result presented in Fig. 3(b) is slightly different from the one reported in our previous paper.[12] This is because the quadrupole interaction defined by (A·18) with force-strengths $\chi_K^{(\pm)}$ determined in a slightly different manner was used in Ref. 12) instead of the H_{QQ}^{int} defined by (2·7).

We now summarize the result of the RPA calculation, shown in Fig. 3(b), as follows:

1) The energy of the γ-vibration built on the g-band depends only weakly on ω_{rot}. The slight decrease of the RPA energy with increasing ω_{rot} is mainly caused by the slight decrease of the pairing deformation Δ_g of the g-band. This result is in clear agreement with the observed properties of the γ-band.

2) The excitation energies of the negative-signature γ-vibrations built on the s-band is

*) The $f_{K=0}^{(+)}$ values considerably deviate from unity, since, as pointed out in Ref. 26) for the neighboring nucleus ^{168}Er, the first excited 0^+ state in ^{164}Er may not be a good β-vibrational state. However, the $\varkappa_{K=0}^{(+)}$ value is not essential for the γ-vibrations, and therefore we do not attempt in this paper to improve the description of the 0^+ state.

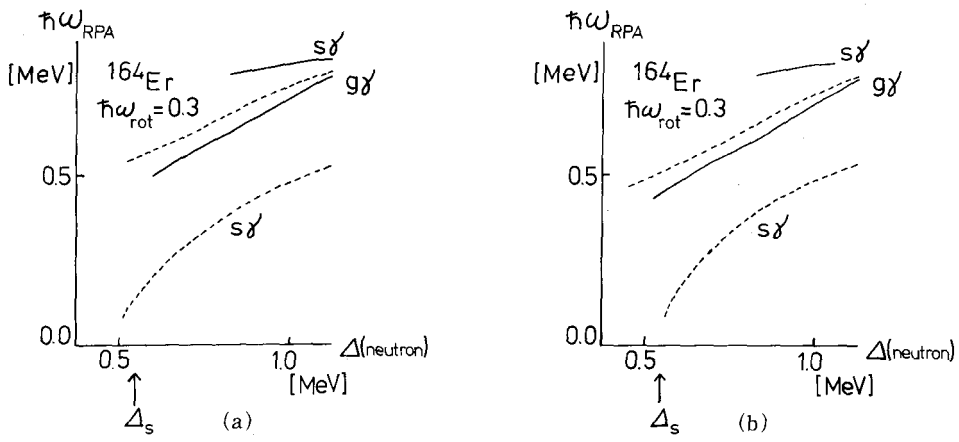

Fig. 4. Dependence of the theoretical γ-vibrational energies upon the magnitude of the neutron pairing deformation. The solid (dashed) lines show the excitations with positive (negative) signature. This is the example calculated at $\hbar\omega_{\rm rot}=0.30$ MeV. The self-consistent value of the pairing deformation for the s-band (Δ_s) is indicated by an arrow.
(a) Result of the five major shell calculation.
(b) Result of the three major shell calculation.

remarkably lowered so that the order of signature splitting is reversed in comparison with that of the γ-band built on the g-band. This is mainly because the low-energy negative-signature two-quasiparticle states built on the s-band acquire an appreciable amount of the transition strength of the Y_{22} type (in comparison with those built on the g-band).[12]

It should be emphasized here that the point 2) above does not imply that the γ-band built on the s-band is a candidate for the observed new band: Firstly, the calculated energies of the negative-signature γ-band built on the s-band are too low to be identified with the new intersecting band. Secondly, the theoretical result for the γ-vibrations excited from the s-band is quite sensitive to the magnitude of the pairing deformation Δ. Figure 4 shows how the RPA energies depend on the values of the neutron pairing deformation used. We see that the negative-signature γ-vibration built on the s-band would be situated in close vicinity to the occurrence of an imaginary RPA solution, if the self-consistent value for the s-band, $\Delta\approx 0.55$ MeV, was used in the RPA calculation.

The above consideration favours the interpretation of the new band as the second-lowest aligned two-quasiparticle band (s'-band), although we need more data especially for the positive-signature sector to establish such an interpretation.

§ 7. Concluding remarks

We have seen in § 6 how the excitation of the rotation-aligned two-quasiparticles modifies the nature of the γ-vibrational mode. The presented numerical result may be taken as an indication of an onset in the s-band of the instability toward triaxial deformation.

As the quasiparticle is a mixture of particle and hole excitaion with comparable amplitudes, the excitation of the aligned two-quasiparticles does not by itself bring about a significant triaxial bulge in the density distribution. On the other hand, it should be stressed that they considerably reduce the magnitude of the pairing deformation Δ through the blocking effect. Thus, we may say that the aligned quasiparticle does play

a role of softening the system toward triaxial shape by reducing the stability of the axial symmetric shape mainly *through the decrease of the pairing deformation.*

Clearly, a more detailed analysis of the relationship between the γ-instability and the pairing deformation is necessary, and we shall report in a separate paper a result which explicitly takes the possibility of the triaxial equilibrium deformation into consideration.

Acknowledgements

One of the authors (K. M.) is grateful to R. Bengtsson and S. Frauendorf for invaluable discussions which formed the background of the present work. The computer calculation for this work has been financially supported by Institute for Nuclear Study, University of Tokyo and by Research Center for Nuclear Physics, Osaka University.

Appendix A

We derive the quadrupole-quadrupole interaction (2·7) appropriate for rotating potentials, along the lines of Ref. 14).

As is well known, the single-particle Hamiltonian for spinless particles moving in a rotating harmonic-oscillator potential can be analytically diagonalized:[27]

$$\begin{aligned} h' &= h_{\rm def} - \omega_{\rm rot} l_1 \\ &= \sum_{n=1}^{A} \left(\frac{\boldsymbol{p}^2}{2M} + \frac{1}{2} M \sum_{i=1,2,3} \omega_i^2 x_i^2 - \omega_{\rm rot} (\boldsymbol{x} \times \boldsymbol{p})_1 \right)_n \\ &= \sum_{n=1}^{A} \left(\frac{1}{2} M \boldsymbol{v}'^2 + \frac{1}{2} M \omega_0^2 \sum_i x_i''^2 \right)_n \\ &= \sum_{n=1}^{A} \left(\sum_i \hbar \Omega_i \left(\alpha_i^\dagger \alpha_i + \frac{1}{2} \right) \right)_n , \end{aligned} \tag{A·1}$$

where $\boldsymbol{v}' = \boldsymbol{p}/M - \boldsymbol{\omega}_{\rm rot} \times \boldsymbol{x}$ and x_i'' are the doubly stretched coordinates defined by $x_i'' = (\omega_i'/\omega_0) x_i$ with

$$\omega_1' = \omega_1, \quad \omega_2' = \sqrt{\omega_2^2 - \omega_{\rm rot}^2}, \quad \omega_3' = \sqrt{\omega_3^2 - \omega_{\rm rot}^2}, \tag{A·2}$$

$\hbar\omega_0$ being an arbitrary energy unit. Obviously, the oscillator frequency ω_1 along the rotational axis is unaltered by the Coriolis term, i.e., $\Omega_1 = \omega_1$. The total energy of the independent-particle system is given in the rotating frame, by

$$E' = \hbar\Omega_1 \Sigma_1 + \hbar\Omega_2 \Sigma_2 + \hbar\Omega_3 \Sigma_3 , \tag{A·3}$$

$$\Sigma_i = \sum_\beta \langle \beta | \alpha_i^\dagger \alpha_i + \frac{1}{2} | \beta \rangle \rho_\beta , \tag{A·4}$$

where ρ_β are the occupation numbers of the single-particle states labeled by β.

Now, let us assume that the velocity distribution of our system is isotropic in the rotating frame (this is equivalent to the requirement of self-consistency between the density distribution and the velocity-independent potential):[21),27)]

$$\Omega_1 \Sigma_1 = \Omega_2 \Sigma_2 = \Omega_3 \Sigma_3 \equiv C . \tag{A·5}$$

The expectation values of $x_i''^2$ are then given as

$$\langle\sum_{n=1}^{A}(x_1''^2)_n\rangle=\langle\sum_{n=1}^{A}(x_2''^2)_n\rangle=\langle\sum_{n=1}^{A}(x_3''^2)_n\rangle=\frac{\hbar C}{M\omega_0^2}. \tag{A·6}$$

Following the Landau prescription to derive the residual interaction, let us calculate the second derivative of E' with respect to ρ. By making use of (A·5) and (A·6) we find that

$$\frac{\partial^2 E'}{\partial\rho_\beta\partial\rho_\gamma}=-\frac{4\pi}{15}\frac{M^2\omega_0^4}{\hbar(\Omega_1\Omega_2\Omega_3\Sigma_1\Sigma_2\Sigma_3)^{1/3}}\cdot 2\sum_{K=0,2}\langle\beta|\tilde{Q}_K^{(+)}|\beta\rangle\langle\gamma|\tilde{Q}_K^{(+)}|\gamma\rangle$$

$$=-\langle\beta\gamma|\sum_{K=0,2}\varkappa_K^{(+)}\tilde{Q}_K^{(+)\dagger}\tilde{Q}_K^{(+)}|\beta\gamma\rangle, \tag{A·7}$$

where

$$\varkappa_0^{(+)}=\varkappa_2^{(+)}=\frac{4\pi}{15}\frac{M\omega_0^2}{(\langle\sum_{n=1}^{A}(x_1''^2)_n\rangle\langle\sum_{n=1}^{A}(x_2''^2)_n\rangle\langle\sum_{n=1}^{A}(x_3''^2)_n\rangle)^{1/3}}. \tag{A·8}$$

Here, $\tilde{Q}_K^{(+)}$ are the modified quadrupole operators written in terms of the doubly stretched coordinates x_i'', and are related to the ordinary quadrupole operators $\hat{Q}_K^{(+)}$,

$$\hat{Q}_0^{(+)}=\sqrt{\frac{5}{16\pi}}\sum_{n=1}^{A}(2x_3^2-x_1^2-x_2^2)_n,\quad \hat{Q}_2^{(+)}=\sqrt{\frac{15}{16\pi}}\sum_{n=1}^{A}(x_1^2-x_2^2)_n \tag{A·9}$$

by

$$\tilde{Q}_0^{(+)}=\sqrt{\frac{5}{16\pi}}\frac{2\omega_3'^2-\omega_1'^2-\omega_2'^2}{3\omega_0^2}\sum_{n=1}^{A}(\boldsymbol{x}^2)_n$$

$$+\frac{4\omega_3'^2+\omega_1'^2+\omega_2'^2}{6\omega_0^2}\hat{Q}_0^{(+)}-\frac{\omega_1'^2-\omega_2'^2}{2\sqrt{3}\omega_0^2}\hat{Q}_2^{(+)}, \tag{A·10}$$

$$\tilde{Q}_2^{(+)}=\sqrt{\frac{15}{16\pi}}\frac{\omega_1'^2-\omega_2'^2}{3\omega_0^2}\sum_{n=1}^{A}(\boldsymbol{x}^2)_n-\frac{\omega_1'^2-\omega_2'^2}{2\sqrt{3}\omega_0^2}\hat{Q}_0^{(+)}+\frac{\omega_1'^2+\omega_2'^2}{2\omega_0^2}\hat{Q}_2^{(+)}. \tag{A·11}$$

It is easily confirmed that

$$\langle\tilde{Q}_0^{(+)}\rangle=\langle\tilde{Q}_2^{(+)}\rangle=0. \tag{A·12}$$

The residual interaction derived above is to be regarded as a part of the quadrupole interaction H_{QQ}^{int} that may be generally written as

$$H_{QQ}^{\text{int}}=-\frac{1}{2}\sum_{K=0,2}\varkappa_K^{(+)}\{\tilde{Q}_K^{(+)}\}^2-\frac{1}{2}\sum_{i=1,2,3}\varkappa^{(i)}\{\tilde{Q}^{(i)}\}^2, \tag{A·13}$$

where

$$\tilde{Q}^{(i)}=\frac{\omega_j'\omega_k'}{\omega_0^2}\hat{Q}^{(i)},\qquad (i,\ j,\ k\ ;\ \text{cyclic}) \tag{A·14}$$

$$\hat{Q}^{(i)}=\sqrt{\frac{15}{4\pi}}\sum_{n=1}^{A}(x_jx_k)_n$$

$$=i\hat{Q}_1^{(+)},\ -\hat{Q}_1^{(-)},\ -i\hat{Q}_2^{(-)}\qquad \text{for } i=1,\ 2,\ 3. \tag{A·15}$$

The force-strengths $\chi^{(i)}$ cannot be uniquely determined by the Landau prescription alone. To determine $\chi^{(i)}$, we require that the combination, $h_{\rm def}+H_{QQ}^{\rm int}$, should commute with l_i in the RPA order:

$$[l_i,\ h_{\rm def}+H_{QQ}^{\rm int}]_{\rm RPA}=[l_i,\ h_{\rm def}]-\sum_j \chi^{(j)}\langle[l_i,\ \tilde{Q}^{(j)}]\rangle \tilde{Q}^{(j)}=0\,. \tag{A·16}$$

Then, we obtain

$$\begin{aligned}\chi^{(i)}&=-\frac{4\pi}{15}\frac{M\omega_0^4}{\omega_j'^2\omega_k'^2}\frac{\omega_j^2-\omega_k^2}{\langle\sum_{n=1}^{A}(x_j^2-x_k^2)_n\rangle}\quad (i,\ j,\ k:\ \text{cyclic})\\ &=\chi_1^{(+)},\ \chi_1^{(-)},\ \chi_2^{(-)}\qquad \text{for } i=1,\ 2,\ 3.\end{aligned} \tag{A·17}$$

We note that the first term of $H_{QQ}^{\rm int}$ does not contribute to (A·16) since $\langle[l_i,\ \tilde{Q}_{K=0,2}^{(+)}]\rangle=0$. We furthermore note that all force-strengths $\chi_K^{(\pm)}$ coincide in the limit, $\omega_{\rm rot}=0$, except that $\chi_2^{(-)}$ is undefined in the prolate limit, $\omega_1=\omega_2$.

In Ref. 12) we used the following interaction:

$$H'_{QQ}=-\frac{1}{2}\sum_{K=0,2}\chi_K^{(+)}\{\hat{Q}_K^{(+)}\}^2-\frac{1}{2}\sum_{i=1,2,3}\chi^{(i)}\{\hat{Q}^{(i)}\}^2\,. \tag{A·18}$$

$$(\chi^{(i)}=\chi_1^{(+)},\ \chi_1^{(-)},\ \chi_2^{(-)}\quad \text{for } i=1,2,3)$$

Apparently, this is merely a part of $H_{QQ}^{\rm int}$ given by (A·13), and $\chi_K^{(\pm)}$ are related to $\varkappa_K^{(\pm)}$ by

$$\chi_0^{(+)}=\varkappa_0^{(+)}\left(\frac{\omega_1'^2+\omega_2'^2+4\omega_3'^2}{6\omega_0^2}\right)^2+\varkappa_2^{(+)}\left(\frac{\omega_1'^2-\omega_2'^2}{2\sqrt{3}\omega_0^2}\right)^2, \tag{A·19}$$

$$\chi_2^{(+)}=\varkappa_0^{(+)}\left(\frac{\omega_1'^2-\omega_2'^2}{2\sqrt{3}\omega_0^2}\right)^2+\varkappa_2^{(+)}\left(\frac{\omega_1'^2+\omega_2'^2}{2\omega_0^2}\right)^2, \tag{A·20}$$

$$\chi^{(i)}=\frac{\omega_j'^2\omega_k'^2}{\omega_0^4}\varkappa^{(i)}.\qquad (i,\ j,\ k;\ \text{cyclic}) \tag{A·21}$$

With the use of the deformation parameters α_0 and α_2 defined through rewriting $h_{\rm def}$ as

$$h_{\rm def}=h_{\rm sph}-\alpha_0\hat{Q}_0^{(+)}-\alpha_2\hat{Q}_2^{(+)}, \tag{A·22}$$

we obtain from (A·17) and (A·21) the following relations:

$$\sqrt{3}\alpha_0+\alpha_2=\chi_1^{(+)}(\sqrt{3}\langle\hat{Q}_0^{(+)}\rangle+\langle\hat{Q}_2^{(+)}\rangle), \tag{A·23}$$

$$\sqrt{3}\alpha_0-\alpha_2=\chi_1^{(-)}(\sqrt{3}\langle\hat{Q}_0^{(+)}\rangle-\langle\hat{Q}_2^{(+)}\rangle), \tag{A·24}$$

$$\alpha_2=\chi_2^{(-)}\langle Q_2^{(+)}\rangle. \tag{A·25}$$

Appendix B

We can easily shift the energy of the NG mode in the negative-signature sector to zero by adding

$$H_{\rm res}^{(-)}=-\frac{1}{2\mathcal{J}_x}(\hat{J}_y^2+\hat{J}_z^2) \tag{B·1}$$

to the Hamiltonian (2·10), since the angular-momentum operators $\hat{J}_i$ commute in the RPA

order with the combination $-\omega_{\rm rot}\hat{J}_x^{\dagger}H_{\rm res}^{(-)}$ when $\mathcal{J}_x=\langle\hat{J}_x\rangle/\omega_{\rm rot}$. The addition of $H_{\rm res}^{(-)}$ does not affect the other RPA modes that commute with the NG mode.

The above recipe may be regarded as an application of the general method of introducing the residual interaction[26]

$$H_{\rm res}=-\frac{1}{2}\sum_k\frac{[h_{\rm sp},\,i\hat{J}_k]^2}{\langle[[h_{\rm sp},\,i\hat{J}_k],\,i\hat{J}_k]\rangle} \tag{B·2}$$

that restores in the RPA order the symmetry broken by the single-particle Hamiltonian $h_{\rm sp}$. Alternatively, the $H_{\rm res}^{(-)}$ may be viewed as a part of the intrinsic Hamiltonian[7] $H_{\rm intri}=H-H_{\rm rot}$ with $H_{\rm rot}=\sum_n h_n(\hat{\boldsymbol{J}}^2)^n$; namely, we get (B·1) by expanding $H_{\rm intri}$ around the equilibrium, $\langle\hat{J}_x\rangle=\omega_{\rm rot}\mathcal{J}_x$ and $\langle\hat{J}_y\rangle=\langle\hat{J}_z\rangle=0$. There are no difference between the use of $H_{\rm intri}$ and that of H' adopted in the text, as far as the microscopic structures of the RPA vibrations are concerned.

Appendix C

Let us assume a case where the RPA Hamiltonian $H^{(2)}$ does not fulfil the symmetry property with respect to $\hat{J}_x$. In the language of the boson-expansion theory, this means that $[H^{(2)},\hat{J}_x^{(1)}]\neq 0$ in the RPA order, where the superscripts denote the order with respect to the boson operators[6] that correspond to the quasiparticle pairs $(A^{\dagger},A)$ given in (2·11). In this case, we can easily construct the modified Hamiltonian $H'^{(2)}$ defined by

$$H'^{(2)}=H^{(2)}-\frac{1}{2}\frac{[H^{(2)},\,i\hat{J}_x^{(1)}]^2}{[[H^{(2)},\,i\hat{J}_x^{(1)}],\,i\hat{J}_x^{(1)}]} \tag{C·1}$$

that obviously commutes with $\hat{J}_x^{(1)}$.

Now, the exact commutation relation $[H,\hat{J}_x]=0$ implies in the RPA order that[6]

$$[H^{(2)},\,\hat{J}_x^{(1)}]+[H^{(1)},\,\hat{J}_x^{(2)}]=0\,. \tag{C·2}$$

With the use of (C·2), we can rewrite (C·1) as

$$H'^{(2)}=H^{(2)}+\frac{1}{2}\frac{[H^{(1)},\,i\hat{J}_x^{(2)}]^2}{[[H^{(1)},\,i\hat{J}_x^{(2)}],\,i\hat{J}_x^{(1)}]}\,. \tag{C·3}$$

The form (C·3) may be more useful than (C·1), because the case considered would occur when the total Hamiltonian expressed in terms of the boson expansion contains a linear term $H^{(1)}$; for instance, the $H^{(1)}$ represents the specific components that are excluded from the Coriolis term, $\omega_{\rm rot}\hat{J}_x$, in order to remove the g-s interaction. It is remarkable that we can express the effect of $H^{(1)}$ in a from of separable interaction as in the expression (C·3).

References

1) A. Bohr and B. R. Mottelson, *Proc. Int. Conf. Nuclear Structure, Tokyo*, 1977 [J. Phys. Soc. Japan Suppl. **44**(1978)], p.157.
2) R. Bengtsson and S. Frauendorf, Nucl. Phys. **A327** (1979), 139.
3) S. Frauendorf, Physica Scripta **24** (1981), 349.
4) H. J. Mang, Phys. Rep. **18** (1975), 325.
5) P. Ring and P. Schuck, *The Nuclear Many-Body Problem* (Springer-Verlag, 1980).
6) E. R. Marshalek, Nucl. Phys. **A275** (1977), 416.

7) D. Janssen and I. N. Mikhailov, Nucl. Phys. **A318** (1979), 390.
8) E. R. Marshalek, Nucl. Phys. **A331** (1979), 429.
9) J. L. Egido, H. J. Mang and P. Ring, Nucl. Phys. **A339** (1980), 390.
10) V. G. Zelevinsky, Nucl. Phys. **A344** (1980), 109.
11) T. Horibata and N. Onishi, Prog. Theor. Phys. **67** (1982),190.
12) Y. R. Shimizu and K. Matsuyanagi, Prog. Theor. Phys. **67** (1982), 1637, 1641; *Proc.* 1982 *INS Int. Symp. Dynamics of Nuclear Collective Motion,* p.110.
13) A. Bohr, *Proc. Int. School of Physics "Enrico Fermi",* course LXIX (Academic Press, 1977), p.3.
14) T. Kishimoto et al., Phys. Rev. Lett. **35** (1975), 552.
T. Kishimoto, *Proc.* 1980 *RCNP Int. Symp. Highly Excited States in Nuclear Reactions, Osaka,* p.145.
15) E. R. Marshalek and J. O. Rasmussen, Nucl. Phys. **43** (1963), 438.
16) T. Suzuki and D.J. Rowe, Nucl. Phys. **A289** (1977), 461.
17) C. G. Andersson, J. Krumlinde, G. Leander and Z. Szymanski, Nucl. Phys. **A361** (1981), 147.
18) H. Kurasawa, Prog. Theor. Phys. **64** (1980), 2055.
19) I. Hamamoto, Nucl. Phys. **A271** (1976), 15.
20) Y. Tanaka and S. Suekane, Prog. Theor. Phys. **66** (1981), 1639.
21) A. Bohr and B. R. Mottelson, *Nuclear Structure* Vol. II, (W. A. Benjamin Inc., 1975).
22) R. Bengtsson and Jing-Ye Zhang, *Proc. of the Nuclear Physics Workshop, Trieste,* 1981 (North-Holland, 1982), p. 165.
23) S. W. Yates et al., Phys. Rev. **C21** (1980), 2366.
24) N. R. Johnson, D. Cline, S. W., Yates, F. S. Stephens, L. L. Riedinger and R. M. Ronningen, Phys. Rev. Lett. **40** (1978), 151.
25) O. C. Kistner, A. W. Sunyar and E. der Mateosian, Phys. Rev. **C17** (1978), 1417.
26) A. Bohr and B. R. Mottelson, Physica Scripta **25** (1982), 28.
27) G. Ripka, J. P. Blaizot and N. Kassis, in *Heavy Ions, High Spin States and Nuclear Structure* Vol. I, (IAEA Vienna, 1975), p. 445.
28) N. I. Pyatov and D. I. Salamov, Nukleonika **22** (1977), 127.

Prog. Theor. Phys. Vol. 70, No. 1, July 1983, Progress Letters

Residual Interactions between Aligned Quasiparticles and Pairing Deformation Changes in ^{165,166}Yb and ^{164}Er

Yoshifumi R. SHIMIZU and Kenichi MATSUYANAGI
Department of Physics, Kyoto University, Kyoto 606
(Received February 12, 1983)

We explicitly evaluate the residual interactions between aligned quasiparticles that are associated with the decrease of the pairing deformation Δ. The result of analysis supports the suggestion by Roy et al. that the residual interactions arise mainly from the blocking effects.

The up-to-date recognition of the major role played by the rotational alignment of quasiparticle angular momenta in the band-crossing phenomena[1),2)] sheds a new light on the mechanism of the pairing deformation change along the yrast line: Namely, the pairing deformation Δ is expected to decrease stepwise at the band-crossing points due to the blocking effects of the aligned quasiparticles, if both the band-band interactions and the dependence of Δ on the rotational frequency $\omega_{\rm rot}$ within individual bands (due to the collective rotations) are weak.

In this letter, we present a result of analysis of the recent experimental data[3),4)] for ^{165,166}Yb and ^{164}Er, that typically exhibit the theoretical picture stated above. In these nuclei, the interactions between the ground band (g-band) and the Stockholm band (s-band) are known to be weak.[3),4)]

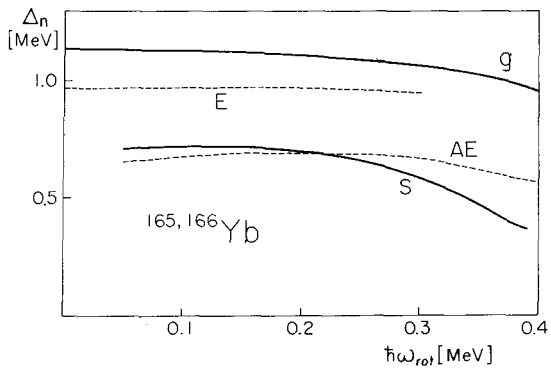

Fig. 1. Theoretical values of the neutron pairing deformation Δ for the g-band and the quasiparticle configurations AB, AE and E in ^{165,166}Yb, plotted as functions of $\omega_{\rm rot}$. The pairing force strength G is determined such that $\Delta_g(\omega_{\rm rot}=0) = \Delta_{oe}=1.139$ MeV. The quasiparticle Hamiltonian is diagonalized in the $N_{\rm osc}=4,5$ and 6 shells with the deformation parameter $\delta_{\rm osc}=0.246$. The parametrization of the deformed single-particle Hamiltonian, $h_{\rm def}$, is the same as in Ref. 11).

Figure 1 shows the self-consistent values of Δ calculated for several bands in ^{165,166}Yb. Here, as in Ref. 3), the capital letters A, B and E are used to denote the lowest $(\pi, r)=(+, -i)$ quasiparticle (qp) state, the lowest $(+, +i)$ qp state, and the lowest $(-, -i)$ qp state, respectively, where π and r mean the parity and the signature. Thus, e.g., the configuration-AE means the lowest-energy negative-parity band with odd angular momenta. We obtained this result by solving the quasiparticle Hamiltonian in a rotating deformed potential[2)]

$$H'=h_{\rm def}-\Delta(\hat{P}^{\dagger}+\hat{P})-\lambda\hat{N}-\omega_{\rm rot}\hat{J}_x \qquad (1)$$

with the self-consistency conditions

$$\Delta=G\langle\phi|\hat{P}|\phi\rangle, \quad N=\langle\phi|\hat{N}|\phi\rangle. \qquad (2)$$

Here, the state vectors $|\phi\rangle$ are in general a few quasiparticle excited states that correspond to individual rotational bands of interest. We constructed these state vectors such that their internal structures smoothly change as a function of $\omega_{\rm rot}$: To make a one-to-one correspondence between the observed bands and the qp configurations in a rotating potential through the band-crossing region, we constructed the diabatic qp representation[5)] by removing a small part of the Coriolis term $-\omega_{\rm rot}\hat{J}_x$, that originates from the neutron $i_{13/2}$ orbit.[6),7)]

We find in Fig. 1 that the 10~15% (30~40%) reduction of Δ occurs due to the one-quasiparticle (two-quasiparticle) alignment. In the following, let us test this theoretical prediction against available experimental data.

Decrease of the band-crossing frequency in odd-A nuclei

In Fig. 2 is made a comparison between the

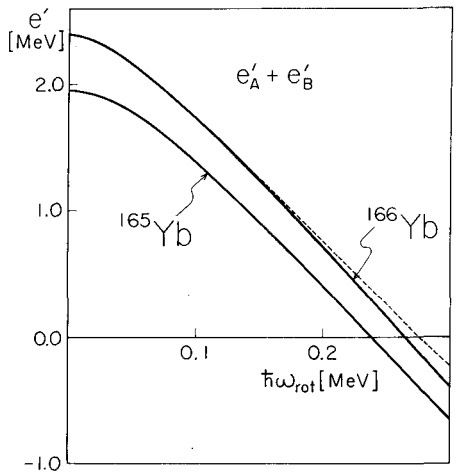

Fig. 2. Comparison between the excitation energies, $e_A' + e_B'$, measured from the configuration E in ^{165}Yb and those measured from the g-band in ^{166}Yb. The self-consistent pairing deformations Δ are used for both cases. For reference, the energies calculated with the value of Δ fixed at $\omega_{rot}=0$ are also shown by broken line.

excitation energies of the aligned quasiparticles AB evaluated by using the selfconsistent value of Δ for the qp configuration E and those calculated with the use of Δ appropriate to the g-band. It is seen that the band-crossing frequency between the configurations E and EAB shifts toward a smaller value (in comparison with the g-s crossing frequency) in odd-A nuclei due to the decrease of Δ. This is exactly the phenomenon which Garrett et al. found in experiments.[8]

Residual interactions in the configurations AB and AE

Very recently, this quantity has been discussed by Roy et al.[3] and by Herskind:[9] The residual interactions v between the quasiparticles, e.g., A and B, may be defined as

$$e'_{AB}(\omega_{rot}) = e_A'(\omega_{rot}) + e_B'(\omega_{rot}) + v_{AB}(\omega_{rot}), \quad (3)$$

where e'_{AB}, e_A', e_B' are excitation energies (at a given value of ω_{rot}) of the qp configurations AB, A and B, measured from the g-band chosen as a reference band. This is an important quantity to measure the independency of the quasiparticle motions in a rotating potential.

Following Refs. 3) and 9), let us assume that major part of v comes from the reduction of Δ due to the blocking effect of the aligned quasiparticles AB, and let us compare the relative energies

$$\varepsilon'_{AB} = \langle\phi_{AB}|H'|\phi_{AB}\rangle - \langle\phi_g|H'|\phi_g\rangle \quad (4)$$

with the sum of the constituent single-qp energies

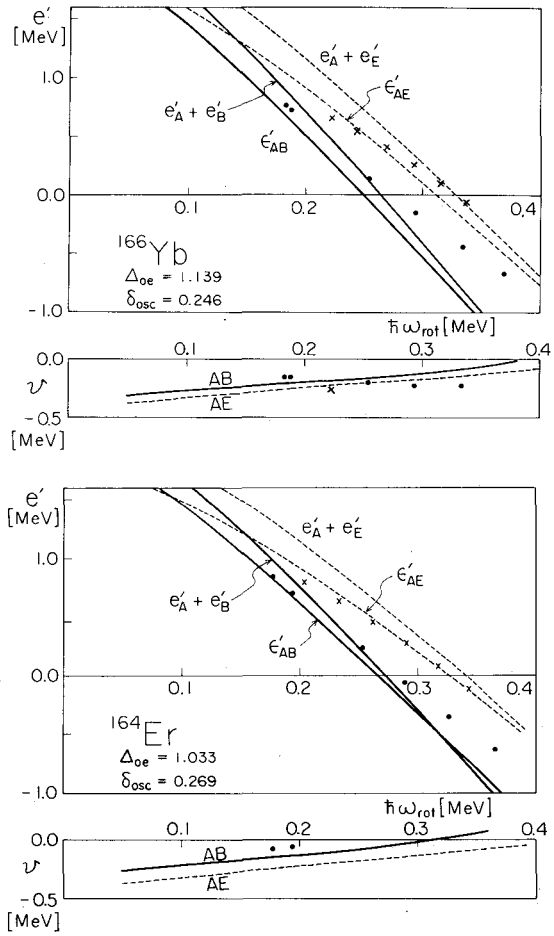

Fig. 3. In the above part, the relative energies ε'_{AB} and ε'_{AE} defined in the text, are compared with the sums $(e_A'+e_B')$ and $(e_A'+e_E')$, respectively. The differences between these quantities are identified with the residual interactions, v_{AB} and $v_{AE'}$ and are shown in the lower part of the figure. The full (broken) lines are used for the configuration AB (AE). Experimental data[3),4)] evaluated in the manner explained in the text are shown by the symbols ● and × for the configurations AB and AE, respectively. The parameters used are: $\delta_{osc}=0.246$, $\Delta_{oe}=1.139$ MeV, $\mathcal{I}_0=29.0\,\mathrm{MeV}^{-1}\hbar^2$, $\mathcal{I}_1=136.0\,\mathrm{MeV}^{-3}\hbar^4$ for ^{166}Yb; $\delta_{osc}=0.269$, $\Delta_{oe}=1.033$ MeV, $\mathcal{I}_0=32.6$ $\mathrm{MeV}^{-1}\hbar^2$, $\mathcal{I}_1=92.5\,\mathrm{MeV}^{-3}\hbar^4$ for ^{164}Er, where $\mathcal{I}_0$ and $\mathcal{I}_1$ are Harris parameters to express the rotational energies of the reference g-band.

$(e_A'+e_B')$ measured from the g-band. Here, $|\phi_{AB}\rangle$ and $|\phi_g\rangle$ are the state vectors with the self-consistent values of Δ, that respectively represent the s-band and the g-band. In Fig. 3, the empirical values of e'_{AB} and v_{AB} are compared with theoretical values of ε'_{AB} and $v_{AB}^{\rm cal}\equiv\varepsilon'_{AB}-(e_A'+e_B')$ calculated with the use of the pairing-force strength G that reproduces the odd-even mass difference Δ_{oe}. The figure is drawn by choosing the g-band as a common reference band. Thus, the empirical values of v_{AB} are extracted from the average values of $(e_A'+e_B')$ for adjacent odd-A nuclei with the use of the same Δ_{oe}.

The theoretical values of $v_{AB}(v_{AE})$ shown in Fig. 3 are seen to be about the same magnitude with the experimental values; thus supporting our assumption on the main origin of them. On the other hand, the calculation tends to overestimate the aligned angular momenta although the quantities ε'_{AB} and ε'_{AE} seem to agree better with experimental data than the sums $(e_A'+e_B')$ and $(e_A'+e_E')$.

To further test our assumption, let us compare the above numerical results with the qualitative estimates based on the following schematic models.

Degenerate model

For the degenerate system with pair degeneracy Ω, the solution of the blocking BCS equation for the pairing Hamiltonian $H_P=-G\tilde{P}^\dagger\tilde{P}$ can be written as

$$\Delta_\nu=\left(1-\frac{\nu}{\Omega}\right)\Delta_{\nu=0}\,, \tag{5}$$

$$\langle\phi_{\nu+2}|H_P|\phi_{\nu+2}\rangle-\langle\phi_\nu|H_P|\phi_\nu\rangle=2\Delta_\nu\,, \tag{6}$$

where ν denotes the seniority. One can easily confirm that Eq. (6) coincides with the exact solution; this fact implies that the additional energy to excite two-quasiparticles from the seniority-ν state, $2\Delta_\nu$, is exactly given within the independent-quasiparticle model, i.e., the residual interaction is zero in this special model.

Uniform level-density model

For the constant level density $g=2/d$, the solution of the blocking BCS equation is approximately written as

$$\Delta_\nu\approx\sqrt{1-\nu d/\Delta_0}\cdot\Delta_0\,, \tag{7}$$

$$\langle\phi_{\nu+2}|H_P|\phi_{\nu+2}\rangle-\langle\phi_\nu|H_P|\phi_\nu\rangle\approx2\Delta_\nu-d\,. \tag{8}$$

This estimate has been utilized by Hamamoto[10] and Herskind[9] to suggest that $v\approx-d\approx-300$ keV.

The numbers we found for ^{166}Yb and ^{164}Er shown in Fig. 3, $v\approx-200$ keV, are indeed close to the estimate based on the uniform level-density model. This agreement can be taken as an additional support to our assumption on the origin of v.

Finally, we want to emphasize the following points: The physical meaning of the quantity Δ characterizing the quasiparticle energy diagram in the rotating shell model (RSM)[2] is the pairing deformation of the reference configuration from which the excitation energies of the states in question are measured. Namely, it is not necessary for the RSM to assume that the self-consistent values of Δ for the excited qp configuration are the same as the one for the reference configuration. In fact, the presented result of realistic calculation indicates that the independent-quasiparticle picture of the RSM holds quite well for the relative quantities like $\langle\phi_{\nu+2}|H'|\phi_{\nu+2}\rangle-\langle\phi_\nu|H'|\phi_\nu\rangle$, and it can be extended in such a way that neglected effects are treated as residual interactions.

We hope that this kind of analysis provides a basis for the study of the mechanism of pairing phase transition which is expected to occur at slightly higher spin region than considered here, where several quasiparticles would align their angular momenta.

The computer calculation for this work has been financially supported by Research Center for Nuclear Physics, Osaka University.

1) A. Bohr and B. R. Mottelson, Physica Scripta **24** (1981), 71.
2) R. Bengtsson and S. Frauendorf, Nucl. Phys. **A327** (1979), 139.
3) N. Roy et al., Nucl. Phys. **A382** (1982), 125.
4) S. W. Yates et al., Phys. Rev. **C21** (1980), 2366.
5) S. Frauendorf, in *Nuclear Physics*, edited by C. H. Dasso, R. A. Broglia and A. Winther (North-Holland, 1982), p. 111.
6) Y. Tanaka and S. Suekane, Prog. Theor. Phys. **66** (1981), 1639.
7) Y. R. Shimizu and K. Matsuyanagi, Prog. Theor. Phys. **70** (1983), 144.
8) J. D. Garrett et al., Phys. Rev. Lett. **47** (1981), 75.
9) B. Herskind, *Proc. of* 1982 *INS Int. Symp. on Dynamics of Nuclear Collective Motion*, p. 443.
10) I. Hamamoto, *ibid.*, p. 78.
11) A. Bohr and B. R. Mottelson, *Nuclear Structure*, vol. II (W. A. Benjamin Inc., 1975).

Progress of Theoretical Physics, Vol. 71, No. 5, May 1984

Incipient Triaxial Deformations of the Rotation-Aligned Bands

—— *Equilibrium Shapes Determined by the Isotropic Velocity Distribution Condition* ——

Yoshifumi R. SHIMIZU and Kenichi MATSUYANAGI

Department of Physics, Kyoto University, Kyoto 606

(Received September 1, 1983)

Shape changes of the rotation-aligned s-bands in Er isotopes are evaluated as functions of rotational frequency by requiring that average velocity distribution at equilibrium shall be isotropic in the rotating frame. Numerical results clearly indicate that small triaxial deformations are induced by excitations of the aligned quasiparticles.

§ 1. Introduction

In recent years, the yrast spectroscopy has rapidly developed so that we can now perform a detailed investigation on the mechanism of shape changes of rotating nuclei along the yrast line.[1] In particular, the decrease of the B(E2) values observed[2] for the s-bands in nuclei with $N \approx 90$ seems to indicate an onset of triaxial deformation associated with the alignment of the quasiparticle angular momenta.[3] It has also been pointed out[4),5] that the properties of the signature splittings for aligned quasiparticle configurations strongly depend on the magnitude and sign of the axial asymmetry.

The first purpose of this paper is to investigate how the equilibrium deformation depends on configuration of the aligned quasiparticles and changes as a function of the rotational frequency $\omega_{\rm rot}$. For this purpose, we perform numerical calculations for the g- and s-bands covering the regions both before and after the band-crossing frequency $\omega_{\rm cri}$: This calculation including the crossing region is made possible by using the diabatic quasiparticle representation[6] described in our previous paper.[7] The second purpose is to demonstrate the feasibility of a simple method of finding the equilibrium shape; namely, to characterize the equilibrium by the property that the average velocity distribution is isotropic in the rotating frame. We call this requirement "isotropic velocity distribution (IVD) condition". The method proposed is not as systematic as the widely-used methods like the Strutinsky method[8] and the constrained Hartree-Bogoliubov method with effective interactions.[9),10] However, it is well adapted for use in conjuction with the modified harmonic-oscillator (h.o.) potential, and in fact it makes the calculations of equilibrium shapes quite simple. Of course, the pairing potential is easily incorporated. This method is semiclassical in nature, but we believe that this characteristic is quite consistent with the idea of the rotating shell model,[11] where the rotating potential itself is described semiclassically in terms of the cranking concept while intrinsic quasiparticle excitations are treated quantum-mechanically.

Our model is formulated in §2 with the use of a deformed potential where the $\boldsymbol{l}^2$- and $\boldsymbol{l}\cdot\boldsymbol{s}$-terms of the Nilsson potential are modified to be written in terms of the doubly stretched coordinates. In §3 the result of numerical calculations for Er isotopes with $90 \leqq N \leqq 98$ is reported, which indicates an occurrence of incipient triaxial deformation in

the s-bands. In §4 we discuss the relationship between the IVD condition and other known methods like energy-minimization methods and semiclassical approximation methods. Conclusions are given in §5.

§ 2. Isotropic velocity distribution in a rotating frame

2. 1. *Single-particle Hamiltonian*

We start with the quasiparticle Hamiltonian in a rotating frame:

$$h' = h_{\rm def} - \Delta(\hat{P}^\dagger + \hat{P}) - \lambda\hat{N} - \omega_{\rm rot}\hat{J}_1 , \tag{2·1}$$

where $h_{\rm def}$ describes the single-particle motions in a deformed potential and other notations are the same as in Ref. 7). As for $h_{\rm def}$, let us adopt the following modified h.o. Hamiltonian:[12]

$$h_{\rm def} = h_{\rm sph}(\boldsymbol{x} \to \tilde{\boldsymbol{x}}), \tag{2·2}$$

$$h_{\rm sph} = \frac{\boldsymbol{p}^2}{2M} + \frac{1}{2}M\omega_0{}^2\boldsymbol{x}^2 + h_{ll} + h_{ls} , \tag{2·3}$$

$$h_{ll} + h_{ls} = v_{ll}\hbar\omega_0(\boldsymbol{l}^2 - \langle \boldsymbol{l}^2\rangle_{N_{\rm osc}}) + v_{ls}\hbar\omega_0 \boldsymbol{l}\cdot\boldsymbol{s} , \tag{2·4}$$

where $\boldsymbol{x} \to \tilde{\boldsymbol{x}}$ means that the spacial coordinates $\boldsymbol{x}$ in $h_{\rm sph}$ are replaced with the doubly stretched coordinates $\tilde{\boldsymbol{x}}$ defined by $\tilde{x}_i = (\omega_i/\omega_0)x_i$.[12] We note that this scaling is applied also to the conventional $\boldsymbol{l}^2$- and $\boldsymbol{l}\cdot\boldsymbol{s}$- terms in order to approximately take into account the deformation effect on them.*) It was confirmed that this modification of the $\boldsymbol{l}^2$- and $\boldsymbol{l}\cdot\boldsymbol{s}$- terms does not significantly affect the single-particle spectrum. However, we will see below that it greatly simplifies an application of the IVD condition to determining the equilibrium shape of rotating nuclei.

As is well known, the anisotropic h.o. part of h' is readily combined with the centrifugal potential contained in $-\omega_{\rm rot}\hat{J}_1$ so that

$$\frac{\boldsymbol{p}^2}{2M} + \frac{1}{2}M\sum_{i=1,2,3}\omega_i{}^2 x_i{}^2 \to \frac{\boldsymbol{\pi}^2}{2M} + \frac{1}{2}M\omega_0{}^2\boldsymbol{x}''{}^2 , \tag{2·5}$$

where

$$x_i'' \equiv \frac{\omega_i{}^{\rm eff}}{\omega_0}x_i , \qquad \omega_i{}^{\rm eff} = \sqrt{\omega_i{}^2 - (1-\delta_{i1})\omega_{\rm rot}^2} , \tag{2·6}$$

$$\boldsymbol{\pi} = \boldsymbol{p} - M\boldsymbol{\omega}_{\rm rot}\times\boldsymbol{x} , \qquad \boldsymbol{\omega}_{\rm rot} = (\omega_{\rm rot}, 0, 0). \tag{2·7}$$

Thus, the doubly stretched coordinate $\boldsymbol{x}''$ defined in the rotating frame transforms the rotating h.o. ellipsoid into a sphere.

2. 2. *Condition of isotropic velocity distribution*

It is well known for the rotating h.o. potential that the IVD condition is equivalent to the requirement that the shape of the density distribution should be proportional to that

*) The mean value of the $\boldsymbol{l}^2$ operator in the $N_{\rm osc}$ shell, $\langle \boldsymbol{l}^2\rangle_{N_{\rm osc}} = \frac{1}{2}N_{\rm osc}(N_{\rm osc}+3)$, is to be scaled[12] by $N_{\rm osc} \to (\omega_1/\omega_0)n_1 + (\omega_2/\omega_0)n_2 + (\omega_3/\omega_0)n_3$. In an operator form, this term after the scaling can be expressed as $\frac{1}{2}\{(\boldsymbol{p}^2/2M\omega_0 + M\omega_0\tilde{\boldsymbol{x}}^2/2)^2 - ((\omega_1+\omega_2+\omega_3)/2\omega_0)^2\}$.

of the velocity-independent potential in the uniformly rotating frame.[13),14)] We now show that this property holds in a very good approximation also for the more realistic Hamiltonian (2·1) under consideration.

To evaluate the velocity distribution, let us calculate the commutators $[x_i p_i,\ h']$, and we obtain

$$\frac{1}{2i}[x_i p_i,\ h']=\frac{\pi_i^2}{2M}-\frac{1}{2}M\omega_0^2 x_i''^2+\delta K_i+\delta P_i$$
$$-(1-\delta_{i1})\frac{1}{2}\{l_1\omega_{\rm rot}-M(x_2^2+x_3^2)\omega_{\rm rot}^2\}, \tag{2·8}$$

where

$$\delta K_i=\frac{1}{2i}[x_i p_i,\ h_{ll}(\boldsymbol{x}\to\tilde{\boldsymbol{x}})+h_{ls}(\boldsymbol{x}\to\tilde{\boldsymbol{x}})]$$
$$=v_{ll}\hbar\omega_0\left[(\tilde{\boldsymbol{x}}^2 p_i^2-\tilde{x}_i^2\boldsymbol{p}^2)-\frac{1}{2}\left\{\frac{\boldsymbol{p}^2}{2M\omega_0}+\frac{M\omega_0\tilde{\boldsymbol{x}}^2}{2},\ \frac{p_i^2}{2M\omega_0}-\frac{M\omega_0\tilde{x}_i^2}{2}\right\}\right]$$
$$+v_{ls}\hbar\omega_0\Big[\sum_{j,k=1,2,3}\epsilon_{ijk}s_k(\tilde{x}_i p_j+\tilde{x}_j p_i)\Big], \tag{2·9}$$

$$\delta P_i=\frac{1}{2i}[x_i p_i,\ -\Delta\cdot(\hat{P}^\dagger+\hat{P})]. \tag{2·10}$$

Here the symbol $\{\ ,\ \}$ denotes the anticommutator and ϵ_{ijk} the three-dimensional totally antisymmetric tensor. By taking the expectation value of both sides of (2·8) with respect to an eigenstate of h', the squared velocity distributions in the rotating frame are calculated to be

$$\frac{1}{2}M\Big\langle\sum_{n=1}^{A}(v_i^2)_n\Big\rangle=\frac{1}{2}M\omega_0^2\Big\langle\sum_{n=1}^{A}(x_i''^2)_n\Big\rangle-(1-\delta_{i1})\frac{1}{2}(\mathcal{J}-\mathcal{J}_{\rm rig})\omega_{\rm rot}^2, \tag{2·11}$$

where $\boldsymbol{v}$ is the velocity in the rotating frame, $\boldsymbol{v}=\boldsymbol{\pi}/M$, and

$$\mathcal{J}\equiv\Big\langle\sum_{n=1}^{A}(l_1)_n\Big\rangle/\omega_{\rm rot},\qquad \mathcal{J}_{\rm rig}\equiv M\Big\langle\sum_{n=1}^{A}(x_2^2+x_3^2)_n\Big\rangle \tag{2·12}$$

with $l_1=x_2p_3-x_3p_2$. In deriving Eq. (2·11), the contributions of δK_i, (2·9), resulting from the commutator with the $\tilde{\boldsymbol{l}}^2$- and $\tilde{\boldsymbol{l}}\cdot\boldsymbol{s}$- terms are neglected because of the following reason: Since the $\tilde{\boldsymbol{l}}$ operator is diagonal with respect to the major quantum number $N_{\rm osc}=n_1+n_2+n_3$, the operators δK_i contain only the terms that change $N_{\rm osc}$ by ±2. Although the cranking term $-\omega_{\rm rot}\hat{J}_1$ contains the components that bring about the $\Delta N_{\rm osc}=\pm2$ mixings in the eigenstates of h', these components accompany a very small factor $(\omega_{\rm rot}/\omega_0)^2\times$ (deformation parameter)^2. Therefore, the expectation values $\langle\delta K_i\rangle$ are negligible. We can also confirm that the expectation values $\langle\delta P_i\rangle$, resulting from the commutator with the pairing potential, exactly vanish (see Appendix A). As for the second term on the r.h.s. of Eq. (2·11), we know that it exactly vanishes in the case of pure h.o. potential, because $\mathcal{J}=\mathcal{J}_{\rm rig}$ in this case.[13)] Although this term appears in a general case, its magnitude is smaller than the first term by a factor $(\omega_{\rm rot}/\omega_0)^2$. Moreover, we can confirm that it is absent in the Thomas-Fermi-like approximation discussed in §4.1. Thus, under the approximation of neglecting 1) the $\Delta N_{\rm osc}=\pm2$ mixing effects due to the

cranking term and 2) the second term in Eq. (2·11), the following property holds for the rotating modified h.o. potential h': The requirement of

$$(\omega_1^{\text{eff}})^2\langle\sum_{n=1}^{A}(x_1^2)_n\rangle=(\omega_2^{\text{eff}})^2\langle\sum_{n=1}^{A}(x_2^2)_n\rangle=(\omega_3^{\text{eff}})^2\langle\sum_{n=1}^{A}(x_3^2)_n\rangle, \tag{2·13}$$

which implies the self-consistency between the density distribution and the velocity-independent potential in the rotating frame, is equivalent to the IVD condition

$$\langle\sum_{n=1}^{A}\langle v_1^2)_n\rangle=\langle\sum_{n=1}^{A}(v_2^2)_n\rangle=\langle\sum_{n=1}^{A}(v_3^2)_n\rangle. \tag{2·14}$$

We note that the above argument would not apply to the ordinary Nilsson Hamiltonian, because $\langle\delta K_i\rangle$ might not be neglected in this case.

It is clear that Eq. (2·14) together with the volume conservation condition*)

$$\omega_1\omega_2\omega_3=\omega_0^3 \tag{2·15}$$

is sufficient to determine the quadrupole shape parameters (β, γ). Various definitions of (β, γ) and their relations to ω_i are summarized in Appendix B. In the succeeding sections, we show that the IVD condition works very well as a principle to determine the equilibrium shapes of rotating nuclei.

§ 3. Equilibrium shapes of the *g*- and *s*- bands in Er isotopes

3. 1. *Details of calculation*

Our objective is to determine as functions of ω_{rot} the shape parameters (β and γ) and the pairing parameters (Δ and λ) for individual rotational bands in the yrast region. They are determined such that Eqs. (2·14), (2·15) and the BCS equations

$$G\langle\hat{P}^\dagger\rangle=\Delta \quad \text{and} \quad \langle\hat{N}\rangle=N\,, \tag{3·1}$$

for both protons and neutrons are satisfied simultaneously. Here the symbol $\langle\ \rangle$ means the expectation values with respect to the specific quasiparticle configurations $|\phi\rangle$ that correspond to the rotational bands of interest. These state vectors $|\phi\rangle$ are constructed with use of the diabatic quasiparticle representation[6] which ensures that the internal structures of individual rotational bands persist through the band-crossing region. We use the method of Ref. 7) for constructing the diabatic representation.

We solve the above-mentioned set of six equations which determine the parameters of the quasiparticle Hamiltonian (2·1) by means of the six-dimensional Newtonian method. In solving these equations, we explicitly use, as the single-particle space to diagonalize (2·1), the $N_{\text{osc}}=3\sim7$ shells for neutrons and $N_{\text{osc}}=2\sim6$ shells for protons, while the contributions from the lower N_{osc}-shells are evaluated with the help of the analytical expressions (see §4. 3 below). As mentioned in §2. 1, the $\Delta N_{\text{osc}}=\pm2$ mixing effects of the cranking term $-\omega_{\text{rot}}\hat{J}_1$ are neglected. On the other hand, we find it important to take into account all the N_{osc}-shells to determine the equilibrium shape.

*) This equation may be regarded as an approximation for situation with small values of $\omega_{\text{rot}}/\omega_0$ to

$$\langle\sum_{n=1}^{A}(x_1^2)_n\rangle\cdot\langle\sum_{n=1}^{A}(x_2^2)_n\rangle\cdot\langle\sum_{n=1}^{A}(x_3^2)_n\rangle=\text{const}$$

or $\omega_1^{\text{eff}}\omega_2^{\text{eff}}\omega_3^{\text{eff}}=\omega_0^3$, which are equivalent under the IVD condition.

The values of v_{tt} and v_{ts} in $h_{\rm def}$ are taken from the Bohr and Mottelson's textbook,[12] while the pairing-force strengths G are parametrized as $G=G_0/A$ and G_0 is fixed at ^{164}Er to give $\Delta_n=1.04$ MeV and $\Delta_p=1.06$ MeV for the ground state. We use the same oscillator length $b^2=\hbar/M\omega_0$ with $\hbar\omega_0=41A^{-1/3}$MeV for both neutrons and protons, because it is found that the calculated equilibrium deformations are changed only within 1% by an explicit consideration of the difference in the root-mean square radii between neutrons and protons.

It should be emphasized that there are no adjustable parameters at all in the calculational scheme described above.

3. 2. *Result of calculations for ground-state deformations*

Figure 1 shows the theoretical ground-state deformations for Dy, Er and Yb isotopes with $86\leqq N\leqq 98$. The equilibrium shapes obtained are always axially symmetric. The agreement between the theoretical and experimental values of $\delta_{\rm osc}$ is satisfactory, except that the calculation tends to slightly (5%~10%) underestimate $\delta_{\rm osc}$. We also present in Fig. 2 the curvatures of the energy surface at the equilibrium,

$$C_\beta\equiv\frac{\partial^2 E}{\partial\beta^2},\qquad C_\gamma\equiv\frac{1}{\beta^2}\frac{\partial^2 E}{\partial\gamma^2}. \qquad (3\cdot2)$$

It is seen that the C_β value increases with increasing N in the region $90\leqq N\leqq 98$, while the C_γ value is approximately constant. Thus, our calculation correctly reproduces the well-known shape transition at $N\approx 90$ from spherical to prolate shapes.

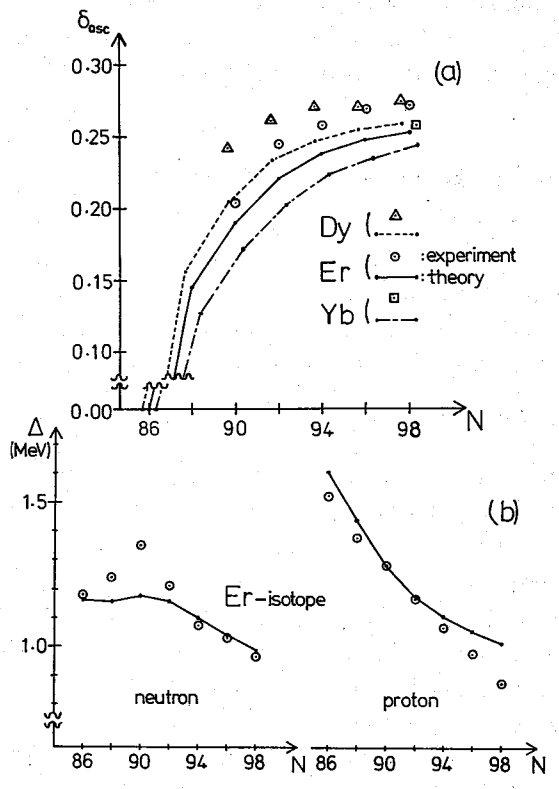

Fig. 1. (a) Equilibrium quadrupole deformations $\delta_{\rm osc}$ of the ground states of Dy, Er and Yb isotopes. The calculated values are shown by lines, while the experimental data taken from Ref. 18) are denoted by symbols △, ⊙, ⊡.

(b) Pairing deformations Δ_n and Δ_p of the ground states of Er isotopes. The experimental values denoted by the symbol ⊙ are obtained by using the third difference formula of the binding energies.

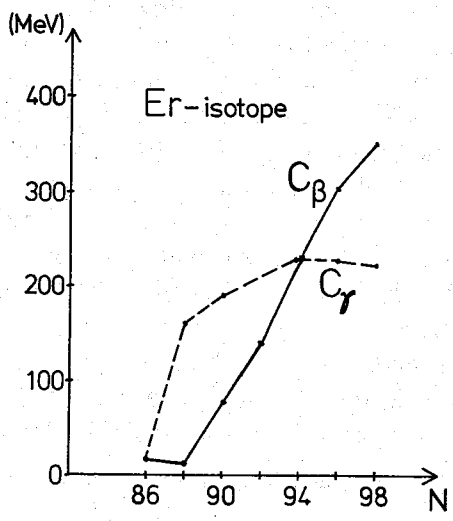

Fig. 2. Curvatures of the energy surfaces, C_β and C_γ, evaluated for the ground states of Er isotopes.

3. 3. *Onset of triaxiality at $\omega_{\rm rot}\neq 0$ in the s-band*

Figure 3 shows the equilibrium deformations (β, γ) of the g- and s-bands calculated as functions of $\omega_{\rm rot}$. We see that, within a given band, the β value stays almost constant, while the absolute value of γ slowly increases as $\omega_{\rm rot}$ increases. It is quite interesting to notice that the sign of γ of the s-band changes as the neutron number changes, and that it is in general not the same as the sign of the g-band. This is a clear manifestation of the role of the rotation-aligned quasiparticles in determining the equilibrium shapes of rotating nuclei. In particular, we note that the tendency toward positive γ (i.e., against the occurrence of the oblate shape with respect to the rotation axis) dominates over that toward negative γ already at $N=94$ (see Fig. 4). This result agrees with the argument of Ref. 5) based on the analysis of classical orbits of the aligned quasiparticles.

To see the dependence of (β, γ) on the pairing deformation Δ, we also indicate by the symbol $\times$ in Fig. 4 the (β, γ) values for the s-bands that would be obtained if the self-consistent values of Δ for neutrons of the s-bands are replaced with those valid for the g-bands. Since the actual values for the s-bands are 30%~40% smaller than those for the g-bands, the small shift from the self-consistent result implies that the equilibrium quadrupole deformations depend on Δ only weakly. Needless to say, this insensitivity to Δ does not mean that the pairing deformation is unimportant to dynamical properties. In fact, as emphasized in Ref. 7), properties of the γ-vibration around the axial symmetric deformation are quite sensitive to the magnitude of Δ. The dependence on Δ of the vibrational properties around the triaxial equilibrium will be discussed in our forthcoming paper.

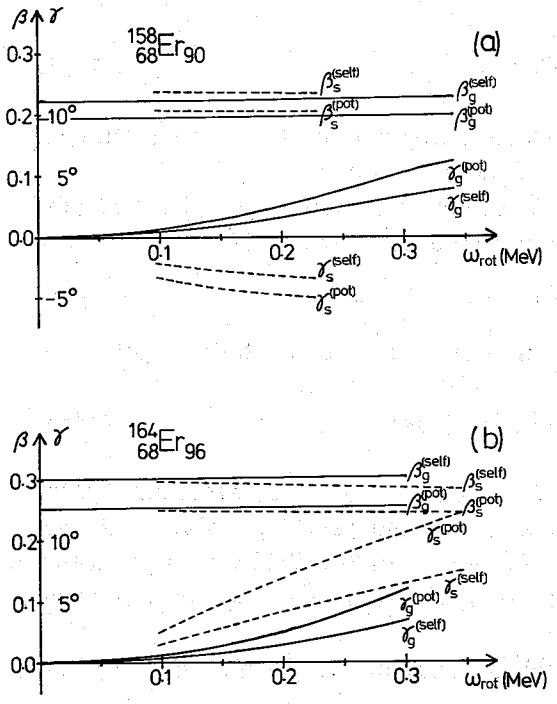

Fig. 3. Equilibrium deformations, $(\beta^{(\rm self)}, \gamma^{(\rm self)})$ and $(\beta^{(\rm pot)}, \gamma^{(\rm pot)})$, of the g- and s- bands calculated as functions of $\omega_{\rm rot}$. The definitions of these quantities are given in Appendix B. (a) ^{158}Er$_{90}$, (b) ^{164}Er$_{96}$.

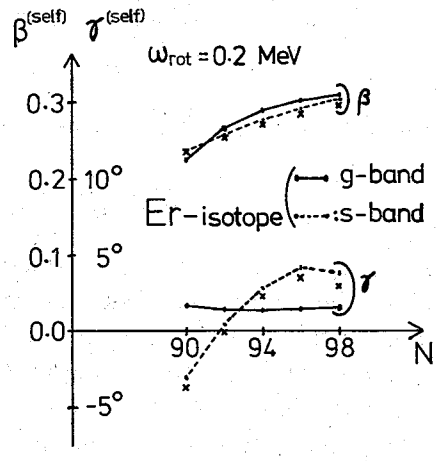

Fig. 4. Equilibrium deformations $(\beta^{(\rm self)}, \gamma^{(\rm self)})$ of the g- and s- bands calculated at $\hbar\omega_{\rm rot}=0.2$ MeV for Er isotopes as functions of the neutron number N. For the meaning of the symbol $\times$, see the text.

§ 4. Discussion on the IVD condition

4. 1. *Relation to the semiclassical approximation*

In order to see the semiclassical nature of the IVD condition, let us consider the distribution function $f(\boldsymbol{x}, \boldsymbol{p})$ in phase space, which is obtained by Wigner-transforming the density matrix $\rho(\boldsymbol{x}, \boldsymbol{x}')$. For systems with rotational and time-reversal invariance, it is rather easy to confirm that the IVD condition is fulfilled. The distribution function for such systems, $f_0(\boldsymbol{x}, \boldsymbol{p})$, has the property

$$\int d\boldsymbol{x} f_0(\boldsymbol{x}, \boldsymbol{p}) = F_0(\boldsymbol{p}^2). \tag{4·1}$$

Thus, the average squared velocity, $\int d\boldsymbol{x}d\boldsymbol{p}v_i^2 f_0(\boldsymbol{x}, \boldsymbol{p})$, is independent of the direction $i(=1, 2, 3)$.

Next, let us consider the rotating deformed nuclei by introducing a prescription which is of semiclassical nature. Namely, let us assume that effects of the deformation and the rotation can be taken into account in a good approximation by the scaling in both coordinates and momenta, $\boldsymbol{x} \to \boldsymbol{x}''$ and $\boldsymbol{p} \to \boldsymbol{\pi}$, with $\boldsymbol{x}''$ and $\boldsymbol{\pi}$ being defined by Eqs. (2·6) and (2·7), i.e., if we assume that

$$f_{\omega \neq 0}(\boldsymbol{x}, \boldsymbol{p}) = f_0(\boldsymbol{x}'', \boldsymbol{\pi}), \tag{4·2}$$

then we readily see that

$$\int d\boldsymbol{x} f_\omega(\boldsymbol{x}, \boldsymbol{p}) = F_0(\boldsymbol{\pi}^2). \tag{4·3}$$

This implies that the average velocity distribution is isotropic in the rotating frame, i.e., the quantity $\int d\boldsymbol{x}d\boldsymbol{p}\pi_i^2 f_\omega(\boldsymbol{x}, \boldsymbol{p})$ is independent of the direction i.

If we additionally adopt the Thomas-Fermi-like approximation that $f_0(\boldsymbol{x}, \boldsymbol{p})$ can be written as a function of the single-particle Hamiltonian $h_{\rm sp}$ alone,[15] i.e.,

$$f_0(\boldsymbol{x}, \boldsymbol{p}) = f_0(h_{\rm sp}(\boldsymbol{x}, \boldsymbol{p})), \tag{4·4}$$

then for the case $h_{\rm sp} = h_{\rm sph}$ adopted in §2 it is easy to derive the following equation:

$$\left\langle \sum_{n=1}^{A} \left(\frac{\pi_i^2}{2M} \right)_n \right\rangle = \frac{1}{2} M\omega_0^2 \langle \sum_{n=1}^{A} (x_i''^2)_n \rangle, \tag{4·5}$$

where the expectation values are defined as $\langle \hat{O} \rangle \equiv \int d\boldsymbol{x}d\boldsymbol{p} \hat{O}(\boldsymbol{x}, \boldsymbol{p}) f_\omega(\boldsymbol{x}, \boldsymbol{p})$ for any operator $\hat{O}$. Thus, the equivalence between conditions (2·13) and (2·14) is established under these approximations. Although Eq. (4·5) is different from Eq. (2·11) in that it does not contain the second term appearing in the latter, this difference does not seem essential at least for situations with $\omega_{\rm rot}/\omega_0 \ll 1$.

Finally, we note that one can determine higher multipole deformations by utilizing higher moments of velocity distributions.

4. 2. *Comparison with other approaches*

It is well known[13),14] that in the case of the nonrotating h.o. potential the equilibrium deformation determined by the IVD condition is equivalent to the one obtained by

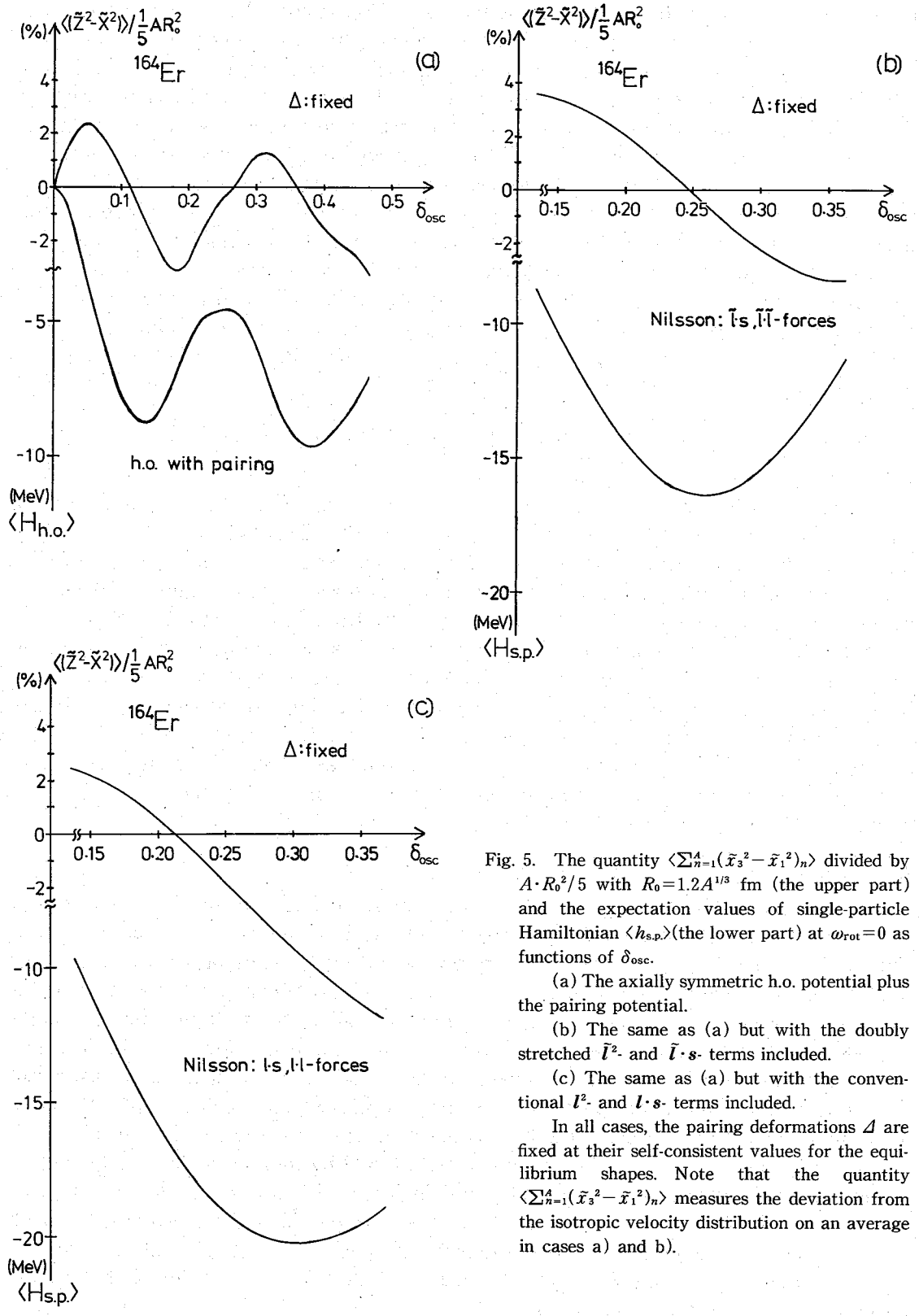

Fig. 5. The quantity $\langle\sum_{n=1}^{A}(\tilde{x}_3^2-\tilde{x}_1^2)_n\rangle$ divided by $A\cdot R_0^2/5$ with $R_0=1.2A^{1/3}$ fm (the upper part) and the expectation values of single-particle Hamiltonian $\langle h_{\text{s.p.}}\rangle$(the lower part) at $\omega_{\text{rot}}=0$ as functions of δ_{osc}.

(a) The axially symmetric h.o. potential plus the pairing potential.

(b) The same as (a) but with the doubly stretched $\tilde{\boldsymbol{l}}^2$- and $\tilde{\boldsymbol{l}}\cdot\boldsymbol{s}$- terms included.

(c) The same as (a) but with the conventional $\boldsymbol{l}^2$- and $\boldsymbol{l}\cdot\boldsymbol{s}$- terms included.

In all cases, the pairing deformations Δ are fixed at their self-consistent values for the equilibrium shapes. Note that the quantity $\langle\sum_{n=1}^{A}(\tilde{x}_3^2-\tilde{x}_1^2)_n\rangle$ measures the deviation from the isotropic velocity distribution on an average in cases a) and b).

minimizing the sum of the single-particle energies, $\langle h_{\rm sp}\rangle$, under the volume-conservation condition (2·15). Figure 5(a) shows that this property holds well even in the presence of the pairing potential. It has been expected that such an equivalence will never exactly hold for a realistic potential like the Nilsson potential. However, we find in Fig. 5(b) that the equilibrium deformation determined by the IVD condition agrees surprisingly well with the one minimizing the $\langle h_{\rm def}\rangle$ *if the single-particle Hamiltonian* $h_{\rm def}$, *Eq.*(2·2), *defined in terms of the doubly-stretched coordinates is adopted.* We feel that this agreement is not accidental but indicates an existence of physical reasons to be studied more deeply. In fact, our numerical calculation shows that the minimum point of $\langle h_{\rm def}\rangle$ sensitively depends on the details of the single-particle Hamiltonian. This point may be seen by comparing Fig. 5(b) with Fig. 5(c) where the ordinary $\boldsymbol{l}^2$- and $\boldsymbol{l}\cdot\boldsymbol{s}$- terms are used. We also mention that the minimum point in Fig. 5(c) would decrease by about 20% if the conventional approximate expression $\frac{1}{2}N_{\rm osc}(N_{\rm osc}+3)$ for the $\langle \boldsymbol{l}^2\rangle_{N_{\rm osc}}$ term is replaced with the exact expression

$$\langle \boldsymbol{l}^2\rangle_{N_{\rm osc}}=\frac{1}{6}\left[\left(\frac{\omega_1}{\omega_2}+\frac{\omega_2}{\omega_1}\right)+\left(\frac{\omega_2}{\omega_3}+\frac{\omega_3}{\omega_2}\right)+\left(\frac{\omega_3}{\omega_1}+\frac{\omega_1}{\omega_3}\right)\right]\frac{1}{2}N_{\rm osc}(N_{\rm osc}+3). \tag{4·6}$$

Bengtsson, Chen, Zhang and Åberg[16] calculated the shapes of $^{160}Yb_{90}$ at high spin and Egido, Mang and Ring[9] those for $^{164}Er_{96}$. The former result, which was obtained by minimizing the expectation value of the single-particle Hamiltonian in a rotating frame, agrees fairly well with our result for $^{158}Er_{90}$ with the same neutron number. The latter result, which is obtained by the constrained Hartree-Bogoliubov method to the conventional pairing-plus-quadrupole (P+QQ) Hamiltonian,[17] is also qualitatively similar to our result for the same nucleus (except for the apparent difference in the treatment of the band-crossing region). It should be noted, however, that there are significant differences in the deformation parameters used; for instance, as is summarized in Appendix B, the equality $\gamma^{(\rm pot)}=\gamma^{(\rm den)}$ is imposed in the latter method as a self-consistency condition, whereas at the equilibrium deformation determined by our method, the value of $\gamma^{(\rm pot)}$ is about twice as large as that of $\gamma^{(\rm den)}$.

4. 3. *Treatment of the low* $N_{\rm osc}$ *shells*

In contrast to the familiar P+QQ model, our method to determine the equilibrium deformation does not presuppose a truncation of the shell-model space. Namely, expectation values appearing in our equations are always meant to be taken with respect to all nucleons in the nucleus. In practice, however, we find it possible to evaluate the contributions from the low $N_{\rm osc}$ shells analytically. Let us consider the state in which all single-particle states of $h_{\rm def}$ are completely filled up to some major quantum number $\mathring{N}_{\rm osc}$, and call it "the inner core". Because the effects of the $\tilde{\boldsymbol{l}}^2$- and $\tilde{\boldsymbol{l}}\cdot\boldsymbol{s}$- terms in $h_{\rm def}$ vanish in the expectation values taken with respect to the inner core, the quantity like $\langle Q^{(+)}_{2\mu}\rangle^{(\rm core)}$ can be analytically calculated by using the anisotropic h.o. wave functions (see Appendix B).

The appropriate value of $\mathring{N}_{\rm osc}$, may be easily found by looking at the single-particle occupation probabilities obtained by diagonalizing the BCS Hamiltonian, $h_{\rm def}-\Delta(\hat{P}^\dagger+\hat{P})-\lambda\hat{N}$. Actually one may choose $\mathring{N}_{\rm osc}=3$ for neutrons and $\mathring{N}_{\rm osc}=2$ for protons, although the more accurate numerical results obtained by the choice $\mathring{N}_{\rm osc}=2$ for neutrons and $\mathring{N}_{\rm osc}=1$ for protons are presented in §3: We examined that the former choice changes the latter numerical results at most 2%.

The inner core plays an indispensable role in determining the equilibrium shapes, even when its contribution to the mass-quadrupole moment $\langle Q_{2\mu}^{(+)}\rangle$ is only about 10% (for the case presented in §3). Because the dependence of the quantity $\langle Q_{2\mu}^{(+)}\rangle$ on the deformation parameters is quite different between the inner core and the total system, the omission of the core contribution would lead to quite different equilibrium deformations. In particular, we note an approximate relation $a_{2\mu}^{(\mathrm{core})} \approx \frac{1}{2} a_{2\mu}^{(\mathrm{self})}$, which is explicitly derived in Appendix B.

§ 5. Conclusions

We have evaluated as functions of ω_{rot} the quadrupole deformations of the g- and s-bands by employing the semiclassical requirement that the equilibrium state should fulfill the IVD condition in the uniformly rotating frame. The method used to determine the equilibrium shapes has been shown to work very well, and the result of numerical calculations clearly indicates that incipient triaxial deformations are certainly induced by excitations of the aligned quasiparticles. It is also found that the sign of the triaxiality parameter γ changes from negative to positive as the neutron number N goes from 90 to 98. However, the absolute magnitudes of $\gamma^{(\mathrm{self})}$ obtained are always smaller than the amplitudes of zero-point vibrations, which are estimated[19] from the properties of the γ-vibrational states to reach about 9°. This fact poses a new problem of elucidating the characteristics of the γ-vibrational modes around the equilibrium shapes with small triaxiality. We shall discuss this problem in a forthcoming paper by combining the method of this paper with the model formulated in Ref. 7) which treats collective correlations between quasiparticles moving in the rotating potential.

Acknowledgements

We thank Dr. T. Kunihiro and Dr. S. Nishizaki for helpful discussions.

The computer calculation for this work has been supported in part by the Grant-in-Aid for Scientific Research of the Japan Ministry of Education, Science and Culture, and in part by Research Center for Nuclear Physics, Osaka University.

Appendix A

The expectation values of the commutator between the pairing potential $\Delta(\hat{P}^{\dagger}+\hat{P})$ and an Hermite operator $\hat{F}_k = \frac{1}{2}\sum_{i,j}\langle i|(x_k p_k + p_k x_k)|j\rangle c_i^{\dagger} c_j$ may be written as

$$\langle[\hat{F}_k, \Delta(\hat{P}^{\dagger}+\hat{P})]\rangle = \Delta\{\langle[\hat{F}_k, \hat{P}^{\dagger}]\rangle - \langle[\hat{F}_k, \hat{P}^{\dagger}]\rangle^*\}. \quad (k=1, 2, 3) \qquad (\mathrm{A}\cdot 1)$$

This equation shows that the expectation values of δP_i defined by (2·10) are zero, if the matrix elements of $[\hat{F}_k, \hat{P}^{\dagger}]$ are real. In fact, it is always possible to choose a phase convention such that the matrix elements like $\langle i|(x_k p_k + p_k x_k)|j\rangle$ and $\langle c_i^{\dagger} c_j^{\dagger}\rangle$ appearing on the r.h.s. of Eq. (A·1) become real. We note that this argument applies also for a general pairing potential which contains, e.g., the quadrupole-pairing component.

Appendix B

Deformation parameters

The deformation parameters (β, γ) may be defined through the quantities $(a_{00}, a_{2\mu})$ as

$$\beta=\sqrt{{a_{20}}^2+{a_{22}}^2} \quad \text{or} \quad \beta'=\sqrt{{a_{20}}^2+{a_{22}}^2}/a_{00} \tag{B·1}$$

$$\tan\gamma=a_{22}/a_{20}\,. \tag{B·2}$$

There are several definitions of $(a_{00}, a_{2\mu})$ with different physical meanings.

(1) $a_{00}^{(\mathrm{den})}$, $a_{2\mu}^{(\mathrm{den})}$ and $a_{00}^{(\mathrm{self})}$, $a_{2\mu}^{(\mathrm{self})}$ These are defined by

$$a_{00}^{(\mathrm{den})}=\langle\sum_{n=1}^{A}(\boldsymbol{x}^2)_n\rangle/\langle\sum_{n=1}^{A}(\boldsymbol{x}''^2)_n\rangle, \tag{B·3}$$

$$a_{2\mu}^{(\mathrm{den})}=\frac{4\pi}{5}\langle Q_{2\mu}^{(+)}\rangle/\langle\sum_{n=1}^{A}(\boldsymbol{x}''^2)_n\rangle, \tag{B·4}$$

where

$$Q_{20}^{(+)}=\sqrt{\frac{5}{16\pi}}\sum_{n=1}^{A}(2{x_3}^2-{x_1}^2-{x_2}^2)_n\,, \tag{B·5}$$

$$Q_{22}^{(+)}=\sqrt{\frac{15}{16\pi}}\sum_{n=1}^{A}({x_1}^2-{x_2}^2)_n\,. \tag{B·6}$$

The quantities $(a_{00}^{(\mathrm{den})}, a_{2\mu}^{(\mathrm{den})})$ are specifically denoted as $(a_{00}^{(\mathrm{self})}, a_{2\mu}^{(\mathrm{self})})$ when the expectation values are evaluated at the equilibrium states satisfying the IVD condition.

(2) $a_{00}^{(\mathrm{pot})}$, $a_{2\mu}^{(\mathrm{pot})}$ These are defined by

$$a_{00}^{(\mathrm{pot})}=\omega_{\mathrm{sph}}^2/{\omega_0}^2\,, \qquad a_{2\mu}^{(\mathrm{pot})}=a_{2\mu}/M{\omega_0}^2\,, \tag{B·7}$$

where $\omega_{\mathrm{sph}}^2=({\omega_1}^2+{\omega_2}^2+{\omega_3}^2)/3$ and $a_{2\mu}(\mu=0, 2)$ are the quantities related to the anisotropic h.o. Hamiltonian $h_{\mathrm{def}}^{(0)}$ through

$$h_{\mathrm{def}}^{(0)}=\frac{\boldsymbol{p}^2}{2M}+\frac{1}{2}M\omega_{\mathrm{sph}}^2\boldsymbol{x}^2-\sum_{\mu=0,2}a_{2\mu}Q_{2\mu}^{(+)}\,. \tag{B·8}$$

(3) $a_{00}^{(\mathrm{L})}$, $a_{2\mu}^{(\mathrm{L})}$ These are also defined through the deformation of the potential, but the quantities $(\omega_{\mathrm{sph}}^{(\mathrm{L})}, a_{2\mu}^{(\mathrm{L})})$ are here defined by rewriting the $h_{\mathrm{def}}^{(0)}$ in terms of the stretched coordinates $x_i'=\sqrt{\omega_i/\omega_0}\,x_i$ as

$$h_{\mathrm{def}}^{(0)}=\frac{\boldsymbol{p}^2}{2M}+\frac{1}{2}M\omega_{\mathrm{sph}}^{(\mathrm{L})2}\boldsymbol{x}'^2-\sum_{\mu=0,2}a_{2\mu}^{(\mathrm{L})}Q_{2\mu}'^{(+)}\,. \tag{B·9}$$

The deformation parameter $\epsilon^{(\mathrm{L})}$ used by the Lund group is related to $\beta^{(\mathrm{L})}$ (defined in terms of $a_{2\mu}^{(\mathrm{L})}$) by

$$\epsilon^{(\mathrm{L})}=\sqrt{\frac{45}{16\pi}}\,2\beta^{(\mathrm{L})}, \tag{B·10}$$

and the sign of γ used by them is opposite to our convention.

(4) $a_{00}^{(\mathrm{core})}$, $a_{2\mu}^{(\mathrm{core})}$ These are defined in the same way as ($a_{00}^{(\mathrm{den})}$, $a_{2\mu}^{(\mathrm{den})}$), but the expectation values are here taken with respect to the inner core wave functions only, i.e., with respect to the states constructed by completely filling the nucleons up to a given $N_{\mathrm{osc}}=\mathring{N}_{\mathrm{osc}}$ shell.

By explicit calculations, we find that these deformation parameters are compactly written down in terms of the oscillator frequencies ω_i as follows:

$$a_{00}=\frac{1}{3}\omega_0{}^p(\omega_1{}^{-p}+\omega_2{}^{-p}+\omega_3{}^{-p}), \tag{B·11}$$

$$a_{20}=\sqrt{\frac{\pi}{45}}\mathrm{sign}(p)\cdot\omega_0{}^p(2\omega_3{}^{-p}-\omega_1{}^{-p}-\omega_2{}^{-p}), \tag{B·12}$$

$$a_{22}=\sqrt{\frac{\pi}{15}}\mathrm{sign}(p)\cdot\omega_0{}^p(\omega_1{}^{-p}-\omega_2{}^{-p}), \tag{B·13}$$

where $p=2$, -2, -1 and 1 for $a^{(\mathrm{self})}$, $a^{(\mathrm{pot})}$, $a^{(\mathrm{L})}$ and $a^{(\mathrm{core})}$, respectively.

It may be convenient to parameterize ω_i as

$$\omega_1=\bar{\omega}\left(1+\frac{1}{3}\delta_{20}-\frac{1}{3}\delta_{22}\right), \tag{B·14}$$

$$\omega_2=\bar{\omega}\left(1+\frac{1}{3}\delta_{20}+\frac{2}{3}\delta_{22}\right), \tag{B·15}$$

$$\omega_3=\bar{\omega}\left(1-\frac{2}{3}\delta_{20}-\frac{1}{3}\delta_{22}\right), \tag{B·16}$$

with $\bar{\omega}=\frac{1}{3}(\omega_1+\omega_2+\omega_3)$ being determined by the volume-conservation condition $\omega_1\omega_2\omega_3=\omega_0{}^3$. To indicate the importance of distinguishing the different definitions summarized above, we show a numerical example for $\delta_{20}=0.3$ and $\delta_{22}=0.1$:

$$\begin{aligned}
&\beta^{(\mathrm{self})} &&=0.454, && \gamma^{(\mathrm{self})} &&=7.9^\circ.\\
&\beta^{(\mathrm{pot})} &&=0.376, && \gamma^{(\mathrm{pot})} &&=16.3^\circ.\\
&\epsilon^{(\mathrm{L})} &&=0.346, && \gamma^{(\mathrm{L})} &&=13.9^\circ.\\
&2\beta^{(\mathrm{core})} &&=0.430, && \gamma^{(\mathrm{core})} &&=9.7^\circ.
\end{aligned}$$

It should be noted that, for the quantities ($a_{00}^{(\mathrm{self})}$, $a_{2\mu}^{(\mathrm{self})}$), the frequencies ω_i in expressions (B·11)~(B·13) are to be replaced with the effective frequencies $\omega_i{}^{\mathrm{eff}}$ defined by (2·6), for the case $\omega_{\mathrm{rot}}\neq 0$.

If we start with the spherical j-j coupling shell model with the ordinary quadrupole force[17] and make a Hartree approximation, then we would obtain a deformed potential of form (B·8) with the quantities $\alpha_{2\mu}$ satisfying the relation

$$\alpha_{22}/\alpha_{20}=\langle Q_{22}^{(+)}\rangle/\langle Q_{20}^{(+)}\rangle. \tag{B·17}$$

The l.h.s. is the same as $a_{22}^{(\mathrm{pot})}/a_{20}^{(\mathrm{pot})}$ while the r.h.s. is equal to $a_{22}^{(\mathrm{self})}/a_{20}^{(\mathrm{self})}$. Thus, it is evident from Eqs. (B·11)~(B·13) that Eq. (B·17) is not compatible with the IVD condition. Namely, the equilibrium shapes calculated by adopting the ordinary quadrupole force may in general be different from those calculated in this paper. The difference is significant; in fact the numerical example listed above indicates that the γ value corre-

sponding to the l.h.s., $\gamma^{(\mathrm{pot})}$, and the one corresponding to the r.h.s., $\gamma^{(\mathrm{self})}$, differs by almost factor two.

References

1) See, e.g., G. A. Leander et al., Nucl. Phys. **A400** (1983), 97c.
2) H. Emling et al., Phys. Lett. **98B** (1981), 169.
   N. R. Johnson, *Proc. of the 1982 INS Sym. on Dynamics of Nuclear Collective Motion,* Mt. Fuji, p. 144.
3) P. Ring, A. Hayashi, K. Hara, E. Emling and E. Grosse, Phys. Lett. **110B** (1982), 423.
4) S. Frauendorf and F. R. May, Phys. Lett. **125B** (1983), 245.
5) I. Hamamoto and B. R. Mottelson, Phys. Lett. **127B** (1983), 281.
6) S. Frauendorf, in *Nuclear Physics,* edited by C. H. Dasso, R. A. Broglia and A. Winther (North-Holland, 1982), p. 111.
7) Y. R. Shimizu and K. Matsuyanagi, Prog. Theor. Phys. **70** (1983), 144.
8) G. Anderson et al., Nucl. Phys. **A268** (1976), 205.
9) J. L. Egido, H. J. Mang and P. Ring, Nucl. Phys. **A339** (1980), 390.
10) J. Fleckner, U. Mosel, P. Ring and H. J. Mang, Nucl. Phys. **A331** (1979), 288.
11) R. Bengtsson and S. Frauendorf, Nucl. Phys. **A327** (1979), 139.
12) A. Bohr and B. R. Mottelson, *Nuclear Structure,* Vol. II. (W. A. Benjamin Inc., 1975), see especially p. 219 and p. 594.
13) See, e.g., G. Ripka, J. P. Blaizot and N. Kassis, in *Heavy Ions, High Spin States and Nuclear Structure,* Vol. I, IAEA Vienna 1975, p. 445.
14) V. G. Zelevinsky, Sov. J. Nucl. Phys. **22** (1976), 565.
15) D. M. Brink and M. Di Toro, Nucl. Phys. **A372** (1981), 151.
16) R. Bengtsson, Y-S. Chen, J-Y. Zhang and S. Åberg, Nucl. Phys. **A405** (1983), 221.
17) D. R. Bès and R. A. Sorensen, *The Pairing-Plus-Quadrupole Model, Advances in Nuclear Physics* (Plenum Press), Vol. 2 (1969), p. 129.
18) K. E. G. Löbner, M. Vetter and V. Hönig, Nuclear Data Tables, **A7** (1970), 495.
19) A. Bohr and B. R. Mottelson, Physica Scripta **25** (1982), 28.

Progress of Theoretical Physics, Vol. 72, No. 4, October 1984

Interplay of Gamma-Vibrations and Aligned-Quasiparticles at High-Spin Yrast Region

Yoshifumi R. SHIMIZU and Kenichi MATSUYANAGI

Department of Physics, Kyoto University, Kyoto 606

(Received May 25, 1984)

On the basis of the self-consistently determined diabatic quasiparticle representation, RPA calculations in the rotating frame are performed for the γ-vibrations around the triaxial equilibrium shapes. The doubly stretched quadrupole forces are used as residual interactions. It is found that the negative-signature γ-vibrational modes created on the s-band well retain their collective characters, while the positive-signature modes tend to lose their identities with increasing rotational frequency.

§ 1. Introduction

In recent years, the rotating shell model (RSM)[1] has become a basis for discussing high-spin yrast spectroscopic data. One of the keys to the success of the RSM is the construction of an orthogonal basis in the rotating frame of reference, called "diabatic quasiparticle representation",[2] which is associated with the rotating deformed potential. In contrast to the "adiabatic representation" which is conventionally adopted in calculations in terms of the constrained Hartree-Bogoliubov method,[3),4] the use of "diabatic representation" enables us to unambiguously specify individual rotational bands in which internal structures of the quasiparticle state vectors smoothly change as functions of the rotational frequency $\omega_{\rm rot}$. Such an unambiguous specification of the rotating frame is especially important in the band-crossing region in order to avoid the shortcoming[5] of the semiclassical (cranking-model) description of the band-band interactions.

In our previous paper,[6] we developed an RPA approach based on the RSM, and investigated the effects of the alignment of quasiparticle angular momenta on collective properties of the γ vibrations in ^{164}Er. It turned out that the negative-signature γ-vibrations built on the Stockholm band (s-band) appear in immediate vicinity to the occurrence of an imaginary RPA solution, indicating an instability toward triaxial deformations. We then performed in Ref. 7) a self-consistent calculation of the equilibrium deformations for both the g- and s-band as a function of $\omega_{\rm rot}$, and found that small triaxial deformations are indeed induced in the s-band due to the excitations of the aligned quasiparticles.

In this paper, we perform an RPA calculation for γ vibrations around the rotating *triaxial* equilibrium shapes which are self-consistently determined. The RPA calculations for the same problem have been reported by Egido, Mang and Ring[8] (see also Refs. 9) ~13)). However, their calculation is based on the adiabatic representation in which strong band-band interactions inevitably occur over a rather wide range of angular momenta. Thus, physical interpretation of their calculated results is not always clear-cut.

In §2 we briefly review the basic framework of our RPA approach based on the diabatic quasiparticle representation. Here, we shall construct the RPA excitations not only from the yrast states but also from the excited quasiparticle configurations, and use, as residual interactions, the doubly stretched quadrupole forces.[14)~16] After describing

the calculational details in §3, we present in §4 the result of numerical calculations for ^{164}Er. The result will show that a drastic signature splitting occurs in the γ vibrations created on the s-band; this indicates a significant character change of the γ vibrations induced by the aligned quasiparticles. The main conclusions of this theoretical calculation are summarized in §5.

It should be mentioned that the model developed here is able to describe both the low-lying $\Delta N_{\rm osc}=0$ vibrations and the high-lying $\Delta N_{\rm osc}=2$ excitations (giant quadrupole resonances) simultaneously. Actually, we have performed theoretical calculations also for the latter excitations, and the result is reported in an accompanying paper.[17]

§ 2. The microscopic model

In this section we summarize the basic principles of our model. Mathematical details and precise definitions of the notations used can be found in Refs. 6) and 7).

2. 1. *The self-consistent diabatic basis*

We start with the single-particle Hamiltonian in the frame uniformly rotating with the angular frequency $\omega_{\rm rot}$,

$$h'_{\rm sp}=h_{\rm sp}-\omega_{\rm rot}\hat{J}_x\,, \tag{2·1}$$

where $h_{\rm sp}=h_{\rm def}-\Delta(\hat{P}^\dagger+\hat{P})-\lambda\hat{N}$ and $h_{\rm def}$ is defined by

$$h_{\rm def}=h_{\rm sph}(\boldsymbol{x}\to\tilde{\boldsymbol{x}},\ \boldsymbol{p}), \tag{2·2}$$

$$h_{\rm sph}=\sum_{n=1}^{A}\left\{\frac{\boldsymbol{p}^2}{2M}+\frac{1}{2}M\omega_0{}^2\boldsymbol{x}^2+v_{ls}\boldsymbol{l}\cdot\boldsymbol{s}+v_{ll}(\boldsymbol{l}^2-\langle\boldsymbol{l}^2\rangle_N)\right\}_n. \tag{2·3}$$

Here the notation $\boldsymbol{x}\to\tilde{\boldsymbol{x}}$ implies that the coordinates x_i $(i=1, 2, 3)$ are replaced by the doubly stretched coordinates $\tilde{x}_i\equiv(\omega_i/\omega_0)x_i$. Note that this replacement applies also to the coordinate $\boldsymbol{x}$ contained in $\boldsymbol{l}$ appearing in the $\boldsymbol{l}\cdot\boldsymbol{s}$-, $\boldsymbol{l}^2$- and $\langle\boldsymbol{l}^2\rangle_N$-terms. We can easily diagonalize the $h'_{\rm sp}$ to obtain

$$h'_{\rm sp}=\langle\phi_0|h'_{\rm sp}|\phi_0\rangle+\sum_{\mu}E_\mu a_\mu{}^\dagger a_\mu+\sum_{\bar{\mu}}E_{\bar{\mu}}a_{\bar{\mu}}{}^\dagger a_{\bar{\mu}}\,, \tag{2·4}$$

where $a_\mu{}^\dagger$ and $a_{\bar{\mu}}{}^\dagger$ represent the quasiparticles with the signature quantum number $r=-i$ and $+i$, respectively.

To construct the diabatic representation, we exclude a special part of the Coriolis force that is responsible for the interactions between the ground- and the aligned two-quasiparticle bands (see also Ref. 18)).

To describe individual rotational bands, we have to carefully identify the quasiparticle configurations across the band crossing region such that their internal structures smoothly change as functions of $\omega_{\rm rot}$. This is done in the following way. Let us denote the quasiparticles defined with respect to the yrast configuration $|\phi_{\rm y}\rangle$ by $(\mathring{a}_\mu{}^\dagger,\ \mathring{a}_{\bar{\nu}}{}^\dagger)$; i.e.,

$$\mathring{a}_\mu|\phi_{\rm y}\rangle=\mathring{a}_{\bar{\nu}}|\phi_{\rm y}\rangle=0\,, \tag{2·5}$$

where $|\phi_{\rm y}\rangle$ is constructed to be the lowest-energy state at a given value of $\omega_{\rm rot}$. Then, the quasiparticle configurations describing individual rotational bands take in general the

following form:

$$|\phi_{\text{band}}\rangle=(\prod_{\mu=1}^{n_+}\mathring{a}_\mu^\dagger)(\prod_{\bar{\nu}=1}^{n_-}\mathring{a}_{\bar{\nu}}^\dagger)|\phi_{\text{y}}\rangle;\qquad \omega_{\text{cri}}^{(i)}<\omega_{\text{rot}}<\omega_{\text{cri}}^{(j)}\,. \tag{2·6}$$

Note that the explicit form of $|\phi_{\text{band}}\rangle$ changes whenever the rotational band under consideration crosses with another band; for instance, the configuration corresponding to the g-band changes as

$$|\phi_{\text{g}}\rangle=\begin{cases} |\phi_{\text{y}}\rangle\,, & 0\leq\omega_{\text{rot}}\leq\omega_{\text{cri}}^{(1)}\,,\\ \mathring{a}_A^\dagger\mathring{a}_{\bar{B}}^\dagger|\phi_{\text{y}}\rangle\,, & \omega_{\text{cri}}^{(1)}\leq\omega_{\text{rot}}\leq\omega_{\text{cri}}^{(2)}\,,\\ \mathring{a}_A^\dagger\mathring{a}_{\bar{D}}^\dagger|\phi_{\text{y}}\rangle\,, & \omega_{\text{cri}}^{(2)}\leq\omega_{\text{rot}}\leq\omega_{\text{cri}}^{(3)}\,,\\ \cdots\quad , & \end{cases} \tag{2·7}$$

Here the capital letters are used to label the neutron quasiparticle states as follows: $(\pi,\ r)_n=(+,\ -i)_1\equiv A$, $(+,\ +i)_1\equiv\bar{B}$, $(+,\ -i)_2\equiv C$, $(+,\ +i)_2\equiv\bar{D}$, where the suffix n denotes the energy-ordering among the quasiparticles $\mathring{a}^\dagger$ with the same quantum numbers $(\pi,\ r)$. In a similar way, the configuration for the s-band changes as

$$|\phi_{\text{s}}\rangle=\begin{cases} \mathring{a}_A^\dagger\mathring{a}_{\bar{B}}^\dagger|\phi_{\text{y}}\rangle\,, & 0\leq\omega_{\text{rot}}\leq\omega_{\text{cri}}^{(1)}\,,\\ |\phi_{\text{y}}\rangle\,, & \omega_{\text{cri}}^{(1)}\leq\omega_{\text{rot}}\leq\omega_{\text{cri}}^{(4)},\\ \cdots\quad , & \end{cases} \tag{2·8}$$

The equilibrium deformations are determined as functions of ω_{rot} for each rotational band to simultaneously satisfy the following self-consistency conditions:

$$G\langle\phi_{\text{band}}|\hat{P}|\phi_{\text{band}}\rangle=\Delta\,,\qquad \langle\phi_{\text{band}}|\hat{N}|\phi_{\text{band}}\rangle=N\,, \tag{2·9}$$

(for both protons and neutrons)

$$(\omega_1^{\text{eff}})^2\langle\phi_{\text{band}}|\sum_{n=1}^{\text{A}}(x_1^2)_n|\phi_{\text{band}}\rangle=(\omega_2^{\text{eff}})^2\langle\phi_{\text{band}}|\sum_{n=1}^{\text{A}}(x_2^2)_n|\phi_{\text{band}}\rangle$$

$$=(\omega_3^{\text{eff}})^2\langle\phi_{\text{band}}|\sum_{n=1}^{\text{A}}(x_3^2)_n|\phi_{\text{band}}\rangle \tag{2·10}$$

under the volume-conservation constraint $\omega_1^{\text{eff}}\omega_2^{\text{eff}}\omega_3^{\text{eff}}=\omega_0^3$. As discussed in Ref. 7), Eq. (2·10) results from the semiclassical requirement that the velocity distribution in the rotating frame should be isotropic in average. This equation determines the frequencies ω_i of the potential, from which the ordinary deformation parameters $(\beta,\ r)$ or δ_{osc} are immediately calculated.

In this way, we obtain the diabatic quasiparticle representation in which the equilibrium deformations are self-consistently determined as functions of ω_{rot}.

2. 2. *The RPA in the rotating frame*

The residual interactions that are consistent, in the sense of the Landau-Migdal theory,[19] with the single-particle Hamiltonian (2·1) are given by

$$H_{\text{int}}=H_P+H_{QQ}\,, \tag{2·11}$$

$$H_P=-G\tilde{P}^\dagger\tilde{P}\,,\qquad \text{(for both protons and neutrons)} \tag{2·12}$$

$$H_{QQ}=-\frac{1}{2}\sum_{K=0,1,2}\chi_K^{(+)}\tilde{Q}_K^{(+)\dagger}\tilde{Q}_K^{(+)}-\frac{1}{2}\sum_{K=1,2}\chi_K^{(-)}\tilde{Q}_K^{(-)\dagger}\tilde{Q}_K^{(-)}, \tag{2·13}$$

where $\tilde{P}\equiv\hat{P}-\langle\phi_{\rm band}|\hat{P}|\phi_{\rm band}\rangle$ and $\tilde{Q}_K^{(\pm)}$ are the quadrupole operators that are defined in terms of the doubly stretched coordinates x_i'' associated with the rotating deformed potential,

$$x_i''=\frac{\omega_i^{\rm eff}}{\omega_0}x_i, \qquad \omega_i^{\rm eff}=\sqrt{\omega_i^2-(1-\delta_{i1})\omega_{\rm rot}^2}. \tag{2·14}$$

At the equilibrium deformation where Eq. (2·10) holds, we see that $\langle\tilde{Q}_K^{(\pm)}\rangle=0$ for all K and that the force strengths $\chi_K^{(\pm)}$ are given by

$$\left.\begin{aligned}&\chi_0^{(+)}=\chi_1^{(+)}=\chi_2^{(+)}=\frac{4\pi}{5}\frac{M\omega_0^2}{\langle\sum_{n=1}^{A}(\boldsymbol{x}''^2)_n\rangle}\equiv\chi,\\&\chi_1^{(-)}=\chi\frac{\omega_3^2-\omega_1^2}{(\omega_3^{\rm eff})^2-(\omega_1^{\rm eff})^2}, \qquad \chi_2^{(-)}=\chi\frac{\omega_1^2-\omega_2^2}{(\omega_1^{\rm eff})^2-(\omega_2^{\rm eff})^2}.\end{aligned}\right\} \tag{2·15}$$

This H_{QQ} is an obvious generalization of the doubly stretched quadrupole force used in Refs. 14)~16) into the rotating triaxial harmonic-oscillator potential. Since its derivation given in Ref. 6) suffers an ambiguity of factor 2 for the value of χ, we give in the Appendix a revised version of it.

To describe the vibrational excitations, which are associated with the residual interaction (2·11) and are created on a given rotational band $|\phi_{\rm band}\rangle$, it is convenient to use the quasiparticle operators $(a_\mu^\dagger, a_{\bar\nu}^\dagger)$ defined with respect to $|\phi_{\rm band}\rangle$:

$$\left.\begin{aligned}&a_\mu|\phi_{\rm band}\rangle=0; \quad \mu=1, 2, \cdots, \quad \Omega-n_B,\\&a_{\bar\nu}|\phi_{\rm band}\rangle=0; \quad \bar\nu=1, 2, \cdots, \quad \Omega+n_B,\end{aligned}\right\} \tag{2·16}$$

where $n_B\equiv n_+-n_-$. These are obtained from the previous quasiparticle operators $(\mathring{a}_\mu^\dagger, \mathring{a}_{\bar\nu}^\dagger)$ through the following procedure. Let 2Ω be the total number of single-particle states. As is well known, the Hartree-Bogoliubov equation diagonalizing (2·1) has 4Ω solutions. If we identify Ω positive-energy solutions as physical solutions for both signatures, $r=-i$ and $r=+i$, then the vacuum for the quasiparticles $(\mathring{a}_\mu^\dagger, \mathring{a}_{\bar\nu}^\dagger)$ coincides with the yrast configuration. Let $(n_\mu, n_{\bar\nu})$ be the occupation numbers for these quasiparticle states in the configurations $|\phi_{\rm band}\rangle$. Then, the quasiparticle operators $(a_\mu^\dagger, a_{\bar\nu}^\dagger)$ are obtained from $(\mathring{a}_\mu^\dagger, \mathring{a}_{\bar\nu}^\dagger)$ by the following replacements:

$$\begin{aligned}&(-E_\mu, \ V_\mu, \ U_\mu)\longrightarrow(E_{\Omega+\mu}, \ \bar U_{\Omega+\mu}, \ \bar V_{\Omega+\mu}),\\&(-E_{\bar\nu}, \ \bar V_\nu, \ \bar U_\nu)\longrightarrow(E_{\Omega+\nu}, \quad U_{\Omega+\nu}, \ V_{\Omega+\nu})\end{aligned} \tag{2·17}$$

for the states with $n_\mu=1$ and $n_{\bar\nu}=1$, respectively. The other states with $n_\mu=n_{\bar\nu}=0$ remain the same. By the above replacements, the numbers of physical quasiparticle states in each signature sector are changed into

$$\begin{aligned}&\Omega-n_B\equiv\Omega+\sum_{\bar\nu=1}^{\Omega}n_{\bar\nu}-\sum_{\mu=1}^{\Omega}n_\mu,\\&\Omega+n_B\equiv\Omega+\sum_{\mu=1}^{\Omega}n_\mu-\sum_{\bar\nu=1}^{\Omega}n_{\bar\nu}\end{aligned} \tag{2·18}$$

for the $r=-i$ and $r=+i$ sectors, respectively. The quantity n_B is called[4] the blocking number, and is related to the signature r_B of the configuration $|\phi_{\text{band}}\rangle$ through the relation

$$r_B = e^{-i(\pi/2)n_B}. \tag{2·19}$$

Thus, the annihilation operators $\mathring{a}_\mu(\mathring{a}_{\bar{\nu}})$ for the states with $n_\mu=1(n_{\bar{\nu}}=1)$ are now treated as creating the physical excitations $a^\dagger_{\Omega+\mu}$ $(a^\dagger_{\Omega+\nu})$ with negative energies and with opposite signature. The procedure described above was actually carried out in Ref. 6) although it was mentioned only briefly.

In terms of the quasiparticle operators defined above, the RPA excitations $X_n^{(\pm)\dagger}$ are constructed as

$$X_n^{(\pm)\dagger} = \sum_{(\alpha\beta)} \{\psi_n^{(\pm)}(\alpha\beta) a_\alpha^\dagger a_\beta^\dagger + \varphi_n^{(\pm)}(\alpha\beta) a_\beta a_\alpha\}, \tag{2·20}$$

where $(\alpha\beta)=(\mu\bar{\nu})$ for the $r=+1$ sector, and $(\alpha\beta)=(\mu\nu)$ or $(\bar{\mu}\bar{\nu})$ for the $r=-1$ sector. Note that $X_n^{(\pm)\dagger}$ contains, besides the ordinary pair-creation terms like $\mathring{a}_\mu^\dagger \mathring{a}_{\bar{\nu}}^\dagger$, the terms like $\mathring{a}_\mu^\dagger \mathring{a}_\nu$ which scatter the quasiparticles already present in the reference configuration $|\phi_{\text{band}}\rangle$. The excitation energies $\hbar\omega_n^{(\pm)}$ and the transition amplitudes like $\langle\phi_{\text{band}}|[\tilde{Q}_K^{(\pm)}, X_n^{(\pm)}]|\phi_{\text{band}}\rangle$ are obtained as usual by solving, in the RPA, the equation of motion $[h'_{\text{sp}}+H_{\text{int}}, X_n^{(\pm)\dagger}]=\hbar\omega_n^{(\pm)} X_n^{(\pm)\dagger}$ and the normalization condition $[X_n^{(\pm)}, X_{n'}^{(\pm)\dagger}] = \delta_{nn'}$.

§ 3. Calculational details

Apparently, our model to describe the vibrational excitations at a finite rotational frequency ω_{rot} contains no adjustable parameters; namely, the equilibrium deformations and the residual interactions can be self-consistently determined in principle. However, in order to compare our results of numerical calculation with experimental data, we have to make the following phenomenological adjustments in practice:

1) The force-strengths $\varkappa_K^{(\pm)}$ are multiplied by the constants $f_K^{(\pm)}$. The values of $f_0^{(+)}$ and $f_2^{(+)}$ are determined to reproduce the experimental excitation energies of the β- and γ-vibrations at $\hbar\omega_{\text{rot}}=0$, while $f_1^{(\pm)}$ to restore, within the model space (i.e., the space explicitly taken into account in the numerical calculations), the rotational invariance broken by h_{def}.

2) The expectation value $\langle\sum_{n=1}^{A}(x_i^2)_n\rangle$ consists of two parts;

$$\langle\sum_{n=1}^{A}(x_i^2)_n\rangle = \langle\sum_{\text{valence}}(x_i^2)_n\rangle + \langle\sum_{\text{core}}(x_i^2)_n\rangle.$$

The first term represents the contributions from the nucleons inside the model space, while the second term, those outside the model space. The latter is analytically evaluated in terms of ω_i and then multiplied by a factor α_{ren} to reproduce the experimental values of the ground-state quadrupole deformation.

In the actual calculation for ^{164}Er, we explicitly took into account the three major shells; $N_{\text{osc}}=4$, 5, 6 for neutrons and $N_{\text{osc}}=3$, 4, 5 for protons. The following values of $f_K^{(\pm)}$ were then obtained; $f_0^{(+)}=2.257$, $f_1^{(+)}=f_1^{(-)}=1.590$, $f_2^{(+)}=1.491$, $f_2^{(-)}=1.465$, and the value $\alpha_{\text{ren}}=0.817$ was found to reproduce the experimental data $\delta_{\text{osc}}=0.269$. [Note that the $f_2^{(-)}$ value was actually determined at $\hbar\omega_{\text{rot}}=0.05$ MeV where we have a small triaxiality.

In our previous calculation, we assumed $\varkappa_2^{(-)}=\varkappa_2^{(+)}$ because $\varkappa_2^{(-)}$ is undefined in the prolate limit.]

There are some obvious reasons for using such "renormalization" constants:

1) Some truncation of the model space is unavoidable. (We examined in Ref. 6) that the result of 5-major-shell calculations is almost perfectly reproduced in the 3-major-shell calculations by using appropriate values for $f_K^{(\pm)}$.)

2) The $\Delta N_{\rm osc}=2$ terms in the Coriolis force are neglected in the actual calculations. (This is because their effects are much smaller, by a factor $(\omega_{\rm rot}/\omega_0)^2\times\delta_{\rm osc}^2$, than the effects of the $\Delta N_{\rm osc}=0$ terms.)

3) The specific terms in the Coriolis force are eliminated in order to construct the diabatic representation. Furthermore, our $(\boldsymbol{l}\cdot\boldsymbol{s})$- and $(\boldsymbol{l}^2-\langle\boldsymbol{l}^2\rangle_N)$-terms depend on the ω_i's after the scaling $\boldsymbol{x}\to\tilde{\boldsymbol{x}}$ mentioned in §2. 1. Thus, the exact decoupling of the Nambu-Goldstone modes is not guaranteed if we use the value of $\varkappa$ given by (2·15) in the actual calculation.

It should be emphasized that we have no adjustable parameters at $\omega_{\rm rot}\neq 0$, once the above renormalization constants are determined at $\omega_{\rm rot}=0$.

§ 4. Gamma bands in ^{164}Er at high spin

Figure 1 shows the result of the RPA calculations for ^{164}Er, which are based on the triaxial equilibrium deformations. The calculated triaxiality parameters γ[7] are about $\gamma^{(\rm self)}=3°$ and 6° at $\hbar\omega_{\rm rot}=0.3$ MeV for the g-band and the s-band, respectively. [Note that the above values of $\gamma^{(\rm self)}$ correspond to $\gamma^{(\rm pot)}=6°$ and $\gamma^{(\rm pot)}=11°$, respectively, which

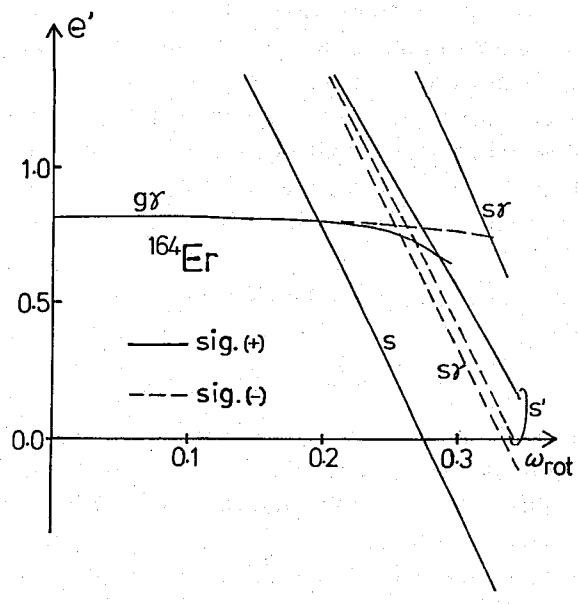

Fig. 1. Theoretical excitation energies for the positive-parity states in ^{164}Er. These are measured from the g-band, and plotted as functions of $\omega_{\rm rot}$. The solid (dashed) lines represent the states with positive (negative) signature. The $g\gamma$ ($s\gamma$) denotes the γ-band built on the g-band (s-band). The letter $s(s')$ denotes the lowest (second-lowest) aligned two-quasiparticle states.

characterize the deformation of the potential. Thus the difference in the definition of the triaxiality parameters is quite significant especially for small γ.] In this figure, the yrast spectrum is drawn by measuring the excitation energies from the rotating frame of reference associated with the g-band. Let us notice a significant difference in the RPA frequencies between the γ-vibrations built on the g-band ($g\gamma$-modes) and those built on the s-band ($s\gamma$-modes). Below, we discuss their properties in detail.

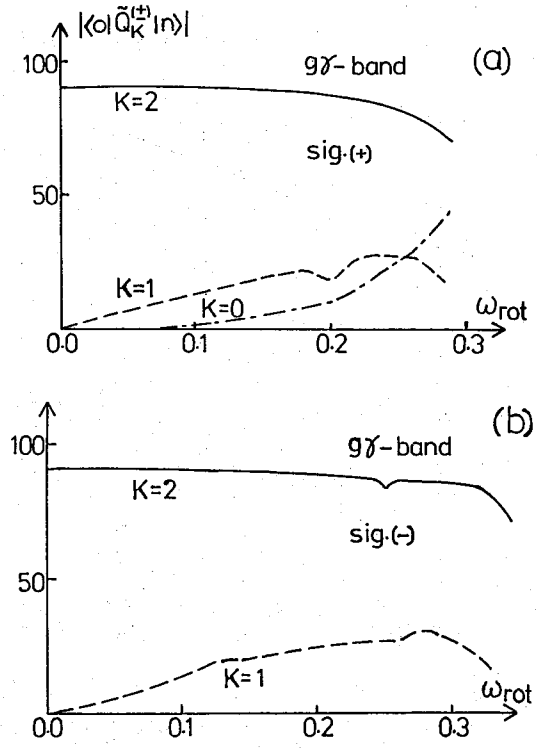

Fig. 2. (a) The absolute values of the RPA transition amplitudes $|\langle 0|\tilde{Q}_K^{(+)}|n\rangle|$ for the $g\gamma$ modes with positive signature in ^{164}Er, plotted as a function of ω_{rot}. The unit is fm^2. The solid, dashed and dotted-dashed lines are used for $K=2$, $K=1$ and $K=0$, respectively.

(b) The same as (a) but for the negative-signature modes.

4.1. *Properties of the γ-vibrations built on the g-band*

Figure 2 shows the RPA transition amplitudes $|\langle 0|\tilde{Q}_K^{(\pm)}|n(\pm)\rangle|$ for the $g\gamma$-modes. We see that the components $K=1$ and $K=0$ gradually increase with increasing ω_{rot}, indicating the effects of the Coriolis force. However, the signature-splitting is small, and no drastic change occurs in the properties of the $g\gamma$-modes up to $\hbar\omega_{rot}\simeq 0.3$ MeV. The small wiggles seen at $\hbar\omega_{rot}\simeq 0.20$ MeV in (a) and at $\hbar\omega_{rot}\simeq 0.26$ MeV in (b) are due to the crossings with the s-band and the lowest-energy negative-signature two-quasiparticle band, respectively. This result of calculation indicates that the interactions between these bands are weak. Above $\hbar\omega_{rot}\simeq 0.3$ MeV, the identification of the $g\gamma$ modes becomes increasingly difficult because of the fragmentation of the transition amplitudes into several non-collective two-quasiparticle states. For $\hbar\omega_{rot}\gtrsim 0.35$ MeV, the identity of the g-band itself tends to be lost because the g-band goes away far from the yrast line, and thus it becomes inappropriate for the reference band. The properties of the $g\gamma$ modes mentioned above are essentially the same with those in our previous paper, which implies that the triaxial equilibrium deformation of the g-band is too small to affect the $g\gamma$-modes.

4.2. *Properties of the γ-vibrations built on the s-band*

Figure 3 shows the excitation energies and the transition amplitudes of the $s\gamma$ modes, which are obtained by treating the s-band as the RPA vacuum. By comparing Fig. 3(a) with Fig. 3(b), we see that the negative-signature $s\gamma$ modes appear much lower in energy than the positive-signature $s\gamma$ modes. Furthermore, the former well retain their collectivities in the whole region of ω_{rot} investigated, while the latter tend to lose their identities in the region $\hbar\omega_{rot}>0.23$ MeV due to the fragmentation of their collectivities

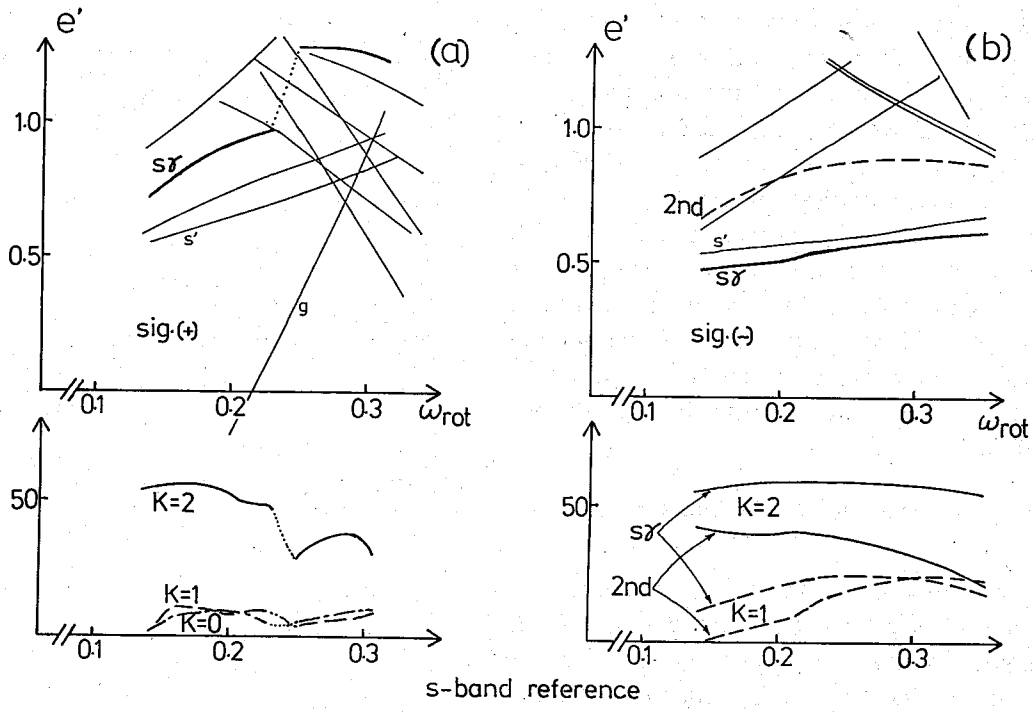

Fig. 3. (a) The excitation energies of the positive-signature states measured from the s-band in ^{164}Er are plotted as functions of $\omega_{\rm rot}$ for both the unperturbed two-quasiparticle states and the collective $s\gamma$ modes (the upper part). The absolute values of the RPA transition amplitudes $|\langle 0|\tilde{Q}_K^{(+)}|n\rangle|$ for the $s\gamma$ modes (the lower part). The solid, dashed and dotted-dashed lines are used for $K=2$, $K=1$ and $K=0$, respectively.

(b) The same as (a) but for the negative-signature modes. Notice that the dashed lines are used in the upper figure to show the second-lowest RPA solution.

into several non-collective two-quasiparticle states.

In order to get a qualitative understanding of the reason why the properties of the $s\gamma$ modes are strongly dependent on their signature quantum numbers, we have computed, in the RPA, the strength functions

$$\mathcal{S}_K^{(\pm)}(\omega)\equiv\sum_n \delta(\hbar\omega-\hbar\omega_n^{(\pm)})|\langle 0|\tilde{Q}_K^{(\pm)}|n(\pm)\rangle|^2$$

$$=\frac{1}{\pi}\mathrm{Im}\ \mathcal{R}_{KK}^{(\pm)}(\omega)$$

with the use of the energy-averaging parameter $\mathrm{Im}(\hbar\omega)=0.02$ MeV, where $\mathcal{R}_{KK}^{(\pm)}$ denote the response functions. It should be mentioned here that the K-mixing effects, which stem from the Coriolis force and are represented by the coupled RPA dispersion equation (2·25) of Ref. 6), play an important role in determining these quantities.[17] To exhibit their role, we compare in Figs. 4 and 5 below the results of the exactly calculated strength functions with those of approximate calculations in which the K-mixing effects are artificially switched off. Generally speaking, we find that the K-mixings act to enhance the collectivity of the most collective solution of the coupled RPA equation. For the positive-signature sector shown in Fig. 4, however, the concentration of the collectivity is not remarkable enough. In fact, at $\hbar\omega_{\rm rot}=0.2$ MeV (Fig. 4(a)), an appreciable fraction of the

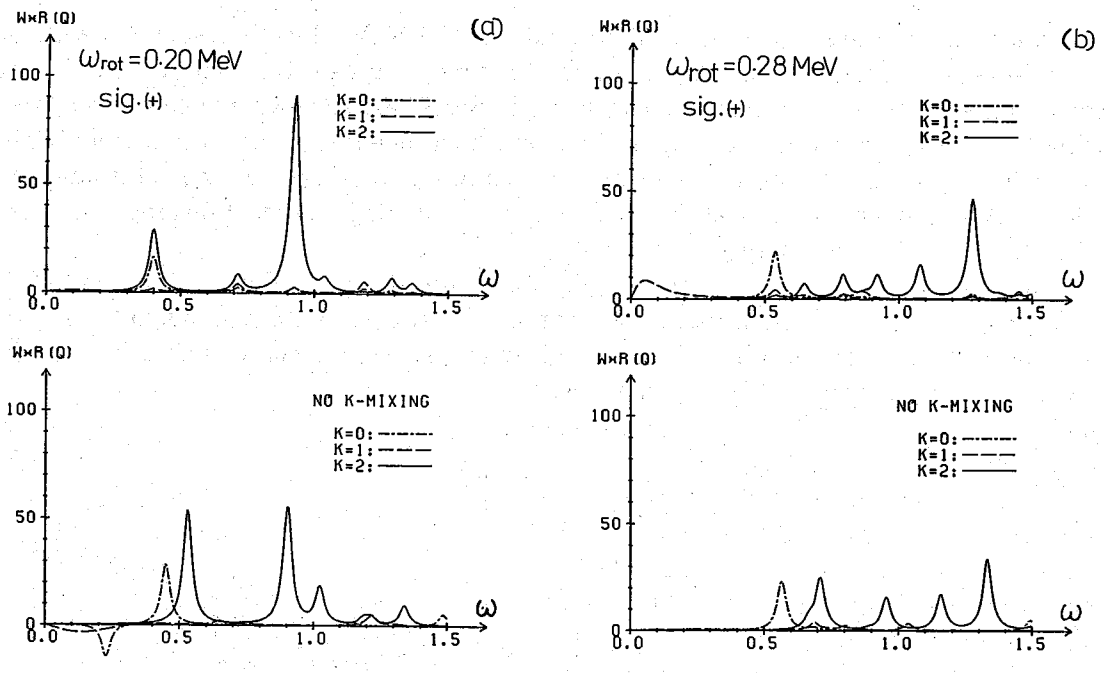

Fig. 4. The RPA strength functions at $\hbar\omega_{\rm rot}=0.20$ MeV (a) and 0.28 MeV (b) for the positive-signature excitations from the s-band in ^{164}Er. The ordinate indicates the values of $\mathrm{Im}(\hbar\omega)\times\mathrm{Im}(\mathcal{R})$ in units of $b_0^4=(\hbar/M\omega_0)^2=(5.56\ \mathrm{fm}^2)^2$. The value $\mathrm{Im}(\hbar\omega)=0.02$ MeV is adopted. The solid, dashed and dotted-dashed lines are used for $K=2$, $K=1$ and $K=0$, respectively. In the lower parts of these figures, the strength functions obtained by artificially switching off the K-mixings in the RPA dispersion equation are shown for reference. Note that the peak around $\omega=0$, seen in the upper part of (b), represents the effect of the Nambu-Goldstone mode which is not exactly separated out in the numerical calculation.

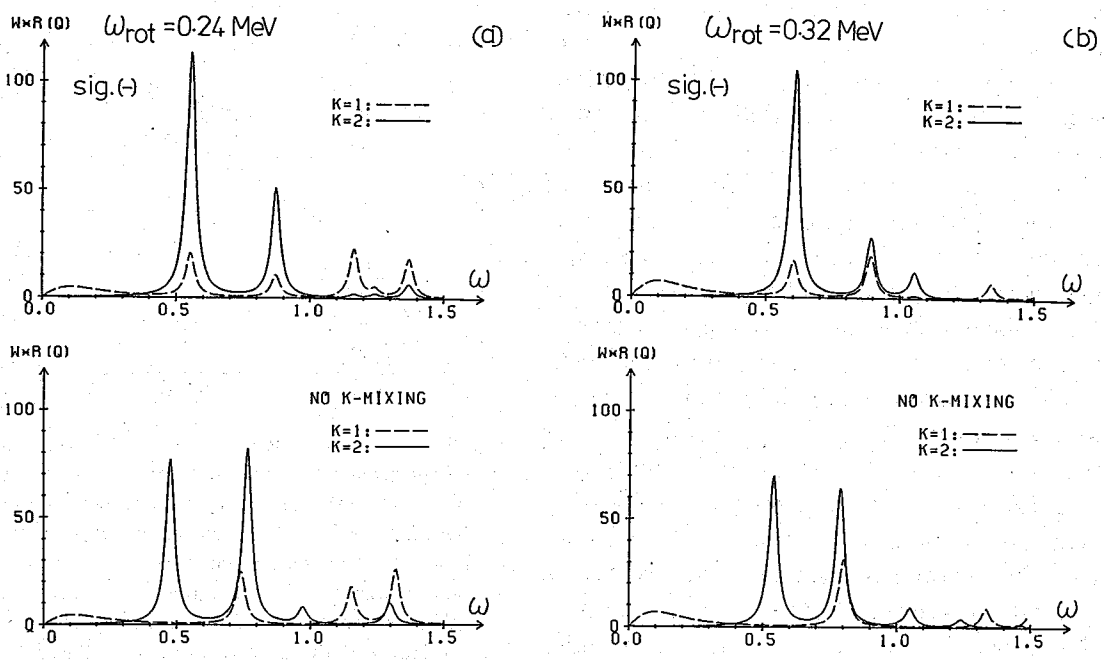

Fig. 5. The RPA strength functions at $\hbar\omega_{\rm rot}=0.24$ MeV (a) and 0.32 MeV (b) for the negative-signature excitations from the s-band in ^{164}Er. See the caption of Fig. 4.

transition strength remains in the peak around $\hbar\omega \simeq 0.4$ MeV which is associated with the second-lowest aligned two-quasiparticle state (s' band). This is the main reason why the transition amplitudes for the $s\gamma$ modes (shown in Fig. 3) are somewhat reduced compared with those for the $g\gamma$ modes (shown in Fig. 2) in which such fragmentations are negligible. This kind of fragmentation mechanism becomes more significant as the rotational frequency $\omega_{\rm rot}$ increases so that at $\hbar\omega_{\rm rot}=0.28$ MeV (Fig. 4(b)) the peak-height associated with the $s\gamma$ mode is no more predominant.

Next, let us discuss the negative-signature sector shown in Fig. 5. At $\hbar\omega_{\rm rot}=0.24$ MeV (Fig. 5(a)) we see again that a part of the transition strength remains in the second peak associated with the aligned two-quasiparticle state. In contrast to the positive-signature case, however, the collective $s\gamma$ mode appears in the present case as the lowest-energy solution of the RPA. This is an important reason why the negative-signature $s\gamma$ mode retains its identity in the whole region of $\omega_{\rm rot}$ considered. In fact, the $s\gamma$ mode remains also at $\hbar\omega_{\rm rot}=0.32$ MeV (Fig. 5(b)) as a predominant peak.

In addition to the stability against the fragmentation of the transition strength, the negative-signature $s\gamma$ mode is found to possess an interesting property; that is, its collectivity is always enhanced by the K-mixing effects mentioned above. This is manifestly seen by comparing the upper and the lower part of Fig. 5. Consequently, the ratio $|\langle 0|\tilde{Q}^{(-)}_{K=1}|s\gamma\rangle|/|\langle 0|\tilde{Q}^{(-)}_{K=2}|s\gamma\rangle|$ becomes conspicuously large compared with other modes (see Fig. 3). It can be shown that this ratio indicates the degree of character-change of the γ-vibrations into the wobbling modes of motion which are expected[20),21)] to appear as the characteristic modes in nuclei with axial-symmetry breaking. The property of the RPA dispersion equation that the negative-signature γ-vibrations change into the wobbling motions was first pointed out by Janssen and Mikhailov.[10)] It is easily confirmed that the above ratio increases with increasing triaxiality and reaches unity at the limiting case of the precession modes[22)~24)] built on the oblate high-K isomers (the rotations around the symmetry axis). In the light of this general theoretical picture, it is quite tempting to regard the above-mentioned property of the negative-signature $s\gamma$ modes

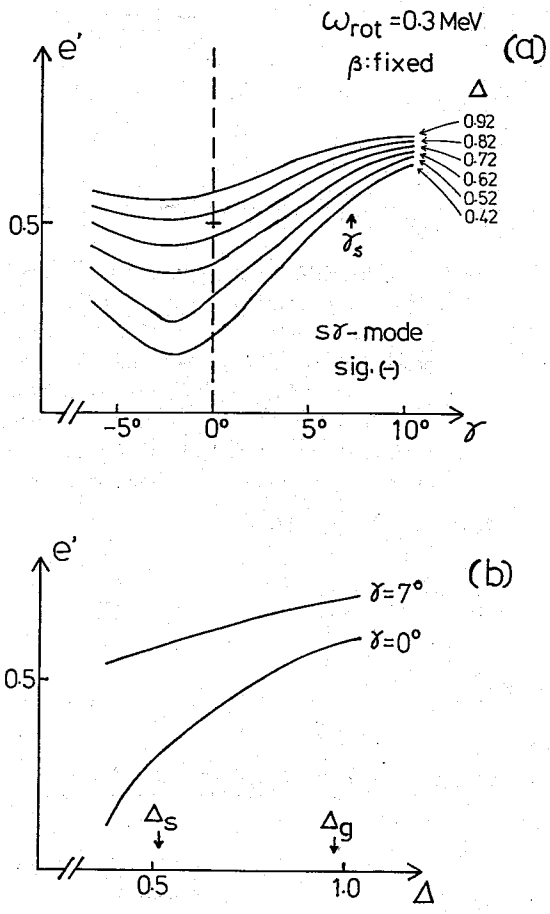

Fig. 6. The dependence of the RPA excitation energies for the negative-signature $s\gamma$ modes at $\hbar\omega_{\rm rot}=0.3$ MeV upon the triaxial deformation parameter $\gamma^{(\rm den)}$ and the neutron pairing deformation Δ_n. The equilibrium value of γ for the s-band is indicated by the arrow in (a), while the self-consistent values of Δ_n for the g- and s-band are indicated by the arrows in (b). The deformation parameter β and the quadrupole-force strengths are fixed at their self-consistent values.

as an incipient trend of the character change toward the wobbling modes of excitation. In fact, however, the actual calculated value[7] of the triaxial deformation $\gamma^{(\mathrm{self})}$ ($\gamma^{(\mathrm{pot})}$) is only 8°(13°) at $\hbar\omega_{\mathrm{rot}}=0.35$ MeV, and its sign is in the direction opposite to the oblate shape. Thus, a more extensive investigation seems necessary to reach a definite conclusion about the mechanism of character-change of the γ-vibrations associated with the change of the equilibrium shape at high spin.

Figure 6 illustrates how the RPA excitation energies change when the deformations of the single-particle potential are treated as free parameters. This manifestly demonstrates that the instability of the $s\gamma$ modes encountered in our previous calculation (Fig. 4 of Ref. 6)) disappears when the equilibrium shape is determined self-consistently. It should be emphasized again that the excitation energies of the $s\gamma$ modes displayed in Fig. 1 have been obtained by using the self-consistent values for the pairing- and the quadrupole-deformation of the s-band, although, somewhat accidentally, it looks quite similar to Fig. 3(b) of Ref. 6). Thus, the insufficiency in our previous calculations[6] has been overcome in the present paper, while the statements made in Ref. 6) on the experimental data are unchanged.

§ 5. Conclusions

On the basis of the self-consistent diabatic quasiparticle representation, the RPA calculations in the rotating frame have been performed for the γ-vibrational modes around the triaxial equilibrium deformations. The doubly stretched quadrupole forces have been used as the residual interactions. It was found that the negative-signature γ-vibrational modes built on the s-band well retain their collective characters, while the positive-signature modes tend to lose their identities with increasing ω_{rot}. We have discussed that such drastic signature splittings may be caused by a subtle difference (between the positive- and negative-signature sectors) in the interplay of γ-vibrational and aligned-quasiparticle modes of motion at high-spin.

We can now summarize the major effects of the rotation-aligned two-quasiparticles on the collective properties of the s-band as follows:

1) reduce, about 30~40%, the pairing deformation Δ through the blocking effects.[6),25)]
2) induce a small triaxiality in the equilibrium shape.[7)]
3) induce a large signature-splitting in the γ-vibrational modes.

We expect that the above conclusions apply rather generally, although the numerical results are presented only for ^{164}Er. (Quantitatively, of course, the magnitude and the sign of the triaxiality parameter γ depend on the neutron number.[7)])

The high-spin γ-vibrational bands, especially the negative-signature trajectories, are expected to sensitively indicate the nature of the collective motions of rapidly rotating nuclei. Thus, the possibility to interpret the calculated result of this paper as an incipient trend of the character change of the γ-vibrations into the wobbling motions has been pointed out. To explore such a character change of the collective vibrational modes along the yrast line, associated with increasing number of aligned quasiparticles, we desire to have more experimental data for them.

Acknowledgements

We thank Dr. K. Ando for his suggestion that was very helpful to clarify the derivation of the doubly-stretched quadrupole force given in the Appendix. One of the authors (Y.R.S.) is indebted to Japan Society for the Promotion of Science for financial support. The computer calculation for this work has been supported in part by the Grant-in-Aid for Scientific Research from the Ministry of Education, Science and Culture (No. 58540153), and in part by Research Center for Nuclear Physics, Osaka University.

Appendix

We give a revised derivation of the doubly stretched quadrupole-quadrupole interactions.

Let us consider the harmonic-oscillator potential model:

$$\hat{h}=\sum_{n=1}^{A}\sum_{i=1}^{3}\left\{\frac{1}{2}M(\hat{v}_i^2)_n+\frac{1}{2}M\omega_i^2(\hat{x}_i^2)_n\right\}. \tag{A·1}$$

In order to apply the Landau-Migdal theory, we should relate the single-particle potential to the density matrix. For this purpose, we invoke the self-consistency between the density distribution and the equi-potential shape with the volume-conservation condition $\omega_1\omega_2\omega_3=\omega_0^3$:

$$\omega_1^2\langle\sum_{n=1}^{A}(\hat{x}_1^2)_n\rangle=\omega_2^2\langle\sum_{n=1}^{A}(\hat{x}_2^2)_n\rangle=\omega_3^2\langle\sum_{n=1}^{A}(\hat{x}_3^2)_n\rangle. \tag{A·2}$$

Introducing a fixed single-particle basis $\{|a\rangle\}$ and a density matrix (ρ_{ba}) corresponding to the Slater-determinantal state $|\phi\rangle$ in this basis, we then express the frequencies (ω_i) of the oscillator potential as functionals of (ρ_{ba}):

$$\omega_i\{\rho\}=\omega_0\left[\frac{\{(\mathrm{tr}\rho\hat{x}_1^2)(\mathrm{tr}\rho\hat{x}_2^2)(\mathrm{tr}\rho\hat{x}_3^2)\}^{1/3}}{(\mathrm{tr}\rho\hat{x}_i^2)}\right]^{1/2}, \tag{A·3}$$

where

$$\langle\phi|\sum_{n=1}^{A}(\hat{O})_n|\phi\rangle=\mathrm{tr}\rho\hat{O}=\sum_{ab}\langle a|\hat{O}|b\rangle\rho_{ba} \tag{A·4}$$

for an arbitrary single-particle operator $\hat{O}$. Equation (A·3) defines the single-particle potential which is dependent on the density matrix.

The effective interaction is obtained by functionally derivating the total independent-particle energy $E\equiv\mathrm{tr}\rho\hat{h}$:

$$\langle ac|\hat{V}|bd\rangle\equiv\frac{\delta^2E}{\delta\rho_{dc}\delta\rho_{ba}}=\sum_{i=1}^{3}M\omega_i\langle a|\hat{x}_i^2|b\rangle\frac{\delta\omega_i}{\delta\rho_{dc}}. \tag{A·5}$$

Here we have used the fact that the rearrangement term,

$$\mathrm{tr}\left(\rho\frac{\delta\hat{h}}{\delta\rho_{ba}}\right)\propto\sum_{i=1}^{3}\frac{1}{\omega_i}\frac{\delta\omega_i}{\delta\rho_{ba}}, \tag{A·6}$$

vanishes under the volume-conservation constraint. We note that this property generally

holds for density dependent zero-range forces as long as they are velocity independent. Owing to this property, the variation of the independent-particle energy E with respect to the volume-conserving deformation change is equivalent to that of the exact total energy.

By using (A·3), we can easily calculate the functional derivative of (ω_i) appearing in (A·5):

$$\frac{\delta\omega_i}{\delta\rho_{ba}}=-\frac{1}{2}\langle\phi|\sum_{n=1}^{A}(\tilde{\boldsymbol{x}}^2)_n|\phi\rangle^{-1}\omega_i\sum_{j=1}^{3}(3\delta_{ij}-1)\left(\frac{\omega_j}{\omega_0}\right)^2\langle a|\hat{x}_j{}^2|b\rangle. \tag{A·7}$$

Inserting (A·7) into (A·5), we finally obtain the effective interaction:

$$\langle ac|\hat{V}|bd\rangle=-\varkappa\sum_{K=0,2}\langle a|\tilde{Q}_K{}^{(+)}|b\rangle\langle c|\tilde{Q}_K{}^{(+)}|d\rangle \tag{A·8}$$

with $\varkappa$ given by (2·15). Apparently, extension of this argument to the rotating harmonic-oscillator case is straightforward.

In the above treatment, the single-particle basis $\{|a\rangle\}$ is fixed. On the other hand, it is also possible to consider the state $|\phi\rangle$ that follows the change of the potential induced by the variation of the density matrix. Namely, we can always set the $|\phi\rangle$ to be the eigenstate of the Hamiltonian (A·1) during the variation. In this case, we obtain in place of (A·7):

$$\frac{\delta\omega_i}{\delta\rho_a}=-\langle\phi|\sum_{n=1}^{A}(\tilde{\boldsymbol{x}}^2)_n|\phi\rangle^{-1}\omega_i\sum_{j=1}^{3}(3\delta_{ij}-1)\left(\frac{\omega_j}{\omega_0}\right)^2\langle a|\hat{x}_j{}^2|a\rangle, \tag{A·9}$$

where (ρ_a) is the density matrix in such a single-particle basis $\{|a\rangle\}$ that diagonalizes (A·1). Here, it should be emphasized that (A·9) contains the contributions from

$$\frac{\partial}{\partial\omega_j}\langle a|\hat{x}_i{}^2|a\rangle=-\frac{1}{\omega_j}\delta_{ij}\langle a|\hat{x}_i{}^2|a\rangle, \tag{A·10}$$

because the basis $\{|a\rangle\}$ is now dependent on (ω_i). As a result, the force-strength $\varkappa$ is increased by a factor of two. This treatment gives the quadrupole-quadrupole interaction in which the effect of the high-frequency vibrations (core polarizations) is renormalized into the force-strength. Needless to say, however, the previous value $\varkappa$ given by (2·15) should be used when we explicitly take both the $\Delta N_{\rm osc}=0$ and $\Delta N_{\rm osc}=2$ excitations into account in the RPA.

References

1) R. Bengtsson and S. Frauendorf, Nucl. Phys. **A327** (1979), 139.
2) S. Frauendorf, in *Nuclear Physics*, edited by C. H. Dasso, R. A. Broglia and A. Winther (North-Holland, 1982), p.111.
3) H. J. Mang, Phys. Rep. **18** (1975), 325.
4) P. Ring and P. Schuck, *The Nuclear Many-Body Problem* (Springer-Verlag, 1980).
5) I. Hamamoto, Nucl. Phys. **A271** (1976), 15.
6) Y. R. Shimizu and K. Matsuyanagi, Prog. Theor. Phys. **70** (1983), 144.
7) Y. R. Shimizu and K. Matsuyanagi, Prog. Theor. Phys. **71** (1984), 960.
8) J. L. Egido, H. J. Mang and P. Ring, Nucl. Phys. **A339** (1980), 390.
9) E. R. Marshalek, Nucl. Phys. **A275** (1977), 416.
10) D. Janssen and I. N. Mikhailov, Nucl. Phys. **A318** (1979), 390.
11) E. R. Marshalek, Nucl. Phys. **A331** (1979), 429.
12) V. G. Zelevinsky, Nucl. Phys. **A344** (1980), 109.
13) T. Horibata and N. Onishi, Prog. Theor. Phys. **67** (1982), 190.
14) T. Kishimoto, *Proc. 1980 RCNP Int. Symp. Highly Excited States in Nuclear Reactions, Osaka*, p. 145. T. Kishimoto et al., Phys. Rev. Lett. **35** (1975), 552.

15) T. Suzuki and D. J. Rowe, Nucl. Phys. **A289** (1977), 461.
16) E. R. Marshalek, Phys. Rev. Lett. **51** (1983), 1534; Phys. Rev. **C29** (1984), 640.
17) Y. R. Shimizu and K. Matsuyanagi, Prog. Theor. Phys. **72** (1984), No. 5.
18) Y. Tanaka and S. Suekane, Prog. Theor. Phys. **66** (1981), 1639.
19) A. B. Migdal, *Theory of Finite Fermi Systems and Application to Atomic Nuclei* (Wiley Interscience, 1967).
20) A. Bohr and B. R. Mottelson, *Nuclear Structure* Vol. II (W. A. Benjamin Inc., 1975).
21) A. K. Kerman and N. Onishi, Nucl. Phys. **A361** (1981), 179.
22) H. Kurasawa, Prog. Theor. Phys. **64** (1980), 2055; **66** (1981), 1317; **68** (1982), 1594.
23) C. G. Andersson, J. Krumlinde, G. Leander and Z. Szymanski, Nucl. Phys. **A361** (1981), 147.
24) A. Akbarov, A. V. Ignatyuk, I. N. Mikhailov, Kh. L. Molina, R. G. Nazmitdinov and D. Janssen, Yadern. Fiz. **33** (1981), 1480 [Sov. J. Nucl. Phys. **33** (1981), 794].
25) Y. R. Shimizu and K. Matsuyanagi, Prog. Theor. Phys. **70** (1983), 319.

Progress of Theoretical Physics, Vol. 72, No. 5, November 1984

Monopole and Quadrupole Giant Resonances in Rotating Triaxially Deformed Nuclei

Yoshifumi R. SHIMIZU and Kenichi MATSUYANAGI

Department of Physics, Kyoto University, Kyoto 606

(Received July 23, 1984)

Isoscalar monopole and quadrupole giant resonances in rotating triaxially deformed nuclei are studied by means of the RPA based on the rotating shell model. The deformation parameters are selfconsistently determined as functions of rotational frequency, and the doubly stretched monopole and quadrupole forces are used as residual interactions. It is found that the properties of these modes—the excitation energies, the splitting and the mixing of the strength—predicted by the harmonic-oscillator potential model are well realized in the realistic calculation. The result indicates that the high frequency rotations affect the properties of these giant resonances mainly through the change of the deformation parameters.

§1. Introduction

One of the most exciting topics in the recent studies of high-spin states is the observations of the giant resonances (GR) built on the states with high rotational frequencies.[1),2)] Although the experimentally observed resonances are regarded as the isovector dipole type, it is expected that the GR's of other types built on the high-spin states will also be detected in the near future. These GR's might play important roles in the heavy-ion reaction mechanism as doorway states and in the deexcitation process above the yrast line. Therefore it is very important to investigate the GR's excited on the high-spin states.

Up to now, several theoretical works have been done for this subject.[3)~7)] However, realistic calculations for the monopole and quadrupole resonances (GMR and GQR) in rotating deformed nuclei have not been reported except Ref. 5). In this paper we shall present realistic calculations for the strength functions of the isoscalar GMR and GQR built on the yrast states. In our previous papers,[8)~10)] we have developed an RPA approach based on the rotating shell model where the deformation parameters are selfconsistently determined as functions of the rotational frequency. Although attentions were focussed in Ref. 10) on the low-lying γ-vibrational modes, our approach can also be applicable to describe the high-lying giant vibrations.

One of the characteristic features of our approach is the use of the residual interaction composed of the multipole operators defined in terms of the doubly stretched coordinates.[11)~13)] As is well known, the conventional quadrupole force gives a too large splitting of the GQR in deformed nuclei in contradiction to the experimental data.[11),14),15)] It seems for us that the theoretical calculation of Ref. 5) suffers from this shortcoming. It will be demonstrated in this paper that the doubly stretched monopole and quadrupole forces correctly describe not only the splitting but also the coupling between the GMR and GQR.[12)]

In §2 we briefly review the basic framework of our approach, where a general derivation of the response functions is also given paying attention to the presence of the zero-energy modes. In §3 analytical solutions for the coupled RPA dispersion equations

are presented for the case of the non-rotating but triaxially deformed harmonic-oscillator (h.o.) potential model. After describing the calculational details in §4, we present in §5 the results of realistic calculations for ^{158}Er and ^{164}Er. Conclusions are drawn in §6.

§ 2. Formulation

In this section*) we first give a derivation of the RPA response functions in a general form, putting particular attention to the treatment of the Nambu-Goldstone (NG) modes. We then discuss the residual interaction which will be used in later sections.

2. 1. *The RPA response functions*

A starting point for the calculation of the response functions is the resolvent operator $\hat{G}(\omega)\equiv(\hat{H}-\omega)^{-1}$; for the Hamiltonian $\hat{H}=\hat{H}_0+\hat{V}$, it satisfies

$$\hat{G}(\omega)=\hat{G}_0(\omega)-\hat{G}_0(\omega)\hat{V}\hat{G}(\omega), \tag{2·1}$$

where $\hat{G}_0(\omega)\equiv(\hat{H}_0-\omega)^{-1}$. In the RPA this equation is approximated by the matrix equation expressed in the "RPA vector space" which is spanned by two-quasiparticle states.[16] The part relevant to the RPA of an arbitrary one-body operator is uniquely represented by a vector in this vector space:

$$F\equiv\begin{pmatrix} f(\alpha\beta) \\ \bar{f}^*(\alpha\beta)\end{pmatrix}\longleftrightarrow \hat{F}=\sum_{\alpha<\beta}\{f(\alpha\beta)a_\alpha^\dagger a_\beta^\dagger+\bar{f}^*(\alpha\beta)a_\beta a_\alpha\}, \tag{2·2}$$

where $a_\alpha^\dagger(a_\alpha)$ are the quasiparticle creation (annihilation) operators. As is well known the RPA vector space is accompanied with an inner product $\langle F_1, F_2\rangle$, which is defined in terms of the indefinite metric tensor $\boldsymbol{I}$:[16),**)]

$$\langle F_1, F_2\rangle\equiv[\hat{F}_1^\dagger, \hat{F}_2]_{\mathrm{RPA}}=F_1^\dagger \boldsymbol{I} F_2, \qquad \boldsymbol{I}=\begin{pmatrix}1 & 0\\ 0 & -1\end{pmatrix}. \tag{2·3}$$

The matrix $G(\omega)$ corresponding to $\hat{G}(\omega)$ is easily obtained once the RPA eigenvalue problem is solved. Generally speaking, the RPA spectrum consists of complex energies.[16] Among them special attention should be paid to the zero-energy solutions associated with the NG modes.[16),17)] In the following we assume that the dimensionality of the cell in the Jordan normal form of the Hamiltonian matrix in the RPA is one for non-zero solutions and two for zero-energy solutions.[18),19)] For non-zero complex solutions, the eigenvalues and eigenvectors appear in quartet:

$$\{(\omega_n, X_n), (-\omega_n^*, \bar{X}_n), (\omega_n^*, X_n'), (-\omega_n, \bar{X}_n')\}, \tag{2·4}$$

where

$$X_n=\begin{pmatrix}\psi_n(\alpha\beta)\\ \varphi_n(\alpha\beta)\end{pmatrix}\longleftrightarrow \hat{X}_n^\dagger=\sum_{\alpha<\beta}\{\psi_n(\alpha\beta)a_\alpha^\dagger a_\beta^\dagger+\varphi_n(\alpha\beta)a_\beta a_\alpha\},$$

$$\bar{X}_n=\begin{pmatrix}\varphi_n^*(\alpha\beta)\\ \psi_n^*(\alpha\beta)\end{pmatrix}\longleftrightarrow \hat{\bar{X}}_n, \text{ and similar equations for } X_n' \text{ and } \bar{X}_n', \tag{2·5}$$

*) Throughout this section, we shall use the unit of $\hbar=1$.

**) The subscript RPA attached to the commutator means that it should be evaluated within the RPA.

and the only non-vanishing norm between them is

$$N_n^{-1}=\langle X_n', X_n\rangle=-\langle \bar{X}_n, \bar{X}_n'\rangle. \tag{2·6}$$

Needless to say, $(\omega_n, X_n)\equiv(\omega_n^*, X_n')$ for real solutions and $(\omega_n, X_n)\equiv(-\omega_n^*, \bar{X}_n)$ for pure imaginary solutions, so that only the two among those appear (i.e., in doublet) for these cases. For zero-energy solutions, the eigenvalues are two-fold degenerate. Accordingly there are two vectors (J_a, C_a) of the form

$$J_a=\begin{pmatrix} j_a(\alpha\beta) \\ j_a^*(\alpha\beta)\end{pmatrix}, \qquad C_a=\begin{pmatrix} c_a(\alpha\beta) \\ -c_a^*(\alpha\beta)\end{pmatrix}. \tag{2·7}$$

Here $\hat{J}_a$ corresponds to the NG modes and $\hat{C}_a$ satisfies

$$[\hat{H}, \hat{C}_a]_{\mathrm{RPA}}=\hat{J}_a\,. \tag{2·8}$$

We define the moment of inertia tensor g_{ab} as an inner product of them,

$$g_{ab}\equiv\langle J_a, C_b\rangle, \tag{2·9}$$

which is real and symmetric. In terms of $\hat{C}_a$, the angle operators satisfying $[\hat{J}_a, i\hat{\Phi}_b]_{\mathrm{RPA}}=\delta_{ab}$ are expressed as

$$i\hat{\Phi}_a=\sum_b (g^{-1})_{ab}\hat{C}_b\,. \tag{2·10}$$

Explicitly separating out the contribution from the zero-energy solutions, we obtain $G(\omega)$ as

$$G(\omega)=G^{(C)}(\omega)+G^{(Z)}(\omega), \tag{2·11}$$

$$G^{(C)}(\omega)=\sum_{\substack{\omega_n\\ \neq 0}}\left\{N_n\left(\frac{X_n * X_n'^{\dagger}}{\omega_n-\omega}+\frac{\bar{X}_n' * \bar{X}_n^{\dagger}}{\omega_n+\omega}\right)+N_n^*\left(\frac{X_n' * X_n^{\dagger}}{\omega_n^*-\omega}+\frac{\bar{X}_n * \bar{X}_n'^{\dagger}}{\omega_n^*+\omega}\right)\right\}, \tag{2·12}$$

$$G^{(Z)}(\omega)=\sum_{a,b}(g^{-1})_{ab}\left\{\frac{J_a * J_b^{\dagger}}{-\omega^2}+\frac{C_a * J_b^{\dagger}+J_a * C_b^{\dagger}}{-\omega}\right\}. \tag{2·13}$$

Here we used the notation $X * Y^{\dagger}$ representing a matrix constructed from two vectors X and Y, which is defined by

$$A^{\dagger}(X * Y^{\dagger})B=\langle A, X\rangle\langle Y, B\rangle. \tag{2·14}$$

As is mentioned above, the second term in the curly bracket in Eq. (2·12) should be dropped with setting $X_n'=X_n$ and $\bar{X}_n'=\bar{X}_n$ ($\bar{X}_n=X_n$ and $\bar{X}_n'=X_n'$) for real (pure imaginary) solutions.

The response function for operators A and B is given in the RPA by [20]

$$\begin{aligned}\mathcal{R}_{AB}(\omega)&\equiv A^{\dagger}G(\omega)B\\ &=\sum_{\substack{\omega_n\\ \neq 0}}\left\{\left(\frac{\mathcal{A}^*(n)\mathcal{B}'(n)}{\omega_n-\omega}+\frac{\bar{\mathcal{A}}'(n)\bar{\mathcal{B}}^*(n)}{\omega_n+\omega}\right)+\left(\frac{\mathcal{A}'^*(n)\mathcal{B}(n)}{\omega_n^*-\omega}+\frac{\bar{\mathcal{A}}(n)\bar{\mathcal{B}}'^*(n)}{\omega_n^*+\omega}\right)\right\}\\ &\quad+\sum_{a,b}(g^{-1})_{ab}\left\{\frac{\mathcal{A}_J^*(a)\mathcal{B}_J(b)}{-\omega^2}+\frac{\mathcal{A}_c^*(a)\mathcal{B}_J(b)+\mathcal{A}_J^*(a)\mathcal{B}_c(b)}{-\omega}\right\},\end{aligned} \tag{2·15}$$

where

$$\mathcal{A}(n)\equiv N_n^{*1/2}[\hat{X}_n,\ \hat{A}]_{\mathrm{RPA}},\qquad \mathcal{A}^*(n)=N_n^{1/2}[\hat{A},\ \hat{X}_n^{\dagger}]_{\mathrm{RPA}},\ \text{etc.},$$
$$\mathcal{A}_J(a)\equiv[\hat{J}_a,\ \hat{A}]_{\mathrm{RPA}},\qquad \mathcal{A}_C(a)\equiv[\hat{C}_a,\ \hat{A}]_{\mathrm{RPA}}. \tag{2·16}$$

The quantities $\mathcal{A}(n)$, $\mathcal{A}^*(n)$ above are the transition amplitudes between the ground state and the RPA eigenstates. Similarly the unperturbed response function is given by

$$R_{AB}(\omega)\equiv A^{\dagger}G_0(\omega)B$$
$$=\sum_{\alpha<\beta}\left\{\frac{a^*(\alpha\beta)b(\alpha\beta)}{E_{\alpha\beta}-\omega}+\frac{\bar{a}(\alpha\beta)\bar{b}^*(\alpha\beta)}{E_{\alpha\beta}+\omega}\right\},\quad E_{\alpha\beta}\equiv E_\alpha+E_\beta. \tag{2·17}$$

The strength function for the transition operator $\hat{F}$ in the RPA is defined by[20]

$$S_F(\omega)\equiv\frac{1}{\pi}\mathrm{Im}\mathcal{R}_{FF}(\omega)$$
$$=\sum_n\delta(\omega_n-\omega)|\langle n|\hat{F}|0\rangle|^2. \tag{2·18}$$

Note that the second equality holds only if all the RPA eigenvalues are real and positive. If we perform an energy averaging by setting $\mathrm{Im}(\omega)$ to be finite, the NG modes affect the strength functions for the operators which do not commute with $\hat{J}_a$'s. This problem can be avoided, however, by using the modified operator $\hat{F}_c$ which is designed to commute with $\hat{J}_a$'s:

$$\hat{F}\longrightarrow\hat{F}_c\equiv\hat{F}+\sum_a[\hat{F},\ \hat{J}_a]_{\mathrm{RPA}}i\hat{\Phi}_a. \tag{2·19}$$

It can be easily shown that any interaction $\hat{V}$ is represented in the RPA as a sum of separable forces*)

$$V=-\sum_{\rho=1}^{N}\chi_\rho O_\rho O_\rho^{\dagger}\longleftrightarrow\hat{V}=-\frac{1}{2}\sum_{\rho=1}^{N}\chi_\rho\hat{O}_\rho\hat{O}_\rho, \tag{2·20}$$

where N is the rank of the matrix V corresponding to $\hat{V}$, and $\hat{O}_\rho^{\dagger}=\hat{O}_\rho$. As a result the equation for the Green's function (2·1) is reduced to that for the response functions for the operators ($\hat{O}_\rho$):

$$\mathcal{R}=(1-R\chi)^{-1}R, \tag{2·21}$$

where $\mathcal{R}$, R and χ are $N\times N$-matrices defined by

$$(\mathcal{R})_{\rho\sigma}\equiv\mathcal{R}_{O_\rho O_\sigma},\quad (R)_{\rho\sigma}\equiv R_{O_\rho O_\sigma},\quad (\chi)_{\rho\sigma}\equiv\delta_{\rho\sigma}\chi_\rho. \tag{2·22}$$

Finally we note that the response function $\mathcal{R}_{AB}$ for arbitrary operators $\hat{A}$ and $\hat{B}$ can be calculated from the unperturbed ones as follows:

$$\mathcal{R}_{AB}=R_{AB}+(R\chi R)_{AB}+(R\chi\mathcal{R}\chi R)_{AB}. \tag{2·23}$$

Note that the first and the second terms are necessary when $\mathrm{Im}(\omega)$ is finite.

2. 2. *The Hamiltonian*

Our starting point for the description of the giant resonances in rotating deformed nuclei is the selfconsistent rotating shell model (RSM). The details of the RSM+RPA

*) In this representation of $\hat{V}$ the exchange contributions to the Hamiltonian matrix should be excluded.

approach are described in Refs. 8)~10).

We adopt the single-particle Hamiltonian,

$$\hat{H}_0=\hat{h}_{\rm def}-\Delta(\hat{P}^\dagger+\hat{P})-\lambda\hat{N}-\omega_{\rm rot}\hat{J}_1\,, \tag{2·24}$$

where $\hat{h}_{\rm def}$ is defined in terms of the doubly stretched coordinates $\tilde{x}_i=(\omega_i/\omega_0)x_i$ ($i=1, 2, 3$) by

$$\hat{h}_{\rm def}=\hat{h}_{\rm sph}(\boldsymbol{x}\to\tilde{\boldsymbol{x}},\ \boldsymbol{p}). \tag{2·25}$$

Here the replacement $\boldsymbol{x}\to\tilde{\boldsymbol{x}}$ applies to all $\boldsymbol{x}$ including the $\boldsymbol{l}\cdot\boldsymbol{s}$ and $\boldsymbol{l}^2$-terms in $\hat{h}_{\rm sph}$ which is the spherical limit of the Nilsson-type Hamiltonian. The frequencies of the h.o. potential and the pairing deformation Δ are determined selfconsistently by the isotropic velocity-distribution (IVD) condition with the volume-conserving constraint and the BCS equations.

The residual interactions adopted are

$$\hat{V}=\hat{H}_P+\hat{H}_M+\hat{H}_Q \tag{2·26}$$

with

$$\hat{H}_P=-\sum_{\tau=n,p}G_\tau\tilde{P}_\tau^\dagger\tilde{P}_\tau\,, \tag{2·27}$$

$$\hat{H}_M=-\frac{1}{2}\chi_{00}^{(+)}\tilde{Q}_{00}^{(+)}\tilde{Q}_{00}^{(+)}\,, \tag{2·28}$$

$$\hat{H}_Q=-\frac{1}{2}\sum_{K=0,1,2}\chi_{2K}^{(+)}\tilde{Q}_{2K}^{(+)\dagger}\tilde{Q}_{2K}^{(+)}-\frac{1}{2}\sum_{K=1,2}\chi_{2K}^{(-)}\tilde{Q}_{2K}^{(-)\dagger}\tilde{Q}_{2K}^{(-)}\,, \tag{2·29}$$

where $\tilde{P}_\tau\equiv\hat{P}_\tau-\langle\hat{P}_\tau\rangle$ and $\tilde{Q}_{LK}^{(\pm)}\equiv\hat{Q}_{LK}^{(\pm)}(\boldsymbol{x}\to\boldsymbol{x}'')-\langle\hat{Q}_{LK}^{(\pm)}(\boldsymbol{x}\to\boldsymbol{x}'')\rangle$ are the multipole operators*) that are defined in terms of the doubly stretched coordinates $x_i''\equiv(\omega_i^{\rm eff}/\omega_0)x_i$ associated with the rotating h.o. potential with effective frequencies $\omega_i^{\rm eff}\equiv\sqrt{\omega_i^2-(1-\delta_{i1})\omega_{\rm rot}^2}$. Note that the property $\langle\hat{Q}_{2K}^{(\pm)}(\boldsymbol{x}\to\boldsymbol{x}'')\rangle=0$ holds owing to the IVD condition. The force strengths of the monopole and quadrupole interactions are expressed as

$$\chi_{LK}^{(\pm)}=f_{LK}^{(\pm)}\chi\,,\qquad \chi=\frac{4\pi}{5}\frac{M\omega_0^2}{\langle\sum_{n=1}^{A}(\boldsymbol{x}''^2)_n\rangle}\,. \tag{2·30}$$

The factors ($f_{20}^{(+)}$, $f_{22}^{(+)}$) are determined by employing the Landau-Migdal theory and ($f_{21}^{(+)}$, $f_{21}^{(-)}$, $f_{22}^{(-)}$) by the decoupling conditions for the Nambu-Goldstone modes ($\hat{J}_x$, $i\hat{J}_y$, $\hat{J}_z$).[8] On the other hand the factor $f_{00}^{(+)}$ is determined as in the work of Kishimoto[12] from the requirement that $A^{-1/3}$-dependence of ω_0 is rigorously satisfied in the h.o. potential model:

$$f_{20}^{(+)}=f_{21}^{(+)}=f_{22}^{(+)}=1\,,\quad f_{21}^{(-)}=\frac{\omega_3^2-\omega_1^2}{(\omega_3^{\rm eff})^2-(\omega_1^{\rm eff})^2}\,,\quad f_{22}^{(-)}=\frac{\omega_1^2-\omega_2^2}{(\omega_1^{\rm eff})^2-(\omega_2^{\rm eff})^2}\,,$$

*) The operators $\hat{Q}_{LK}^{(\pm)}$ ($L=0, 2$) are defined by

$$\hat{Q}_{LK}^{(\pm)}\equiv\frac{1}{\sqrt{2(1+\delta_{K0})}}(\hat{Q}_{LK}\pm\hat{Q}_{L-K}),\qquad \hat{Q}_{LK}=\sum_{n=1}^{A}(r^2Y_{LK})_n\,,$$

where ($\pm$) denote the signature quantum numbers $r=\pm1$. The 3rd axis is chosen as a quantization axis.

$$f_{00}^{(+)}=1\,. \tag{2·31}$$

The residual interactions, Eqs. (2·26)~(2·29), are cast into form (2·20) with $(\hat{O}_\rho)\equiv(\tilde{Q}_\rho)$,

$$\begin{cases}(\tilde{Q}_\rho)\equiv(\tilde{P}_{n+},\ i\tilde{P}_{n-},\ \tilde{P}_{p+},\ i\tilde{P}_{p-},\ \tilde{Q}_{00}^{(+)},\ \tilde{Q}_{20}^{(+)},\ i\tilde{Q}_{21}^{(+)},\ \tilde{Q}_{22}^{(+)})\\ (\chi_\rho)\equiv(G_n/2,\ G_n/2,\ G_p/2,\ G_p/2,\ \chi_{00}^{(+)},\ \chi_{20}^{(+)},\ \chi_{21}^{(+)},\ \chi_{22}^{(+)})\end{cases}\quad\text{for the } r=+1 \text{ sector}, \tag{2·32}$$

where $\tilde{P}_{\tau\pm}=\tilde{P}_\tau{}^\dagger\pm\tilde{P}_\tau$, and

$$\begin{cases}(\tilde{Q}_\rho)\equiv(\tilde{Q}_{21}^{(-)},\ i\tilde{Q}_{22}^{(-)})\\ (\chi_\rho)\equiv(\chi_{21}^{(-)},\ \chi_{22}^{(-)})\end{cases}\quad\text{for the } r=-1 \text{ sector}. \tag{2·33}$$

Thus, the number N of the separable forces is 8(2) for the $r=+1$ ($r=-1$)-sector. We can express the operators $\tilde{Q}_{LK}^{(\pm)}$ in terms of the original multipole operators $\hat{Q}_{LK}^{(\pm)}$ as

$$\tilde{Q}_\rho=\sum_\sigma \hat{Q}_\sigma C_{\sigma\rho}\,, \tag{2·34}$$

where the conversion matrix (C) is explicitly given in §3.*) Accordingly, the strengths of $\hat{Q}_{LK}^{(\pm)}$'s are obtained from the diagonal matrix elements of

$$\tilde{\mathcal{R}}\equiv(C^{-1})^\dagger\mathcal{R}C^{-1}. \tag{2·35}$$

Finally, it should be noted that the response functions derived in this section are defined in the rotating frame. Accordingly, to make a comparison with experimental data, we have to transform them into the laboratory frame. This transformation is easily done when the single-particle potential is axially symmetric about the rotation axis.[6] It is not easy, however, in the general case.

§ 3. The triaxial harmonic-oscillator potential model

In this section we give the analytical solutions for the GMR and GQR at $\omega_{\rm rot}=0$ in the h.o. potential model with triaxial equilibrium deformation.

In the absence of rotations, the response matrix is decoupled into the "Nambu-Goldstone sector" composed of $(\tilde{Q}_{21}^{(+)},\ \tilde{Q}_{21}^{(-)},\ \tilde{Q}_{22}^{(-)})$ and the "Landau-Migdal sector" composed of $(\tilde{Q}_{00}^{(+)},\ \tilde{Q}_{20}^{(+)},\ \tilde{Q}_{22}^{(+)})$,

$$R=R^{(\rm NG)}\otimes R^{(\rm LM)}\,. \tag{3·1}$$

With the selfconsistency condition (the IVD condition), their explicit expressions are given as

$$R^{(\rm NG)}=\prod_{i=1}^{3}R^{(i)}\,,\qquad R^{(i)}\chi^{(i)}=\frac{1}{2}f^{(i)}(p_i{}^{(+)}+p_i{}^{(-)}) \tag{3·2}$$

*) In §3 the matrix (C) is given for $\omega_{\rm rot}=0$. For the rotating case, (ω_i) should be replaced by $(\omega_i{}^{\rm eff})$.

and

$$R^{(\mathrm{LM})}\chi^{(\mathrm{LM})}=\begin{bmatrix} \frac{f_0}{5}\frac{1}{3}(p_1+p_2+p_3), & \frac{f_2}{2}\frac{1}{3\sqrt{5}}(2p_3-p_1-p_2), & \frac{f_2}{2}\frac{1}{\sqrt{15}}(p_1-p_2) \\ \frac{f_0}{5}\frac{\sqrt{5}}{6}(2p_3-p_1-p_2), & \frac{f_2}{2}\frac{1}{6}(4p_3+p_1+p_2), & \frac{f_2}{2}\frac{1}{2\sqrt{3}}(p_2-p_1) \\ \frac{f_0}{5}\frac{\sqrt{15}}{6}(p_1-p_2), & \frac{f_2}{2}\frac{1}{2\sqrt{3}}(p_2-p_1), & \frac{f_2}{2}\frac{1}{2}(p_1+p_2) \end{bmatrix}, \tag{3·3}$$

where

$$p_i^{(\pm)}\equiv p_{jk}^{(\pm)} \quad (i,\ j,\ k\text{-cyclic}), \qquad p_i\equiv p_{ii}^{(+)},$$

$$p_{ij}^{(\pm)}\equiv\frac{(\omega_i\pm\omega_j)^2}{(\omega_i\pm\omega_j)^2-\omega^2}, \tag{3·4}$$

$$f_0\equiv f_{00}^{(+)},\quad f_2\equiv f_{20}^{(+)}=f_{22}^{(+)},\quad (f^{(i=1,2,3)})\equiv(f_{21}^{(+)},\ f_{21}^{(-)},\ f_{22}^{(-)}). \tag{3·5}$$

In this section we leave the factor $f_{LK}^{(\pm)}$ whose actual values are given by Eq. (2·31) unspecified as long as possible, since the results are then applicable to the isovector modes as well.[13),21)]

Below we shall parametrize ω_i as

$$\omega_i{}^2=\omega_p{}^2\left\{1+\alpha\cos\left(\frac{2\pi}{3}i-\gamma\right)\right\}, \qquad (i=1,\ 2,\ 3) \tag{3·6}$$

where ω_p is determined by $\omega_1\omega_2\omega_3=\omega_0{}^3$, and $(\varepsilon,\ \gamma)$ are related to $(\beta^{(\mathrm{pot})},\ \gamma^{(\mathrm{pot})})$ of Ref. 9) through

$$\alpha=-\frac{4}{3}\varepsilon=-\frac{4}{3}\sqrt{\frac{45}{16\pi}}\beta^{(\mathrm{pot})},$$

$$\gamma=\gamma^{(\mathrm{pot})}. \tag{3·7}$$

3. 1. *Nambu-Goldstone sector*

The RPA eigen-frequencies ω are determined by the poles of $\mathcal{R}$. Thus, from

$$\begin{aligned} g^{(i)}(\Omega)&\equiv(W_i^{(\pm)}-\Omega)(W_i^{(-)}-\Omega)(1-R^{(i)}\chi^{(i)}) \\ &=-\Omega^2+x^{(i)}(W_i^{(+)}+W_i^{(-)})\Omega-(2x^{(i)}-1)W_i^{(+)}W_i^{(-)} \\ &=0, \end{aligned} \tag{3·8}$$

where $W_i^{(\pm)}\equiv((\omega_j\pm\omega_k)/2\omega_p)^2$ and $\Omega\equiv(\omega/2\omega_p)^2$, we obtain

$$\Omega_\pm=x^{(i)}\frac{1}{2}\{(W_i^{(+)}+W_i^{(-)})\pm[W_i^{(+)2}+2aW_i^{(+)}W_i^{(-)}+W_i^{(-)2}]^{1/2}\} \tag{3·9}$$

with

$$a=(1-x^{(i)})/x^{(i)}, \qquad x^{(i)}\equiv 1-f^{(i)}/2. \tag{3·10}$$

The Ω_+ and Ω_- correspond to the high- and the low-lying modes, respectively.

The transition amplitudes $t(\tilde{Q}^{(i)})$ for the operators $(\tilde{Q}^{(i=1,2,3)})\equiv(\tilde{Q}_{21}^{(+)},\ \tilde{Q}_{21}^{(-)},\ \tilde{Q}_{22}^{(-)})$ are given by the residues of $\mathcal{R}^{(i)}$ so that, with the definition

$$\Omega D^{(i)}\equiv(W_i^{(+)}-\Omega)(W_i^{(-)}-\Omega)R^{(i)}(\Omega)\chi$$

$$=\frac{1}{2}\{W_i^{(+)}(W_i^{(-)}-\Omega)+W_i^{(-)}(W_i^{(+)}-\Omega)\}, \tag{3·11}$$

we obtain

$$|t(\tilde{Q}^{(i)})|^2_{\Omega_\pm}=\frac{\sqrt{\Omega_\pm}D^{(i)}(\Omega_\pm)}{(\Omega_\mp-\Omega_\pm)}\left(\frac{\omega_p}{\omega_0}\right)T_{\rm cl} \tag{3·12}$$

for the $\Omega=\Omega_\pm$ modes, where $T_{\rm cl}$ is related to the classical sum rule value $S_{\rm cl}$ for the operator r^2Y_{2K} as

$$T_{\rm cl}\equiv\frac{\hbar\omega_0}{\chi}=\frac{5}{4\pi}\frac{\hbar}{M\omega_0}\langle\sum_{n=1}^{A}(\tilde{x}^2)_n\rangle=\frac{1}{\hbar\omega_0}\frac{1}{5}S_{\rm cl}. \tag{3·13}$$

Finally the transition strengths for the original multipole operators $\hat{Q}^{(i)}$ are readily obtained by multiplying Eq. (3·12) by the inverse of the conversion coefficients

$$C^{(i)}=\omega_j\omega_k/{\omega_0}^2. \qquad (i,\ j,\ k\text{-cyclic}) \tag{3·14}$$

Their explicit expressions are given up to the first order in ε in Table I. In Fig. 1 the properties of the exact solutions are displayed as functions of γ.

For the selfconsistent values, $f^{(i)}=1$, the expression above reduces to

$$\omega=\begin{cases}\omega_{\rm NG}=0\\ \omega_{\rm GR}=\sqrt{{\omega_j}^2+{\omega_k}^2}\end{cases} \tag{3·15}$$

and

$$|t(\hat{Q}^{(i)})|^2_{\rm GR}=\frac{1}{\sqrt{2}}\left(\frac{2{\omega_0}^2}{{\omega_j}^2+{\omega_k}^2}\right)^{3/2}T_{\rm cl},$$

$$[\omega|t(\hat{Q}^{(i)})|^2]_{\rm NG}=\frac{4\pi}{15}\frac{1}{5}S_{\rm cl}\left(\frac{{\omega_0}^2}{\omega_j\omega_k}\right)^4\left\{\left(\frac{\omega_j}{\omega_0}\right)^2-\left(\frac{\omega_k}{\omega_0}\right)^2\right\}\Big/\mathcal{J}_i, \tag{3·16}$$

where $\mathcal{J}_i$ are the cranking moment of inertia around the i-axis:

$$\mathcal{J}_i\equiv M\langle\sum_{n=1}^{A}({x_j}^2+{x_k}^2)_n\rangle. \tag{3·17}$$

3. 2. *Landau-Migdal sector*

The eigen-frequencies of the RPA modes belonging to this sector are determined by a cubic equation:

$$g^{(\rm LM)}(\Omega)\equiv(W_1-\Omega)(W_2-\Omega)(W_3-\Omega)\det(1-R^{(\rm LM)}\chi^{(\rm LM)})$$

$$=-\Omega^3+(x_0+2x_2)\Omega^2-x_2(2x_0+x_2)\left(1-\frac{1}{4}\alpha^2\right)\Omega$$

$$+x_0{x_2}^2\left(1-\frac{3}{4}\alpha^2+\frac{1}{4}\alpha^3\cos3\gamma\right)=0, \tag{3·18}$$

where $W_i\equiv(2\omega_i/2\omega_p)^2$, $\Omega\equiv(\omega/2\omega_p)^2$ and

$$x_0=1-f_0/5, \qquad x_2=1-f_2/2. \tag{3·19}$$

Here we have used parametrization (3·6). The solutions Ω_n are given by Cardano's

formula,

$$\Omega_n=\frac{1}{3}(x_0+x_2)+\frac{2}{3}(x_0-x_2)\sqrt{p}\cos\left(\theta+\frac{2\pi}{3}n\right)\quad(n=0,\ 1,\ 2) \tag{3·20}$$

with

$$\theta=\frac{1}{3}\tan^{-1}\sqrt{(p^3/q^2)-1}\ ,$$

$$\begin{cases} p\equiv 1+\dfrac{x_2(2x_0+x_2)}{(x_0-x_2)^2}\dfrac{3}{4}\alpha^2\ , \\ q\equiv 1+\dfrac{x_0}{x_0-x_2}\dfrac{9}{4}\alpha^2+\dfrac{x_0{x_2}^2}{(x_0-x_2)^2}\dfrac{27}{8}\alpha^3\cos 3\gamma\ . \end{cases} \tag{3·21}$$

In the limit $\gamma\to 0$, the solutions Ω_0, Ω_1 and Ω_2 coincide with the monopole ($L=0$, $K=0$) and the $K=0$ and $K=2$ quadrupole GR, respectively.

The transition amplitudes for the operators $(\tilde{Q}_\rho,\ (\rho=1,\ 2,\ 3))\equiv(\tilde{Q}^{(+)}_{00},\ \tilde{Q}^{(+)}_{20},\ \tilde{Q}^{(+)}_{22})$ are calculated to be

$$[t^*(\tilde{Q}_\rho)t(\tilde{Q}_\sigma)]_\Omega=\frac{\sqrt{\Omega}\,D^{(\mathrm{LM})}_{\rho\sigma}(\Omega)}{(\Omega'-\Omega)(\Omega''-\Omega)}\left(\frac{\omega_p}{\omega_0}\right)T_{\mathrm{cl}}\quad(\rho,\ \sigma=1,\ 2,\ 3) \tag{3·22}$$

with

$$\Omega D^{(\mathrm{LM})}\equiv(W_1-\Omega)(W_2-\Omega)(W_3-\Omega)R^{(\mathrm{LM})}\chi\ , \tag{3·23}$$

where Ω' and Ω'' represent the solutions other than Ω. These transition amplitudes are readily converted into those for the multipole operators $\tilde{Q}^{(+)}_{LK}$ by multiplying the inverse of the conversion matrix (see Eq. (2·35)),

$$C^{(\mathrm{LM})}=\begin{bmatrix} \frac{1}{3}(w_1+w_2+w_3), & \frac{\sqrt{5}}{6}(2w_3-w_1-w_2), & \frac{\sqrt{15}}{6}(w_1-w_2) \\ \frac{1}{3\sqrt{5}}(2w_3-w_1-w_2), & \frac{1}{6}(4w_3+w_1+w_2), & \frac{1}{2\sqrt{3}}(w_2-w_1) \\ \frac{1}{\sqrt{15}}(w_1-w_2), & \frac{1}{2\sqrt{3}}(w_2-w_1), & \frac{1}{2}(w_1+w_2) \end{bmatrix},\quad w_i\equiv(\omega_i/\omega_0)^2$$

$$=(R^{(\mathrm{LM})}\chi^{(\mathrm{LM})})^T[f_0\to 5,\ f_2\to 2;\ p_i\to w_i]. \tag{3·24}$$

The explicit expressions for the matrix elements of $D^{(\mathrm{LM})}$ are found to be

$$D^{(\mathrm{LM})}_{11}=\frac{1}{5x_0}\left\{\left(\Omega-x_2\left(1+\frac{1}{2}\alpha\right)\right)\left(\Omega-x_2\left(1-\frac{1}{2}\alpha\right)\right)\right\},$$

$$D^{(\mathrm{LM})}_{22}=\frac{1}{2x_2}\left\{(\Omega-x_0)\left(\Omega-x_2\left(1-\frac{1}{2}\alpha\cos\gamma\right)\right)-\frac{1}{2}x_0x_2\alpha^2\sin^2\gamma\right\},$$

$$D^{(\mathrm{LM})}_{33}=\frac{1}{2x_2}\left\{(\Omega-x_0)\left(\Omega-x_2\left(1+\frac{1}{2}\alpha\cos\gamma\right)\right)-\frac{1}{2}x_0x_2\alpha^2\cos^2\gamma\right\},$$

$$D^{(\mathrm{LM})}_{12}=\frac{1}{\sqrt{5}}\left(\frac{1}{2}\alpha\right)\left\{(\Omega-x_2)\cos\gamma+\frac{1}{2}x_2\alpha\cos 2\gamma\right\},$$

$$D_{13}^{(\mathrm{LM})}=\frac{1}{\sqrt{5}}\left(\frac{1}{2}\alpha\right)\left\{(\Omega-x_2)\sin\gamma-\frac{1}{2}x_2\alpha\sin 2\gamma\right\},$$

$$D_{23}^{(\mathrm{LM})}=\frac{1}{2}\left(-\frac{1}{2}\alpha\sin\gamma\right)\{(\Omega-x_0)-x_0\alpha\cos\gamma\}. \tag{3·25}$$

Their analytical expressions are given in the lowest order in ε in Table I. In Fig. 1 the properties of the exact solutions are displayed as functions of γ.

Table I. Properties of the GMR and GQR in the triaxial h.o. potential model. Expressions are given in the lowest order with respect to ε. For the modes belonging to the NG-sector, $x^{(i)}(i=1, 2, 3)$ are simply denoted by x. For other notations, see the text.

Nambu-Goldstone sector

mode		excitation energy ω/ω_0	transition strength $\lvert t_\rho\rvert^2/T_{\mathrm{cl}}$
$\mathcal{Q}_1(\tilde{Q}_{21}^{(+)})$	low	$\sqrt{\frac{2x-1}{x}}\varepsilon\left\lvert\cos\gamma+\frac{1}{\sqrt{3}}\sin\gamma\right\rvert$	$\frac{1}{\sqrt{x^3(2x-1)}}\frac{1}{2}\varepsilon\left\lvert\cos\gamma+\frac{1}{\sqrt{3}}\sin\gamma\right\rvert$
	high	$2\sqrt{x}\left(1-\frac{1}{6}\varepsilon(\cos\gamma-\sqrt{3}\sin\gamma)\right)$	$\frac{1}{2\sqrt{x}}\left(1+\frac{1}{2}\varepsilon(\cos\gamma-\sqrt{3}\sin\gamma)\right)$
$\mathcal{Q}_2(\tilde{Q}_{21}^{(-)})$	low	$\sqrt{\frac{2x-1}{x}}\varepsilon\left\lvert\cos\gamma-\frac{1}{\sqrt{3}}\sin\gamma\right\rvert$	$\frac{1}{\sqrt{x^3(2x-1)}}\frac{1}{2}\varepsilon\left\lvert\cos\gamma-\frac{1}{\sqrt{3}}\sin\gamma\right\rvert$
	high	$2\sqrt{x}\left(1-\frac{1}{6}\varepsilon(\cos\gamma+\sqrt{3}\sin\gamma)\right)$	$\frac{1}{2\sqrt{x}}\left(1+\frac{1}{2}\varepsilon(\cos\gamma+\sqrt{3}\sin\gamma)\right)$
$\mathcal{Q}_3(\tilde{Q}_{22}^{(-)})$	low	$\sqrt{\frac{2x-1}{x}}\frac{2}{\sqrt{3}}\varepsilon\lvert\sin\gamma\rvert$	$\frac{1}{\sqrt{x^3(2x-1)}}\frac{1}{\sqrt{3}}\varepsilon\lvert\sin\gamma\rvert$
	high	$2\sqrt{x}\left(1+\frac{1}{3}\varepsilon\cos\gamma\right)$	$\frac{1}{2\sqrt{x}}(1-\varepsilon\cos\gamma)$

Landau-Migdal sector

mode	excitation energy ω/ω_0	transition strength $\lvert t_\rho\rvert^2/T_{\mathrm{cl}}$ for $\tilde{Q}_{LK}^{(+)}$
$\mathcal{Q}_0(\tilde{Q}_{00}^{(+)})$	$2\sqrt{x_0}$	$\tilde{Q}_{00}^{(+)}$: $\frac{1}{5\sqrt{x_0}}$
		$\tilde{Q}_{20}^{(+)}$: $\frac{1}{2\sqrt{x_2}}\left(\frac{1}{2}\sqrt{\frac{x_2}{x_0}}\right)\left(\frac{x_2}{x_0-x_2}\frac{4}{3}\varepsilon\cos\gamma\right)^2$
		$\tilde{Q}_{22}^{(+)}$: $\frac{1}{2\sqrt{x_2}}\left(\frac{1}{2}\sqrt{\frac{x_2}{x_0}}\right)\left(\frac{x_2}{x_0-x_2}\frac{4}{3}\varepsilon\sin\gamma\right)^2$
$\mathcal{Q}_1(\tilde{Q}_{20}^{(+)})$	$2\sqrt{x_2}\left(1-\frac{1}{3}\varepsilon\right)$	$\tilde{Q}_{00}^{(+)}$: $\frac{1}{5\sqrt{x_0}}\left(\frac{1}{2}\sqrt{\frac{x_0}{x_2}}\right)\left(\frac{x_0}{x_0-x_2}\frac{4}{3}\varepsilon\cos\frac{3}{2}\gamma\right)^2$
		$\tilde{Q}_{20}^{(+)}$: $\frac{1}{2\sqrt{x_2}}\left\{(1+\varepsilon)\cos\frac{1}{2}\gamma+\frac{x_0}{x_0-x_2}\frac{2}{3}\varepsilon\sin 3\gamma\sin\frac{1}{2}\gamma\right\}\cos\frac{1}{2}\gamma$
		$\tilde{Q}_{22}^{(+)}$: $\frac{1}{2\sqrt{x_2}}\left\{(1+\varepsilon)\sin\frac{1}{2}\gamma-\frac{x_0}{x_0-x_2}\frac{2}{3}\varepsilon\sin 3\gamma\cos\frac{1}{2}\gamma\right\}\sin\frac{1}{2}\gamma$
$\mathcal{Q}_2(\tilde{Q}_{22}^{(+)})$	$2\sqrt{x_2}\left(1+\frac{1}{3}\varepsilon\right)$	$\tilde{Q}_{00}^{(+)}$: $\frac{1}{5\sqrt{x_0}}\left(\frac{1}{2}\sqrt{\frac{x_0}{x_2}}\right)\left(\frac{x_0}{x_0-x_2}\frac{4}{3}\varepsilon\sin\frac{3}{2}\right)^2$
		$\tilde{Q}_{20}^{(+)}$: $\frac{1}{2\sqrt{x_2}}\left\{(1-\varepsilon)\sin\frac{1}{2}\gamma-\frac{x_0}{x_0-x_2}\frac{2}{3}\varepsilon\sin 3\gamma\cos\frac{1}{2}\gamma\right\}\sin\frac{1}{2}\gamma$
		$\tilde{Q}_{22}^{(+)}$: $\frac{1}{2\sqrt{x_2}}\left\{(1-\varepsilon)\cos\frac{1}{2}\gamma+\frac{x_0}{x_0-x_2}\frac{2}{3}\varepsilon\sin 3\gamma\sin\frac{1}{2}\gamma\right\}\cos\frac{1}{2}\gamma$

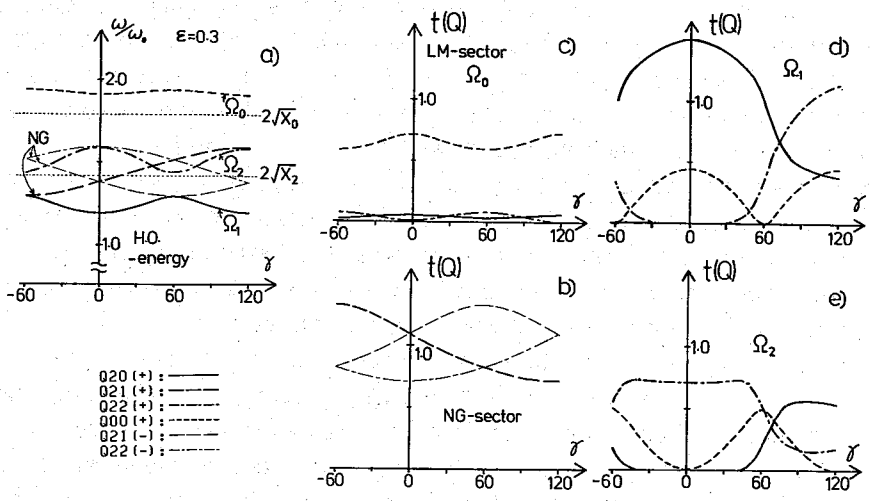

Fig. 1. Dependence on the triaxiality γ of the properties of the GMR and GQR in the h.o. potential model. ε is fixed at a value 0.3. (a) Excitation energies $\hbar\omega$ in units of $\hbar\omega_0$. (b) Transition strengths $|t_\nu|^2$ with respect to the operators $(\hat{Q}^{(+)}_{21}, \hat{Q}^{(-)}_{21}, \hat{Q}^{(-)}_{22})$ for the modes belonging to the NG-sector. The unit is $T_{\rm cl}$. (c), (d) and (e) Transition strengths with respect to the operators $(\hat{Q}^{(+)}_{00}, \hat{Q}^{(+)}_{20}, \hat{Q}^{(+)}_{22})$ for the eigenmodes Ω_0, Ω_1 and Ω_2 belonging to the LM-sector, which respectively correspond to the monopole, the $K=0$ and $K=2$ quadrupole GR in the limit $\gamma\to 0$. A factor $5\sqrt{x_0}(2\sqrt{x_2})$ is multiplied for the $\hat{Q}^{(+)}_{00}(\hat{Q}^{(+)}_{2K})$-strength in order to normalize these values to unity in the spherical limit.

From this table, we can evaluate the mixing strengths between the GMR and the GQR as

$$\frac{[|t(\hat{Q}^{(+)}_{20})|^2+|t(\hat{Q}^{(+)}_{22})|^2]_{\Omega_0}}{[|t(\hat{Q}^{(+)}_{20})|^2+|t(\hat{Q}^{(+)}_{22})|^2]_{\Omega_1,\Omega_2}}\simeq\frac{\frac{1}{2}\sqrt{\frac{x_2}{x_0}}\left(\frac{x_2}{x_0-x_2}\frac{4}{3}\varepsilon\right)^2}{1\pm\varepsilon}, \tag{3·26}$$

$$\frac{|t(\hat{Q}^{(+)}_{00})|^2_{\Omega_1}+|t(\hat{Q}^{(+)}_{00})|^2_{\Omega_2}}{|t(\hat{Q}^{(+)}_{00})|_{\Omega_0}}\simeq\frac{1}{2}\sqrt{\frac{x_0}{x_2}}\left(\frac{x_0}{x_0-x_2}\frac{4}{3}\varepsilon\right)^2. \tag{3·27}$$

As is clearly seen from these expressions, the expansion with respect to ε is accompanied by a factor $1/(x_0-x_2)$, which is approximately proportional to an inverse of the energy difference between the GMR and the GQR. For the selfconsistent values, $f^{(+)}_{LK}=1(x_0=\frac{5}{4}$ and $x_2=\frac{1}{2})$, this factor takes 0.3 and therefore the expansion is dangerous already for $\varepsilon\lesssim 0.3$. Thus we need to use the exact expressions for such cases. In fact, as is clearly seen from Fig. 1(a), the ordering of the excitation energies predicted by the first-order approximation with respect to ε is changed in the oblate limit due to the higher-order contributions.

Finally it should be mentioned that we have used the REDUCE II for analytically evaluating Eqs. (3·18) and (3·25).

§ 4. Details of calculation

For the description of the GR, it is necessary to use a sufficiently large shell-model space. We have therefore taken into account 5-oscillator shells, i.e., $N_{\rm osc}=3-7$ and $2-6$

for neutrons and protons, respectively. In fact the classical energy-weighted sum-rule values are exhausted in this model space (Table II). As for the force parameters, we have used the selfconsistent value of $\kappa_{LK}^{(\pm)}(L=0, 2)$ for the doubly stretched multipole forces, although the renormalization factors $f_{2K}^{(\pm)}\approx 1.07-1.12$, are required to reproduce the experimental data for the low-lying quadrupole vibrational modes.*)

In the calculations with such a large model space, it is important to take into account the $N_{\rm osc}$-dependence of the strength $v_{l\cdot l}$ of the $\boldsymbol{l}^2$-terms in the Nilsson potential. If this $N_{\rm osc}$-dependence is neglected, the unperturbed strength distributions of the monopole and the quadrupole operators deviate appreciably from $2\hbar\omega_0$. We therefore use the values of $v_{l\cdot s}$ and $v_{l\cdot l}$ newly determined by Bengtsson and Ragnarsson.[22]

Since the giant resonances in the high-spin region are considered to be excited on the compound states with rather high excitation energies from the yrast line,[1),2)] inclusion of the finite temperature effects may be preferable. However, according to the calculations in Refs. 3) and 4), these effects do not change the essential features of the strength functions for GR's. Therefore, we have neglected them for simplicity. Furthermore, we use in this paper the adiabatic quasiparticle basis because the fine structure of the yrast states is not important for properties of GR's under consideration.

As for the energy-averaging parameter $\mathrm{Im}(\omega)$, we adopt the values 0.5 MeV and 1.0 MeV for Fig. 2 and Figs. 3~6, respectively.

§ 5. Results of calculation

5. 1. *The GMR and GQR built on the ground state*

Figure 2 shows the calculated strength functions for the monopole and quadrupole operators acting on the ground state of ^{158}Er: Figure 2(a) is the result of full calculations and Fig. 2(b) the result in which only the $\Delta N_{\rm osc}=\pm 2$ matrix elements are taken into account.

The excitation energies of the GQR and of the GMR are reproduced about 10.5 MeV and 16.5 MeV, respectively. This result qualitatively agrees with the prediction of the h.o. potential model, $\sqrt{2}\hbar\omega_0=10.7$ MeV and $\sqrt{16/5}\hbar\omega_0=13.6$ MeV. On the other hand, the calculated value is about 1 MeV lower (higher) than the experimental data for the GQR (GMR) obtained by the electron scattering.[15] The main reason for this small discrepancy is that, as is displayed in the lower part of Fig. 1, the unperturbed strengths are shifted considerably from the region of $2\hbar\omega_0\approx 15.2$ MeV due to the $\boldsymbol{l}^2$-terms.[4] The calculated splitting of the GQR is about 1 MeV, which well coincides with the prediction of the h.o. potential model (about $\sqrt{2}\hbar\omega_0\times\frac{2}{3}\varepsilon\approx 1.3$ MeV for $\varepsilon\approx 0.18$).[11)~13)] It is also seen that the calculated ratios of the strengths between different K-components agree well with the h.o. model predictions listed in Table I. The experimental data[11),14),15)] indicate that the deformation broadens the width of the GQR about the same magnitude with this theoretical calculation.

As for the coupling between the GMR and GQR, the calculated result indicates that the mixing of strengths is small. This result is slightly different from the estimate in terms of the h.o. potential model, Eqs. (3·26) and (3·27), which suggests that the $\hat{Q}_{00}^{(+)}$-

*) In Ref. 8) the contribution to $\langle\sum_{n=1}^{A}(\boldsymbol{x}''^2)_n\rangle$ from the outside of the model space was neglected in calculating κ, resulted in the inappropriate values $f_{2K}^{(\pm)}\approx 1.03$.

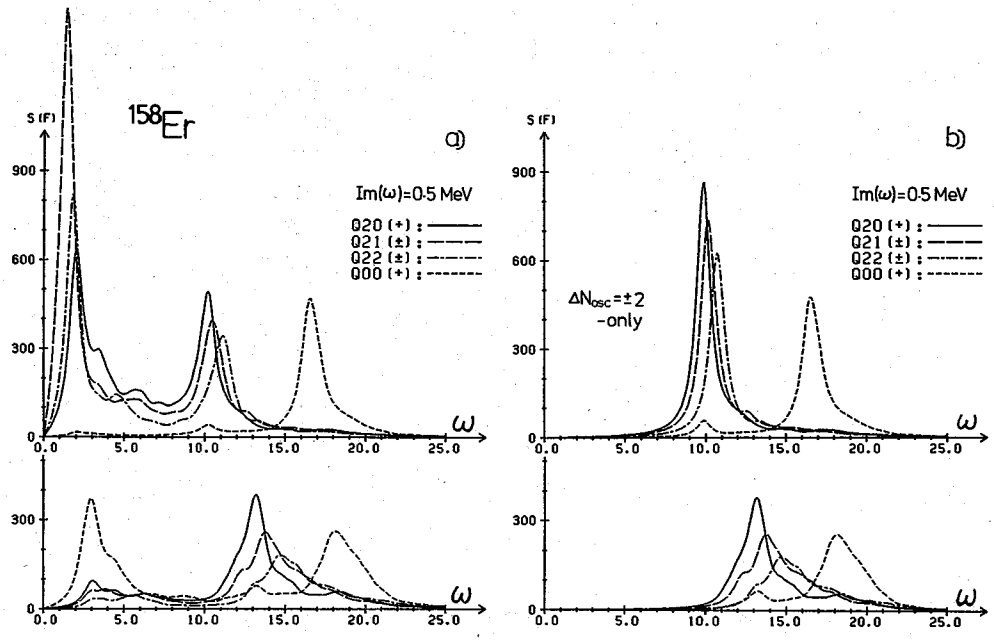

Fig. 2. Strength functions for the operators $\hat{Q}^{(\pm)}_{LK}$ acting on the ground state of ^{158}Er. Im $(\hbar\omega)=0.5$ MeV is adopted. (a) Both the $\Delta N_{\rm osc}=0$ and ± 2 excitations are taken into account. (b) Only the $\Delta N_{\rm osc}=\pm 2$ excitations are taken into account. The upper (lower) parts show the RPA (unperturbed) strength functions in units of $b_0^4/\hbar\omega_0$. A factor 5/2 is multiplied for the $\hat{Q}^{(\pm)}_{00}$-strength in order to make the value comparable with those of $\hat{Q}^{(\pm)}_{2K}$-strengths.

strength of the GQR ($K=0$) is noticeably large while the $\hat{Q}^{(+)}_{20}$-strength of the GMR is small.[12] The origin of this difference is easily understood from the analysis in §3, which indicates that the mixing of the strengths is quite sensitive to the energy difference between the GMR and GQR. Thus, the shift of about 3 MeV from the h.o. prediction in the excitation energy of the GMR, mentioned above, causes such a difference.

Figure 2 furthermore shows that considerable amount of the quadrupole strength is distributed over the energy region between 0 and 8 MeV. Consequently, only about 55% of the oscillator strength is exhausted by the GQR's, as is displayed in Table II. This value is similar to that of Dumitrescu and Hamamoto,[23] but smaller than that of Zawiscka, Speth and Pal[24] who used the density-dependent zero-range forces of Migdal and Larkin. Since only the attractive (isoscalar) quadrupole interaction is taken into account in our calculations, it seems necessary to investigate in detail the effects of the isovector-quadrupole and the quadrupole-pairing interactions, in order to understand this difference.

The low-energy peaks around 1~2 MeV in the RPA strength functions correspond to the low-lying $\beta(K=0)$, $\gamma(K=2)$ and the NG($K=1$) modes. They deviate about 1 MeV from the experimentally observed positions since we have not adjusted the force parameters.

On the other hand, the low-energy peak of the unperturbed $\hat{Q}^{(+)}_{00}$-strength (in the lower part of Fig. 2(a)) is due to the presence of the pairing field. This peak disappears in the RPA because the NG modes associated with the pairing rotations guarantee the decoupling condition $[\hat{Q}^{(+)}_{00}, \hat{N}]_{\rm RPA}=0$ to hold.

Table II. Calculated distributions of the oscillator strengths for the operators $\hat{Q}^{(\pm)}_{LK}$ acting on the ground state of ^{158}Er. These are nomalized by the values integrated up to 30 MeV. The deformation parameter $\delta_{\rm osc}$ used is 0.184. The numbers in the parentheses show the distributions obtained when only the $\Delta N_{\rm osc}=\pm 2$ excitations are taken into account. The calculated and the classical energy-weighted sum rule values are given in units of $\hbar\omega_0 b_0^4=226.7$ MeV fm^4.

mode	distribution of oscillator strength						EWSR-value	
	0-3	3-8	8-13	13-19	19-30	(MeV)	cal.	classical
$\hat{Q}^{(+)}_{00}$	0.0 (0.0)	1.0 (0.1)	5.1 (5.3)	85.6 (86.4)	8.3 (8.2)	(%)	137.1 (135.8)	122.3
$\hat{Q}^{(+)}_{20}$	10.9 (0.0)	20.1 (0.6)	55.5 (84.8)	9.5 (11.1)	4.0 (3.5)		346.9 (303.1)	346.2
$\hat{Q}^{(+)}_{21}$	17.1 (0.0)	14.3 (0.4)	53.6 (83.0)	10.6 (12.3)	4.4 (4.3)		333.7 (291.9)	320.4
$\hat{Q}^{(+)}_{22}$	14.5 (0.0)	12.3 (0.3)	54.5 (79.3)	12.5 (14.0)	6.2 (6.4)		277.6 (249.6)	265.5

5. 2. *The GMR and GQR built on the high-spin yrast states*

In Fig. 3 we display the strength functions for the operators $\hat{Q}^{(\pm)}_{LK}$ acting on the yrast states of ^{164}Er with $\hbar\omega_{\rm rot}=0.0$, 0.2, 0.4 and 0.6 MeV. The deformation parameters of the yrast states are selfconsistently determined and are listed in Table III. The calculation indicates that this nucleus has rather stable deformation of approximately prolate shape up to considerably high angular momentum, accompanying, however, the slowly increasing triaxial deformation. This calculated result is similar to that of Ref. 25).

At $\omega_{\rm rot}\neq 0$ the GQR splits into five peaks corresponding to the five components of the quadrupole operators $\hat{Q}^{(+)}_{2K=0,1,2}$ and $\hat{Q}^{(-)}_{2K=1,2}$. Similarly to the GR's excited on the ground state, we find that the result of realistic calculations for the excitation energies, the splitting, and the strengths for these modes well agree with the prediction of the triaxially deformed h.o. potential model. Concerning the dependence on the rotational frequency $\omega_{\rm rot}$, we notice that the excitation energies of the GMR and GQR decrease at $\hbar\omega_{\rm rot}=0.4$ MeV about 0.5 MeV (Fig. 3(c)). The main reason for this is that at this rotational frequency the neutron pairing gap vanishes due to the excitation of four aligned quasi-neutrons and the proton pairing gap is also reduced due to two aligned quasi-protons. This decrease of the excitation energies is smaller in magnitude than that of the GDR reported in Ref. 3), since the pairing reduction affects only little the $2\hbar\omega_0$ excitations across the Fermi-surface (which are the important components of the GMR and GQR but are absent in the case of GDR).

It is seen that qualitative features of the GMR and GQR are not much affected by the high-frequency rotations, except that the fragmentation width of each component, especially that of $K=1$ (Fig. 3(c) and (d)), is increased noticeably due to the K-mixing effects of the Coriolis force. Therefore it can be stated (at least for $\hbar\omega_{\rm rot}\lesssim 0.6$ MeV) that the rapid rotations influence the GMR and GQR mainly through the equilibrium-deformation change of the single-particle potential.

In Fig. 4 we also show the strength functions for the yrast states of ^{158}Er with $\hbar\omega_{\rm rot}=0.0$, 0.35, 0.5 and 0.7 MeV. The corresponding deformation parameters are listed in Table III. This nucleus appears to be relatively soft against the deformation, and thus a

Table III. Selfconsistently determined deformation parameters and the expectation values of $\hat{J}_1$ for the yrast states of ^{164}Er and ^{158}Er. The unit for Δ_n, Δ_p and $\hbar\omega_{\rm rot}$ is MeV.

	$\hbar\omega_{\rm rot}$	$\langle\hat{J}_1\rangle$	Δ_n, Δ_p		$(\beta, \gamma)^{\rm (self)}$		(ε, γ)	
^{164}Er	0.00	0.0	1.032,	0.984	0.303,	0.0	0.241,	0.0
	0.20	5.7	0.929,	0.928	0.306,	2.1	0.243,	3.6
	0.40	36.2	0.0,	0.610	0.257,	8.3	0.213,	13.1
	0.60	53.3	0.0,	0.0	0.197,	14.0	0.170,	20.2
^{158}Er	0.0	0.0	1.348,	1.198	0.216,	0.0	0.180,	0.0
	0.35	31.4	0.0,	0.803	0.213,	−2.4	0.177,	−3.2
	0.50	46	0.0,	0.661	0.119,	−60.0	0.119,	−60.0
	0.70	64	0.0,	0.0	0.216,	−60.0	0.229,	−60.0

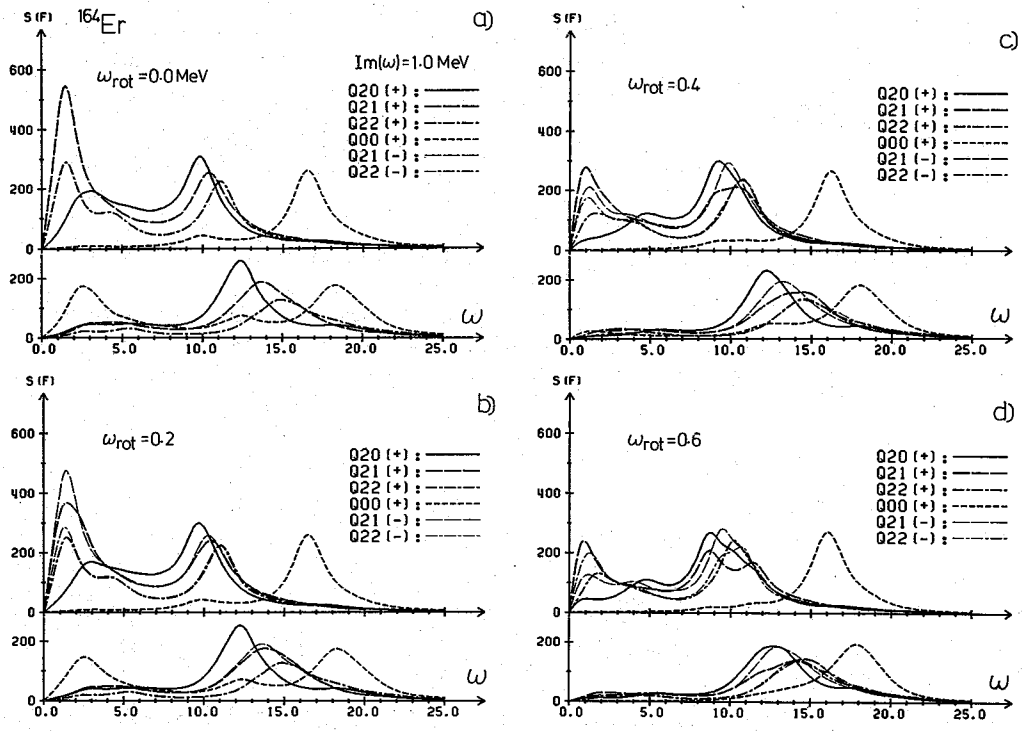

Fig. 3. Strength functions for the operators $\hat{Q}^{(\pm)}_{LK}$ acting on the yrast states of ^{164}Er. Im($\hbar\omega$)=1.0 MeV is adopted. (a), (b), (c) and (d) are evaluated at $\hbar\omega_{\rm rot}$=0.0, 0.2, 0.4 and 0.6 MeV, respectively. The calculated deformation parameters of the yrast states are listed in Table III. See also the caption to Fig. 2.

phase transition to the oblate shape with respect to the rotation axis (high K-isomer) occurs in the present calculation at $I \lessapprox 50$, again in accordance with the result of Ref. 25). The strength function after the oblate shape is realized (Fig. 4(c) and (d)) appears to contradict the h.o. model prediction at first sight, namely the splitting of the GQR appears too large. However it should be recalled that we have done the calculation in the rotating frame. In the oblate case, we can easily transform the calculated result into the laboratory frame as follows:

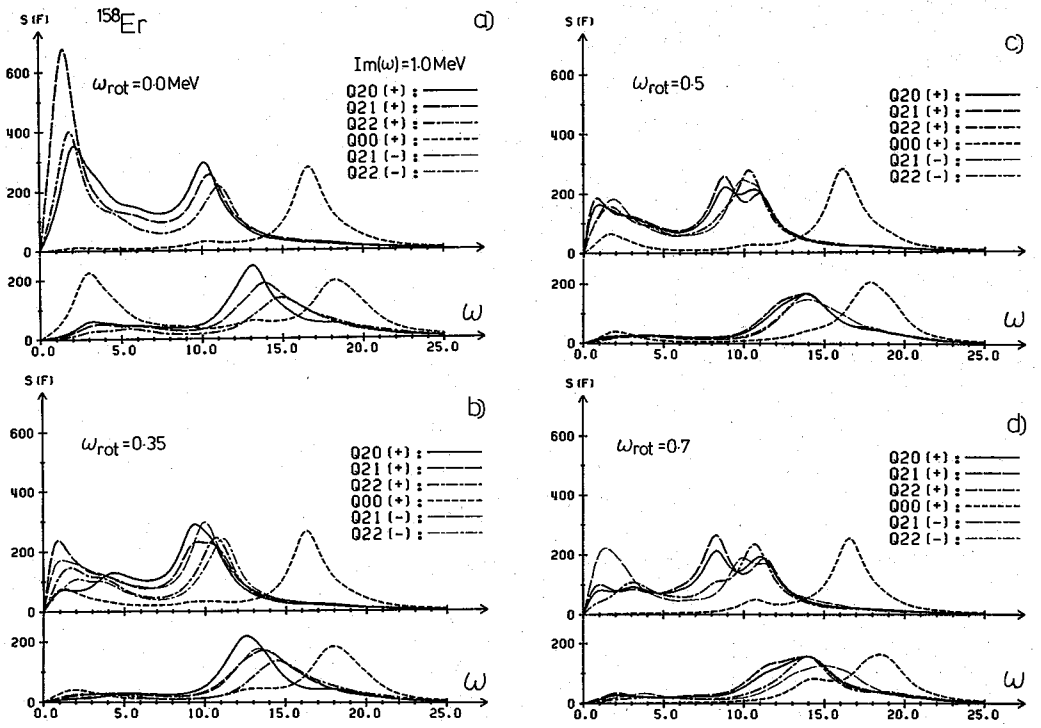

Fig. 4. The same as Fig. 3 but for ^{158}Er. (a), (b), (c) and (d) are the strength functions calculated at $\hbar\omega_{\rm rot}=0.0$, 0.35, 0.5 and 0.7 MeV, respectively. Note that, in (c) and (d), the $\tilde{Q}^{(-)}_{21}$- and $\tilde{Q}^{(-)}_{22}$-strengths exactly coincide since the oblate shape is realized. See also Table III.

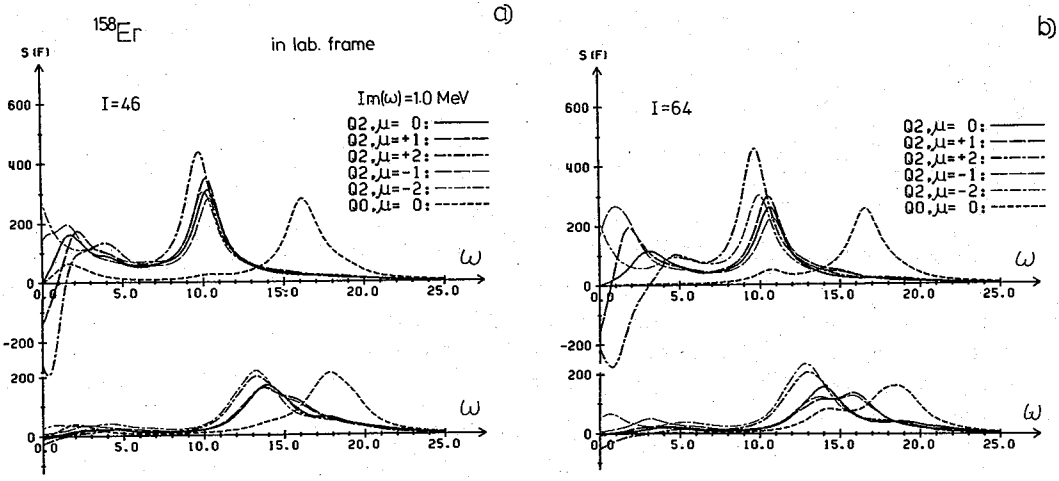

Fig. 5. Strength functions in the laboratory frame for the operators $\mathring{Q}_{L\mu}$ acting on high-K isomeric states in ^{158}Er. (a) and (b) correspond to Fig. 4(c) and (d) calculated at $I=46\hbar$ and $64\hbar$ (see Table III).

$$S^{(\rm lab)}_{\mathring{Q}_{2\mu}}(\omega)=S^{(\rm rot)}_{\mathring{Q}_{2\mu}}(\omega-\mu\omega_{\rm rot}), \tag{5·1}$$

where $\mathring{Q}_{2\mu}$ is the quadrupole operator whose components are defined with respect to the rotation axis (the lst-axis), i.e.,

$$\mathring{Q}_{2\mu} \equiv \sum_{K=-2}^{2} \mathcal{D}^{(2)}_{\mu K}\left(\frac{\pi}{2}, \frac{\pi}{2}, 0\right) \hat{Q}_{2K} . \tag{5·2}$$

Note that there is an important relation for $S^{(\mathrm{lab})}_{\mathring{Q}_{2\mu}}$,

$$S^{(\mathrm{lab})}_{\mathring{Q}_{2\mu}}(\omega) = -S^{(\mathrm{lab})}_{\mathring{Q}_{2-\mu}}(-\omega). \tag{5·3}$$

We show in Fig. 5(a) and (b) the strength functions for the operator $\mathring{Q}_{2\mu}$ transformed into the laboratory frame, which correspond to Fig. 4(c) and (d). From this figure we find that, for instance, the two peaks in the $\hat{Q}^{(+)}_{21}$-strength seen in Fig. 4(c) and (d) correspond to the $\mu=+2$ and -2 -components of the $\mathring{Q}_{2\mu}$ operator and hence their excitation energies are respectively shifted by $+2\hbar\omega_{\mathrm{rot}}$ and $-2\hbar\omega_{\mathrm{rot}}$ by this transformation. Thus, the splitting is reduced by $4\hbar\omega_{\mathrm{rot}}$ in the laboratory frame, recovering the agreement with the h.o. potential prediction in §3. Note, however, that small splittings between $+\mu$ and $-\mu$ -components arise due to the Coriolis effects, in addition to those among the $\mu=0$, 1 and 2 -components by the deformation effects. Furthermore a difference in the strengths between the $+\mu$ and $-\mu$ -components is conspicuous. It should be noticed that in the transformation of the strength function into the laboratory frame the coupling terms in the response matrix play an important role. Therefore the prescription adopted in Ref. 3), which neglects the coupling terms, does not seem to be a good approximation at least for the GQR under consideration. The results obtained above qualitatively agree with the predictions of Ref. 6) where the GQR built on the high-K isomers are investigated within the cranked h.o. potential model. In this connection, we also mention that the negative peaks seen in the low-frequency parts of the $\mathring{Q}_{2\mu=+2}$-strengths in Fig. 5(a) and (b) are associated with the negative-energy transitions from the yrast states with angular momentum I to states with $I-2$ (see Eq. (5·3)), which occur in the description where the yrast states are regarded as the vacuum states.

Finally we give in Fig. 6 the quantities

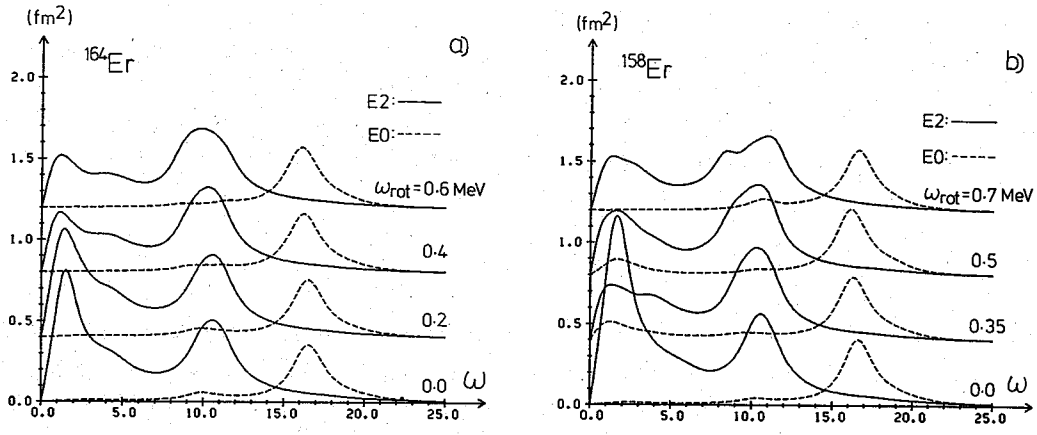

Fig. 6. The quantities defined by Eq. (5·4) in the rotating frame, which are related to the photo- and/or electro-reaction cross sections. The unit is fm². (a) and (b) are those for ^{164}Er and ^{158}Er, respectively. In (a) ((b)), the four curves correspond to (a)~(d) of Fig. 3 (Fig. 4) which are shifted from the bottom by 0.0, 0.4, 0.8 and 1.2 fm², respectively.

$$\tau(E2;\ \omega)=\frac{4\pi^2}{15}\left(\frac{e^2}{\hbar c}\right)\frac{(\hbar\omega_0)^3}{(\hbar c)^2}\left(\frac{Z}{A}\right)^2\sum_{\substack{K=0,1,2\\ r=+,-}}S_{Q_{2K}^{(r)}}(\omega),$$

$$\tau(E0;\ \omega)=2\pi^3\left(\frac{e^2}{\hbar c}\right)\frac{(\hbar\omega_0)^3}{(\hbar c)^2}\left(\frac{Z}{A}\right)^2 S_{Q_{00}^{(+)}}(\omega), \tag{5·4}$$

which are related to the photo- and/or electro-reaction cross sections in the long wavelength limit.[26] Four curves in this figure correspond from the bottom to the calculations (a), (b), (c) and (d) of Fig. 3 (Fig. 4) for ^{164}Er (^{158}Er). From this figure we see that, as the angular momentum becomes larger, the peak energies of the GMR and GQR slightly move reflecting the change of equilibrium deformation of the single-particle potential, while the width of the GQR increases as a consequence of the K-mixing effects of the Coriolis forces. The change in these quantities are not drastic, however.

§ 6. Conclusions

We have performed realistic calculations of the strength functions for the isoscalar giant monopole and quadrupole resonances built on the high-spin yrast states. The doubly stretched monopole and quadrupole forces with selfconsistent values of force parameters are used as residual interactions. For the case of non-rotating but triaxially deformed harmonic-oscillator potential, we have derived the analytical solutions of the coupled RPA equations describing these modes. We have found that the calculated properties of the GMR and GQR—the excitation energies, the splitting and the mixing of the strengths—are well characterized by these analytical expressions. It has also been shown that these properties, especially the small splitting of the GQR, are quite consistent with the experimental observations.[15] This result demonstrates the importance of the "nuclear selfconsistency" emphasized by Kishimoto.[11),12]

It has been found that the high frequency rotation affects the properties of the GMR and GQR mainly through the change of the deformation parameters (including pairing fields), except that the K-mixings caused by the Coriolis force considerably broaden the width of each component of the GQR.

The drastic change might not occur in the quantities like the inclusive photo-emission cross sections, because the splitting of the GQR induced by the triaxial deformation is small. Therefore it is hoped that more high-precision measurements (e.g., those distinguishing each component of the GQR), will be done to extract information about the structural change of nuclei caused by the rapid rotations.

Acknowledgements

We thank Professor P. Ring, Dr. K. Ando and Dr. S. Nishizaki for fruitful discussions. One of the authors (Y. R. S.) is indebted to Japan Society for the Promotion of Science for financial support. The computer calculation for this work has been supported in part by the Grant-in-Aid for Scientific Research of the Japan Ministry of Education, Science and Culture (No. 58540153), and in part by Research Center for Nuclear Physics, Osaka University.

References

1) J. O. Newton et al., Phys. Rev. Lett. **46** (1981), 1383.
B. Haas et al., Phys. Lett. **120B** (1983), 79.
A. M. Sandorfi et al., Phys. Lett. **130B** (1983), 19.
2) W. Hennerici et al., Nucl. Phys. **A396** (1983), 329c.
3) J. L. Egido and P. Ring, Phys. Rev. **C25** (1982), 3239.
M. E. Faber, J. L. Egido and P. Ring, Phys. Lett. **127B** (1983), 5.
P. Ring, L. M. Robledo, J. L. Egido and M. Faber, Nucl. Phys. **A419** (1984), 261.
4) S. N. Fedotkin, I. N. Mikhailov and R. G. Nazmitdinov, Phys. Lett. **121B** (1983), 15.
I. N. Mikhailov, R. G. Nazmitdinov and S. N. Fedotkin, Yad. Fiz. **38** (1983), 24 [Sov. J. Nucl. Phys. **38** (1983), 13].
5) O. Civitarese, S. Furui, M. Ploszajczak and A. Faessler, Nucl. Phys. **A408** (1983), 61.
6) H. Kurasawa, Prog. Theor. Phys. **64** (1980), 2055; **66** (1981), 1317; **68** (1982), 1594.
7) A. Akbarov, A. V. Ignatyuk, I. N. Mikhailov, Kh. L. Molina, R. G. Nazmitdinov and D. Janssen, Yad. Fiz. **33** (1981), 1480 [Sov. J. Nucl. Phys. **33** (1981), 794].
E. B. Bal'butsev, Z. Vaishvila and I. N. Mikhailov, Yad. Fiz. **35** (1982), 836 [Sov. J. Nucl. Phys. **35** (1982), 486].
8) Y. R. Shimizu and K. Matsuyanagi, Prog. Theor. Phys. **70** (1983), 144.
9) Y. R. Shimizu and K. Matsuyanagi, Prog. Theor. Phys. **71** (1984), 960.
10) Y. R. Shimizu and K. Matsuyanagi, Prog. Theor. Phys. **72** (1984), 799.
11) T. Kishimoto et al., Phys. Rev. Lett. **35** (1975), 552.
12) T. Kishimoto, *Proc. 1980 RCNP Int. Symp. on Highly Excited States in Nuclear Reactions,* Osaka, p. 145.
13) T. Suzuki and D. J. Rowe, Nucl. Phys. **A289** (1977), 461.
14) A. Schwierczinski et al., Phys. Lett. **55B** (1975), 171.
15) B. S. Dolbilkin et al., Phys. Rev. **C25** (1982), 2255.
16) D. J. Thouless, Nucl. Phys. **21** (1960), 225; **22** (1961), 78.
17) E. R. Marshalek and J. Weneser, Ann. of Phys. **53** (1969), 569.
18) V. I. Arnold, *Mathematical Methods of Classical Mechanics* (Springer-Verlag, 1978).
19) N. Nakanishi, Prog. Theor. Phys. Suppl. No. 51 (1972), 1.
20) P. Ring and P. Schuck, *The Nuclear Many-Body Problem* (Springer-Verlag, 1980).
21) H. Kurasawa and T. Suzuki, Preprint RIFP-559.
22) T. Bengtsson and I. Ragnarsson, Preprint Lund-MPh-84/03.
23) T. S. Dumitriscu and I. Hamamoto, Nucl. Phys. **A383** (1982), 205.
24) D. Zawischa, J. Speth and D. Pal, Nucl. Phys. **A311** (1978), 445.
25) G. Andersson, S. E. Larsson, G. Leander, P. Möller, S. G. Nilsson, I. Ragnarsson and S. Åberg, Nucl. Phys. **A268** (1976), 205.
26) J. M. Eisenberg and W. Greiner, *Nuclear Theory,* Vol. 2, (North-Holland, 1975).

Progress of Theoretical Physics, Vol. 74, No. 2, August 1985

Applicability of the Canonical Quantization Procedure for the Collective Hamiltonian Derived by the Selfconsistent-Collective-Coordinate Method

Masayuki MATSUO and Kenichi MATSUYANAGI

Department of Physics, Kyoto University, Kyoto 606

(Received January 21, 1985)

We investigate the validity of the canonical quantization of the collective Hamiltonian derived by the selfconsistent-collective-coordinate method. Special attention is paid to the boundary condition for the (η^*, η) expansion, which fixes the canonical coordinate system to carry out the quantization procedure. We remove the ambiguity of the boundary condition by requiring that the boson representations obtained by the canonical quantization agree, to the order $1/\Omega$, with those derived by the modified-Marumori boson-expansion method in a certain limit. Numerical examples for an exactly solvable model show that our quantization procedure provides us with remarkably accurate results.

§ 1. Introduction

The selfconsistent-collective-coordinate (SCC) method proposed by Marumori, Maskawa, Sakata and Kuriyama[1] provides us with a classical framework to dynamically extract the collective submanifold from the huge-dimensional phase space associated with the time-evolution of the Hartree-Fock-Bogoliubov (HFB) state vectors. They also proposed a practical way to solve the basic equations of the SCC method, called the (η^*, η) expansion method.[1] It seems to us that the next important subjects to be attacked are 1) to find a procedure to quantize the classical collective Hamiltonian derived by the SCC method, and 2) to apply the SCC method to real nuclear phenomena. Of course, we cannot carry out the second subject without solving the first problem, since the evaluation of excitation spectra and transition probabilities requires the quantization.

In this paper, we show that the canonical quantization with the normal ordering is a suitable procedure for quantizing the classical Hamiltonian evaluated by the fourth-order approximation of the (η^*, η) expansion. Our argument is based on the following investigations: 1) The comparison with the modified-Marumori(mM) boson-expansion method[2),3)] for the case that the collective submanifold is generated by the restricted time-dependent Hartree-Bogoliubov (TDHB) state vectors. 2) The comparison with the exact solutions in a solvable model for the case that the collective submanifold is fully selfconsistently determined without imposing any restriction on the form of the TDHB state vectors. The relation of the (η^*, η) expansion to the mM boson expansion was previously noted by Sakata et al.[4] Also a canonical quantization prescription similar to ours was used in Refs. 5) and 6). However, no detailed investigation on its validity has been carried out up to now. In this paper, we shall argue that our quantization procedure is sufficiently reliable (albeit not exact) to allow us application of the SCC method to real nuclear phenomena. In fact, we have applied[9] the SCC method to elucidate the microscopic structure of anharmonicities of the gamma-vibration in ^{168}Er, and the details will be reported in a forthcoming paper.[10]

As stressed by Kuriyama and Yamamura,[7),8)] the collective submanifold determined

by the SCC method is invariant under the linear canonical transformations for the collective coordinates η^* and η. This invariance results in an arbitrariness of the choice of the boundary condition of the (η^*, η) expansion, which fix the canonical coordinate system for describing the collective submanifold. It is possible, however, to positively utilize this arbitrariness; we thus propose to set up such a boundary condition that is optimally suited to the canonical quantization procedure with the normal ordering. This is the main idea of the present paper.

After briefly reviewing the basic equations of the SCC method in §2, we describe our quantization procedure in §3. The boson representations of physical operators obtained by the quantization are compared in §4 with those derived by the mM boson-expansion method.[2),3)] Here, special attention is paid to the boundary condition for the (η^*, η) expansion, which fixes the canonical coordinate system of the collective submanifold, and we show that the Tamm-Dancoff(TD)-type boundary condition is suitable for the canonical quantization with the normal ordering. In §5 we perform numerical analysis of the exactly solvable three-level model, and confirm the accuracy of our quantization procedure. In §6 conclusions are given and a future problem is remarked.

§ 2. Résumé of the SCC method

In the SCC method,[1)] the collective coordinates (η^*, η) are introduced as c-number variables which parametrize the HFB state vector:

$$|\phi(\eta^*, \eta)\rangle = e^{iG(\eta^*, \eta)}|\phi_0\rangle, \tag{2·1}$$

$$iG(\eta^*, \eta) = \frac{1}{2}\sum_{ij}\{G_{ij}(\eta^*, \eta)a_i^\dagger a_j^\dagger - G_{ij}^*(\eta^*, \eta)a_j a_i\}, \tag{2·2}$$

where $(a_i^\dagger, a_i)$ are the quasiparticle creation and annihilation operators and $|\phi_0\rangle$ is the HFB ground state satisfying $a_i|\phi_0\rangle = 0$. Through the complex functions $G_{ij}(\eta^*, \eta)$, the time dependence of the collective coordinates (η^*, η) determines the time-evolution of the HFB state vector (2·1). Thus, the functions $G_{ij}(\eta^*, \eta)$ define a manifold imbeded in the TDHB phase space, which is called the collective submanifold. At the same time, the TDHB state vector generates the collective subspace in the many-fermion state space.

The fundamental principle to determine the functions $G_{ij}(\eta^*, \eta)$ is the "invariance principle of the time-dependent Schrödinger equation"[11)] which requires that the collective motion under consideration should be maximally decoupled from the remaining (non-collective) degrees of freedom. Combining this principle with the "canonical-variables condition" which requires that the collective variables (η^*, η) should be the canonical variables, we obtain the following set of basic equations of the SCC method:

i) definition of collective Hamiltonian

$$\mathcal{H}(\eta^*, \eta) = \langle\phi_0|e^{-iG(\eta^*, \eta)}He^{iG(\eta^*, \eta)}|\phi_0\rangle - \langle\phi_0|H|\phi_0\rangle, \tag{2·3}$$

ii) equation of collective subspace

$$\delta\langle\phi_0|\left\{e^{-iG(\eta^*, \eta)}He^{iG(\eta^*, \eta)} - \frac{\partial\mathcal{H}}{\partial\eta^*}O^\dagger(\eta^*, \eta) - \frac{\partial\mathcal{H}}{\partial\eta}O(\eta^*, \eta)\right\}|\phi_0\rangle = 0, \tag{2·4}$$

iii) canonical-variables condition

$$\langle\phi_0|O^\dagger(\eta^*,\eta)|\phi_0\rangle=\frac{1}{2}\eta^* \text{ and } \langle\phi_0|O(\eta^*,\eta)|\phi_0\rangle=\frac{1}{2}\eta\,, \tag{2·5}$$

iv) equation of collective motion

$$i\dot{\eta}=\frac{\partial\mathcal{H}}{\partial\eta^*} \quad \text{and} \quad i\dot{\eta}^*=-\frac{\partial\mathcal{H}}{\partial\eta}\,, \tag{2·6}$$

where

$$O^\dagger(\eta^*,\eta)=e^{-iG(\eta^*,\eta)}\frac{\partial}{\partial\eta}e^{iG(\eta^*,\eta)},$$

$$O(\eta^*,\eta)=-e^{-iG(\eta^*,\eta)}\frac{\partial}{\partial\eta^*}e^{iG(\eta^*,\eta)} \tag{2·7}$$

and the variation in (2·4) means that $\delta|\phi_0\rangle=a_i^\dagger a_j^\dagger|\phi_0\rangle$.

Once the collective subspace is determined by the above set of equations, it is straightforward to express arbitrary operators F in terms of (η^*,η): The function $\mathcal{F}(\eta^*,\eta)$ defined by the expectation value,

$$\mathcal{F}(\eta^*,\eta)=\langle\phi_0|e^{-iG(\eta^*,\eta)}Fe^{iG(\eta^*,\eta)}|\phi_0\rangle \tag{2·8}$$

is called the collective representation of the operator F.

A method to solve the basic set of equations, (2·3)~(2·6), is to expand the unknown functions $G_{ij}(\eta^*,\eta)$ and the collective Hamiltonian $\mathcal{H}(\eta^*,\eta)$ in a power series of the collective coordinates (η^*,η) and require that Eqs. (2·3)~(2·6) be satisfied in each order with respect to the powers of (η^*,η). This method successively determines the solutions $G_{ij}(\eta^*,\eta)$ and $\mathcal{H}(\eta^*,\eta)$ starting from the lowest-order terms, and is called the (η^*,η) expansion method.

Thus, the collective subspace is selfconsistently determined within the framework of the SCC method without *a priori* introducing it from the outset. On the other hand, the description in terms of the SCC method is classical in nature. This is known as a property common to all descriptions that use the time-dependent variational principle for the HFB state vectors.[12]

§ 3. Procedure of quantization

To calculate the excitation spectrum and the transition amplitudes of the system, we have to quantize the results obtained by the SCC method. We do this in the following way. Since all the physical quantities are explicitly expressed as polynomials of the collective coordinates (η^*,η), we replace the η^* and η with the boson operators $B^\dagger$ and B which satisfy $[B,B^\dagger]=1$. Concerning the ordering of the boson operators, we adopt the normal ordering. Thus, for instance, the collective Hamiltonian $\mathcal{H}$ is quantized as

$$\mathcal{H}(\eta^*,\eta)\to H_{\text{coll}}(B^\dagger,B)=:\mathcal{H}(B^\dagger,B):\,, \tag{3·1}$$

where : : denotes the normal ordering. By diagonalizing the quantum collective Hamiltonian H_{coll} in the physical subspace in the boson Fock space,

$$\left\{\frac{1}{\sqrt{n!}}(B^\dagger)^n|0)_B\,;\ n=0,\,1,\,\cdots,\,n_{\max}\right\}, \tag{3·2}$$

where $n_{\max}$ corresponds to the maximum number of collective states contained in the collective subspace, we obtain the excitation energies and the eigenvectors. We can also derive the boson representations of transition operators by applying the same quantization procedure to their collective representations $\mathcal{F}(\eta^*, \eta)$. Then, the transition amplitudes are readily evaluated by the matrix elements with respect to the eigenvectors obtained above.

As discussed in the next section, this quantization procedure is motivated by the relationship between the (η^*, η) expansion and the boson-expansion method. Thus, it has nothing to do with the well-known ordering ambiguities in the canonical quantization of the classical mechanics, because it is possible, in principle, to find an optimal quantization procedure by analysing the microscopic structure of the collective subspace. Furthermore, contrary to the quantization procedure employing the Pauli prescription,[13),14)] it is free from the assumption that the collective potential energy just coincides with the expectation value of the original Hamiltonian with respect to the time-even HFB states. This point will be discussed in detail in Ref.10).

§ 4. Applicability of the canonical quantization procedure

In this section, we investigate the validity of our quantization procedure. This is done by making a comparison between the boson representations derived by the procedure and those obtained by the well-known boson-expansion method.

4.1. *Comparison with the boson-expansion method*

Let us assume that the collective subspace is composed of the phonon operators $X^\dagger = \frac{1}{2}\sum_{ij}\psi_{ij}a_i^\dagger a_j^\dagger$ as

$$\left\{|n\rangle = \frac{1}{\sqrt{n!}}N(n)^{-1/2}(X^\dagger)^n|\phi_0\rangle\,;\ n=0,\,1,\,\cdots\right\}, \tag{4·1}$$

where $N(n)\equiv(1/n!)\langle\phi_0|(X)^n(X^\dagger)^n|\phi_0\rangle$. Then, the method which exactly transcribes the dynamics within this subspace into an equivalent one in a boson space is well known, and is called the modified Marumori (mM) boson expansion.[4),5)] This method is fully quantal in nature, and therefore the requirement that the results obtained by our quantization procedure should coincide with those obtained by the boson-expansion method in the limit that the collective subspace is restricted to (4·1) will provide us with a necessary condition for the quantization procedure to be valid. Of course, it is unnecessary for the SCC method to impose such restrictions, and we shall discuss in the next section the case where the collective subspace is selfconsistently determined by the collective dynamics of the system itself.

The collective subspace (4·1) is equivalent to the space generated by the TDHB state

$$\begin{aligned}|\phi(\eta^*, \eta)\rangle &= e^{iG(\eta^*,\eta)}|\phi_0\rangle \\ &= N(\eta^*, \eta)^{-1/2}e^{f(\eta^*,\eta)X^\dagger}|\phi_0\rangle\,,\end{aligned} \tag{4·2}$$

where the normalization function $N(\eta^*, \eta)$ is calculated to be[15]

$$N(\eta^*, \eta)=\exp\left\{\frac{1}{2}\mathrm{Tr}\ \ln(1+\boldsymbol{\phi}^\dagger\boldsymbol{\phi}f^*(\eta^*, \eta)f(\eta^*, \eta))\right\}. \tag{4·3}$$

Here $\boldsymbol{\phi}$ is the matrix notation for the phonon amplitudes ϕ_{ij}. For convenience, we normalize them as

$$\langle\phi_0|[X, X^\dagger]|\phi_0\rangle=\frac{1}{2}\sum_{ij}\phi_{ij}^*\phi_{ij}=\frac{1}{2}\mathrm{Tr}\boldsymbol{\phi}^\dagger\boldsymbol{\phi}=1. \tag{4·4}$$

Because we have imposed the particular form (4·2) for the TDHB state, the unknown function $f(\eta^*, \eta)$ can be determined by the canonical-variables condition (2·5) alone. For the TDHB state (4·2), Eq. (2·5) becomes

$$\eta^*=\left(\frac{\partial f}{\partial\eta}f^*-\frac{\partial f^*}{\partial\eta}f\right)\frac{1}{2}\mathrm{Tr}\left(\frac{\boldsymbol{\phi}^\dagger\boldsymbol{\phi}}{1+\boldsymbol{\phi}^\dagger\boldsymbol{\phi}f^*f}\right). \tag{4·5}$$

A solution to this equation is found to be

$$f(\eta^*, \eta)=\eta\sqrt{\frac{F^{-1}(\eta^*\eta)}{\eta^*\eta}}, \tag{4·6}$$

where $F^{-1}(x)$ is the inverse function of

$$\begin{aligned}F(x)&=\frac{1}{2}\mathrm{Tr}\left(\frac{\boldsymbol{\phi}^\dagger\boldsymbol{\phi}x}{1+\boldsymbol{\phi}^\dagger\boldsymbol{\phi}x}\right)\\&=x+\sum_{n=1}(-1)^n\frac{1}{2}\mathrm{Tr}((\boldsymbol{\phi}^\dagger\boldsymbol{\phi})^{n+1})x^{n+1}.\end{aligned} \tag{4·7}$$

Now that we have determined the TDHB state $|\phi(\eta^*, \eta)\rangle$, we can evaluate the collective representations of arbitrary n-body operators ($n=1, 2, \cdots$). By Wick's theorem, they can be expressed in terms of the collective representations of bilinear quasiparticle operators

$$\langle\phi|a_i^\dagger a_j^\dagger|\phi\rangle=\left(\frac{1}{1+\boldsymbol{\phi}^\dagger\boldsymbol{\phi}F^{-1}(\eta^*\eta)}\boldsymbol{\phi}^\dagger\right)_{ji}\eta^*\sqrt{\frac{F^{-1}(\eta^*\eta)}{\eta^*\eta}}, \tag{4·8a}$$

$$\langle\phi|a_i^\dagger a_j|\phi\rangle=\left(\frac{1}{1+\boldsymbol{\phi}^\dagger\boldsymbol{\phi}F^{-1}(\eta^*\eta)}\boldsymbol{\phi}^\dagger\boldsymbol{\phi}\right)_{ij}F^{-1}(\eta^*\eta), \tag{4·8b}$$

$$\langle\phi|a_ja_i|\phi\rangle=\langle\phi|a_i^\dagger a_j^\dagger|\phi\rangle^*. \tag{4·8c}$$

We can expand the above expressions in a power series with respect to the collective coordinates (η^*, η) as

$$\langle\phi|a_j^\dagger a_j^\dagger|\phi\rangle=(\boldsymbol{\phi}^\dagger)_{ji}\eta^*-((\boldsymbol{\phi}^\dagger\boldsymbol{\phi}-\frac{1}{2}C)\boldsymbol{\phi}^\dagger)_{ji}\eta^*\eta^*\eta+\cdots, \tag{4·9a}$$

$$\langle\phi|a_i^\dagger a_j|\phi\rangle=(\boldsymbol{\phi}^\dagger\boldsymbol{\phi})_{ij}\eta^*\eta-((\boldsymbol{\phi}^\dagger\boldsymbol{\phi}-C)\boldsymbol{\phi}^\dagger\boldsymbol{\phi})_{ij}\eta^*\eta^*\eta\eta+\cdots, \tag{4·9b}$$

where

$$C\equiv\frac{1}{2}\mathrm{Tr}((\boldsymbol{\phi}^\dagger\boldsymbol{\phi})^2). \tag{4·10}$$

Next, let us compare expression (4·9) with the boson representation obtained by the boson-expansion method. In the mM boson-expansion method, one first introduces the ideal boson space $\{|n\rangle=1/\sqrt{n!}\ (B^\dagger)^n|0\rangle;\ n=0, 1, \cdots\}$ which corresponds to the collective subspace (4·1), and then maps the fermion operator F into the boson space such that the matrix element of the mapped operator F_B in the physical subspace of the ideal boson space takes the same value with the matrix element $\langle n|F|m\rangle$ in the fermion space. With the use of the mapping operator $U=\sum_{n=0}|n\rangle\langle n|$, the boson representation F_B is given by

$$F_B=UFU^\dagger=\sum_{n,m}\frac{1}{\sqrt{n!m!}}\langle n|F|m\rangle(B^\dagger)^n:e^{-B^\dagger B}:(B)^m. \tag{4·11}$$

Usually, the above expression is expanded in a power series with respect to the normal ordered product of $B^\dagger$ and B. Thus, for the bilinear quasiparticle operators, we obtain

$$(a_i^\dagger a_j^\dagger)_B=(\boldsymbol{\phi}^\dagger)_{ji}B^\dagger-(N(2)^{-1/2}\boldsymbol{\phi}^\dagger\boldsymbol{\phi}\boldsymbol{\phi}^\dagger+(1-N(2)^{-1/2})\boldsymbol{\phi}^\dagger)_{ji}B^\dagger B^\dagger B+\cdots, \tag{4·12a}$$

$$(a_i^\dagger a_j)_B=(\boldsymbol{\phi}^\dagger\boldsymbol{\phi})_{ij}B^\dagger B-(N(2)^{-1}\boldsymbol{\phi}^\dagger\boldsymbol{\phi}\boldsymbol{\phi}^\dagger\boldsymbol{\phi}+(1-N(2)^{-1})\boldsymbol{\phi}^\dagger\boldsymbol{\phi})_{ij}B^\dagger B^\dagger BB+\cdots, \tag{4·12b}$$

$$(a_ja_i)_B=(a_i^\dagger a_j^\dagger)_B^\dagger, \tag{4·12c}$$

where $N(2)=1-C$. It is seen that the quantity C defined by (4·10) plays in Eq. (4·12) the role of a small parameter. In fact, its reciprocal $\Omega\equiv C^{-1}$ represents an effective number of two-quasiparticle states participating in building up the phonon mode $X^\dagger$ (one can easily confirm that Ω is equal to the degeneracy of the single-particle level in the solvable model discussed in § 4).[16),17)] This argument applies also for making an order-estimate of the (η^*, η) expansion: If we regard

$$\frac{1}{2}\mathrm{Tr}((\boldsymbol{\phi}^\dagger\boldsymbol{\phi})^n)=O(\Omega^{-n+1}),$$

then, as is seen from expressions (4·7) and (4·8), the expansion coefficients of the $(\eta^*)^n(\eta)^m$ term is of order $\Omega^{-(n+m)/2}$. In this sense, the (η^*, η) expansion is equivalent to the Ω^{-1} expansion. Therefore, we can expect a fast convergence for sufficiently collective phonon mode $X^\dagger$ whose Ω is large. In this connection, we quote the recent work of Kishimoto and Tamura,[18)] in which they discuss the convergence property of the boson expansion by formulating it in a form of linked-cluster expansion. According to the above order-estimate, the second terms on the r. h. s. of (4·12a) and (4·12b) contain the contributions starting from $O(\Omega^{-3/2})$ and $O(\Omega^{-2})$, respectively. If we evaluate the leading-order contributions with respect to the Ω^{-1} expansion in the second terms, (4·12) is reduced to

$$(a_i^\dagger a_j^\dagger)_B=(\boldsymbol{\phi}^\dagger)_{ji}B^\dagger-((\boldsymbol{\phi}^\dagger\boldsymbol{\phi}-\frac{1}{2}C)\boldsymbol{\phi}^\dagger)_{ji}B^\dagger B^\dagger B+\cdots, \tag{4·13a}$$

$$(a_i^\dagger a_j)_B=(\boldsymbol{\phi}^\dagger\boldsymbol{\phi})_{ij}B^\dagger B-((\boldsymbol{\phi}^\dagger\boldsymbol{\phi}-C)\boldsymbol{\phi}^\dagger\boldsymbol{\phi})_{ij}B^\dagger B^\dagger BB+\cdots. \tag{4·13b}$$

We find that the above expression just coincides with expression (4·9) under the correspondence rule

$$(\eta^*)^n(\eta)^m\longleftrightarrow(B^\dagger)^n(B)^m. \tag{4·14}$$

This means that the quantization procedure proposed in § 3 reproduces the results of the

mM boson expansion for the bilinear quasiparticle operators $a_i^\dagger a_j^\dagger$ and $a_i^\dagger a_j$ up to the $O(\Omega^{-3/2})$ and $O(\Omega^{-2})$, respectively.

The relationship found above should be distinguished from the well-known one between the boson-expansion method and the TDHB theory[19] in the sense that there is no concept like collective coordinates and collective subspace in the latter case and accordingly the bosons $(B_{ij}^\dagger, B_{ij})$ are introduced so as to directly correspond to the quasiparticle pair operators $(a_i^\dagger a_j^\dagger, a_j a_i)$.

We can also find the agreement similar to the above for the collective Hamiltonian. In the (η^*, η) expansion method, it is evaluated with the use of (4·3) and (4·6) to be

$$\begin{aligned}\mathcal{H}(\eta^*, \eta)=&\langle\phi_0|XHX^\dagger|\phi_0\rangle\eta^*\eta+\frac{1}{2}\langle\phi_0|XXH|\phi_0\rangle(\eta^*\eta^*+\eta\eta)\\&+\frac{1}{2}\langle\phi_0|XXHX^\dagger|\phi_0\rangle(\eta^*\eta^*\eta+\eta^*\eta\eta)\\&+\left\{\frac{1}{4}\langle\phi_0|XXHX^\dagger X^\dagger|\phi_0\rangle-(1-C)\langle\phi_0|XHX^\dagger|\phi_0\rangle\right\}\eta^*\eta^*\eta\eta\\&+\left\{\frac{1}{6}\langle\phi_0|XXXHX^\dagger|\phi_0\rangle-\frac{1}{2}(1-C)\langle\phi_0|XXH|\phi_0\rangle\right\}(\eta^*\eta^*\eta^*\eta+\eta^*\eta\eta\eta)\,.\end{aligned}\tag{4·15}$$

In the ordinary case where the Hamiltonian H consists of the one-body field and the residual two-body interactions, it is easily seen with the help of (4·9) that the $(\eta^*)^n(\eta)^m$ terms are of $O(\Omega^{1-(n+m)/2})$ provided the quadratic terms are regarded as $O(\Omega^0)$. Thus, the higher-order terms in the (η^*, η) expansion decrease with the power of Ω^{-1}. As usual, the fourth-order terms represent the leading-order anharmonicity effects arising from the Pauli principle between the quasiparticles constituting the phonon mode $X^\dagger$, and are of $O(\Omega^{-1})$.

On the other hand, in the mM boson expansion method, the collective boson Hamiltonian is evaluated to be

$$\begin{aligned}H_B=&\langle\phi_0|XHX^\dagger|\phi_0\rangle B^\dagger B+\frac{1}{2}\left(1+\frac{1}{2}C\right)\langle\phi_0|XXH|\phi_0\rangle(B^\dagger B^\dagger+BB)\\&+\frac{1}{2}\left(1+\frac{1}{2}C\right)\langle\phi_0|XXHX^\dagger|\phi_0\rangle(B^\dagger B^\dagger B+B^\dagger BB)\\&+\left\{\frac{1}{4}\langle\phi_0|XXHX^\dagger X^\dagger|\phi_0\rangle-(1-C)\langle\phi_0|XHX^\dagger|\phi_0\rangle\right\}B^\dagger B^\dagger BB\\&+\left\{\frac{1}{6}\langle\phi_0|XXXHX^\dagger|\phi_0\rangle-\frac{1}{2}(1-C)\langle\phi_0|XXH|\phi_0\rangle\right\}(B^\dagger B^\dagger B^\dagger B+B^\dagger BBB)\end{aligned}\tag{4·16}$$

up to the $O(\Omega^{-1})$. We see that (4·16) agrees, aside from the factor $(1+\frac{1}{2}C)$ appearing in the second and third terms on the r. h. s. of this equation, with result (4·15) of the (η^*, η) expansion method under the correspondence rule (4·14). This agreement is remarkable, since we know many examples in which the fourth-order terms determine the major features of the spectrum of anharmonic vibrations.

Finally, we note that such a good agreement would not be obtained if other orderings

(e. g., the Weyl ordering) are adopted instead of the normal ordering. This is evident from the correspondence (4·14) and the comparisons made in this section.

4.2. *Boundary condition for the* (η^*, η) *expansion*

In making a comparison between the boson expansion and the (η^*, η) expansion, special attention should be paid to the boundary condition which fixes the canonical coordinate system for the collective submanifold. The basic equations (2·3)~(2·6) of the SCC method are invariant under the linear canonical transformations

$$\eta^* \to \sigma\eta^* + \tau\eta\ ,$$
$$\eta \to \sigma\eta + \tau\eta^* \qquad (4\cdot17)$$

with the coefficients σ and τ satisfying the relation $\sigma^2-\tau^2=1$. As stressed by Kuriyama and Yamamura,[7),8)] we can therefore choose, within this ambiguity, an arbitrary canonical coordinate system without affecting the structure of the collective submanifold. However, they have not discussed how to fix the canonical coordinate system in connection with the quantization procedure.

In fact, in the previous subsection, we implicitly assumed a specific boundary condition. That is, solution (4·6) for the function $f(\eta^*, \eta)$ which determines the time-evolution of the TDHB state $|\phi(\eta^*, \eta)\rangle$ has been obtained by choosing, as the lowest-order solution of the (η^*, η) expansion, the following specific boundary condition

$$iG^{(1)}(\eta^*, \eta) = \eta X^\dagger - \eta^* X\ . \qquad (4\cdot18)$$

Let us recall that the phonon operator $X^\dagger$ is defined by $X^\dagger = \frac{1}{2}\sum_{ij}\psi_{ij}a_i^\dagger a_j^\dagger$ whose amplitudes ψ_{ij} may be determined by the conventional Tamm-Dancoff (TD) equation. Since the collective coordinates (η^*, η) correspond, under the boundary condition (4·18), to the TD-type phonon operators $(X^\dagger, X)$ in the small amplitude limit, let us call Eq. (4·18) the TD-type boundary condition. In general, for the TDHB state $|\phi(\eta^*, \eta)\rangle$ of form (4·2), the lowest-order solution to the canonical-variables condition (2·5) is written as

$$iG^{(1)}(\eta^*, \eta) = (\sigma\eta + \tau\eta^*)X^\dagger - (\sigma\eta^* + \tau\eta)X \qquad (4\cdot19)$$

with $\sigma^2-\tau^2=1$. This reduces to (4·18) when we set $\sigma=1$ and $\tau=0$. Thus, in addition to the choice of the phonon mode $X^\dagger$, we have to fix the values of σ and τ in order to completely specify the boundary condition. The values of σ and τ can be arbitrarily chosen within the framework of the classical description in terms of the SCC method, because the linear canonical transformation (4·17) is merely a coordinate transformation which change neither the classical equation of motion nor the equation of collective subspace. However, the boundary condition is no longer arbitrary, once the quantization procedure is specified. In fact, we have seen that the TD-type boundary condition is required in order for the good agreement between the collective representation (4·9) and the boson representation (4·12) to hold after the quantization.

The argument of this section may be summarized as follows:

(1) We have to break the invariance under the linear canonical transformation (4·17) by choosing a particular boundary condition suitable for the quantization procedure adopted.

(2) The canonical quantization with the normal ordering is well justified if it is used in conjunction with the TD-type boundary condition (4·18), and if we are concerned with the

4-th order approximation of the (η^*, η) expansion.

§ 5. Simple model analysis

In this section, we investigate the applicability of our quantization procedure for the case where the maximally decoupled collective subspace is dynamically determined, rather than *a priori* given by the truncated TDHB states of form (4·2). Since there is no *quantum* theory capable of treating such a general case, which we can use as a standard theory to compare with, we test the accuracy of our quantization procedure by applying it to an exactly solvable model.

5.1. *The three-level model*

We consider an N-nucleon system which is described by the following model Hamiltonian:[4]

$$H=\sum_{i=1,2} e_i K_{ii}-\frac{1}{2}\sum_{i=1,2} V_i(K_{0i}K_{0i}+K_{i0}K_{i0}) + \frac{1}{2}V_3\{(K_{10}+K_{20})(K_{12}+K_{21})+\text{h. c.}\}, \tag{5·1}$$

$$K_{ij}=\sum_{m=1}^{N} c_{im}^{\dagger}c_{jm}, \qquad (i, j=0, 1, 2) \tag{5·2}$$

where $c_{im}^{\dagger}$ and c_{im} are the operators that create and annihilate nucleons in the magnetic substate m belonging to the i-th level. The single-particle energies of the $i=0$, 1 and 2 levels are set to be 0, e_1 and e_2, respectively $(e_2>e_1>0)$. Each level has degeneracy N. They are denoted by the first term of (5·1). The second term represents the residual interactions that excite the nucleons in the $i=0$ level to the $i=1$ and 2 levels. Let us assume that all the N particles occupy the lowest $i=0$ level in the HF ground state $|\phi_0\rangle$. Then, we obtain two decoupled vibrational modes

$$X_{i(\mathrm{RPA})}^{\dagger}=(\psi_i K_{i0}-\varphi_i K_{0i})/\sqrt{N}, \qquad i=1 \text{ and } 2 \tag{5·3}$$

in the RPA. Their amplitudes (ψ_i, φ_i) and excitation energies $\hbar\omega_i$ can be readily obtained by solving the RPA equations. The third term of (5·1) gives rise to the coupling between the two modes. It is not effective in the RPA order. If $\hbar\omega_1 \ll \hbar\omega_2$ and if the mode-mode coupling is neglected, then the collective subspace may be constructed by using only the lower mode, $X_{i=1(\mathrm{RPA})}^{\dagger}$, in a manner similar to (4·2). However, we should generally expect that the mode-mode coupling becomes increasingly important with increasing amplitude of the collective vibration so that the collective subspace (submanifold) should be determined by taking this dynamical anharmonicity effect into account. The nature of the collective submanifold for this model system was previously studied within the framework of the SCC method by Sakata et al.[4] Our purpose below is to apply our quantization procedure to this collective submanifold and to check the result in comparison with the exact solution. Since the operators K_{ij} satisfy an $SU(3)$ algebra, the exact solution is easily obtained by diagonalizing Hamiltonian (5·1).

5.2. *Application of the SCC method and quantization*

The collective subspace which we are going to determine may be generated by the following TDHB state:

$$|\phi(\eta^*, \eta)\rangle = e^{iG(\eta^*,\eta)}|\phi_0\rangle ,$$

$$iG(\eta^*, \eta) = \sum_{i=1,2}\{G_i(\eta^*, \eta)X^{\dagger}_{i(\mathrm{RPA})} - G_i{}^*(\eta^*, \eta)X_{i(\mathrm{RPA})}\} , \tag{5·4}$$

where $K_{0i}|\phi_0\rangle = 0$ for $i=1$ and 2. If we set $G_2(\eta^*, \eta)=0$, then the coupling to the higher RPA mode is neglected. In this case, the collective subspace reduces to the form discussed in §4, which is assumed in the conventional boson-expansion method. In this section, we dynamically determine the unknown functions $G_1(\eta^*, \eta)$ and $G_2(\eta^*, \eta)$ by means of the (η^*, η) expansion method. The procedure for determining $G_i(\eta^*, \eta)$ and the collective Hamiltonian $\mathcal{H}(\eta^*, \eta)$ is the same as in Sakata et al.,[4] except for the difference in the boundary condition. As discussed in § 4, because of the invariance under the linear canonical transformations, the lowest-order solution of the (η^*, η) expansion can be generally written as

$$\begin{aligned} iG^{(1)}(\eta^*, \eta) &= (\sigma\eta + \tau\eta^*)X^{\dagger}_{1(\mathrm{RPA})} - (\sigma\eta^* + \tau\eta)X_{1(\mathrm{RPA})} \\ &= \eta Y_1{}^{\dagger} - \eta^* Y_1 , \end{aligned} \tag{5·5}$$

$$\mathcal{H}^{(2)}(\eta^*, \eta) = \hbar\omega_1(\sigma^2+\tau^2)\eta^*\eta + \hbar\omega_1\sigma\tau(\eta^*\eta^* + \eta\eta) , \tag{5·6}$$

where

$$Y_1{}^{\dagger} = \sigma X^{\dagger}_{1(\mathrm{RPA})} - \tau X_{1(\mathrm{RPA})} , \tag{5·7}$$

and σ and τ are arbitrary real numbers satisfying the relation $\sigma^2-\tau^2=1$. Here we have adopted the lower RPA mode $X^{\dagger}_{i=1(\mathrm{RPA})}$, because we describe the anharmonic vibration which reduces to it in the small amplitude limit. Sakata et al. fixed the boundary condition by choosing $\sigma=1$ and $\tau=0$. With this choice, the collective coordinates η^* and η correspond, in the lowest-order, to the creation and annihilation operators, $X^{\dagger}_{1(\mathrm{RPA})}$ and $X_{1(\mathrm{RPA})}$, of the RPA vibration. We prefer, however, to fix the boundary condition by

$$\sigma = \phi_1 \quad \text{and} \quad \tau = -\varphi_1 , \tag{5·8}$$

where ϕ_1 and φ_1 are the forward and backward amplitudes of the RPA vibration defined by Eq. (5·3). Obviously, the collective Hamiltonian obtained under this boundary condition is related to the one used by Sakata et al. through the linear canonical transformation; $\eta^* \to \phi_1\eta^* - \varphi_1\eta$ and $\eta \to \phi_1\eta - \varphi_1\eta^*$. The reason for choice (5·8) is that it is better suited to our quantization procedure. To explicitly see this point, let us insert (5·8) into (5·5) and (5·6). Then, we have

$$iG^{(1)} = (\eta K_{10} - \eta^* K_{01})/\sqrt{N} , \tag{5·9}$$

$$\mathcal{H}^{(2)} = e_1\eta^*\eta - V_1(N-1)(\eta^*\eta^* + \eta\eta) . \tag{5·10}$$

Considering that the operators K_{10} and K_{01} correspond to the TD-type phonon operators $X^{\dagger}$ and X discussed in § 4, choice (5·9) is seen to be equivalent to the TD-type boundary condition (4·18). As shown in § 4, this boundary condition guarantees a good agreement between the results obtained by our quantization procedure and by the boson-expansion method, in the limit where the contributions from $G_2(\eta^*, \eta)$ are neglected. Furthermore,

this choice of the boundary condition enables us to apply the (η^*, η) expansion method also to the deformed region where the lower RPA root becomes imaginary.

The model under consideration is special in the sense that the single-particle states contributing to the RPA mode $X^{\dagger}_{i(\mathrm{RPA})}$ are degenerate. In general, it is impossible to construct the TD phonon by a simple linear combination of the collective RPA phonon alone (like Eq. (5·7)). In such general cases, we can still determine the values of σ and τ such that the operator $Y_1{}^{\dagger}$ best resembles the corresponding TD phonon.[10] We shall call the specific RPA boundary condition with such a choice of σ and τ "the optimized RPA boundary condition" in the sense that it best attains the agreement with the mM boson expansion within the restricted TDHB state space considered in § 4. Since the boundary condition (5·8) is a specific example of this prescription, we shall use this term also to it.

We calculated $G_i(\eta^*, \eta)$ up to the third order to obtain the fourth-order collective Hamiltonian $\mathcal{H}^{(4)}(\eta^*, \eta)$. Correspondingly, the collective representations of the transition operators K_{i0} are evaluated up to the third order. By diagonalizing the quantized collective Hamiltonian in the physical boson space with $n_{\max}=N$, we obtain the excitation spectrum and transition probabilities of the three-level model under consideration.

5.3. *Result of numerical calculation*

Figure 1 shows the calculated excitation spectrum for the case $V_3=0$. We see that the result obtained under the optimized RPA boundary condition (5·8) agrees very well with the exact spectrum. The excellent agreement persists beyond the RPA critical point, and holds over the whole region of the interaction strength V_1. On the other hand, the result obtained under the boundary condition ($\sigma=1$ and $\tau=0$) considerably deviates from the exact solution. Of course, it diverges at the RPA critical point. For comparison, we also present in this figure the result which is obtained by quantization with the Weyl ordering,

$$(\eta^*)^n(\eta)^m \to \frac{1}{2^n}\sum_{k=0}^{n}\binom{n}{k}(B^{\dagger})^{n-k}(B)^m(B^{\dagger})^k .$$

We see that this quantization procedure does not give as good agreement as the quantization with the normal ordering.

Figure 2 shows the result for the case V_3

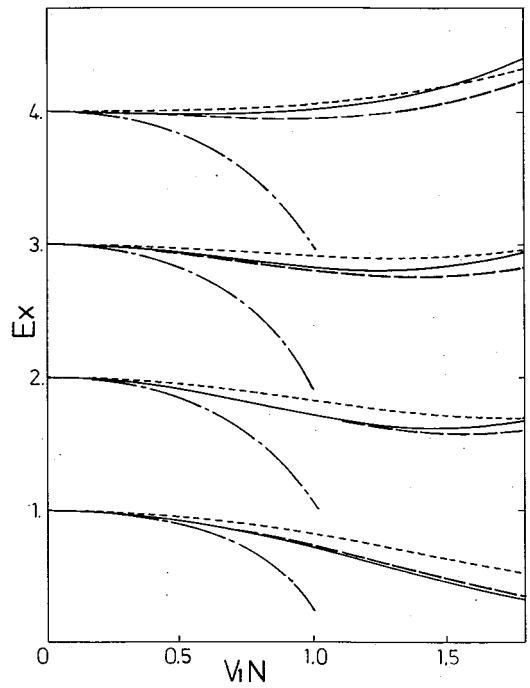

Fig. 1. Excitation energies of collective excited states in the three-level model plotted as functions of the force-strength V_1. The force-strength V_3 responsible for the mode-mode coupling between different RPA vibrations is here put equal to zero. The solid lines represent the exact solutions, while the broken lines the result calculated by our quantization procedure. For reference sake, the result calculated by using the boundary condition ($\sigma=1$ and $\tau=0$) in place of the optimized RPA boundary condition is plotted by the dot-dashed lines. The result calculated by adopting the Weyl ordering in place of the normal ordering is also given by the dotted lines. The parameters used are: $N=10$, $c_1=1.0$, $c_2=3.0$ and $V_2=0$. The RPA critical point corresponds to $V_1N=10/9$.

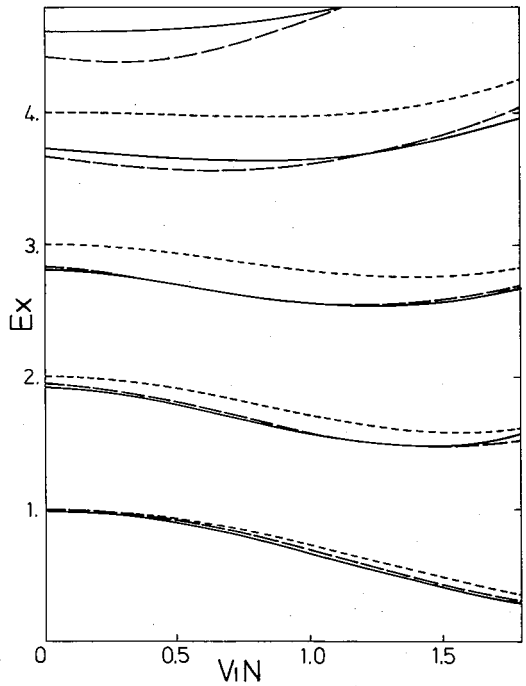

Fig. 2. The same as Fig. 1 except that the force-strength V_3 is here set to be $V_3\sqrt{N}=0.3$. To indicate the energy shifts due to the mode-mode coupling, the excitation energies for $V_3=0.0$, which are shown in Fig. 1 by the broken lines, are again plotted by the dotted lines.

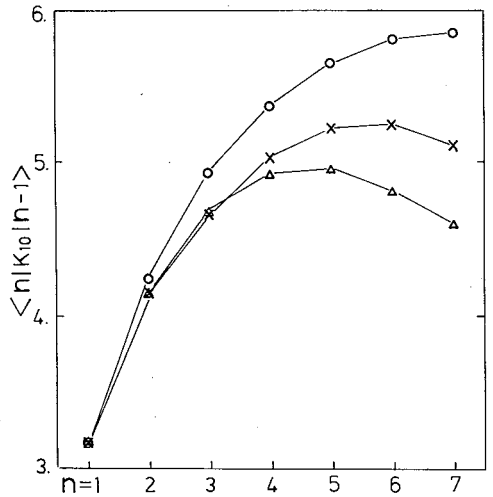

Fig. 3. Transition amplitudes between the n-th and the $(n-1)$-th collective excited states in the three-level model with the parameters $N=10$, $V_1N=0.2$, $V_2N=0.0$, $V_3\sqrt{N}=0.3$, $e_1=1.0$ and $e_2=3.0$. The symbol $\times$ represents the exact solutions, while $\triangle$ the values calculated by our quantization procedure. For reference sake, the values obtained by putting $V_3=0$ in the latter calculation are indicated by the symbol $\circ$.

$\neq 0$. To explicitly indicate the energy shifts due to the mode-mode coupling between the lower and higher RPA vibrations, we also present in this figure the spectrum for the case $V_3=0$. We clearly see that the calculated result agrees surprisingly well with the exact spectrum. This means that the SCC method has succeeded in determining the maximally decoupled collective subspace in such an excellent way as to properly incorporate the effect of the mode-mode coupling. At the same time, this agreement indicates that our quantization procedure is indeed suited to the (η^*, η) expansion under the optimized RPA boundary condition. It should be emphasized that two kinds of boson operators are needed (instead of one kind) to treat the mode-mode coupling under consideration in the conventional boson-expansion methods.

Figure 3 shows the calculated values of the transition amplitudes for the operator K_{10}. Again, we see that the result in which the mode-mode coupling is incorporated agree very well with the exact solution up to the four-phonon state (the fourth collective excited state). This indicates that the convergence of the (η^*, η) expansion is excellent at least for low-lying states.

§ 6. Conclusions

From the analysis made in §§ 4 and 5, we can draw the following conclusions: 1) It is possible to find an optimal canonical coordinate system to carry out the quantization procedure for the collective Hamiltonian derived by the SCC method. 2) We can select

an optimized RPA boundary condition for the (η^*, η) expansion, which is most suitable for the canonical quantization with the normal ordering. Of course, these conclusions admit the possibilities to choose other canonical coordinate systems in conjunction with different quantization procedures. For example, we can quote Ref. 20) in which an adiabatic expansion is used instead of the (η^*, η) expansion.

An interesting future subject is to justify the result of this paper as a (hopefully excellent) approximation to the formulation of Ref. 21) in which a quantum version of the SCC method is proposed. Although the basic ideas to formulate "the invariance principle of the Schrödinger equation" without utilizing the classical framework of the TDHB approximation have already been proposed in Ref. 21), we do not know, at the present time, a feasible method to solve the basic equations of the quantum theory. Thus, it appears to us that the canonical quantization procedure discussed in this paper is a practicable way, free from the adiabatic approximation, to apply the SCC method to real nuclear phenomena. The details for exploiting the result of this paper will be reported in a forthcoming paper[10] dealing with the anharmonic gamma vibrations.

Acknowledgements

We thank the members of the 1984 annual research project on "microscopic theories of large-amplitude collective motions" organized by RIFP for valuable discussions.

References

1) T. Marumori, T. Maskawa, F. Sakata and A. Kuriyama, Prog. Theor. Phys. **64** (1980), 1294.
2) S. G. Lie and G. Holzwarth, Phys. Rev. **C12** (1975), 1035.
3) T. Marumori, K. Takada and F. Sakata, Preprint IP-UT-TNP-Rep. 2, *Lecture at the Winter College on Fundamental Nuclear Physics, Trieste,* 1984, to be published.
4) F. Sakata, Y. Hashimoto, T. Marumori and T. Une, Prog. Theor. Phys. **70** (1983), 163; *Proceedings of* 1982 *INS Int. Symp. on "Dynamics of the Nuclear Collective Motion"*, p. 311.
5) Y. Hashimoto, Genshikaku Kenkyu (circular in Japanese) **26** (1981), 65.
6) A. Kuriyama, Prog. Theor. Phys. Suppl. Nos. 74 & 75 (1983), 66.
7) A. Kuriyama and M. Yamamura, Prog. Theor. Phys. **70** (1983), 1675.
8) M. Yamamura, A. Kuriyama and S. Iida, Prog. Theor. Phys. **71** (1984), 109.
9) M. Matsuo, Prog. Theor. Phys. **72** (1984), 666.
10) M. Matsuo and K. Matsuyanagi, Preprint KUNS 791.
11) T. Marumori, Prog. Theor. Phys. **57** (1977), 112.
12) P. Kramer and M. Saraceno, Lecture Notes in Physics, No. 140 (Springer-Verlag, 1981).
13) K. Kumar and M. Baranger, Nucl. Phys. **A92** (1967), 608.
14) M. Baranger and M. Vénérori, Ann. of Phys. **114** (1978), 123.
15) N. Onishi and S. Yoshida, Nucl. Phys. **80** (1966), 367.
16) G. Holzwarth, D. Janssen and R. V. Jolos, Nucl. Phys. **A261** (1976), 1.
17) S. Iwasaki, F. Sakata and K. Takada, Prog. Theor. Phys. **57** (1977), 1289.
18) T. Kishimoto and T. Tamura, Phys. Rev. **C27** (1983), 341.
T. Tamura and T. Kishimoto, Prog. Theor. Phys. Suppl. Nos. 74&75 (1983), 282.
19) E. R. Marshalek and G. Holzwarth, Nucl. Phys. **A191** (1972), 438.
20) A. Kuriyama, M. Yamamura and S. Iida, Prog. Theor. Phys. **72** (1984), 1273.
21) T. Marumori, F. Sakata, T. Une, Y. Hashimoto and T. Maskawa, Prog. Theor. Phys. **66** (1981), 1651; Prog. Theor. Phys. Suppl. Nos. 74 & 75 (1983), 221.